PHASE 2 INITIAL BOREHOLE DRILLING AND TESTING, IGNACE AREA

WP4b Data Report - Geomechanical Testing of Core for IG_BH03

APM-REP-01332-0252 **June 2022**

Golder Associates Ltd.

NUCLEAR WASTE MANAGEMENT ORGANIZATION
SOCIÉTÉ DE GESTION DES DÉCHETS NUCLÉAIRES

Nuclear Waste Management Organization
22 St. Clair Avenue East, 4th Floor
Toronto, Ontario
M4T 2S3
Canada

Tel: 416-934-9814
Web: www.nwmo.ca

REPORT

PHASE 2 INITIAL BOREHOLE DRILLING AND TESTING, IGNACE AREA

WP4b Data Report - Geomechanical Testing of Core for IG_BH03

Submitted to:

Nuclear Waste Management Organization
4th Floor
22 St. Clair Avenue East
Toronto, Ontario, M4T 2S3

Submitted by:

Golder Associates Ltd.
6925 Century Avenue, Suite #100, Mississauga, Ontario, L5N 7K2, Canada

1671632 (2400B)
NWMO Report: APM-REP-01332-0252

June 2022

Distribution List

NWMO - 1 eCopy

Golder Associates Ltd. - 1 eCopy

WP4B DATA REPORT
GEOMECHANICAL TESTING OF CORE FOR IG_BH03

CLIENT INFORMATION

Project Name: Phase 2 Initial Borehole Drilling and Testing, Ignace Area

Project Number: 1671632

Client PO Number: 2000141 (Formerly 01559 A-TGS)

Document Name: 1671632 (2400B) IG_BH03_WP4B_Report_22Jun2022_r1a_clean.docx

Client: Nuclear Waste Management Organization (NWMO)
22 St. Clair Avenue East, Fourth Floor
Toronto, Ontario
M4T 2S3

Client Contact: Hossein Kasani and Maria Sánchez-Rico Castejón

Email: hkasani@nwmo.ca and msanchez@nwmo.ca

ISSUE/REVISION INDEX

Issue Code	Revision					Revision Details
	No.	By	Rev'd.	App.	Date	
RR	0a	JLC	DD	GWS	April 12, 2022	Draft released for review and comment
RI	1a	JLC	DD	GWS	June 22, 2022	Revised Final released for Information

Issue Codes: RR = Released for Review and Comments, RI = Released for Information

SIGNATURES

Prepared by: ______________________

Joe Carvalho, Ph.D., P.Eng.
Mining & Rock Engineering - Principal

Reviewed by: ______________________

David Dixon, Ph.D., P.Geo.
Senior Geoscientist

Approved by: ______________________

George Schneider, M.Sc., P.Geo.
Senior Geoscientist - Principal

Table of Contents

TABLES

FIGURES

APPENDICES

1.0 INTRODUCTION

The Initial Borehole Drilling and Testing project in the Wabigoon and Ignace Area, Ontario is part of Phase 2 Geoscientific Preliminary Field Investigations of the NWMO's Adaptive Phased Management (APM) Site Selection Phase.

This project involves the drilling and testing of the first of three deep boreholes within the northern portion of the Revell batholith. The second drilled borehole, IG_BH03, is located a direct distance of approximately 21 km southeast of the Wabigoon Lake Ojibway Nation and a direct distance of 43 km northwest of the Town of Ignace. Access to the IG_BH03 drill site is via Highway 17 and primary logging roads, as shown on Figure 1.

The project was carried out by a team led by Golder Associates Ltd. (Golder) on behalf of the NWMO. The overall program is described in the Initial Borehole Characterization Plan (Golder 2018). This report describes the testing methodology and results for Work Package 4B (WP4B): Geomechanical Testing of Core for IG_BH03, which includes Uniaxial Compressive Strength tests (w/ elastic constants), Indirect Tensile (Brazilian) Strength tests, P-wave and S-wave ultrasonic pulse velocity, acoustic emissions (AE) measurements (on UCS tests) and Thermal testing comprising Thermal Conductivity, Thermal Diffusivity, Volumetric Heat Capacity, and Thermal Expansion. Wet and dry density and water content were measured for all tested samples.

2.0 BACKGROUND INFORMATION

2.1 Geological Setting

The approximately 2.7 billion year old Revell batholith is located in the western part of the Wabigoon Subprovince of the Archean Superior Province. The batholith is roughly elliptical in shape trending northwest, is approximately 40 km in length, 15 km in width, and covers an area of approximately 455 km^2. Based on geophysical modelling, the batholith is approximately 2 km to 3 km thick through the center of the northern portion (SGL 2015). The batholith is surrounded by supracrustal rocks of the Raleigh Lake (to the north and east) and Bending Lake (to the southwest) greenstone belts (Figure 2).

Borehole IG_BH03 is located within an investigation area of approximately 19 km^2 in size, situated in the northern portion of the Revell batholith. Bedrock exposure in the area is generally very good due to minimal overburden, few water bodies, and relatively recent logging activities. Ground elevations generally range from 400 to 450 m above sea level. The ground surface broadly slopes towards the northwest as indicated by the flow direction of the main rivers in the area. Local water courses tend to flow to the southwest towards Mennin Lake (Figure 1).

Four main rock units are identified in the supracrustal rock group: mafic metavolcanic rocks, intermediate to felsic metavolcanic rocks, metasedimentary rocks, and mafic intrusive rocks (Figure 2). Sedimentation within the supracrustal rock assemblage was largely synvolcanic, although sediment deposition in the Bending Lake area may have continued past the volcanic period (Stone 2009; Stone 2010a; Stone 2010b). All supracrustal rocks are affected, to varying degrees, by penetrative brittle-ductile to ductile deformation under greenschist- to amphibolite-facies metamorphic conditions (Blackburn and Hinz 1996; Stone et al. 1998). In some locations, primary features, such as pillow basalt or bedding in sedimentary rocks are preserved, in other locations, primary relationships are completely masked by penetrative deformation. Uranium-lead (U-Pb) geochronological analysis of the supracrustal rocks produced ages that range between 2734.6 +/-1.1 Ma and 2725 +/-5 Ma (Stone et al. 2010).

Three main suites of plutonic rock are recognized in the Revell batholith, including, from oldest to youngest: a Biotite Tonalite to Granodiorite suite, a Hornblende Tonalite to Granodiorite suite, and a Biotite Granite to Granodiorite suite (Figure 2). Plutonic rocks of the Biotite Tonalite to Granodiorite suite occur along the southwestern and northeastern margins of the Revell batholith. The principal type of rock within this suite is a white to grey, medium-grained, variably massive to foliated or weakly gneissic, biotite tonalite to granodiorite. One sample of foliated and medium-grained biotite tonalite produced a U-Pb age of 2734.2+/-0.8 Ma (Stone et al. 2010). The Hornblende Tonalite to Granodiorite suite occurs in two irregularly-shaped zones surrounding the central core of the Revell batholith. Rocks of the Hornblende Tonalite to Granodiorite suite range compositionally from tonalite through granodiorite to granite and also include significant proportions of quartz diorite and quartz monzodiorite. One sample of coarse-grained grey mesocratic hornblende tonalite produced a U-Pb age of 2732.3+/-0.8 Ma (Stone et al. 2010). Rocks of the Biotite Granite to Granodiorite suite underlie most of the northern, central and southern portions of the Revell batholith. Rocks of this suite are typically coarse-grained, massive to weakly foliated, and white to pink in colour. The Biotite Granite to Granodiorite suite ranges compositionally from granite through granodiorite to tonalite. A distinct potassium (K)-Feldspar Megacrystic Granite phase of the Biotite Granite to Granodiorite suite occurs as an oval-shaped body in the central portion of the Revell batholith (Figure 2). One sample of coarse-grained, pink, massive K-feldspar megacrystic biotite granite produced a U-Pb age of 2694.0+/-0.9 Ma (Stone et al. 2010).

The bedrock surrounding IG_BH03 is composed mainly of massive to weakly foliated felsic intrusive rocks that vary in composition between granodiorite and tonalite, and together form a relatively homogeneous intrusive complex. Bedrock identified as tonalite transitions gradationally into granodiorite and no distinct contact relationships between these two rock types are typically observed (SRK and Golder 2015; Golder and PGW 2017). Massive to weakly foliated granite is identified at the ground surface to the northwest of the feldspar-megacrystic granite. The granite is observed to intrude into the granodiorite-tonalite bedrock, indicating it is distinct from, and younger than, the intrusive complex (Golder and PGW 2017).

West-northwest trending mafic dykes interpreted from aeromagnetic data extend across the northern portion of the Revell batholith and into the surrounding greenstone belts. One mafic dyke occurrence, located to the northwest of IG_BH01, is approximately 15-20 m wide (Figure 2). All of these mafic dykes have a similar character and are interpreted to be part of the Wabigoon dyke swarm. One sample from the same Wabigoon swarm produced a U-Pb age of 1887+/-13 Ma (Stone et al. 2010), indicating that these mafic dykes are Proterozoic in age. It is assumed based on surface measurements that these mafic dykes are sub-vertical (Golder and PGW 2017).

Long, narrow valleys are located along the western and southern limits of the investigation area (Figure 1). These local valleys host creeks and small lakes that drain to the southwest and may represent the surface expression of structural features that extend into the bedrock. A broad valley is located along the eastern limits of the investigation area and hosts a more continuous, un-named water body that flows to the south. The linear and segmented nature of this waterbody’s shorelines may also represent the surface expression of structural features that extend into the bedrock.

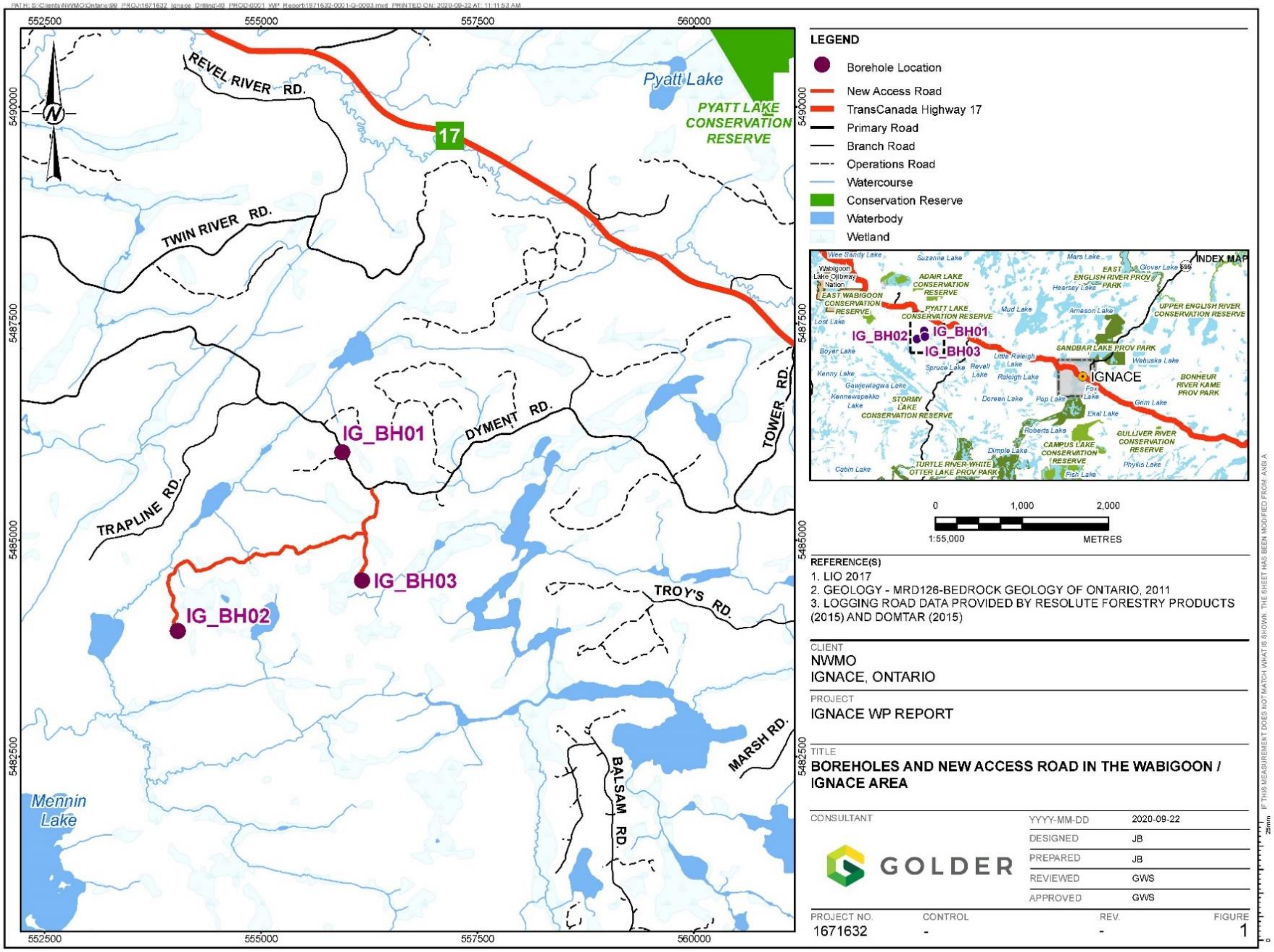

Figure 1: Location of IG_BH01, IG_BH02 and IG_BH03 in Relation to the Wabigoon / Ignace Area

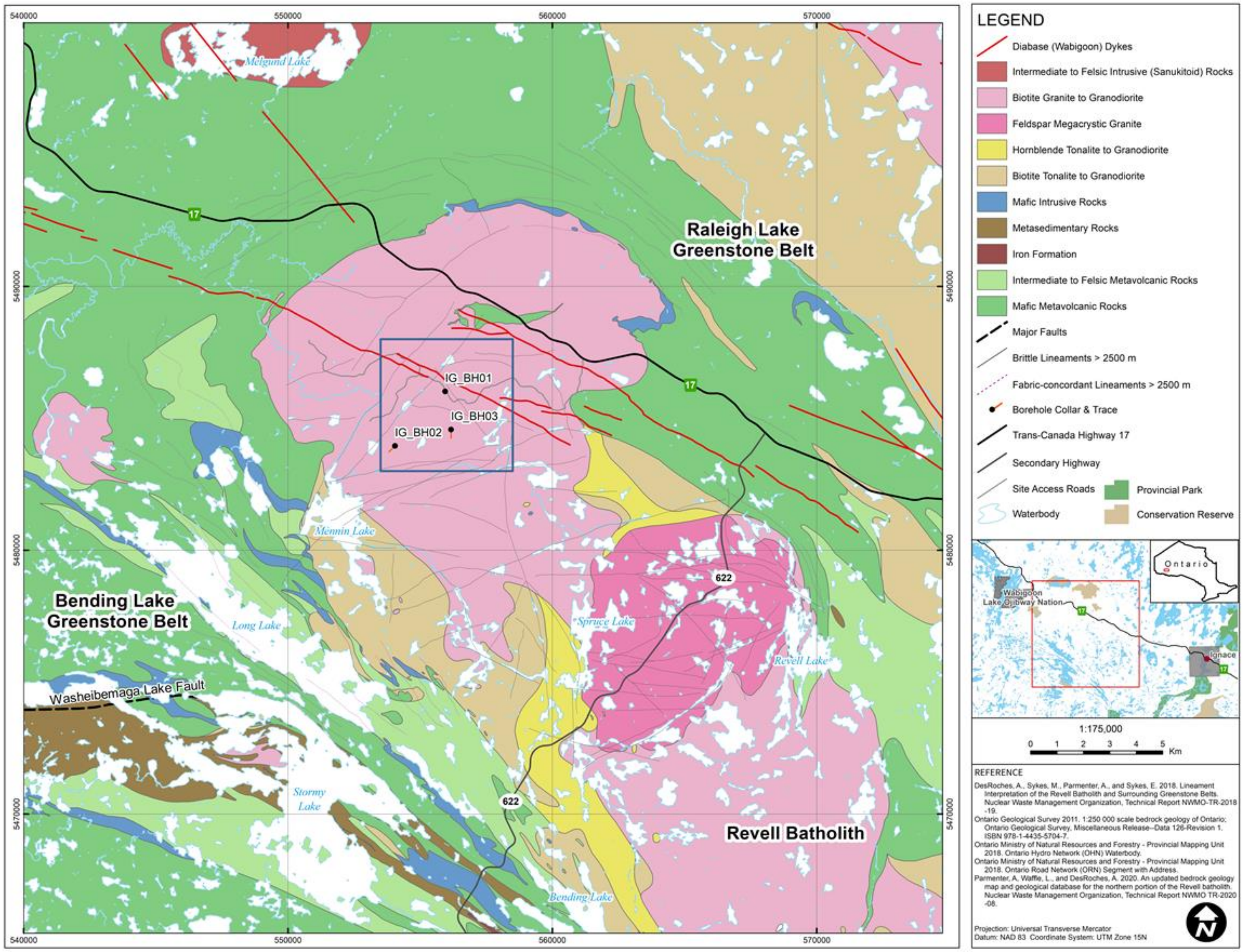

Figure 2: Geological setting and location of boreholes IG_BH01, IG_BH02 and IG_BH03 in the northern portion of the Revell batholith

Regional observations from mapping have indicated that structural features are widely spaced (typical 30 to 500 cm spacing range) and dominantly comprised of sub-vertical joints with two dominant orientations, northeast and northwest trending (Golder and PGW 2017). Interpreted bedrock lineaments generally follow these same dominant orientations in the northern portion of the Revell batholith (Figure 2; DesRoches et al. 2018). Minor sub-horizontal joints have been observed with minimal alteration, suggesting they are younger and perhaps related to glacial unloading. One mapped regional-scale fault, the Washeibemaga Lake fault, trends east and is located to the west of the Revell batholith (Figure 2). Additional details of the lithological units and structures found at surface within the investigation area are reported in Golder and PGW (2017).

2.2 Technical Objectives

The technical objective of the geomechanical laboratory testing and thermal testing program is to assess the key geomechanical and thermal properties of the crystalline host rock mainly within the repository horizon (presently assumed to be between depths of approximately 400 and 600 m) as well as a few samples from outside this horizon.

The testing was undertaken in more than one campaign, as follows:

- Campaign 1: During the drilling of IG_BH03, seven (7) samples were collected and preserved for UCS strength testing and were sent to the CANMET laboratory at the end of the drilling. Also, seven (7) samples were collected and preserved for Indirect Tensile (Brazilian) strength testing and were sent to the CAMNET laboratory for testing at the end of the drilling. Samples were tested in their natural water content state. Nine (9) samples were collected and preserved for thermal testing. Nine (9) thermal samples were tested for Thermal Conductivity, Thermal Diffusivity, and Volumetric Heat Capacity under as-received conditions. Thermal expansion tests deviated from the test plan and needed to be repeated. The thermal conductivity, thermal diffusivity and volumetric heat capacity samples were tested under as-received conditions when they should have been tested in dry conditions, according to the test plan. Therefore, a select few more samples would be also targeted for additional testing under dry conditions.
- Campaign 2: Due to unintentional deviations from the specifications set out in the test plan, that were identified following completion of the initial testing campaign, an additional nine (9) samples were selected for thermal testing. All nine (9) samples were tested for thermal expansion in re-saturated conditions, and a select five (5) samples were tested for thermal conductivity, thermal diffusivity and volumetric heat capacity in dry conditions.

Uniaxial Compressive Strength (UCS) testing of core samples were performed on seven (7) samples to determine the intact unconfined compressive strength and elastic properties (elastic moduli and Poisson’s ratio) of the bedrock. Additional non-destructive testing/measurements for each UCS core sample included:

- Determination of water content and rock density;
- Determination of P-wave and S-wave ultrasonic pulse velocities and determination of ultrasonic elastic constants; and
- Monitoring and recording of incremental and cumulative acoustic emissions throughout each test.

Crack Initiation and Crack Damage stress levels were interpreted from the stress-strain curves for each test and compared to interpreted AE results for verification.

Indirect Tensile (Brazilian) Strength testing of core samples were performed on seven (7) samples (selected adjacent to the UCS samples) to determine the tensile strength of the rock.

Eighteen (18) samples were also selected for thermal property testing, including:

- Determination of volumetric heat capacity;
- Absolute thermal conductivity;
- Thermal diffusivity;
- Thermal expansion; and
- Determination of re-saturated water content, re-saturated and dry density

Initially (Campaign 1), the volumetric heat capacity, thermal conductivity and thermal diffusivity tests were completed on nine (9) samples under re-saturated conditions. An additional nine (9) samples were selected from the stored core; five (5) samples were tested under dry conditions for volumetric heat capacity, thermal conductivity and thermal diffusivity; all additional thirteen (9) samples were tested for thermal expansion under re-saturated conditions. Water content and rock density of test specimens sub-cored from all eighteen (18) samples were determined.

2.3 Description of Testing Procedures

The geomechanical testing program was carried out at the CANMET-MMSL rock mechanics testing facility located in Bells Corners (Ottawa), Ontario. Laboratory tests were carried out according to CANMET-MMSL's Standard Operating Procedures (SOPs), which follow ASTM standard test methods and ISRM suggested methods:

Preparation and Non-destructive Testing

- ASTM D4543-08 & ASTM D4543-19 Standard Practices for Preparing Rock Core as Cylindrical Test Specimens and Verifying Conformance to Dimensional and Shape Tolerances
- ASTM D2216-10 & ASTM D2216-19 Standard Test Methods for Laboratory Determination of Water (Moisture) Content of Soil and Rock by Mass
- ASTM D7263-09 (2018)$^{\varepsilon 2}$, Laboratory Determination of Density (Unit Weight) of Soil Specimens

UCS Testing and Elastic Parameters

- ASTM D7012-14$^{\varepsilon 1}$ Standard Test Methods for Compressive Strength and Elastic Moduli of Intact Rock Core Specimens under Varying States of Stress and Temperatures
- ASTM D2845-08 Standard Test Method for Laboratory Determination of Pulse Velocities and Ultrasonic Elastic Constants of Rock. Note that ASTM D2845-08 has been withdrawn in 2017 without replacement. However, CANMET-MMSL methodology for this test still followed ASTM D2845-08 despite its withdrawal.

Indirect Tensile Strength Testing

- ASTM D3967-16 Standard Test Method for Splitting Tensile Strength of Intact Rock Core Specimens

The thermal testing program was carried out at the RESPEC testing facility located in Rapid City, South Dakota. Laboratory tests were carried out according to RESPEC's Standard Operating Procedures (SOPs), which follow ASTM standard test methods and ISO 22007 standard.

Preparation and Non-destructive Testing

RESPEC follows their internal Test Procedure 02 (TP-02, RSI Standard Procedure for Rock Specimen Preparation, Rev. 4) for sample preparation, which follow ASTM standard test methods:

- ASTM D2216-10 & ASTM D2216-19 Standard Test Methods for Laboratory Determination of Water (Moisture) Content of Soil and Rock by Mass
- ASTM D7263-09 (reapproved 2018)$^{\varepsilon 2}$, Laboratory Determination of Density (Unit Weight) of Soil

For the hot disk specimens which had to be stored between drying and testing, they were double bagged using Ziplock bags and were stored in a room subject to year-round air conditioning.

For the thermal expansion specimens which had to be stored between saturating and testing, they were placed in Ziplock bags with excess water. Specimens were periodically checked to ensure that moist surface conditions were maintained.

Thermal Conductivity, Specific Heat and Thermal Diffusivity

Thermal testing was conducted on full-diameter size core (61 mm). The ends of the specimens are either ground flat in the surface grinder or finished in the lathe depending on the type of rock. The following standard applies:

- ISO 22007-2: 2015(E) Determination of thermal conductivity and thermal diffusivity Part 2: Transient plane heat source (hot disc) method.

Thermal Expansion

Thermal expansion testing was conducted on samples sub-cored to 32 mm (1.25'') diameter. Thermal expansion testing was conducted on saturated samples. Re-saturation for all non-preserved samples preceded thermal expansion testing.

- ASTM D4535-13$^{\varepsilon 1}$ & ASTM D4535-13$^{\varepsilon 2}$, Standard Test Methods for Measurement of Thermal Expansion of Rock Using Dilatometer – Method A (unconfined).

2.4 Test Apparatus and Procedures

2.4.1 Sample Preparation

Preparation of cylindrical specimens for UCS tests, and verification of conformance to dimensional and shape tolerances were done according to the ASTM D4543-19 standard test method. Fresh water was used for cutting and end preparation. Specimen ends were ground flat to within 0.025 mm and parallel to each other as specified by the ASTM standard test method for a loading system with fixed platens.

Specimen dimensions, i.e., average length and diameter, were measured to the nearest 0.01 mm. Cross-sectional area and volume were determined. Specimens were weighted to the nearest 0.1 g, and density was computed to the nearest 0.01 g/cm^3 as well. Zero-pressure P- and S-wave velocities were also measured.

Specimens with a nominal thickness-to-diameter ratio of 0.66 were prepared to carry out splitting tensile (Brazilian) tests.

2.4.2 Uniaxial Compressive Strength (UCS) Tests

UCS tests were carried out using a computer-controlled, servo-hydraulic MTS Rock Mechanics Testing System, Model 815, consisting of a 2.6 MN rated capacity load cell, the load frame itself, the hydraulic power supply, and digital controllers and test software to control experiments. Displacements were converted into strains taking into account the specific dimensions of each test specimen. UCS test specimens were covered by a thin Teflon heat shrink jacket prior the beginning of the test to protect the instrumentation and avoid the projection of fragments, especially when testing brittle materials. Test specimens were loaded up to failure at constant axial displacement rate, e.g., controlled strain rate, equal to 0.0009 mm/sec for 60 mm (nominal) OD specimens, with failure expected between 5 and 10 minutes after the beginning of loading for UCS tests, in accordance with the requirements of the ASTM D7012 standard test method for UCS tests. All data, e.g., time, axial load, axial stress, and axial and circumferential displacements, were sampled and recorded every 0.2 second over the whole test duration, and converted into engineering units afterwards, i.e., conversion of loads and displacements into stresses and strains, respectively.

2.4.2.1 Acoustic Emissions (AE) Data Acquisition

Acoustic emissions were recorded during UCS tests. The system used was a Pocket AE-2™ system manufactured by Physical Acoustics Corporation (PAC). This system is a dual channel 18-bit system connected to Pico™ sensors with a frequency range of 200-750 kHz and a sampling rate of 20 Ms/sec.

Two sensors were fixed on opposite sides of UCS test specimens, at 180 degrees from each other, one sensor being fixed 3 cm above the specimen mid-section, and the second sensor 3 cm below the mid-section, so these were not interfering with the movement of the MTS chain extensometer. Acoustic emission data were recorded systematically. Main features recorded were the number of emissions (or hits) and the waveform signal.

2.4.3 Indirect Tensile Strength (Brazilian) Tests

Tests were performed on the same system used for the UCS testing, but with a smaller load cell for higher accuracy, e.g., a rated capacity of 500 kN. Test specimens were loaded diametrically at a constant load rate of 0.10 kN/sec, with breakage expected sometime between two and five minutes after the beginning of the test. Tests were carried out in conformity with the requirements of the ASTM D3967-16 standard test method for indirect tensile (Brazilian) strength tests. All test data, i.e., time, diametrical load, tensile stress and vertical displacement (Ram LVDT), were recorded every 0.2 seconds over the whole test duration.

2.4.4 Water Content and Density Measurements

The samples were measured and weighed before testing. After testing, they were weighed and placed in the oven to start the drying process. Because of the destructive nature of the UCS and Brazilian tests, there is a possibility that some of the sample material may be lost during testing, which will make it difficult to know the exact volume of the sample after the test. Due to the lower porosity of the rock samples from IG_BH03, any loss, however small, can have a significant effect in the determination of the water content and dry density. Therefore, the more precise way to determine the dry density for samples undergoing destructive testing is using the bulk density and the measured water content.

The density of the bulk samples, as received, is calculated as follows:

Volume of the prepared sample = V

Mass of the prepared sample = M

$$\rho_{\text{bulk}} = \frac{M}{V}$$

The water content of the sample is calculated as follows:

Mass of the sample after testing (initial mass before drying) = M_{init}

Mass of the sample after drying = M_{dry}

$$w = \frac{M_{init} - M_{dry}}{M_{dry}}$$

Calculation of the sample dry density:

$$\rho_{\text{dry}} = \frac{\rho_{\text{bulk}}}{1 + w}$$

Note that when no material is lost, and the mass and volume after the test have not changed, the dry density reverts to

$$\rho_{\text{dry}} = \frac{M_{dry}}{V}$$

2.4.5 Thermal Conductivity, Volumetric Heat Capacity and Thermal Diffusivity

Thermal conductivity, volumetric heat capacity and thermal diffusivity were measured both in as-received (9 samples) and dry conditions (5 samples). Samples tested in the dry state were dried in temperatures not exceeding 80°C prior to testing; after testing, samples were further dried following the same procedure provided for water content measurements described above to a precision not less than 0.01% of the initial sample weight.

Testing was performed using a Thermtest TPS 1500 that heats and measures the thermal gradient across an area. The Transient Plane Source (TPS) sensor was placed between two pieces of material to be measured, each with plane surfaces facing the sensor. The solution to the thermal conductivity equation assumes the sensor is in an infinite medium, so the measurement and subsequent analysis of data must account for the limitation created by the outer boundaries of the material. The TPS sensor contains both a heating element and a temperature measuring sensor. A known amount of power is supplied to the heater for a set amount of time. The temperature gradient is measured as it spreads out from the heat source. From these data, the thermal analyzer can determine the thermal conductivity, volumetric heat capacity and thermal diffusivity.

Thermal conductivity, volumetric heat capacity and thermal diffusivity were measured between room temperature (25°C) and 300°C in 10 temperature intervals for the nine (9) samples tested under as-received water content conditions. The first temperature interval was 15°C and the subsequent intervals were 30°C (Campaign 1). For the five (5) samples tested under dry conditions, five (5) measurements were made between room temperature and 90°C during heating and a repeat measurement during cooling at 60°C followed the heating schedule shown in Table 1 (Campaign 2).

Table 1: Target Temperature Schedule for Hot Disk Tests

Data Point	Target Temperature	Comments
1	20 – 25°C	Room temperature
2	40°C	
3	60°C	
4	80°C	
5	90°C	
6	60°C	Repeat measurement during cooling

2.4.6 Thermal Expansion

Thermal expansion was measured using a Unitherm 1054L apparatus that has been updated to allow automatic control and temperatures ranging from 25°C to 300°C. Tests were performed using a push-rod dilatometer and heating element. The dilatometer system is capable of testing two specimens simultaneously. The test setup is described as unconfined and uniaxial because the specimen is subjected only to atmospheric pressure and deformation is only measured in the axial direction of the specimen.

Thermal expansion was measured between room temperature and 90°C, for the nine (9) re-saturated samples (Campaign 2) following the target temperature schedule shown in Table 2. Two heating-cooling paths were followed with five (5) measurements during heating and a measurement at 60°C during cooling. The rate of heating/cooling between target temperatures did not exceed 1°C/min. A target rate of heating/cooling of 0.5 °C/min was used to ensure that the maximum rate of 1°C/min was not exceeded due to temperature fluctuations. Compliance with this requirement has been demonstrated graphically by plotting temperature rate vs time and included in the metadata deliverable.

Table 2: Target Temperature Schedule for Thermal Expansion Tests

Data Point	Target Temperature	Comments
1	20 – 25°C (room temp)	1st Heating Path
2	40°C	
3	60°C	
4	80°C	
5	90°C	
6	60°C	1st Cooling Path
7	20 – 25°C (room temp)	
8	40°C	2nd Heating Path
9	60°C	
10	80°C	
11	90°C	
12	60°C	2nd Cooling Path
13	20 – 25°C (room temp)	

2.5 Analysis of Data

2.5.1 Zero Pressure P-S Wave Velocity Tests

P (compressive) and S (shear) wave velocities are determined from the time taken by a sinusoidal wave to travel across the test specimen along its longitudinal axis. P and S wave velocities were determined for all UCS specimens prepared for the test program. Dynamic elastic constants are calculated by the following expressions:

$$E_D = \frac{\rho V_S^2 (3V_P^2 - 4V_S^2)}{V_P^2 - V_S^2}$$

$$G_D = \rho V_S^2$$

$$\nu_D = \frac{V_P^2 - 2V_S^2}{2(V_P^2 - V_S^2)}$$

where:

E_D – dynamic Young's modulus
G_D – dynamic shear modulus
ν_D – dynamic Poisson's ratio
V_P – compressive (P) wave velocity
V_S – shear (S) wave velocity
ρ – density

2.5.2 Uniaxial Compressive Strength (UCS) Tests

Raw original data recorded during uniaxial compression tests consist of axial load, and axial and circumferential displacements. Axial displacements are corrected for the compression of steel platens, between which displacements are measured, and the circumferential displacement is corrected for the gap between the measuring chain-extensometer and the specimen side. Engineering stresses and strains are computed using the following formulas:

$$\sigma_1 = \frac{P}{A_0}$$

$$\varepsilon_A = \frac{\Delta L}{L_0}$$

$$\varepsilon_C = \frac{\Delta D}{D_0}$$

where:

σ_1 – axial stress
P – axial load
A_0 – initial cross-sectional area of the specimen
ε_A – axial strain
ε_C – circumferential strain
ΔL – change in specimen length
L_0 – specimen length
ΔD – change in specimen circumference

D_0 – specimen circumference

The volumetric strain (ε_V) is defined by the following expression:

$$\varepsilon_V = \varepsilon_A + 2\varepsilon_C$$

The uniaxial compressive strength (UCS) was determined for all UCS tests carried out during the test program. The Young's modulus (E_{40}) was determined at a nominal stress level of 40% of the UCS, as the slope of the linear regression line through axial stress-axial strain data points over 30-50% of the axial stress interval. The Poisson's ratio (ν_{40}) was determined as the negative of the slope of the linear regression line through circumferential strain-axial strain data points, averaged over the same axial stress interval. Strength is given by the following expression:

$$UCS = \frac{P_C}{A_0}$$

where:

UCS – uniaxial compressive strength
P_C – ultimate axial load on the specimen at failure
As mentioned, strain data are obtained from displacements measured with the mechanical sensors, e.g., axial LVDTs and MTS circumferential chain-extensometer.

The crack damage threshold, σ_{CD}, has been interpreted in this report as the stress level at which the volumetric strain, ε_V, reaches its maximum and starts reversing direction, i.e., the inflexion point on the $\sigma_1 - \varepsilon_V$ graph, hence indicating dilation due to the formation and growth of unstable cracks. Theoretically, it is assumed that the progressive fracturing process starts above the crack damage threshold, leading to the failure of the rock material (Ghazvinian et al., 2012).

The crack initiation threshold, σ_{CI}, has been interpreted in this report as the stress level at which the crack volumetric strain, ε_{VC}, reaches its maximum and starts reversing direction, i.e., the inflection point on the $\sigma_1 - \varepsilon_{VC}$ graph, hence indicating a departure from elasticity, and the development and growth of stable cracks. The crack volumetric strain, ε_{VC}, is determined by the difference between the volumetric strain, ε_V, and the elastic volumetric strain, ε_{VE}, recorded during UCS tests assuming a perfectly linear elastic material, following these expressions:

$$\varepsilon_{VC} = \varepsilon_V - \varepsilon_{VE}$$

$$\varepsilon_{VE} = \frac{1 - 2\nu_{40}}{E_{40}} \sigma_1$$

2.5.3 Acoustic Emissions Data

The counts per time period and cumulative counts per time period of AE hits for each specimen are provided in Appendix B. Recording of the acoustic emissions may not start at the same time as the recording of the strains; therefore, the two records (strains and AE) are time-matched at the peak stress in order to compare the time (and stress) of the crack initiation process. Crack initiation is defined at the time that systematic cracking develops (not the first crack) which can be identified as the change in the slope of the cumulative energy graph. Crack damage starts when individual cracks start to coalesce and create a localized feature; this threshold can be more difficult to identify in the AE data. The data was also provided in raw digital format, which allowed plotting the graphs for cumulative energy vs axial stress in a log-log scale. Figure 3 shows the log-log plot of cumulative energy vs axial stress for sample IG_BH03_UC002.

The AE records seem to suggest different C_i values, although the interpretation can be somewhat subjective. For this reason, the interpretation from the UCS crack volumetric strain is more reliable. Plots of cumulative energy vs axial stress for all the samples are included in APPENDIX B.

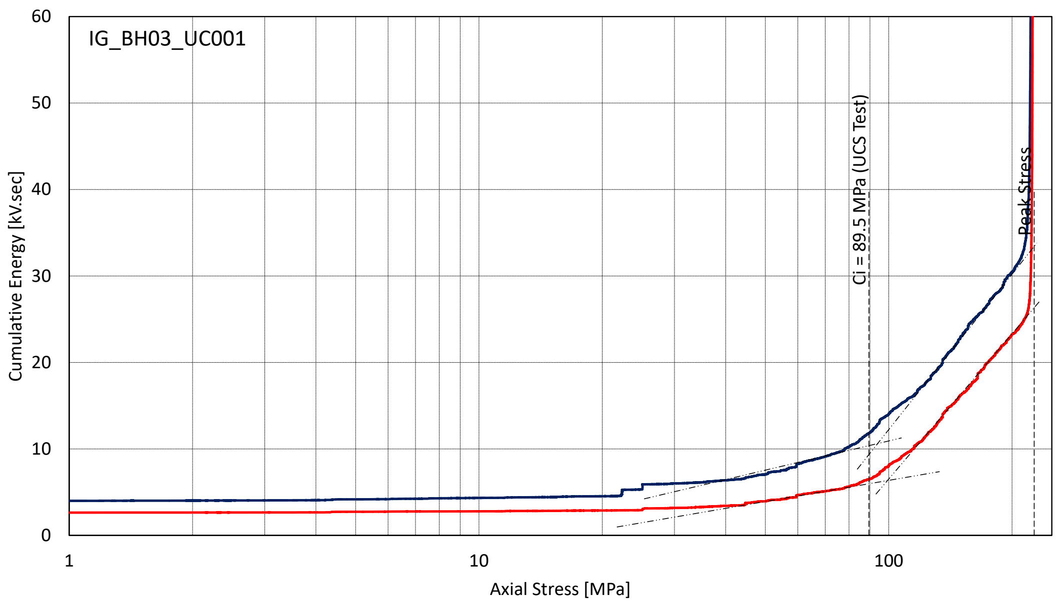

Figure 3: Cumulative energy (in kilovolt.sec) versus axial stress (MPa) measured during UCS testing of sample IG_BH03-UC001 in a log-log scale

2.5.4 Indirect Tensile (Brazilian) Strength Tests

The indirect tensile (Brazilian) strength of a test specimen at failure, σ_T, is given by the following expression:

$$\sigma_T = \frac{2P}{\pi DT}$$

where:

σ_T – tensile strength
P – diametrical load on the specimen at failure
D – diameter of the specimen
T – thickness of the specimen

2.5.5 Thermal Conductivity, Volumetric Heat Capacity and Thermal Diffusivity

The thermal conductivity, k, volumetric heat capacity, C_V, and thermal diffusivity, κ, for each sample were measured at the following 11 temperatures using a Thermtest TPS 1500 for the nine (9) samples tested under as-received water content conditions (Campaign 1):

25°C, 40°C, 70°C, 100°C, 129°C, 159°C, 188°C, 218°C, 247°C, 277°C, and 295°C.

The five (5) samples tested in a dry state were subjected to the heating cycle shown in Table 1.

The thermal diffusivity, κ, can be calculated at each temperature from the thermal conductivity, k, and the volumetric heat capacity, C_V, according to the following relationship:

$$\kappa = \frac{k}{C_V}$$

This relationship provides a check on the results reported by the Thermtest TPS 1500.

If the specific heat, c, is required, it can be obtained from the volumetric heat capacity by dividing it by the density, ρ:

$$c = \frac{C_V}{\rho}$$

2.5.6 Thermal Expansion

The coefficient of linear thermal expansion, α for the seven (7) samples tested in a dry state was measured throughout the heating cycles shown in Table 2.

The displacement measured by the LVDT includes the expansion of sample as well as the components of the apparatus; therefore, it needs to be corrected. Primary machine components that affect measurements are the push rods and the specimen holders. Displacement measurements are referenced to the top of the specimen holders (see Figure 4). The lengthening of the specimen holders is greater than the lengthening of the push rods because they are made from the same material, but the holders are longer; therefore, the LVDTs under-register the specimen displacement.

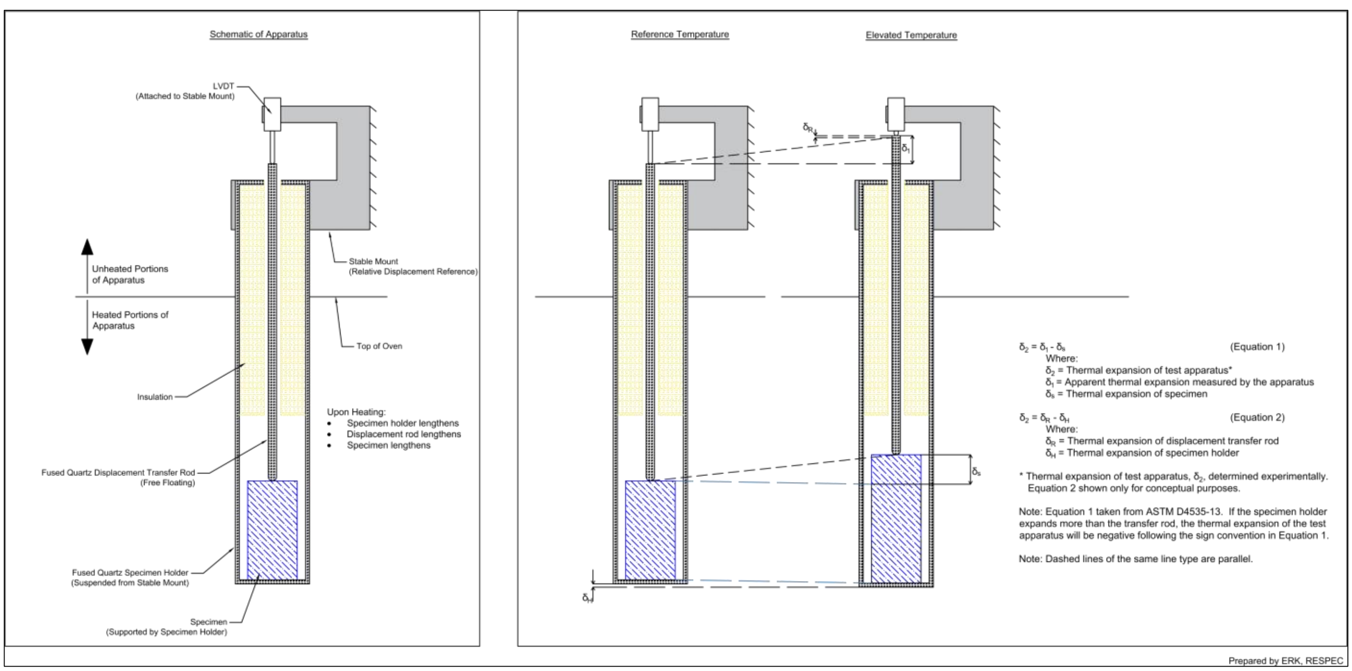

Figure 4: Schematic of the thermal expansion apparatus and components of the displacement correction.

3.0 LABORATORY RESULTS

3.1 Dimensions and Physical Properties of Specimens

The specimen number, top of specimen depth, rock type (according to terminology adopted in WP10 – Golder 2022), specimen dimensions, mass, bulk density (as received), dry density, and water content for all laboratory specimens are shown in Table 3.

Table 3: Dimensions and Physical Properties of Lab Specimens

Sample ID	Depth (mbgs)[1]	Rock Type	Testing Campaign	Diameter (mm)	Length (mm)	L:D Ratio	Mass (g)	Bulk Density[2] (g/cm^3)	Dry Density (g/cm^3)	Water Content[2] (%)
IG_BH03_UC001	415.99	Biotite Granodiorite-tonalite	1	60.78	137.00	2.25	1062.20	2.67	2.67	0.18
IG_BH03_UC002	455.15	Biotite Granodiorite-tonalite	1	60.79	137.01	2.25	1064.25	2.68	2.67	0.17
IG_BH03_UC003	494.50	Biotite Granodiorite-tonalite	1	60.65	137.00	2.26	1057.80	2.67	2.67	0.13
IG_BH03_UC004	540.19	Biotite Granodiorite-tonalite	1	60.72	137.01	2.26	1060.86	2.67	2.67	0.15
IG_BH03_UC005	552.67	Amphibolite	1	60.83	137.01	2.25	1189.68	2.99	2.99	0.04
IG_BH03_UC006	582.55	Biotite Granodiorite-tonalite	1	60.77	137.00	2.25	1065.21	2.68	2.68	0.14
IG_BH03_UC007	662.59	Biotite Granodiorite-tonalite	1	60.79	137.00	2.25	1064.85	2.68	2.68	0.12
IG_BH03_BR001	416.20	Biotite Granodiorite-tonalite	1	60.83	40.01	0.66	310.09	2.67	2.66	0.15
IG_BH03_BR002	455.42	Biotite Granodiorite-tonalite	1	60.82	40.01	0.66	310.90	2.67	2.67	0.12
IG_BH03_BR003	494.73	Biotite Granodiorite-tonalite	1	60.67	40.01	0.66	308.93	2.67	2.67	0.10
IG_BH03_BR004	540.42	Biotite Granodiorite-tonalite	1	60.72	39.98	0.66	309.74	2.68	2.67	0.13
IG_BH03_BR005	551.80	Amphibolite	1	60.89	39.97	0.66	345.90	2.97	2.97	0.08
IG_BH03_BR006	582.82	Biotite Granodiorite-tonalite	1	60.78	40.00	0.66	310.77	2.68	2.67	0.13

Sample ID	Depth (mbgs)[1]	Rock Type	Testing Campaign	Diameter (mm)	Length (mm)	L:D Ratio	Mass (g)	Bulk Density[2] (g/cm^3)	Dry Density (g/cm^3)	Water Content[2] (%)
IG_BH03_BR007	662.81	Biotite Granodiorite-tonalite	1	60.80	40.00	0.66	311.33	2.68	2.68	0.08
IG_BH03_TH001[3,4,7]	304.71 304.75	Biotite Granodiorite-tonalite	1	60.92 60.92	37.19 37.99	N/A	288.23 294.35	2.66 2.66	2.65 2.65	0.16 0.17
IG_BH03_TH002[3,4,7]	358.94 358.98	Biotite Granodiorite-tonalite	1	61.03 61.03	39.13 33.55	N/A	303.87 270.64	2.65 2.76	2.65 2.76	0.05 0.06
IG_BH03_TH003[3,4,7]	416.43 416.47	Biotite Granodiorite-tonalite	1	60.94 60.93	37.64 37.00	N/A	291.57 286.38	2.66 2.65	2.65 2.65	0.11 0.11
IG_BH03_TH004[3,4,7]	454.06 454.10	Biotite Granodiorite-tonalite	1	60.84 60.86	36.64 37.19	N/A	282.62 287.26	2.65 2.66	2.65 2.65	0.12 0.13
IG_BH03_TH005[3,4,7]	495.01 495.05	Biotite Granodiorite-tonalite	1	60.81 60.80	38.02 36.87	N/A	293.45 284.72	2.66 2.66	2.65 2.66	0.14 0.13
IG_BH03_TH006[3,4,7]	539.12 539.16	Biotite Granodiorite-tonalite	1	60.86 60.74	36.96 37.27	N/A	285.99 288.44	2.66 2.67	2.66 2.67	0.14 0.15
IG_BH03_TH007[3,4,7]	548.19 548.23	Amphibolite	1	60.85 60.83	38.34 37.21	N/A	326.75 318.35	2.93 2.94	2.93 2.94	0.04 0.04
IG_BH03_TH008[3,4,7]	581.86 581.90	Biotite Granodiorite-tonalite	1	60.94 60.95	34.58 37.36	N/A	267.97 289.50	2.66 2.66	2.65 2.65	0.08 0.09
IG_BH03_TH009[3,4,7]	800.64 800.68	Biotite Granodiorite-tonalite	1	61.04 61.03	35.61 37.25	N/A	277.80 290.40	2.67 2.66	2.66 2.66	0.18 0.18
IG_BH03_TH011[4,6]	359.31 359.35	Biotite Granodiorite-tonalite	2	61.03 61.03	34.20 34.01	N/A	265.25[8] 264.43[8]	-	2.65 2.66	-
IG_BH03_TH014[4,6]	495.54 495.58	Biotite Granodiorite-tonalite	2	60.80 60.80	33.78 34.24	N/A	260.31[8] 263.59[8]	-	2.65 2.65	-
IG_BH03_TH016[4,6]	548.79 548.83	Amphibolite	2	60.86 60.89	35.43 36.20	N/A	304.42[8] 309.88[8]	-	2.95 2.94	-

Sample ID	Depth (mbgs)[1]	Rock Type	Testing Campaign	Diameter (mm)	Length (mm)	L:D Ratio	Mass (g)	Bulk Density[2] (g/cm³)	Dry Density (g/cm³)	Water Content[2] (%)
IG_BH03_TH017[4,6]	582.25 582.29	Biotite Granodiorite-tonalite	2	60.95 60.95	35.60 35.11	N/A	275.93[8] 272.28[8]	-	2.66 2.66	-
IG_BH03_TH018[4,6]	801.04 801.08	Biotite Granodiorite-tonalite	2	61.04 61.05	35.39 35.89	N/A	275.30[8] 279.02[8]	-	2.66 2.66	-
IG_BH03_TH001[3]	304.79	Biotite Granodiorite-tonalite	1	30.11	79.26	N/A	150.18	2.66	2.66	0.21
IG_BH03_TH002[3]	359.04	Biotite Granodiorite-tonalite	1	29.90	79.02	N/A	147.19	2.65	2.65	0.17
IG_BH03_TH003[3]	416.51	Biotite Granodiorite-tonalite	1	29.91	79.38	N/A	147.63	2.65	2.64	0.22
IG_BH03_TH004[3]	454.14	Biotite Granodiorite-tonalite	1	29.97	79.64	N/A	149.40	2.66	2.65	0.19
IG_BH03_TH005[3]	495.09	Biotite Granodiorite-tonalite	1	30.00	79.53	N/A	149.84	2.67	2.66	0.31
IG_BH03_TH006[3]	539.20	Biotite Granodiorite-tonalite	1	29.63	79.46	N/A	144.37	2.63	2.63	0.11
IG_BH03_TH007[3]		Amphibolite	1	Broken during preparation						
IG_BH03_TH008[3]	581.95	Biotite Granodiorite-tonalite	1	30.08	79.33	N/A	150.03	2.66	2.66	0.20
IG_BH03_TH009[3]	800.72	Biotite Granodiorite-tonalite	1	30.01	79.51	N/A	149.44	2.66	2.65	0.09
IG_BH03_TH010[5,6]	304.96	Biotite Granodiorite-tonalite	2	31.37	79.41	N/A	163.07	2.66	2.65	0.17
IG_BH03_TH011[5,6]	359.20	Biotite Granodiorite-tonalite	2	31.48	79.42	N/A	164.36	2.66	2.65	0.14

Sample ID	Depth (mbgs)[1]	Rock Type	Testing Campaign	Diameter (mm)	Length (mm)	L:D Ratio	Mass (g)	Bulk Density[2] (g/cm^3)	Dry Density (g/cm^3)	Water Content[2] (%)
IG_BH03_TH012[5,6]	416.93	Biotite Granodiorite-tonalite	2	31.53	79.28	N/A	164.59	2.66	2.65	0.17
IG_BH03_TH013[5,6]	454.64	Biotite Granodiorite-tonalite	2	31.20	79.28	N/A	161.31	2.66	2.66	0.22
IG_BH03_TH014[5,6]	495.43	Biotite Granodiorite-tonalite	2	31.38	79.20	N/A	162.59	2.66	2.65	0.17
IG_BH03_TH015[5,6]	538.74	Biotite Granodiorite-tonalite	2	31.15	79.27	N/A	161.03	2.67	2.66	0.18
IG_BH03_TH016[5,6]	548.68	Amphibolite	2	31.27	78.83	N/A	179.14	2.96	2.96	0.1
IG_BH03_TH017[5,6]	582.14	Biotite Granodiorite-tonalite	2	31.58	79.35	N/A	165.84	2.67	2.66	0.18
IG_BH03_TH018[5,6]	800.93	Biotite Granodiorite-tonalite	2	31.39	79.53	N/A	163.96	2.67	2.66	0.16

[1]Top depth of prepared sub-sample (depth along borehole)

[2]Water Content and Bulk Density represent as-received conditions for preserved samples and re-saturated conditions for unpreserved samples. For water content measurement, specimens were oven-dried in accordance with ASTM D2216-19.

[3]Preserved samples tested under as-received water content conditions. (. Wet mass reported. Bulk density represents wet density. Water content represents as-received water content.

[4]Samples for thermal diffusivity, thermal conductivity, and heat capacity (two disks).

[5]Samples for thermal expansion.

[6] Unpreserved samples. Samples were dried at 80°C before testing and at 110°C after testing.

[7] Samples were heated to about 295°C during testing (the data corresponding to 99°C to 295°C are not presented here).

[8] Dry mass reported.

3.2 Laboratory Testing Results

3.2.1 Geomechanical Results

Table 4 shows a summary of the average strength properties for the Biotite Granodiorite-Tonalite determined from the current testing program. Table 5 presents the results of the UCS testing. P and S wave velocities are shown in Table 6 along the derived dynamic elastic moduli.Table 7 presents the results of the Brazilian testing.

Table 4: Average strength properties and elastic moduli for Biotite Granodiorite-Tonalite in the borehole

Rock Type	UCS (MPa)	σ_{CI} (MPa)	σ_{CD} (MPa)	σ_T (MPa)	E_{40} (GPa)	ν_{40}
Average	231.2	92.2	174.5	11.2	71.9	0.180
Std. Dev.	4.76	3.73	6.45	1.05	2.79	0.032

The results of the six UCS tests on Biotite Granodiorite-Tonalite are very consistent and within the range of expected values. The average value for the UCS is 230 MPa (min = 226 MPa; max = 238 MPa). All specimens reached peak strength at an axial strain between 0.37% and 0.41%. Stress-strain graphs and photographs of intact and broken test specimens are shown in APPENDIX A.

Crack Damage (CD) and Crack Initiation (CI) thresholds, or stress levels, determined for all UCS tests carried out during the test program are shown in Table 5. Both crack initiation and crack damage thresholds (σ_{CI} and σ_{CD}) are well correlated with the UCS. Volumetric strain graphs were plotted against the axial stress, σ_1. These are presented in APPENDIX A, adjacent to stress-strain graphs and photographs of all intact and broken test specimens.

The following average relationships were obtained for the Biotite Granodiorite-Tonalite:

$$\sigma_{CI} = 0.40 \times UCS$$

$$\sigma_{CD} = 0.76 \times UCS$$

The results of the indirect tensile (Brazilian) strength tests on Biotite Tonalite are also quite consistent, with an average value for the tensile strength (σ_T) of 11.2 MPa. Load-time and stress-displacement graphs, and photographs of all intact and broken test specimens are shown in APPENDIX C. The relationship between the Brazilian tensile strength and the UCS is as follows:

$$\sigma_T = 0.049 \times UCS$$

The correlation observed between the Young's modulus (E_{40}) and the UCS, both expressed in MPa, is as follows:

$$E_{40} = 311 \times UCS$$

This relationship fits in well with the expected values for granitic rocks (Hoek and Diederichs, 2006). The estimates of elastic moduli from the bench top dynamic testing are about 20% lower than those obtained from the UCS testing. This can be explained by the fact that the samples are in a stress-free state and open micro cracks would yield slower velocities than under a compressed state.

Table 5: Strength and Strain properties determined from UCS tests

Sample ID	Depth (m)[1]	Date Tested	UCS (MPa)	Young's Modulus (GPa)	Poisson's ratio	Axial Strain @ peak (%)	Max. Vol. Strain (%)	Crack Initiation Threshold (MPa)	Crack Damage Threshold (MPa)	Description of Failure Mode[2]
IG_BH03_UC001	415.99	12/11/2019	226.5	70.4	0.133	0.398	0.102	-	176.2	Massive axial splitting
IG_BH03_UC002	455.15	13/11/2019	225.6	75.8	0.210	0.374	0.173	87.0	178.4	Multiple massive shear
IG_BH03_UC003	494.50	13/11/2019	238.0	75.0	0.163	0.404	0.198	96.7	180.3	Massive axial splitting
IG_BH03_UC004	540.19	13/11/2019	229.9	69.3	0.191	0.399	0.191	91.7	172.0	Axial splitting
IG_BH03_UC005	552.67	13/11/2019	214.3	87.8	0.171	0.303	0.138	83.5	185.1	Multiple fractures
IG_BH03_UC006	582.55	14/11/2019	233.1	71.3	0.169	0.408	0.201	94.6	177.5	Multiple massive shear
IG_BH03_UC007	662.59	14/11/2019	234.1	69.8	0.217	0.412	0.181	90.7	162.6	Massive axial splitting

[1]Top depth of prepared sub-sample (depth along borehole)

[2]Massive Failure indicates failure through intact rock

Table 6: Dynamic properties determined from UCS samples

Sample ID	Depth (m)[1]	Date Tested	P-wave Velocity (km/sec)	S-wave Velocity (km/sec)	Dynamic Young's Modulus (GPa)	Dynamic Shear Modulus (GPa)	Dynamic Poisson's ratio
IG_BH03_UC001	415.99	12/11/2019	4.84	2.95	55.9	23.2	0.206
IG_BH03_UC002	455.15	13/11/2019	5.13	3.14	63.3	26.3	0.202
IG_BH03_UC003	494.50	13/11/2019	4.74	2.90	53.9	22.4	0.202
IG_BH03_UC004	540.19	13/11/2019	4.74	2.90	53.9	22.4	0.202
IG_BH03_UC005	552.67	13/11/2019	6.20	3.56	94.9	37.8	0.254

Sample ID	Depth (m)[1]	Date Tested	P-wave Velocity (km/sec)	S-wave Velocity (km/sec)	Dynamic Young's Modulus (GPa)	Dynamic Shear Modulus (GPa)	Dynamic Poisson's ratio
IG_BH03_UC006	582.55	14/11/2019	4.91	2.97	57.3	23.7	0.211
IG_BH03_UC007	662.59	14/11/2019	4.68	2.92	53.9	22.9	0.180

[1]Top depth of prepared sub-sample (depth along borehole)

Table 7: Tensile strength determined from Brazilian tests

Sample ID	Depth (m)[1]	Date Tested	Failure Load (kN)	Tensile Strength (MPa)	Description of Failure Mode
IG_BH03_BR001	416.20	18/11/2019	42.377	11.1	Diametral (central) splitting
IG_BH03_BR002	455.42	18/11/2019	48.266	12.6	Diametral (central) splitting
IG_BH03_BR003	494.73	18/11/2019	35.878	9.4	Diametral (central) splitting
IG_BH03_BR004	540.42	18/11/2019	44.738	11.7	Diametral (central) splitting
IG_BH03_BR005	551.80	18/11/2019	60.219	15.8	Diametral (central) splitting
IG_BH03_BR006	582.82	18/11/2019	42.642	11.2	Diametral (central) splitting
IG_BH03_BR007	662.81	18/11/2019	42.834	11.2	Diametral (central) splitting

[1]Top depth of prepared sub-sample (depth along borehole)

3.2.2 Thermal Results

Table 8 shows a summary of the average thermal properties between room temperature and 90°C or 100°C for each sample measured in the Hot Disk ThermTest TPS 1500, determined from all testing programs. Data for the individual tests and the full range of temperatures are included in APPENDIX D. Figure 5 through Figure 16Figure show plots of the results for the samples grouped by Biotite Granodiorite-Tonalite and Amphibolite. Results from the Hot Disk ThermTest TPS 1500 tests are within the ranges expected for the tested rock types and follow the expected trends with temperature (Robertson, 1988).

Table 8: Thermal properties determined from the Hot Disk ThermTest TPS 1500

Sample ID	Depth (m)[1]	Date Tested	Average Temperature (°C)	Average Volumetric Heat Capacity (MJ/m³°K)	Average Thermal Conductivity (W/m°K)	Average Thermal Diffusivity (mm²/sec)
IG_BH03_TH001[2]	304.71	23/01/2020 to 27/01/2020	26.70	2.13	3.49	1.64
			40.17	2.29	3.45	1.51
			69.78	2.68	3.31	1.24
			99.37	2.68	3.18	1.18
IG_BH03_TH002[2]	358.94	17/01/2020 to 20/01/2020	26.37	1.91	3.02	1.58
			40.17	1.98	3.00	1.52
			69.76	2.17	3.01	1.39
			99.37	2.27	2.96	1.30
IG_BH03_TH003[2]	416.43	15/01/2020 to 16/01/2020	26.37	1.77	2.83	1.60
			40.15	1.86	2.82	1.52
			69.75	2.02	2.82	1.39
			99.35	2.16	2.79	1.29
IG_BH03_TH004[2]	454.06	07/01/2020 to 08/01/2020	26.36	2.13	3.25	1.52
			40.16	2.22	3.23	1.46
			69.77	2.34	3.17	1.35
			99.38	2.49	3.08	1.24
IG_BH03_TH005[2]	495.01	28/01/2020 to 29/01/2020	26.36	2.27	3.39	1.50
			40.17	2.29	3.28	1.43
			69.77	2.60	3.13	1.21
			99.36	2.57	3.04	1.18
IG_BH03_TH006[2]	539.12	21/01/2020 to 22/01/2020	26.44	2.49	3.70	1.48
			40.17	2.55	3.59	1.41
			69.77	2.78	3.45	1.24
			99.36	2.77	3.30	1.19
IG_BH03_TH007[2]	548.19	09/01/2020	26.20	2.43	2.78	1.14

Sample ID	Depth (m)[1]	Date Tested	Average Temperature (°C)	Average Volumetric Heat Capacity (MJ/m³°K)	Average Thermal Conductivity (W/m°K)	Average Thermal Diffusivity (mm²/sec)
		to 10/01/2020	40.19	2.50	2.77	1.11
			69.78	2.73	2.78	1.02
			99.37	2.90	2.76	0.95
IG_BH03_TH008[2]	581.86	13/01/2020 to 14/01/2020	26.39	1.70	2.95	1.73
			40.17	1.78	2.93	1.65
			69.76	1.96	2.92	1.49
			99.38	2.04	2.89	1.41
IG_BH03_TH009[2]	800.64	30/01/2020 to 31/01/2020	26.38	1.92	3.04	1.59
			40.16	1.98	2.95	1.49
			69.76	2.16	2.85	1.32
			99.36	2.26	2.71	1.20
IG_BH03_TH011[3]	359.31	26/05/2021	20.00	2.05	3.38	1.65
			40.00	2.13	3.31	1.56
			60.06	2.26	3.29	1.46
			79.94	2.33	3.24	1.39
			90.04	2.36	3.21	1.36
			60.05[4]	2.21	3.28	1.49
IG_BH03_TH014[3]	495.54	27/05/2021	20.00	2.10	3.16	1.50
			40.01	2.14	3.11	1.45
			60.05	2.26	3.10	1.37
			79.96	2.34	3.06	1.31
			90.05	2.40	3.04	1.27
			60.03[4]	2.27	3.08	1.36
IG_BH03_TH016[3]	548.79	01/06/2021	20.00	2.49	2.76	1.11
			40.00	2.62	2.75	1.05
			60.04	2.81	2.74	0.98
			79.94	2.82	2.73	0.97
			90.04	2.99	2.71	0.91
			60.04[4]	2.76	2.75	1.00
IG_BH03_TH017[3]	582.25	02/06/2021	20.00	2.31	3.56	1.54
			39.99	2.39	3.50	1.47
			60.04	2.53	3.45	1.37

Sample ID	Depth (m)[1]	Date Tested	Average Temperature (°C)	Average Volumetric Heat Capacity ($MJ/m^3 °K$)	Average Thermal Conductivity (W/m°K)	Average Thermal Diffusivity (mm^2/sec)
			79.93	2.59	3.40	1.31
			90.03	2.59	3.36	1.30
			60.03[4]	2.47	3.46	1.40
IG_BH03_TH018[3]	801.04	03/06/2021	20.00	2.15	3.11	1.45
			40.00	2.27	3.06	1.35
			60.05	2.32	3.05	1.32
			79.92	2.43	3.01	1.24
			90.03	2.46	2.99	1.22
			60.05[4]	2.34	3.05	1.31

[1]Top depth of prepared top sub-sample (depth along borehole)

[2]Preserved samples. Samples were tested under as-received water content conditions. Test temperature reached 295°C (the data corresponding to 99°C to 295°C are not presented here)

[3]Unpreserved samples. Samples were dried at 80°C before testing

[4]Measurement to check hysteresis taken at 60°C while cooling; not used for the curve fitting of individual tests.

In general, it is observed that:

- The Volumetric Heat Capacity (C_v) data show that the values increase with an increase in temperature but not in a purely linear manner. There appears to be a slightly decreasing rate of change in C_v with increasing temperature, but the data can be described reasonably using a simple linear regression plot.
- The Thermal Conductivity (k) data shows that the values decrease with an increase in temperature, also not in a purely linear fashion. For the purpose of predicting thermal behaviour a linear fit, which provides a reasonable approximation, can be used for this temperature range.
- The Thermal Diffusivity (κ) shows that the values decrease with an increase in temperature, which is a result of a combination of the trends in the conductivity and heat capacity. A linear fit, which provides a reasonable approximation for this temperature range, can be used.

Best fits for the measurements grouped by rock type included measurement at 60°C while cooling.

Specifically for the Biotite Granodiorite-Tonalite rock:

The Volumetric Heat Capacity (C_v) data collected for 8 water-saturated and 4 dry specimens all show that C_v values increase with an increase in temperature (θ) but not in a purely linear manner (Figure 5 and Figure 6), There appears to be a slightly decreasing rate of change in C_v with increasing temperature, but the data can be described reasonably using a simple linear regression plot. Tests completed on preserved samples containing as-received water content shown in Figure 5 show very consistent C_v versus temperature results and can be described to within approximately 20% by a single regression line. The data for dry specimens was essentially identical to that obtained for the preserved specimens, but with a tighter distribution (within 10% of the regression line).

The Thermal Conductivity (k) data for the eight preserved specimens (Figure 7) shows that the values decrease with an increase in temperature, also not in a purely linear fashion. Dry specimens show a similar trend and exhibit slightly higher k values than observed for preserved materials (Figure 8) but have a tighter distribution. For the purpose of predicting thermal behaviour a linear fit, which provides a reasonable approximation, is provided in the graphs.

The Thermal Diffusivity (κ) for Biotite Tonalite rock is a parameter measured concurrent with the conductivity and heat capacity data presented in Figure 5 through Figure 8. The κ values show a decrease with an increase in temperature, which is a result of a combination of the trends in the conductivity and heat capacity. A linear fit is shown in the graphs, which provides a reasonable approximation for this temperature range.

Note that the sample depths in the graph legends refer to the depth of the original sample as collected (part of the id), not the depth of the sub-samples.

A summary of the equations describing Cv, k and κ are provided in Table 9.

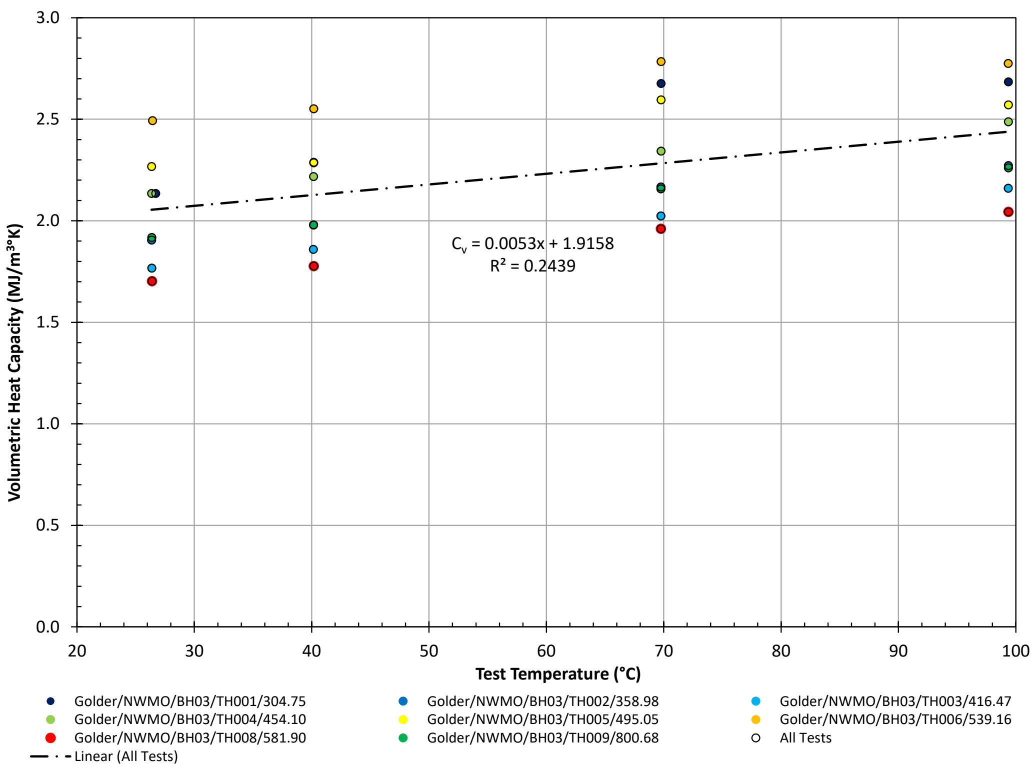

Figure 5: Volumetric heat capacity for preserved samples of Biotite Granodiorite-Tonalite under as-received water content conditions as a function of temperature.

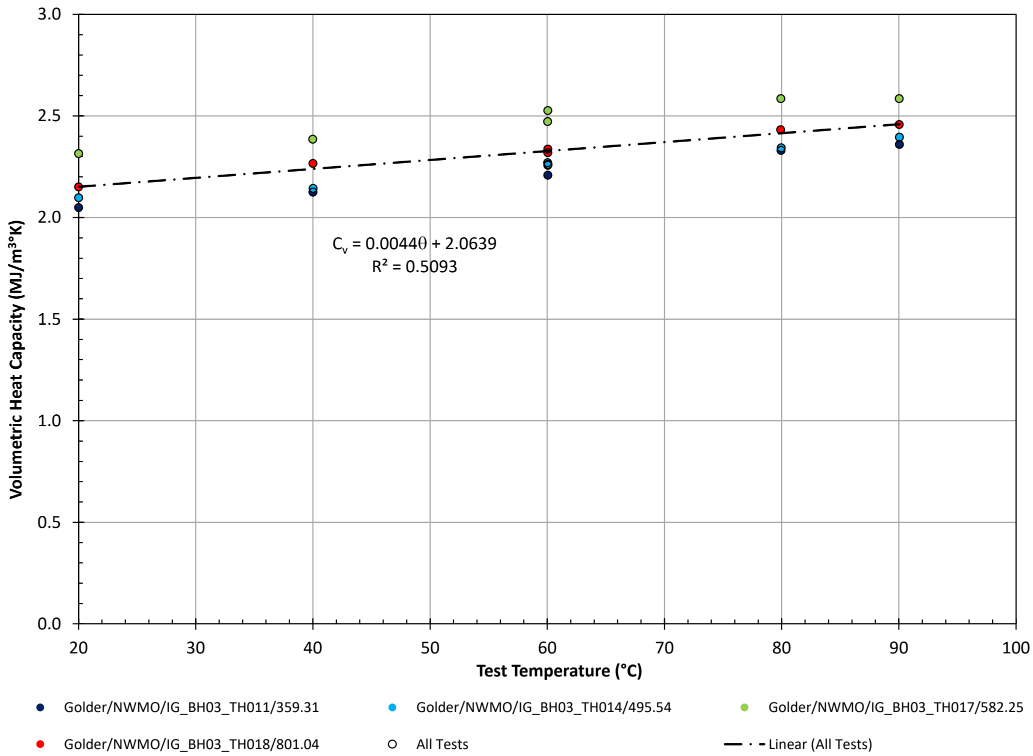

Figure 6: Volumetric heat capacity for dry samples of Biotite Granodiorite-Tonalite as a function of temperature.

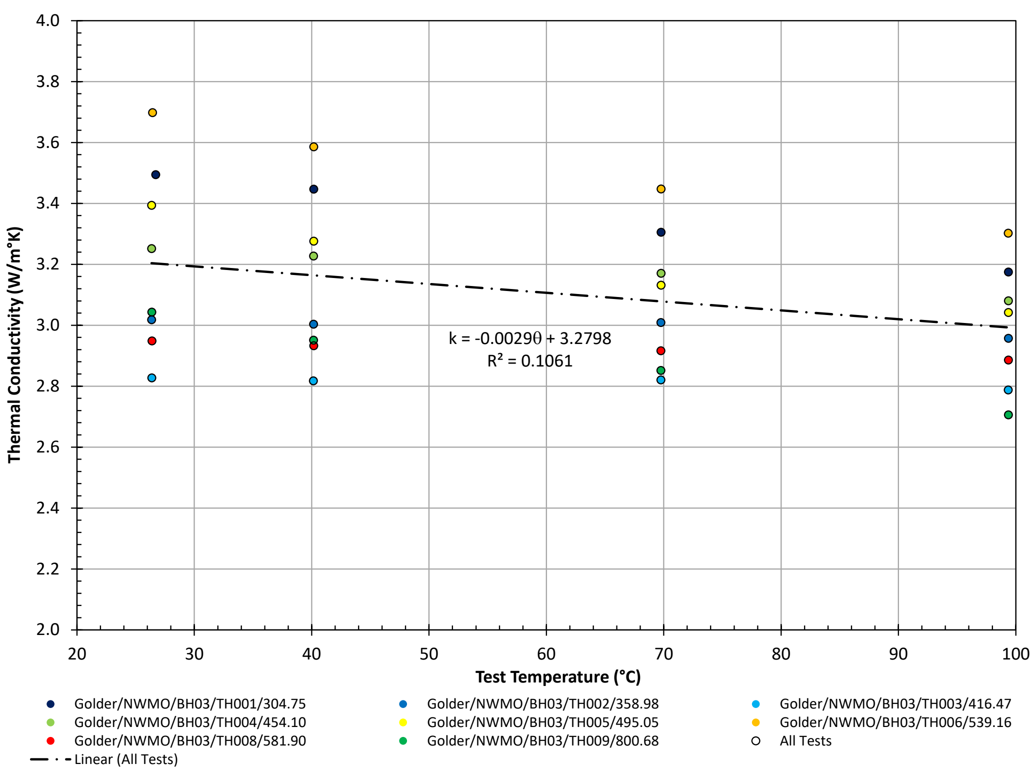

Figure 7: Thermal conductivity for preserved samples of Biotite Granodiorite-Tonalite under as-received water content conditions as a function of temperature

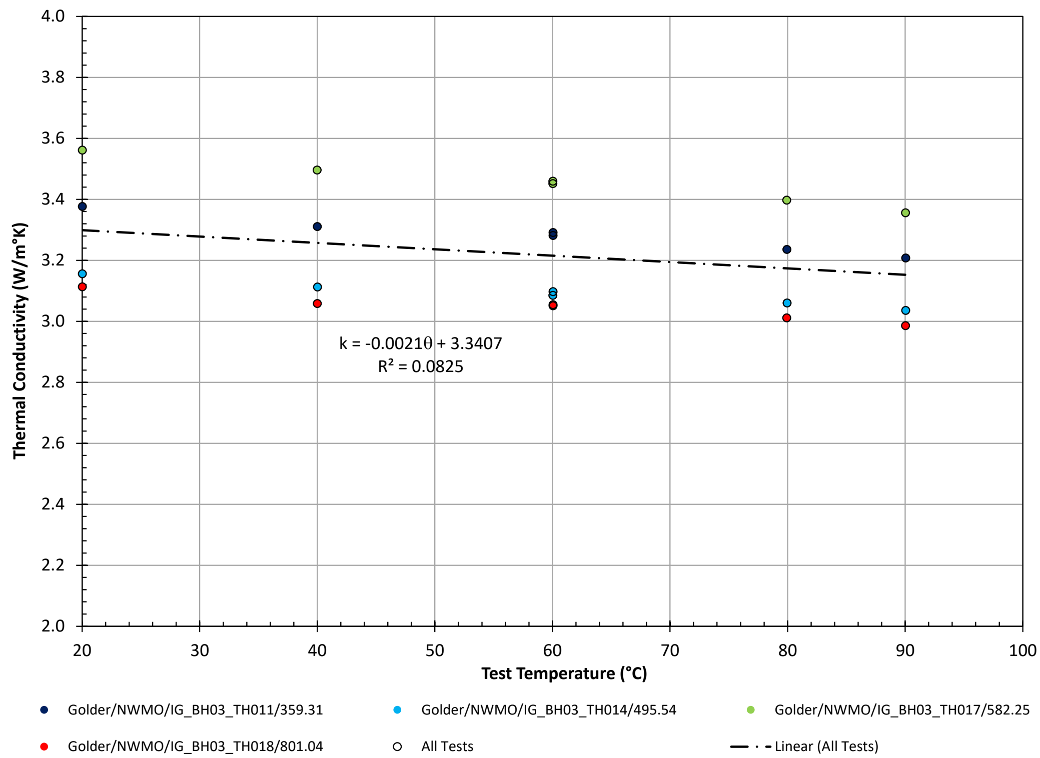

Figure 8: Thermal conductivity for dry samples of Biotite Granodiorite-Tonalite as a function of temperature

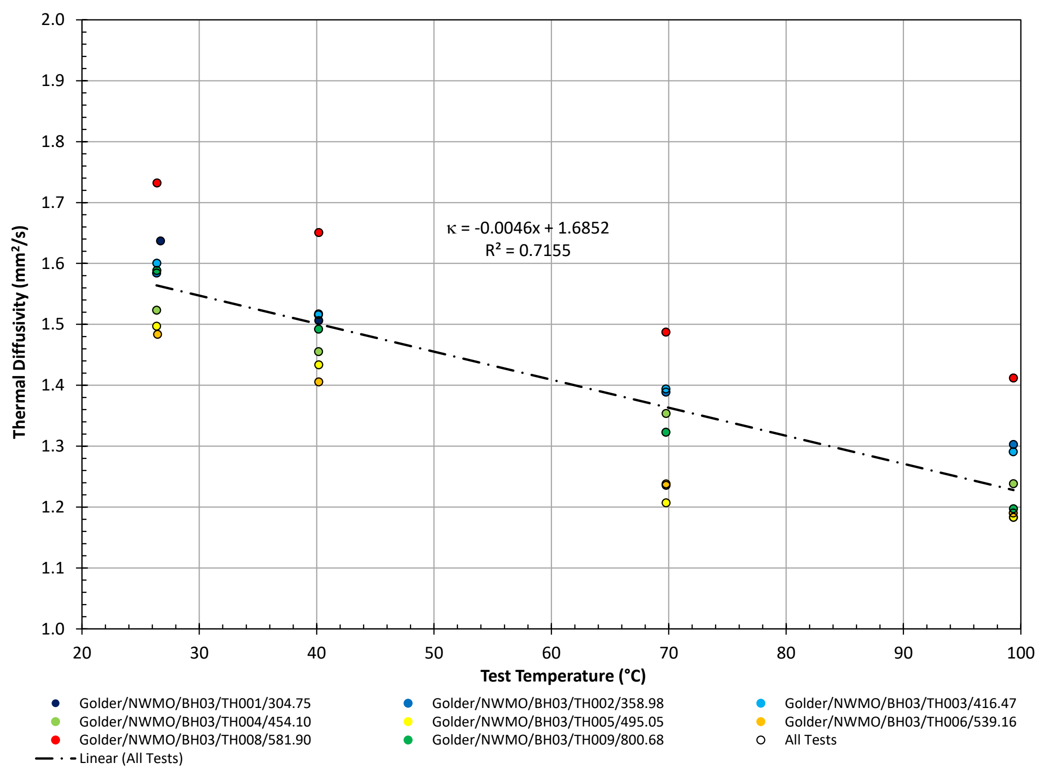

Figure 9: Thermal diffusivity for preserved samples of Biotite Granodiorite-Tonalite under as-received water content conditions as a function of temperature

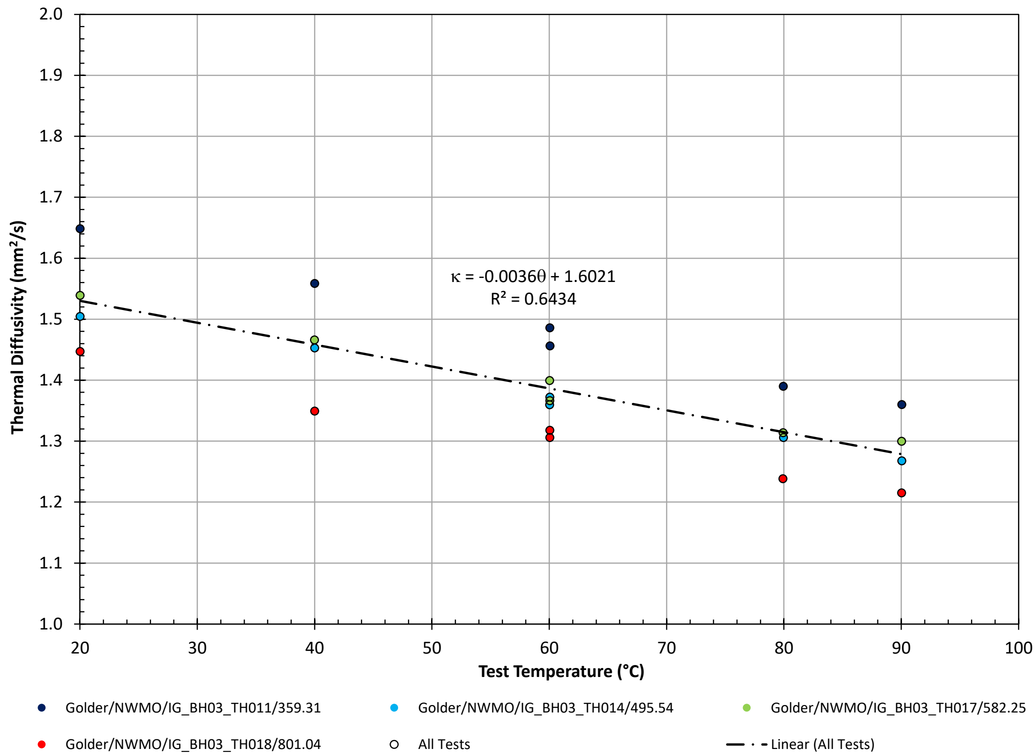

Figure 10: Thermal diffusivity for dry samples of Biotite Granodiorite-Tonalite as a function of temperature

Specifically for Amphibolite

The rock termed Amphibolite is described in the WP3 Data Report – Geological and Geotechnical Core Logging, Photography and Sampling for IG_BH03 (Golder, 2018). One preserved and one dry sample of the Amphibolite rock were tested to determine the thermal properties of this material.

The Volumetric Heat Capacity (C_v) of the preserved and dry samples are presented in Figure 11 and Figure 12, respectively.

The Thermal Conductivity (λ) of the preserved and dry samples are presented in Figure 13 and Figure 14, respectively.

The Thermal Diffusivity (κ) of the preserved and dry samples are presented in Figure 15 and Figure 16, respectively.

Note that the sample depths in the graph legends refer to the depth of the original sample as collected (part of the id), not the depth of the sub-samples.

The equations describing the thermal properties of the Amphibolite are summarized in Table 9.

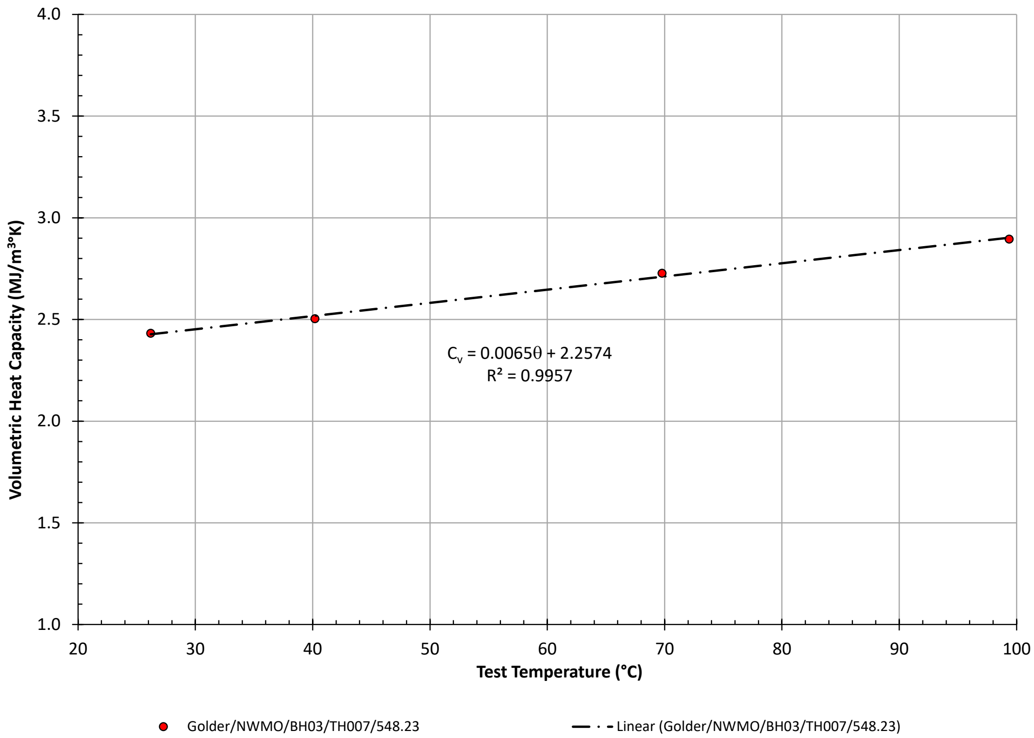

Figure 11: Volumetric heat capacity for preserved sample of Amphibolite as a function of temperature

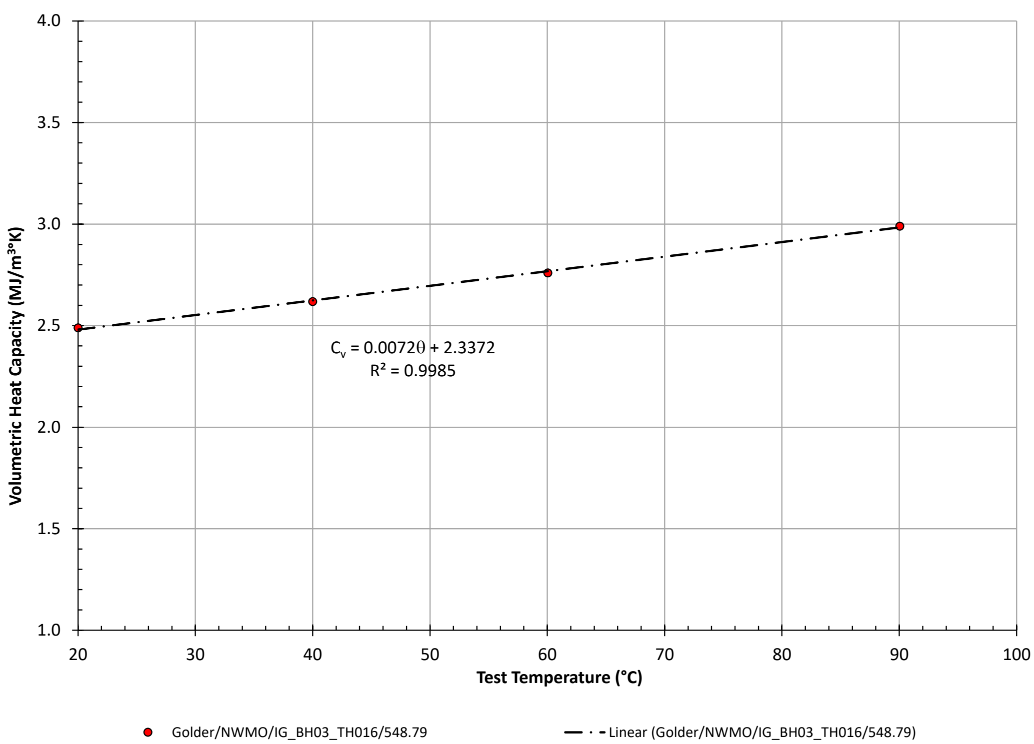

Figure 12: Volumetric heat capacity for dry sample of Amphibolite as a function of temperature

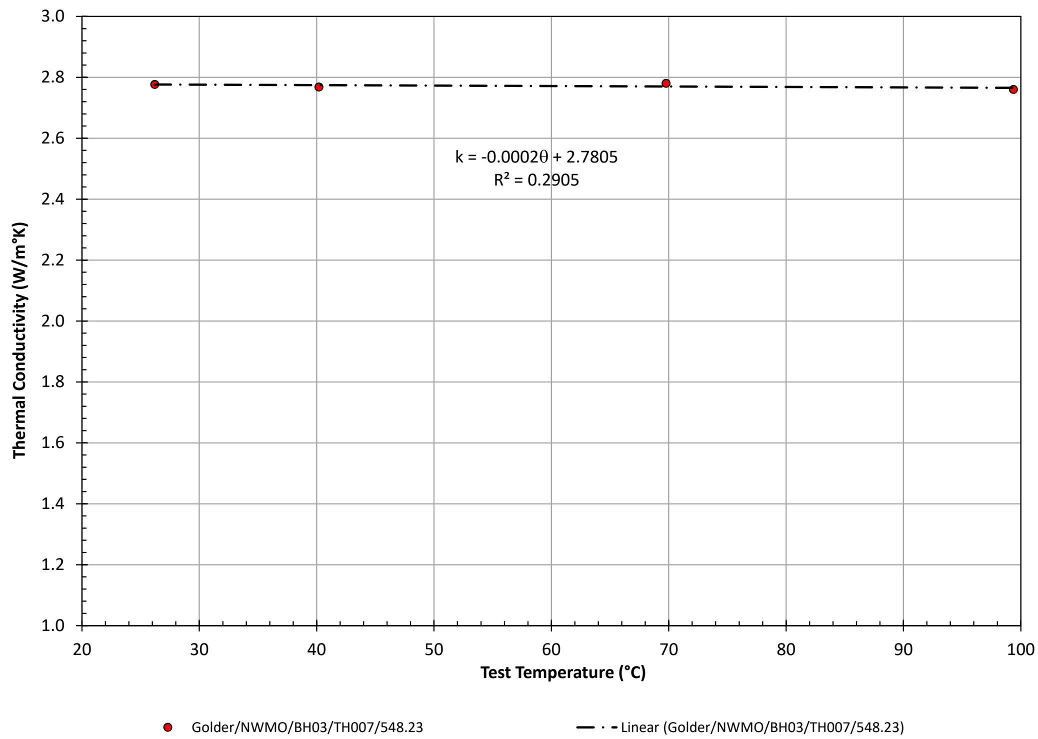

Figure 13: Thermal conductivity for preserved sample of Amphibolite as a function of temperature

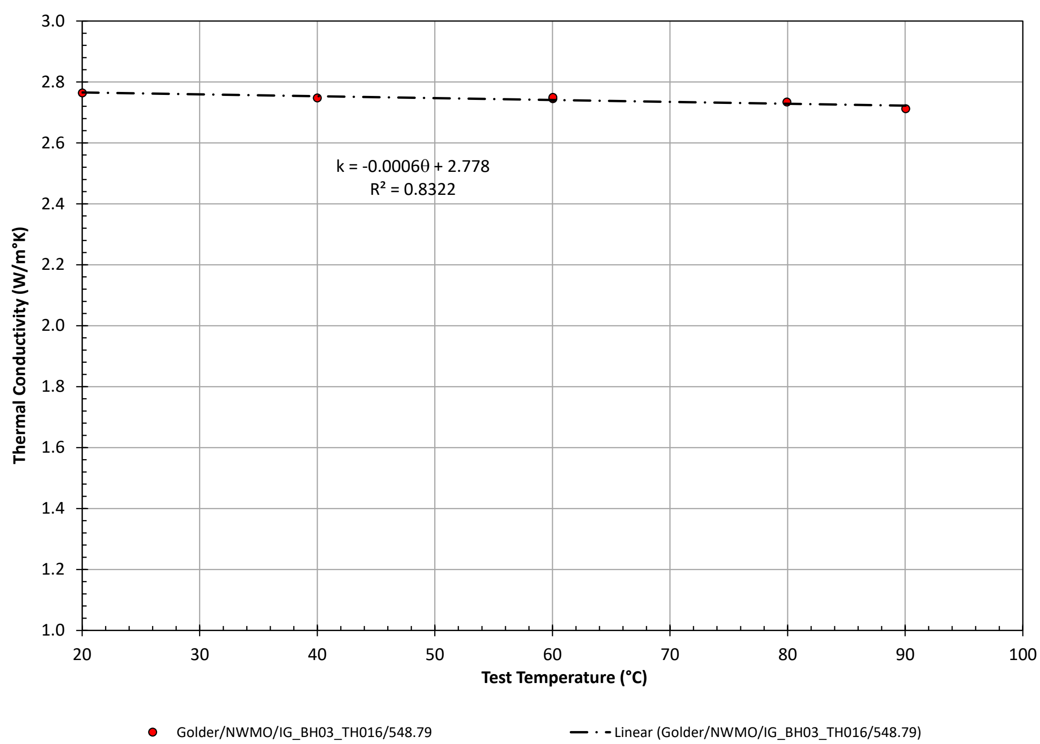

Figure 14: Thermal conductivity for dry sample of Amphibolite as a function of temperature

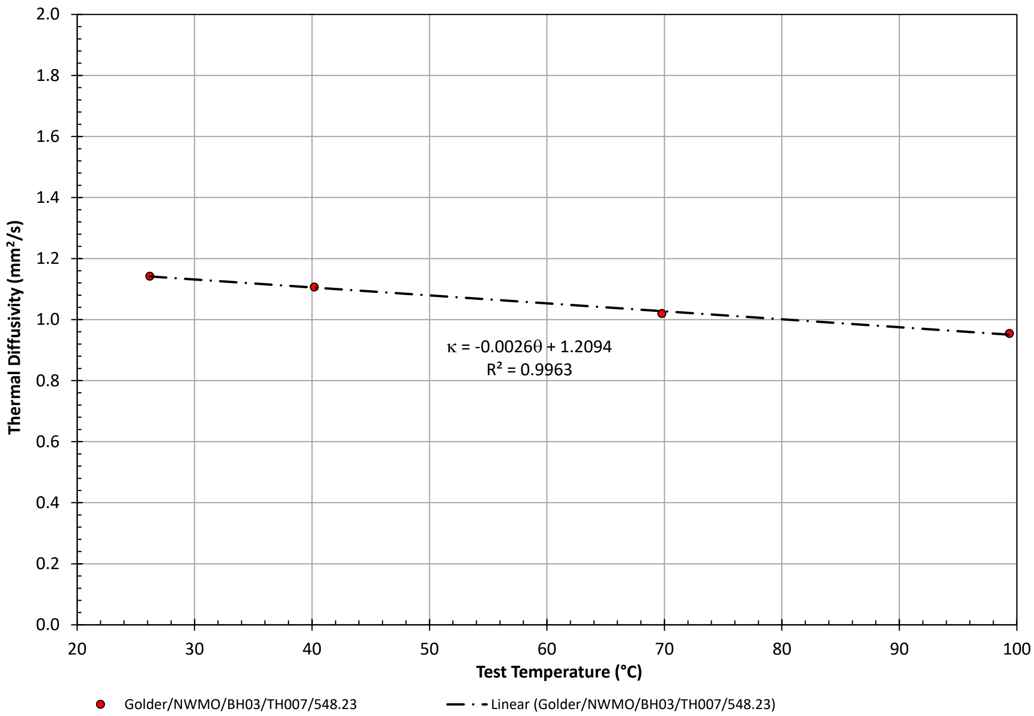

Figure 15: Thermal diffusivity for preserved sample of Amphibolite as a function of temperature

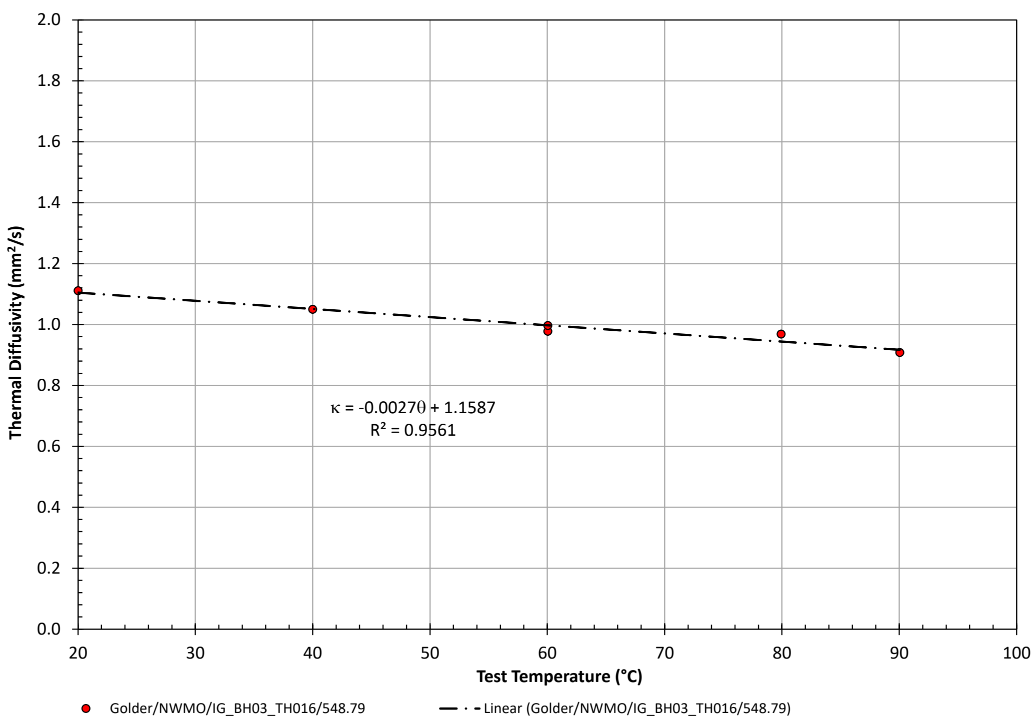

Figure 16: Thermal diffusivity for dry sample of Amphibolite as a function of temperature

The equations describing volumetric heat capacity, thermal conductivity and thermal diffusivity as a function of temperature for different rock types and for wet and dry conditions are provided in Table 9.

Table 9: Summary of equations describing thermal properties Cv, k and κ as a function of temperature for the range ~20°C to 100°C

Rock Type	No. of Samples	C_v (wet) [MJ/(m^3.°K)]	C_v (dry) [MJ/(m^3.°K)]	k (wet) [W/(m.°K)]	k (dry) [W/(m.°K)]	κ (wet) [mm^2/sec]	κ (dry) [mm^2/sec]
Biotite Granodiorite-Tonalite	8(wet)/4(dry)	$C_v = 0.0053\,\theta + 1.93$	$C_v = 0.0044\,\theta + 2.06$	$k = -0.0029\,\theta + 3.28$	$k = -0.0021\,\theta + 3.34$	$\kappa = -0.0045\,\theta + 1.68$	$\kappa = -0.0036\,\theta + 1.60$
Amphibolite	1(wet)/1(dry)	$C_v = 0.0065\,\theta + 2.26$	$C_v = 0.0072\,\theta + 2.34$	$k = -0.0002\,\theta + 2.78$	$k = -0.0006\,\theta + 2.78$	$\kappa = -0.0026\,\theta + 1.21$	$\kappa = -0.0027\,\theta + 1.16$

θ – temperature in °C

Coefficient of linear thermal expansion

Table 10 shows a summary of the coefficient of linear thermal expansion between room temperature and 90°C for each sample measured in the Unitherm 1054L dilatometer, determined from Campaign 2 testing program. The coefficient of linear thermal expansion was calculated from thermal strain vs temperature data points by two methods: 1) as the slope of the linear regression line through the data points and 2) fitting a second order polynomial to the same data and deriving the slope of the polynomial at the target temperatures. Determining coefficient of linear thermal expansion from the linear regression (α_L) seems sufficient given the near linear trend of the data points for the tested temperature range (Table 10). However, the temperature-dependent coefficients of linear thermal expansion ($\alpha_L(\theta)$) were also determined from approach 2 and are summarized in Table 10. Data for the individual tests are included in APPENDIX E. Figure 17 shows plots of the variation of the coefficient of linear thermal expansion, from quadratic fit, with temperature for the re-saturated samples of Biotite Granodiorite-Tonalite and Amphibolite. Results from the Unitherm 1054L dilatometer tests are within the ranges for the tested rock types and follow the expected trends with temperature. The average α_L values as well as the equations describing the coefficient of linear thermal expansion versus temperature ($\alpha_L(\theta)$) are provided for the first and second heating cycles, by rock type, in Table 11.

Table 10: Coefficient of linear thermal expansion determined from the first and second heating cycles and as a function of temperature (from quadratic fit) for the first heating cycle

Sample ID	Depth (m)[1]	Date Tested	Linear fit (range: 20°C - 90°C)		Quadratic fit (range: 20°C - 90°C)	
			α_L (1st heating cycle) (1/°K)	α_L (2nd heating cycle) (1/°K)	Temperature (°C)	$\alpha_L(\theta)$ (1st heating cycle) [1/°K] (1/°K)
IG_BH03_TH010[2]	304.96	01/06/2021 to 04/06/2021	7.96E-06	7.63E-06	20	5.92E-06
					40	7.05E-06
					60	8.18E-06
					80	9.31E-06
					90	9.87E-06
IG_BH03_TH011[2]	359.20	01/06/2021 to 04/06/2021	7.10E-06	7.00E-06	20	5.37E-06
					40	6.33E-06
					60	7.28E-06
					80	8.24E-06
					90	8.72E-06
IG_BH03_TH012[2]	416.93	06/06/2021 to 09/06/2021	7.81E-06	7.64E-06	20	5.80E-06
					40	6.92E-06
					60	8.04E-06
					80	9.16E-06
					90	9.72E-06
IG_BH03_TH013[2]	454.64	06/06/2021	7.54E-06	7.62E-06	20	5.80E-06

Sample ID	Depth (m)[1]	Date Tested	Linear fit (range: 20°C - 90°C)		Quadratic fit (range: 20°C - 90°C)	
			α_L (1st heating cycle) (1/°K)	α_L (2nd heating cycle) (1/°K)	Temperature (°C)	$\alpha_L(\theta)$ (1st heating cycle) [1/°K] (1/°K)
		to 09/06/2021			40	6.77E-06
					60	7.74E-06
					80	8.70E-06
					90	9.18E-06
IG_BH03_TH014[2]	495.43	10/06/2021 to 13/06/2021	6.13E-06	5.99E-06	20	4.21E-06
					40	5.27E-06
					60	6.33E-06
					80	7.39E-06
					90	7.92E-06
IG_BH03_TH015[2]	538.74	10/06/2021 to 13/06/2021	7.31E-06	7.31E-06	20	5.32E-06
					40	6.42E-06
					60	7.52E-06
					80	8.61E-06
					90	9.16E-06
IG_BH03_TH016[2]	548.68	14/06/2021 to 17/06/2021	7.40E-06	8.17E-06	20	6.51E-06
					40	7.00E-06
					60	7.48E-06
					80	7.97E-06
					90	8.21E-06
IG_BH03_TH017[2]	582.14	14/06/2021 to 17/06/2021	8.04E-06	7.95E-06	20	6.35E-06
					40	7.27E-06
					60	8.20E-06
					80	9.12E-06
					90	9.59E-06
IG_BH03_TH018[2]	800.93	18/06/2021 to 21/06/2021	6.47E-06	6.50E-06	20	5.59E-06
					40	6.07E-06
					60	6.55E-06
					80	7.03E-06
					90	7.27E-06

[1]Top depth of prepared sub-sample

[2]Unpreserved samples. Samples were saturated before testing.

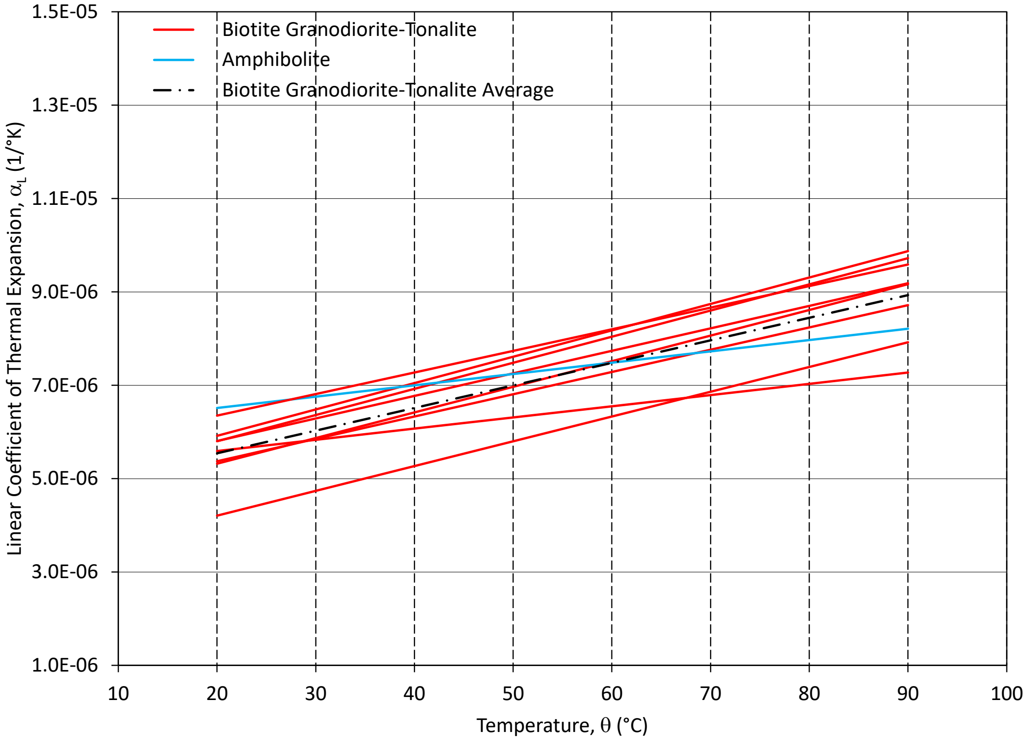

Figure 17: Coefficient of linear thermal expansion, from quadratic fit, as a function of temperature for eight (8) re-saturated samples of Biotite Granodiorite-Tonalite along with the average values as well as the data of one (1) re-saturated sample of Amphibolite

Table 11: Summary of the coefficient of linear thermal expansion, α, average and as a function of temperature for the range ~20°C to 90°C

Rock Type	Average α_L (1st heating cycle) [1/°K]	$\alpha_L(\theta)$ (1st cycle) [1/°K]	α_L (2nd cycle) [1/°K]	$\alpha_L(\theta)$ (2nd cycle) [1/°K]
Biotite Granodiorite-Tonalite	7.30E-06	α_L = 4.84E-08 θ + 4.58E-06	7.22E-06	α_L = 2.96E-08 θ + 5.54E-06
Amphibolite	7.40E-06	α_L = 2.42E-08 θ + 6.03E-06	8.17E-06	α_L = 9.53E-09 θ + 7.63E-06

θ – temperature in °C

4.0 DATA QUALITY

All samples sent to the CANMET laboratory were accounted for and raw testing data were sent back in digital format. The results were checked against expected values and were deemed reasonable. In addition, ratios of moduli to UCS and tensile strength to UCS were within the expected ranges for this rock type. Photographs of the samples before and after testing were also delivered (APPENDIX A). The failure mode is used to determine when the UCS values are representative of the intact rock strength.

The water content for the Brazilian samples is noticeably higher than for the UCS samples. It is conceivable that for rocks with very low and poorly connected porosity, such as the Biotite Tonalite, the drying process will only eliminate surface or near-surface water and the results are affected by the surface area to volume ratios. The surface area to volume ratio for the Brazilian samples is higher than that for the UCS samples, thus resulting in higher water content measurements.

All samples sent to the RESPEC laboratory were accounted for and raw testing data were sent back in digital format. The results were checked against expected values and were deemed reasonable. The Biotite Tonalite saturated samples seem to have a slightly lower thermal conductivity than the dry samples, although there is some overlap between the two sets of data. The volumetric heat capacity does not seem to be affected by the degree of saturation, although it should be noted that the porosities of all tested rocks are very low.

4.1 Uncertainties and Limitations

At this point in the program, the number of samples tested is limited. Although the results of the UCS tests and the Brazilian tests for Biotite Tonalite were very consistent, the sample population is too small to establish statistical data and confidence limits. The number of samples for the other rock types encountered in the borehole is even more limited than that of the Biotite Tonalite. As the program evolves and data from all boreholes becomes available, statistical analyses of the data will provide more information on the degree of confidence.

In the measurement of water content, the samples were weighed before testing and placed in the oven after completion of the test to start the drying process. It has been observed that because of the destructive nature of the UCS and Brazilian tests, some of the sample material may have been lost during testing. Due to the lower porosity of the tonalite, any loss, however small, can have a significant effect in the determination of the water content and dry density.

In this report, the interpretation of Crack Initiation (CI) and Crack Damage (CD) stresses have been based on the maximum crack volumetric strain and the volumetric strain reversal, respectively. A better reported method of interpreting the crack initiation is to follow the Tangent Lateral Stiffness method (Ghazvinian et al., 2012), which considers the same raw data but amplifies the change in lateral strain making identification of systematic diversion more defined. It is recommended this method be used in future work.

Crack damage (CD) is defined as the onset of significant and sustained deviation from linear axial stress vs axial strain behaviour preceding sample failure (Diederichs et al 2004). Volumetric strain reversal may or may not correspond to CD in uniaxial conditions depending on the internal damage mechanisms; therefore, it is recommended that the deviation from the linear section of the stress strain curve be determined by plotting the tangent modulus (slope of the stress strain curve) to identify the onset of the deviation. Alternatively, similarly to the method to determine CI, the Tangent Axial Stiffness can be used to interpret CD. It is recommended that one of these two methods be used in future work.

The number of samples in the thermal testing program are also limited at this time. Samples of Biotite Tonalite were grouped to establish preliminary trends with temperature, while the other rock types were reported by individual tests. As the program evolves and data from all boreholes becomes available, statistical analyses of the data will provide more information on the degree of confidence.

5.0 REFERENCES

ASTM D4543-08, 2008. Standard Practices for Preparing Rock Core as Cylindrical Test Specimens and Verifying Conformance to Dimensional and Shape Tolerances

ASTM D4543-19, 2019. Standard Practices for Preparing Rock Core as Cylindrical Test Specimens and Verifying Conformance to Dimensional and Shape Tolerances

ASTM D2216-10, 2010. Standard Test Methods for Laboratory Determination of Water (Moisture) Content of Soil and Rock by Mass

ASTM D2216-19, 2019. Standard Test Methods for Laboratory Determination of Water (Moisture) Content of Soil and Rock by Mass

ASTM D7263-09 (2018)$^{\varepsilon2}$, 2018. Laboratory Determination of Density (Unit Weight) of Soil Specimens

ASTM D7012-14$^{\varepsilon1}$, 2014. Standard Test Methods for Compressive Strength and Elastic Moduli of Intact Rock Core Specimens under Varying States of Stress and Temperatures

ASTM D3967-16, 2016. Standard Test Method for Splitting Tensile Strength of Intact Rock Core Specimens

ASTM D4535-13$^{\varepsilon1}$ Standard Test Methods for Measurement of Thermal Expansion of Rock Using Dilatometer

ASTM D4535-13$^{\varepsilon2}$ Standard Test Methods for Measurement of Thermal Expansion of Rock Using Dilatometer

ASTM D6026-21 Standard Practice for Using Significant Digits in Geotechnical Data

ASTM D2845-08 Standard Test Method for Laboratory Determination of Pulse Velocities and Ultrasonic Elastic Constants of Rock

Blackburn, C.E. and Hinz, P., 1996. Gold and base metal potential of the northwest part of the Raleigh Lake greenstone belt, northwestern Ontario-Kenora Resident Geologist's District; in Summary of Field Work and Other Activities 1996, Ontario Geological Survey, Miscellaneous Paper 166, p.113-115.

DesRoches, A., Sykes, M., Parmenter, A. and Sykes, E., 2018. Lineament Interpretation of the Revell Batholith and Surrounding Greenstone Belts (Nuclear Waste Management Organization. No. NWMO-TR-2018-19).

Diederichs, M.S., Kaiser, P.K., Eberhardt, E., 2004. Damage initiation and propagation in hard rock during tunnelling and the influence of near-face stress rotation. Int. J. Rock Mech. Min. Sci. 41, 785–812.

Ghazvinian, E., Diederichs, M. and Martin, C.D., 2012. Identification of crack damage thresholds in crystalline rock. Proceedings of the Eurock 2012 International Symposium, Stockholm (Sweden), May 2012, Taylor & Francis Group: 14 p.

Golder (Golder Associates Ltd.), 2018. Phase 2 Initial Borehole Drilling and Testing, Ignace Area - Initial Borehole Characterization Plan for IG_BH03.

Golder and PGW (Paterson Grant and Watson Ltd.), 2017. Phase 2 Geoscientific Preliminary Assessment, Geological Mapping, Township of Ignace and Area, Ontario: APM-REP-01332-0225.

Golder, 2022. WP10 – Phase 2 Initial Borehole Drilling and Testing, Ignace Area - Rock Mass Classification for IG_BH03

Hoek., E. and Diederichs, M.S, 2006. Empirical estimation of rock mass modulus. Int. J. Rock Mech. Min. Sci. 43, 203–215.

ISO 22007-2:2015 (E) Plastics – Determination of thermal conductivity and thermal diffusivity, Part 2: Transient plane heat source (hot disc) method

Robertson, E. C., 1988. Thermal Properties of Rocks, U. S. Geological Survey Open-File Report 88-441, 106 p.

SGL (Sander Geophysics Limited), 2015. Phase 2 Geoscientific Preliminary Assessment, Acquisition, Processing and Interpretation of High-Resolution Airborne Geophysical Data, Township of Ignace, Ontario. Prepared for Nuclear Waste Management Organization (NWMO). NWMO Report Number: APM-REP-06145-0002.

SRK (SRK Consulting, Inc.) and Golder, 2015. Phase 2 Geoscientific Preliminary Assessment, Observation of General Geological Features, Township of Ignace, Ontario. Prepared for Nuclear Waste Management Organization. NWMO Report Number: APM-REP-06145-0004.

Stone, D., 2009. Geology of the Bending Lake Area, Northwestern Ontario; *in* Summary of Field Work and Other Activities 2009. Ontario Geological Survey. Open File Report 6240.

Stone, D., 2010a. Geology of the Stormy Lake Area, Northwestern Ontario; *in* Summary of Field Work and Other Activities 2010. Ontario Geological Survey, Open File Report 6260.

Stone, D., 2010b. Precambrian geology of the central Wabigoon Subprovince area, northwestern Ontario. Ontario Geological Survey, Open File Report 5422.

Stone, D., Halle, J. and Chaloux, E., 1998. Geology of the Ignace and Pekagoning Lake Areas, Central Wabigoon Subprovince; *in* Summary of Field Work and Other Activities 1998, Ontario Geological Survey, Misc. Paper 169.

Stone, D., Davis, D.W., Hamilton, M.A. and Falcon, A., 2010. Interpretation of 2009 Geochronology in the Central Wabigoon Subprovince and Bending Lake Areas, Northwestern Ontario, *in* Summary of Field Work and Other Activities 2010, Ontario Geological Survey, Open File Report 6260.

https://golderassociates.sharepoint.com/sites/13226g/technical work bh03/wp04 core testing/wp04b - geomechanical testing/09 - lab test report/r1/1671632 (2400b)
ig_bh03_wp4b_report_22jun2022_r1a_clean.docx

APPENDIX A

UCS Tests: Stress-Strain Graphs and Photographs of Intact and Broken Test Specimens

Table A-1: List of uniaxial compression test specimens

Specimen No.	Depth (m)[1]	Rock Type	Page
IG_BH03_UC001	415.99	Biotite Granodiorite-Tonalite	A-2
IG_BH03_UC002	455.15	Biotite Granodiorite-Tonalite	A-3
IG_BH03_UC003	494.50	Biotite Granodiorite-Tonalite	A-4
IG_BH03_UC004	540.19	Biotite Granodiorite-Tonalite	A-5
IG_BH03_UC005	552.67	Amphibolite	A-6
IG_BH03_UC006	582.55	Biotite Granodiorite-Tonalite	A-7
IG_BH03_UC007	662.59	Biotite Granodiorite-Tonalite	A-8

[1]Top depth of prepared sub-sample (depth along borehole)

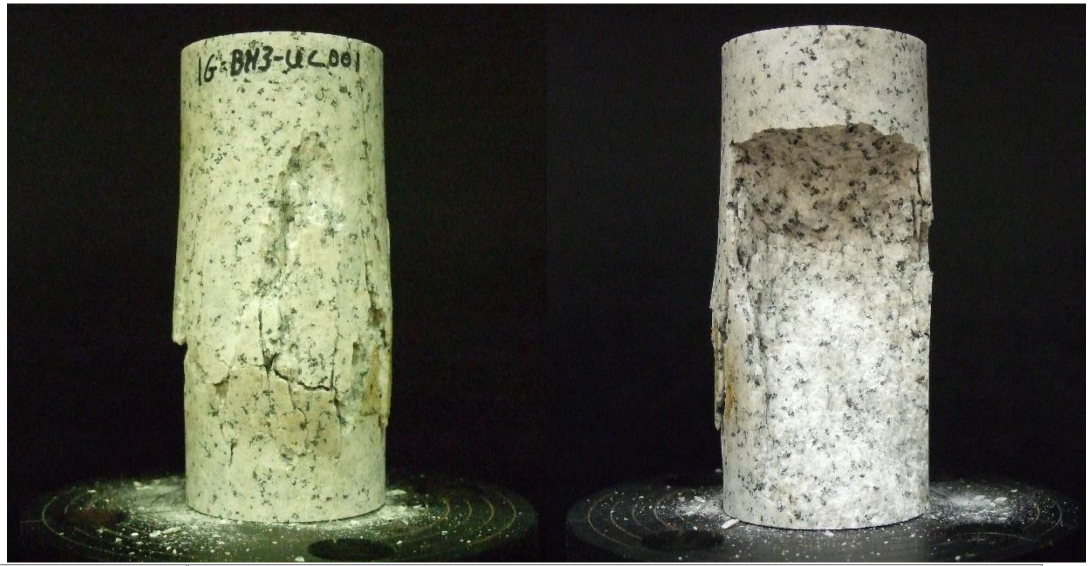

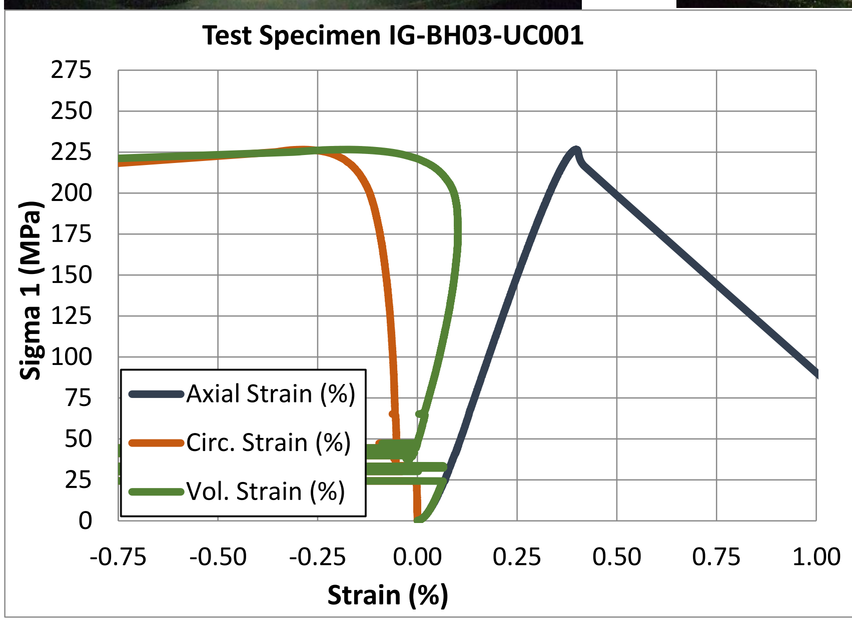

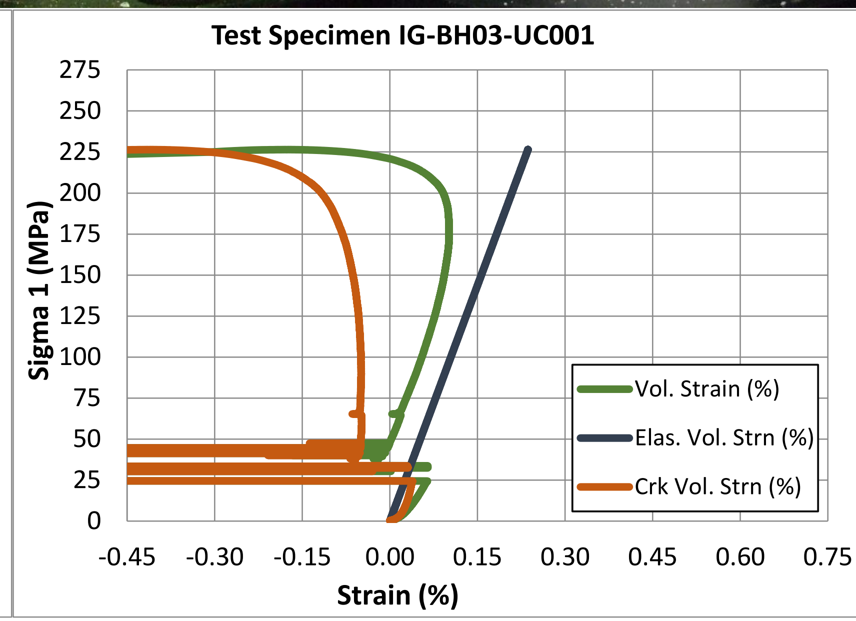

Test Specimen IG_BH03_UC001 – Depth = 415.99 m: Intact and broken specimen photographs and stress-strain curves

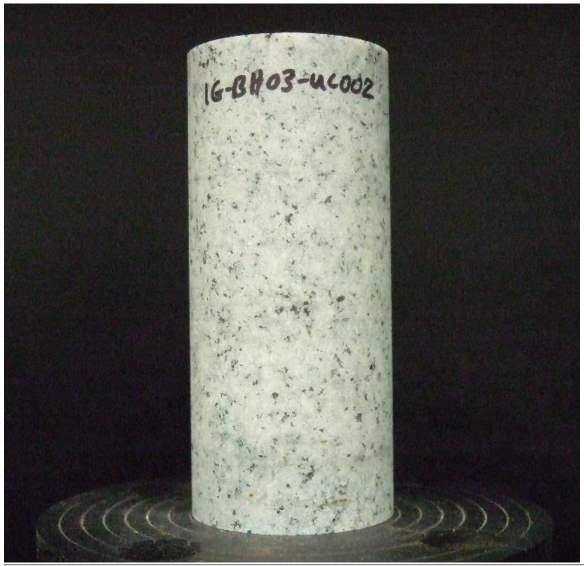

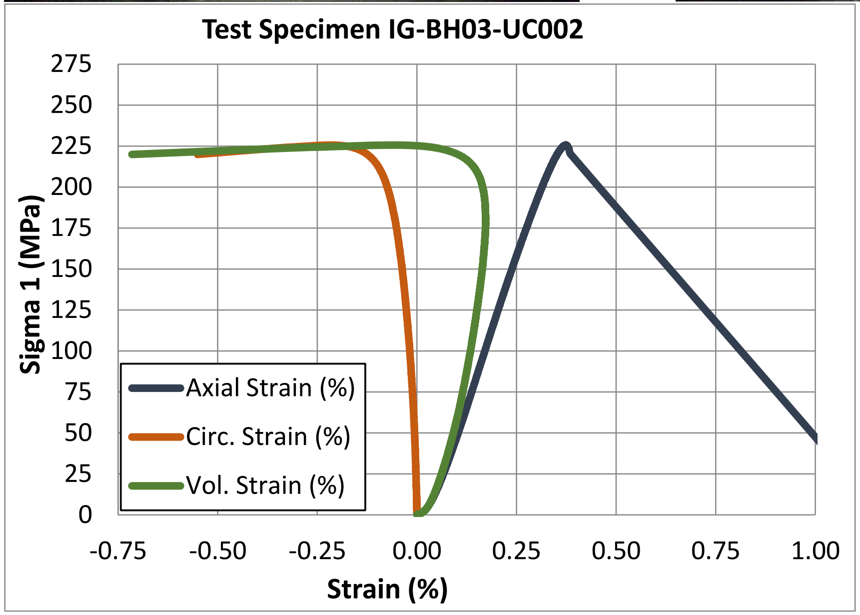

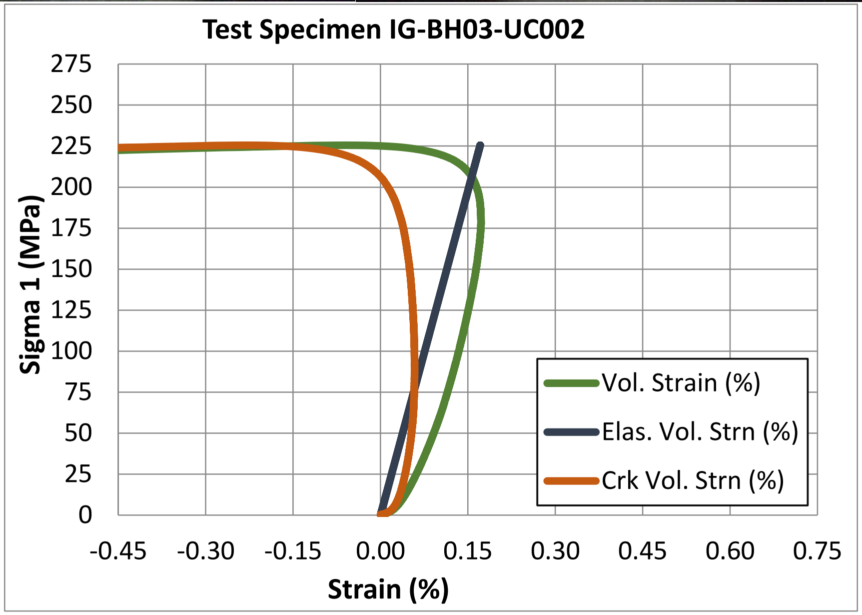

Test Specimen IG_BH03_UC002 – Depth = 455.15 m: Intact and broken specimen photographs and stress-strain curves

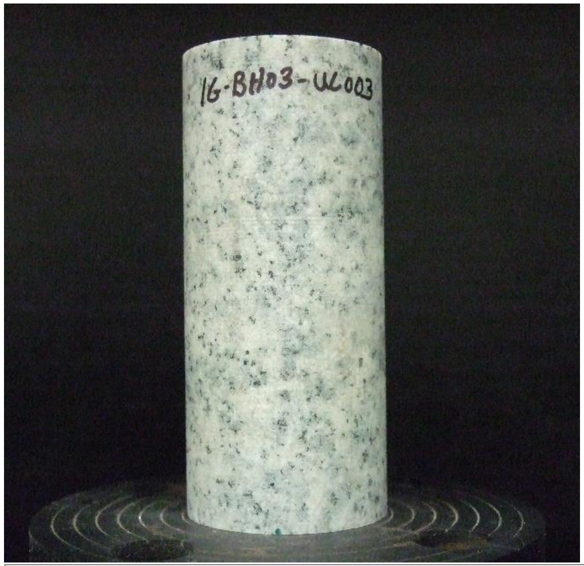

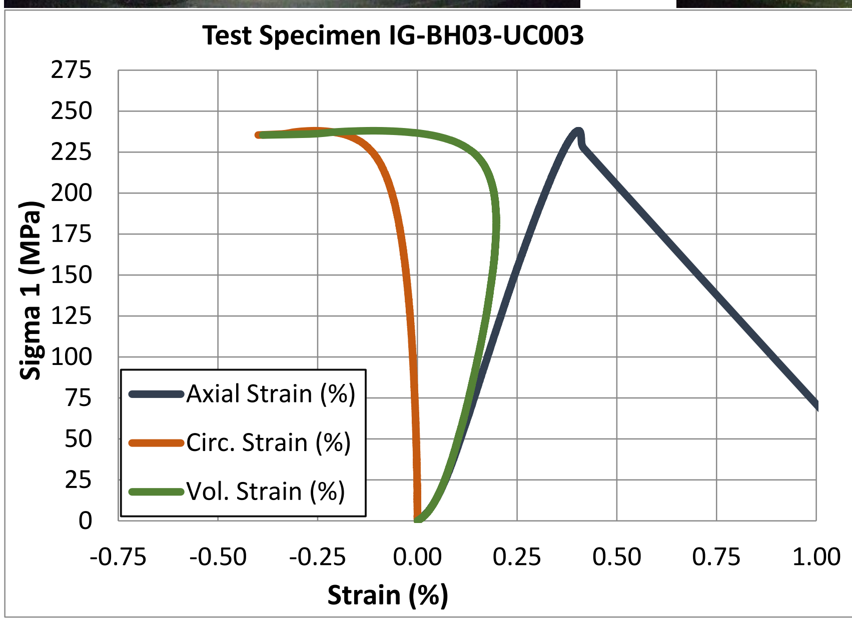

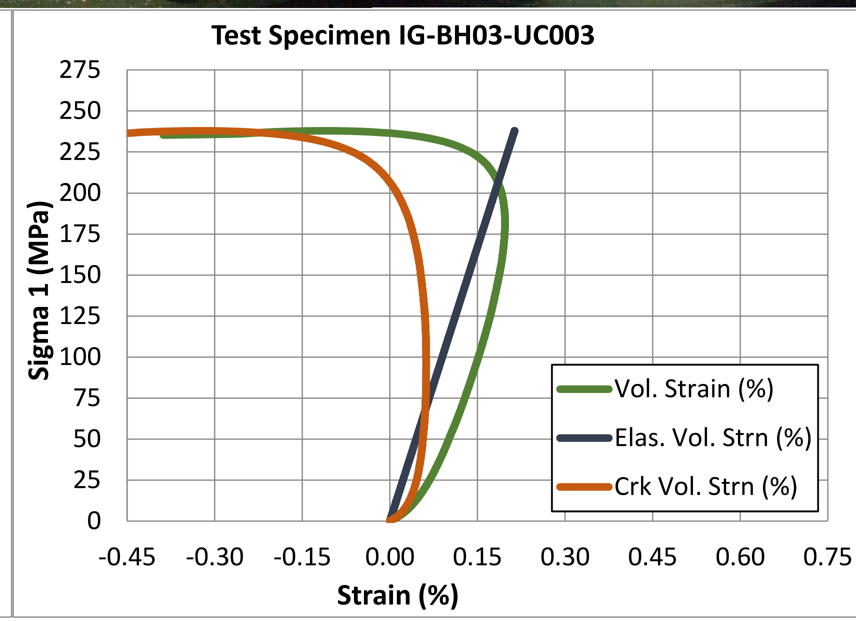

Test Specimen IG_BH03_UC003 – Depth = 494.50 m: Intact and broken specimen photographs and stress-strain curves

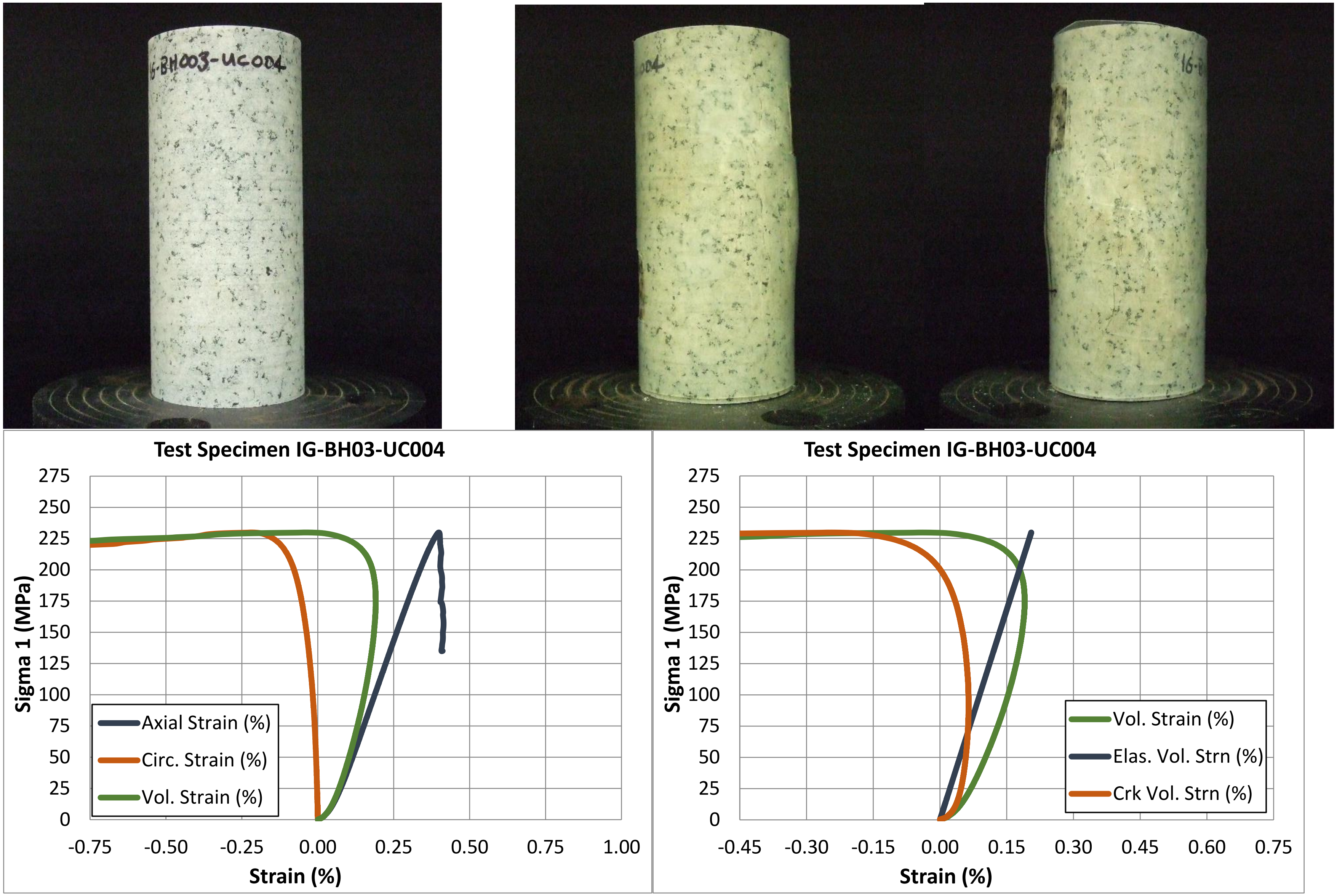

Test Specimen IG_BH03_UC004 – Depth = 540.19 m: Intact and broken specimen photographs and stress-strain curves

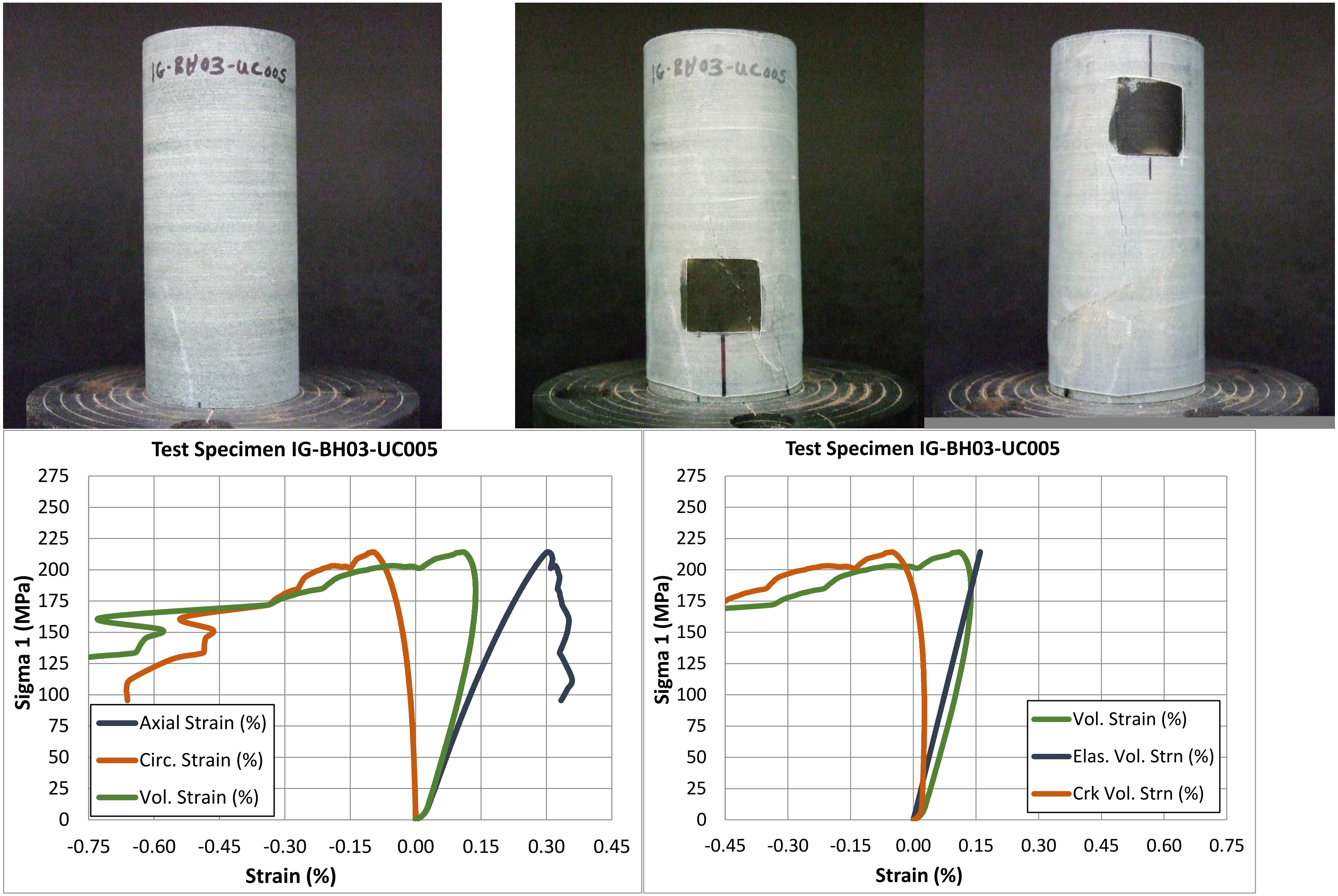

Test Specimen IG_BH03_UC005 – Depth = 552.67 m: Intact and broken specimen photographs and stress-strain curves

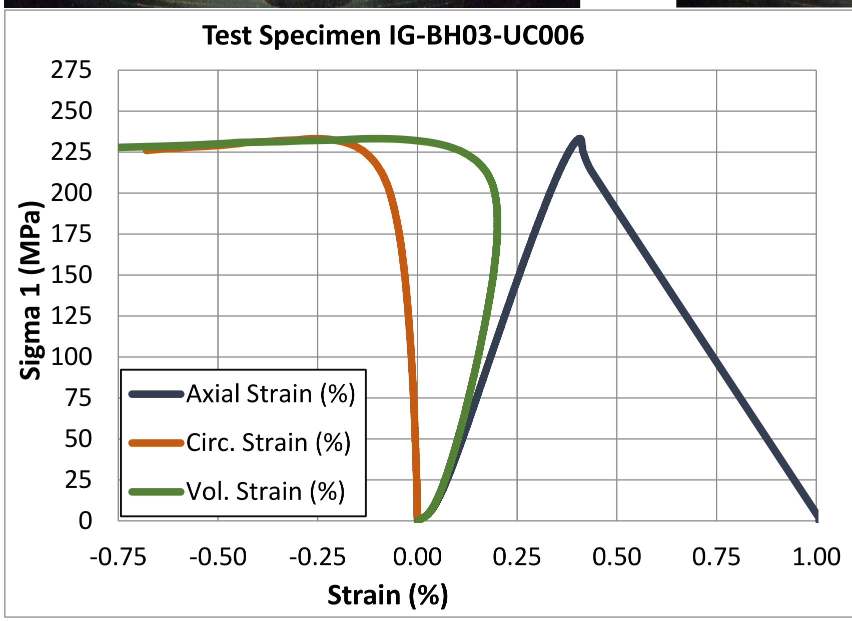

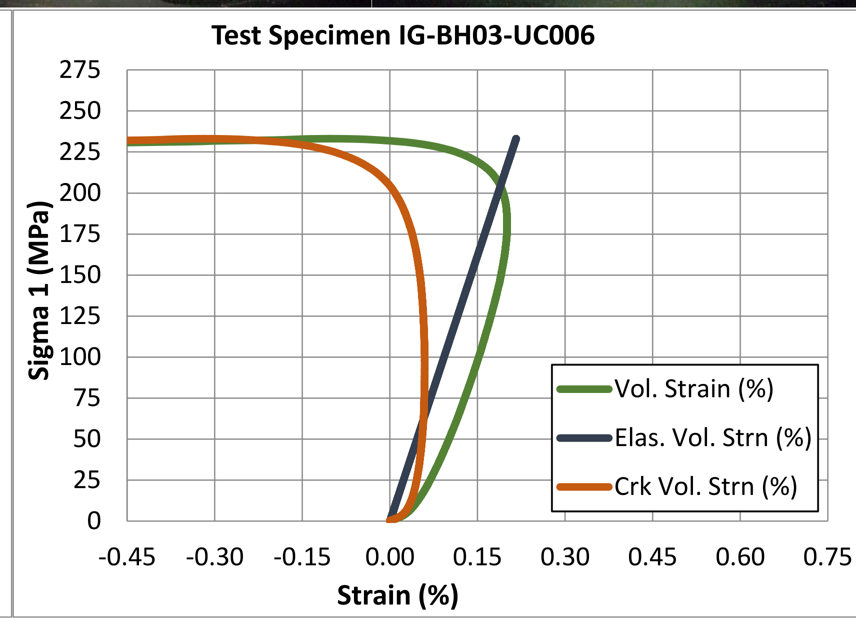

Test Specimen IG_BH03_UC006 – Depth = 582.55 m: Intact and broken specimen photographs and stress-strain curves

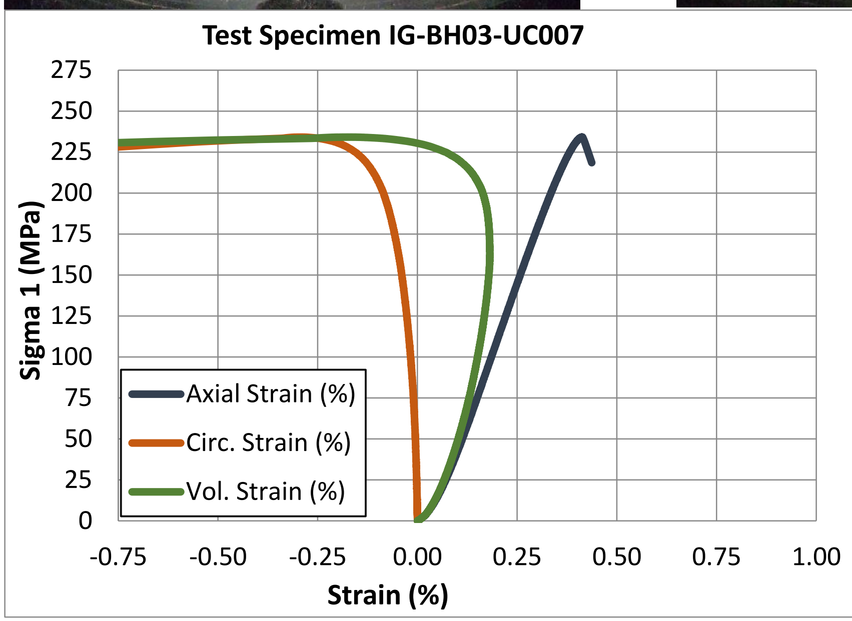

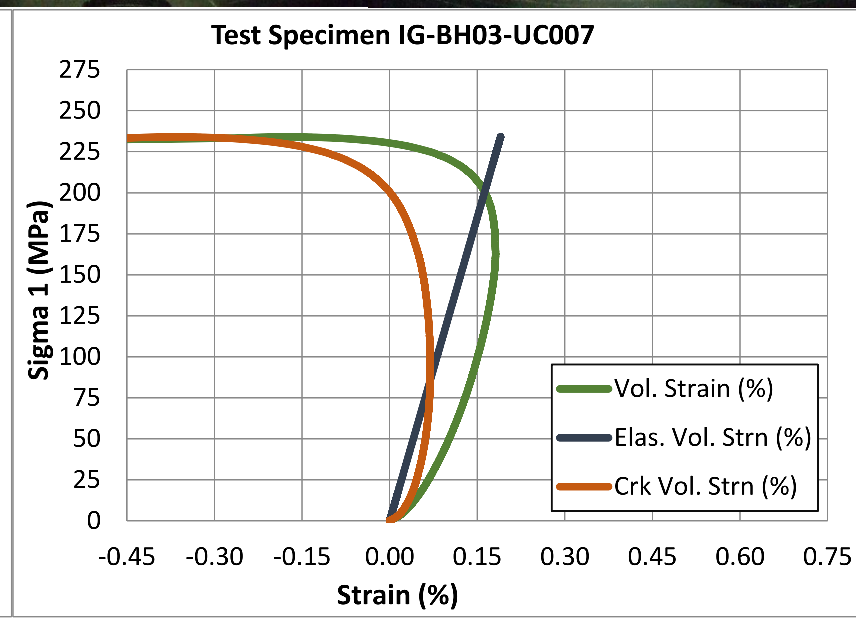

Test Specimen IG_BH03_UC007 – Depth = 662.59 m: Intact and broken specimen photographs and stress-strain curves

APPENDIX B

Acoustic Emission Data and Graph Report

Table B-1: List of uniaxial compression test specimens

Specimen No.	Depth (m)[1]	Rock Type	Page
IG_BH03_UC001	415.99	Biotite Granodiorite-Tonalite	B-2
IG_BH03_UC002	455.15	Biotite Granodiorite-Tonalite	B-3
IG_BH03_UC003	494.50	Biotite Granodiorite-Tonalite	B-4
IG_BH03_UC004	540.19	Biotite Granodiorite-Tonalite	B-5
IG_BH03_UC005	552.67	Amphibolite	B-6
IG_BH03_UC006	582.55	Biotite Granodiorite-Tonalite	B-7
IG_BH03_UC007	662.59	Biotite Granodiorite-Tonalite	B-8

[1]Top depth of prepared sub-sample (depth along borehole)

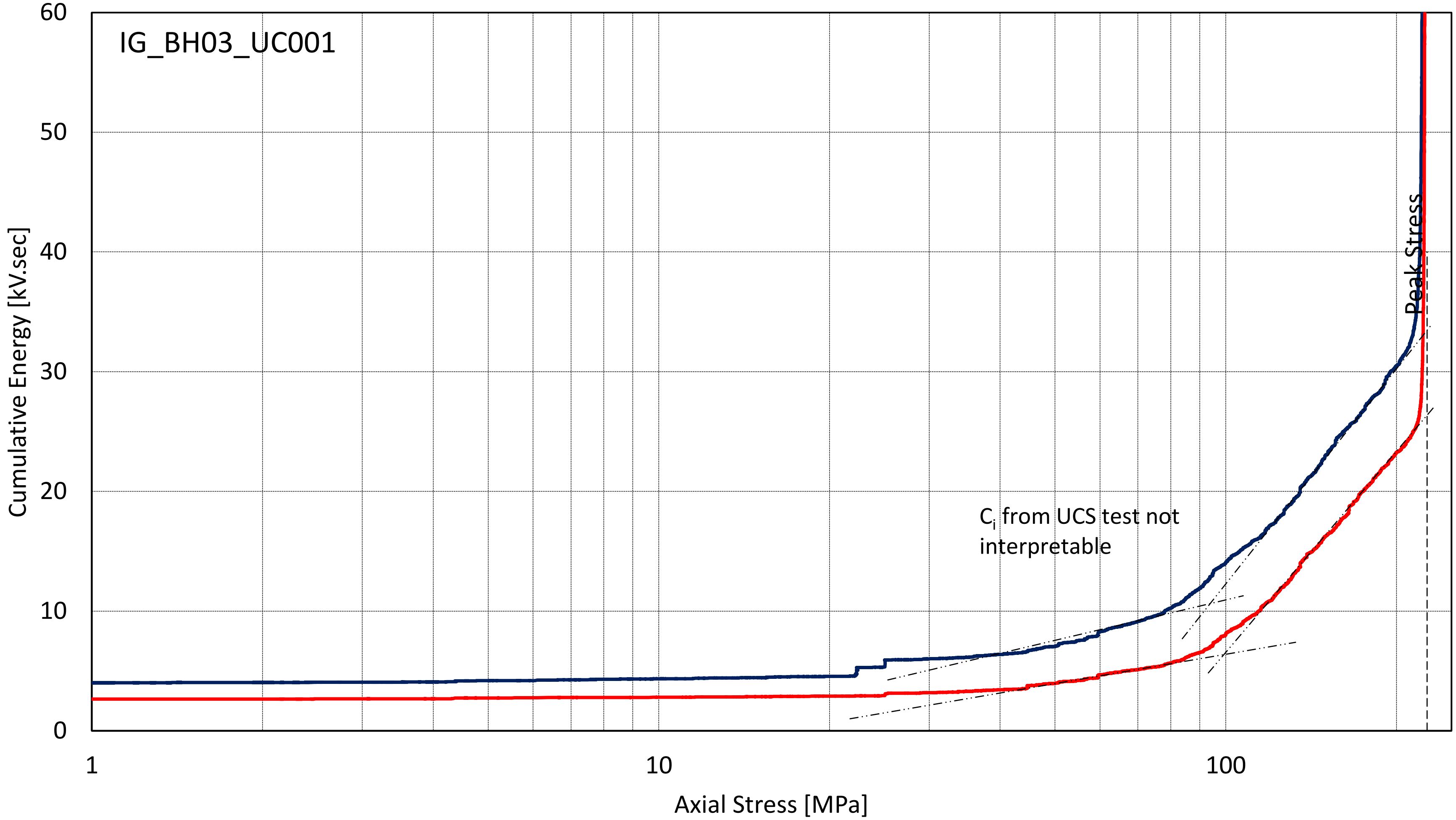

Test Specimen IG_BH03_UC001 – Depth = 415.99 m: Cumulative Energy vs Axial Stress

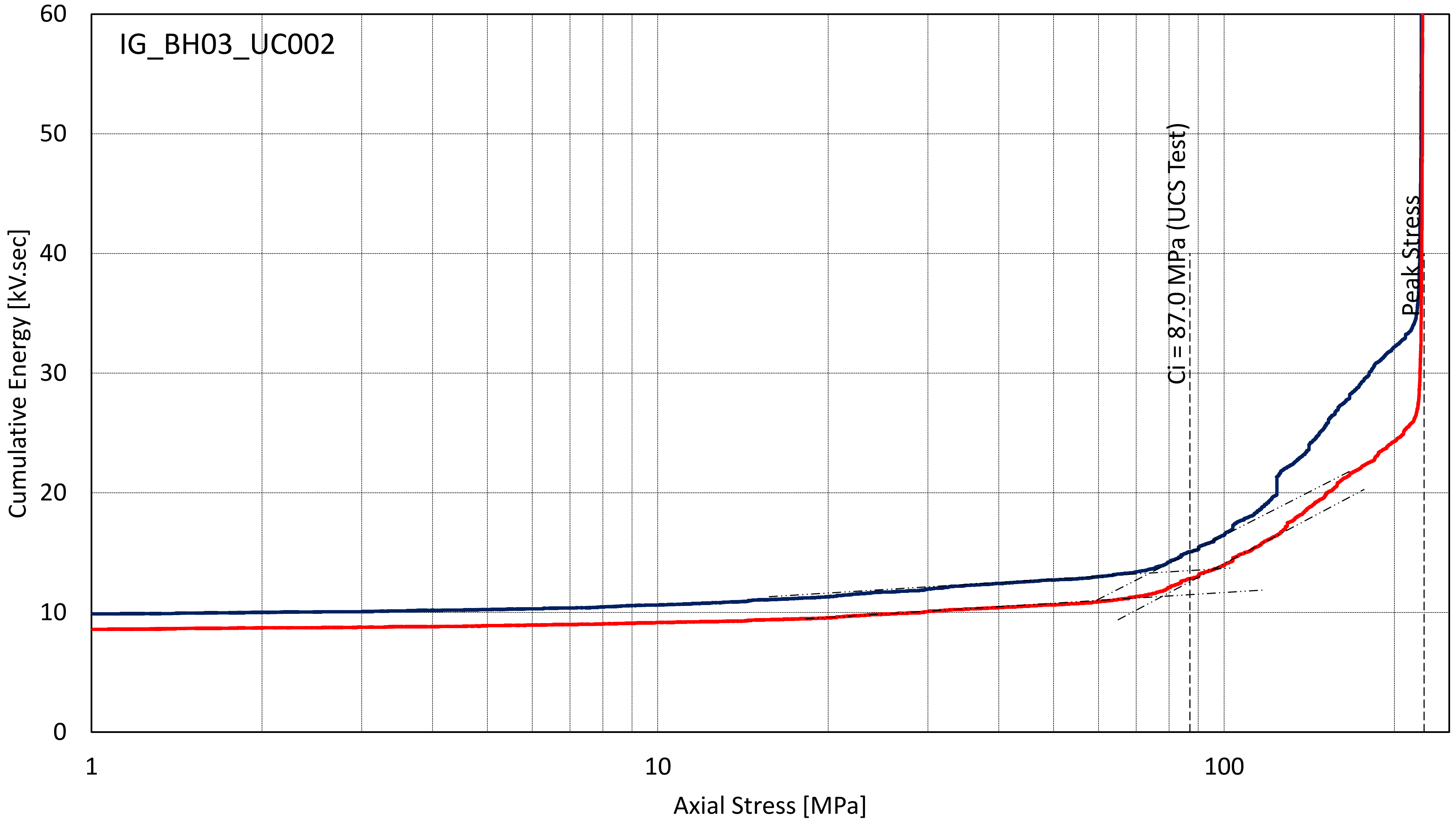

Test Specimen IG_BH03_UC002 – Depth = 455.15 m: Cumulative Energy vs Axial Stress

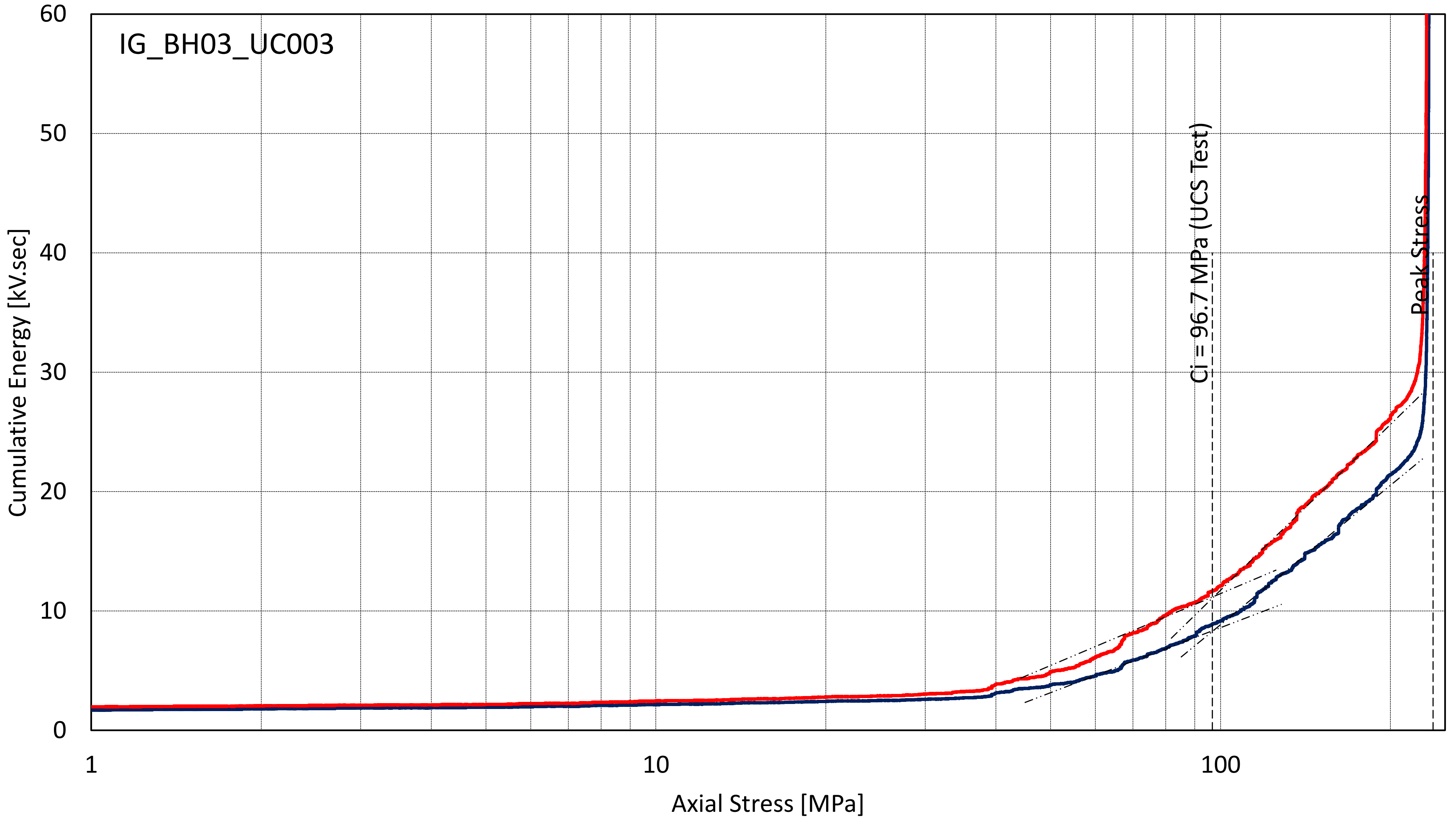

Test Specimen IG_BH03_UC003 – Depth = 494.50 m: Cumulative Energy vs Axial Stress

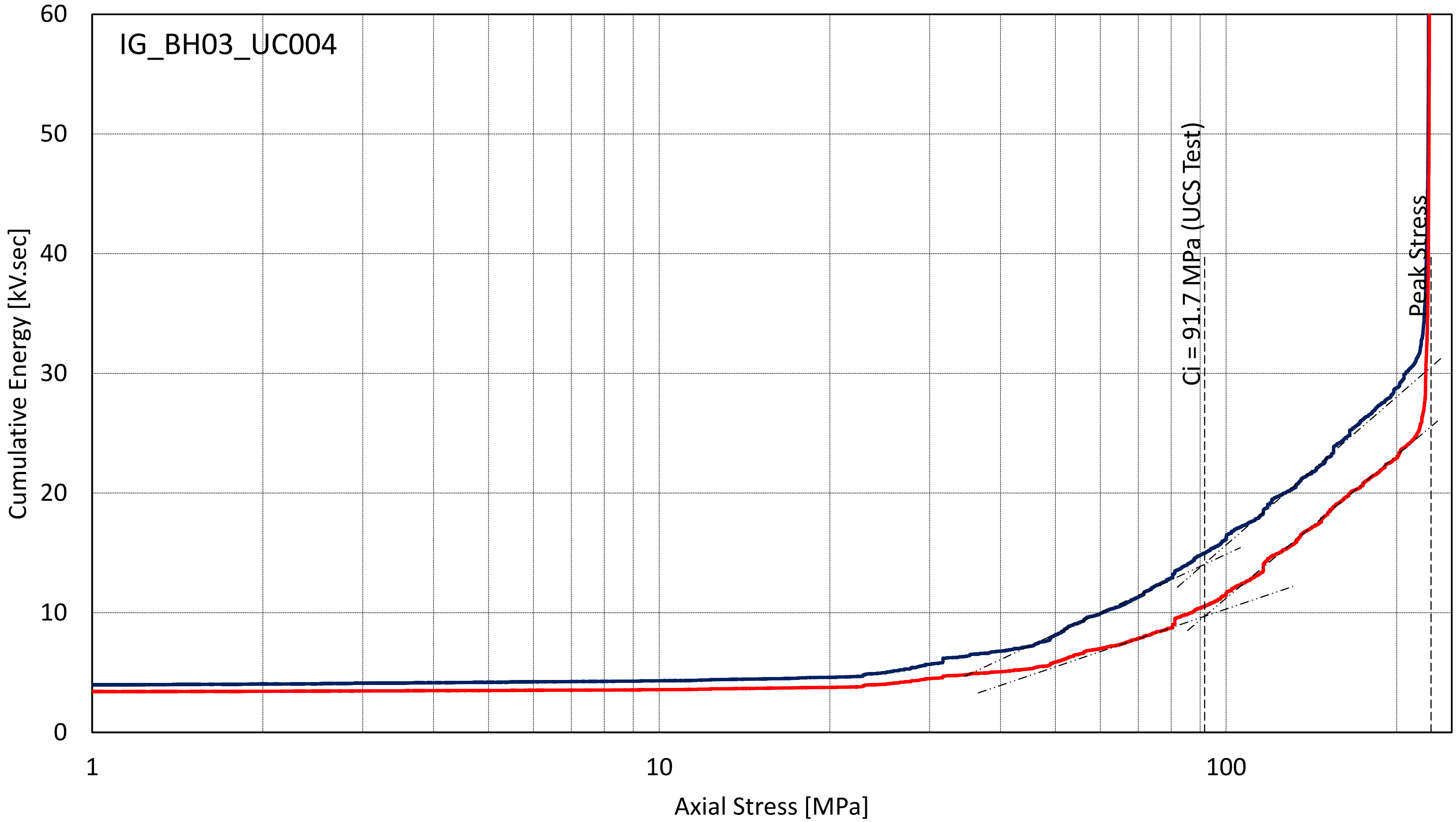

Test Specimen IG_BH03_UC004 – Depth = 540.19 m: Cumulative Energy vs Axial Stress

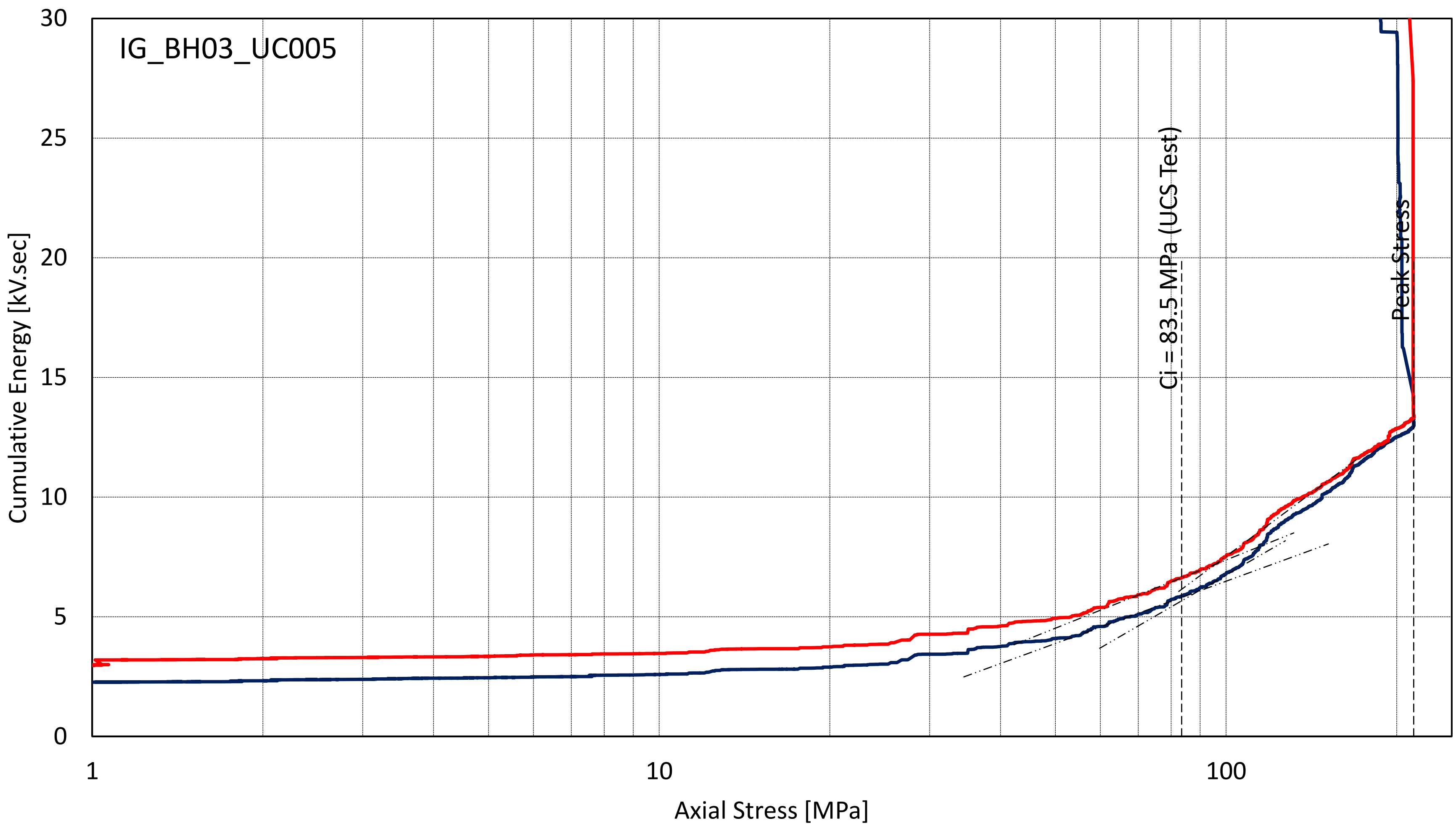

Test Specimen IG_BH03_UC005 – Depth = 552.67 m: Cumulative Energy vs Axial Stress

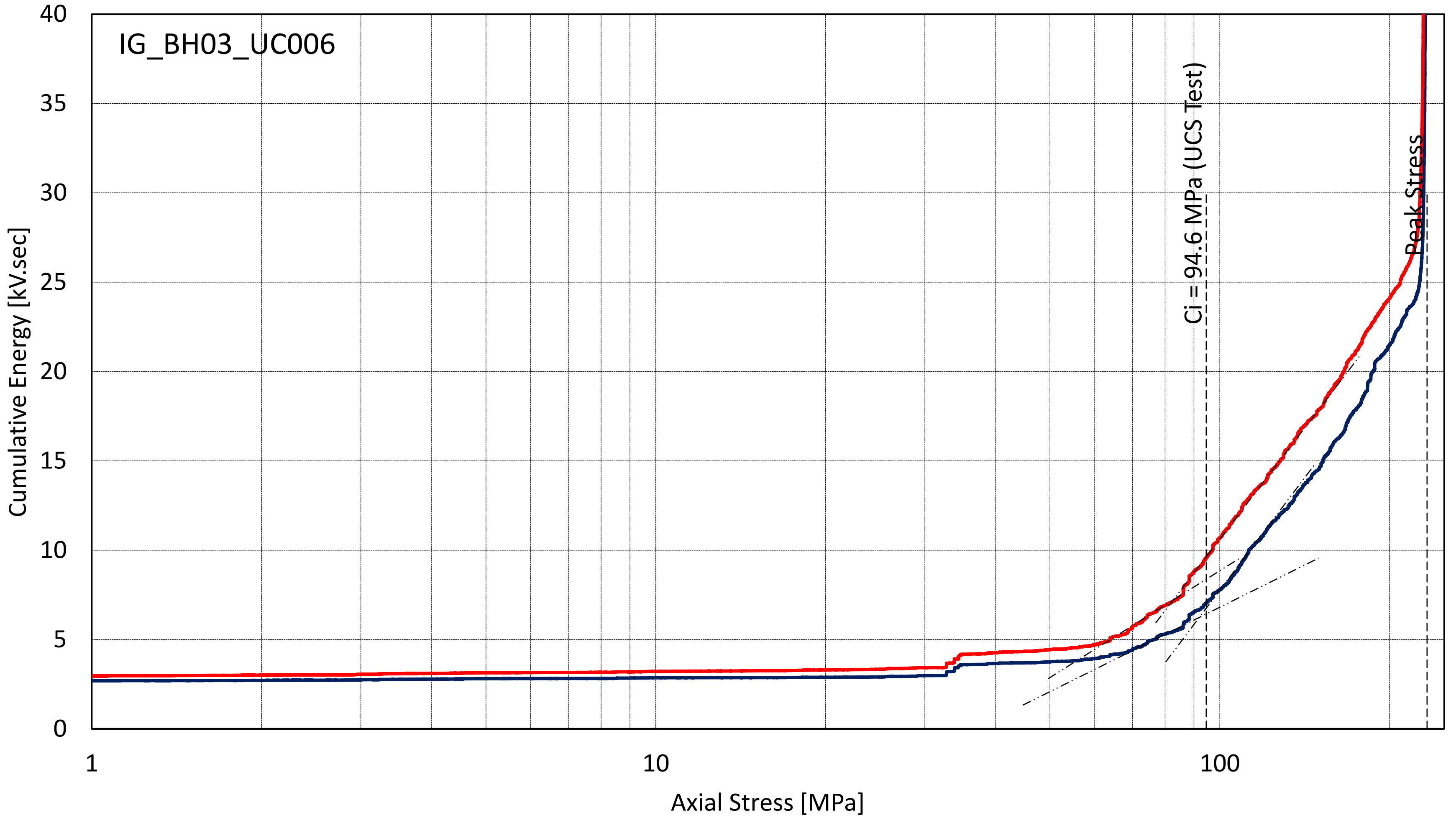

Test Specimen IG_BH03_UC006 – Depth = 582.55 m: Cumulative Energy vs Axial Stress

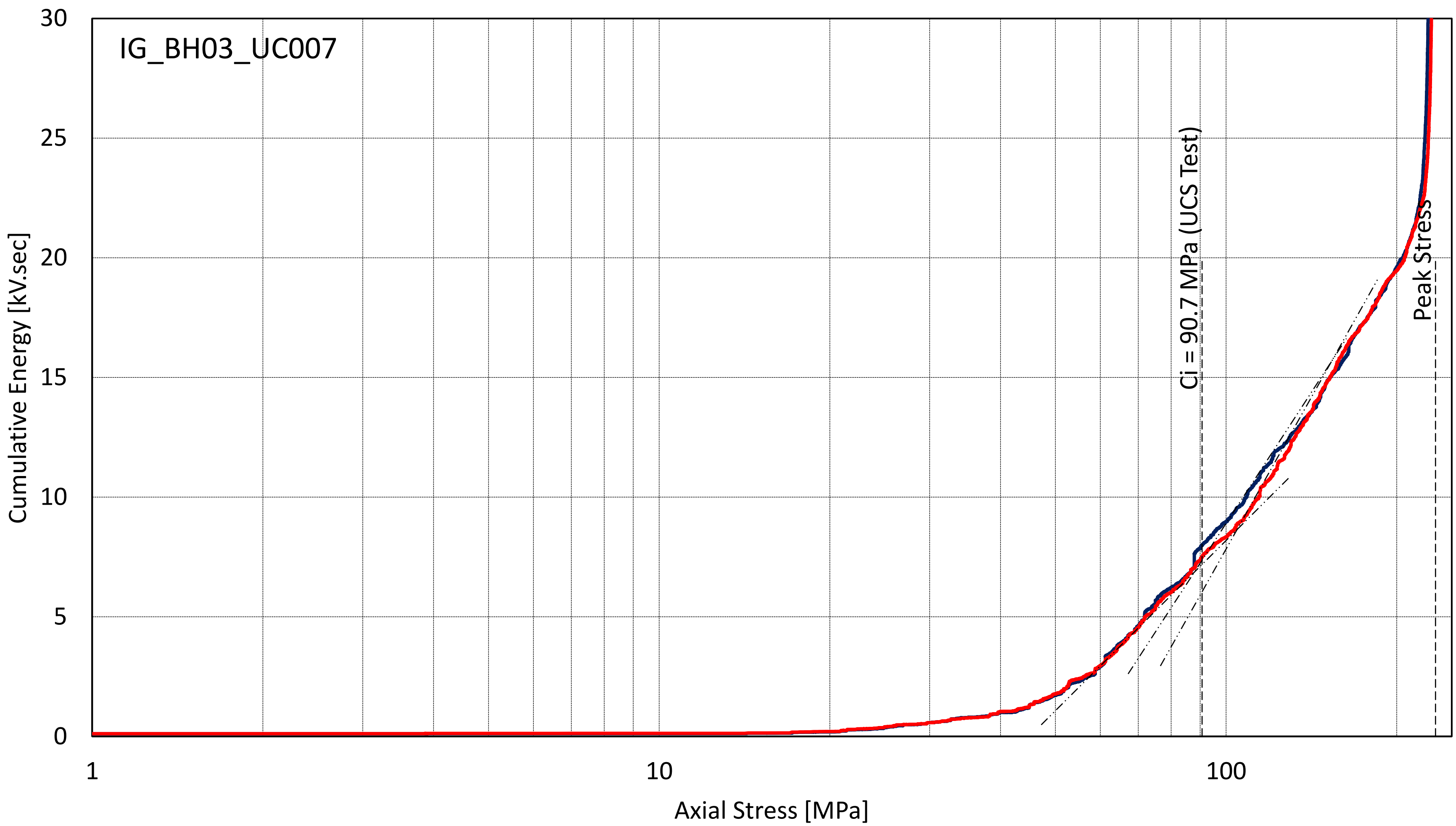

Test Specimen IG_BH03_UC007 – Depth = 662.59 m: Cumulative Energy vs Axial Stress

Test Summary

```
P:\lab data\S Gaines\P-002797.002_Golder_NWMO\Data\Batch 2 (Fall 2019)\AE\IG-UC001\IG-UC001.dta

Total AEHits    :      30543
Total TDDs      :         61
Total Waveforms:       30543
Total Resumes   :          1
Total Pauses    :          1
Total TimeMarks:           0

Channel         AEHits
      1          16543
      2          14000

HIT DRIVEN DATA:
        Feature Chan        Minimum        Maximum        Average        Std Dev
       Risetime    1         0.0000     13066.0000       126.1069       783.4970
         Counts    1         1.0000     31571.0000        72.3571       885.5217
         Energy    1         0.0000     65535.0000        73.0637      1793.8868
       Duration    1         0.0000   1000000.0000      1970.2172     36879.5721
      Amplitude    1        40.0000       100.0000        47.0609         7.7222
      Threshold    1        40.0000        40.0000        40.0000         0.0071
    SigStrength    1         0.0000 11970074624.0000  1353281.8750  96037687.7998
      AbsEnergy    1         0.0000 70041780224.0000  4644582.5000 545327361.3909
    Parametric1    1        -0.2275       235.6523       112.1467        70.6207
       Risetime    2         0.0000     13039.0000       167.1659       934.5461
         Counts    2         1.0000     29961.0000        91.3850       937.4434
         Energy    2         0.0000     65535.0000        72.3105      1693.3107
       Duration    2         0.0000   1000000.0000      2044.6829     33666.3322
      Amplitude    2        40.0000       100.0000        47.4857         8.2425
      Threshold    2        40.0000        40.0000        40.0000         0.0091
    SigStrength    2         0.0000 5232468480.0000  1117166.6250  56257376.6540
      AbsEnergy    2         0.0000 24888891392.0000  3054455.0000 246157376.8761
    Parametric1    2        -0.2275       235.6523       129.8880        69.5059

TIME DRIVEN DATA:
        Feature Chan        Minimum        Maximum        Average        Std Dev
            asl    1        23.0000        60.0000        34.9344         9.4172
            asl    2        18.0000        58.0000        33.0656         9.0080
            asl  104         0.0000         0.0000         0.0000         0.0000
    Parametric1             0.1707       235.5954       117.8511        76.9711
```

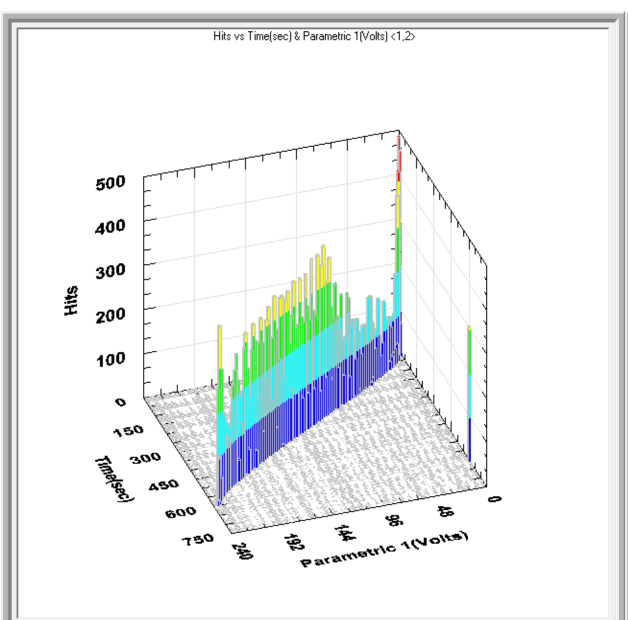

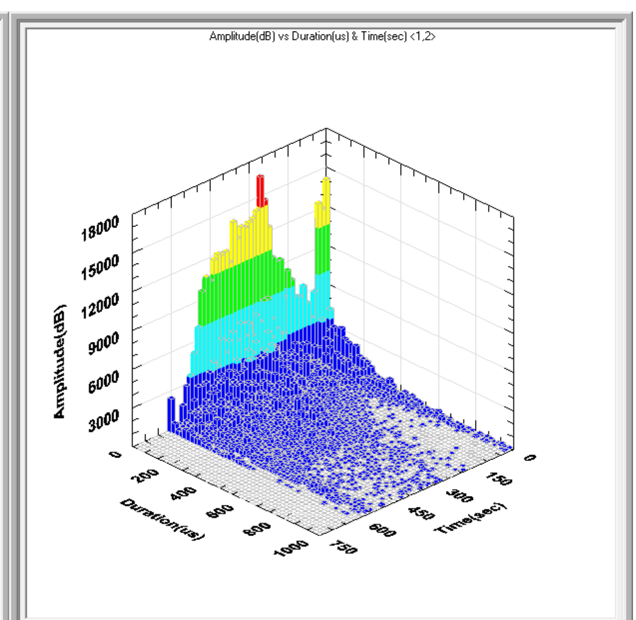

Number of Hits vs. Axial Stress (MPa): Channel 1

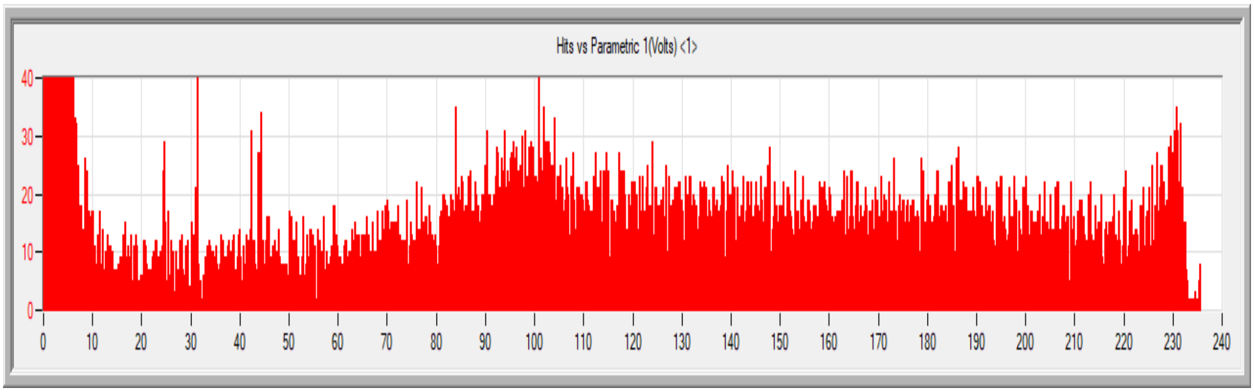

Number of Hits vs. Axial Stress (MPa): Channel 2

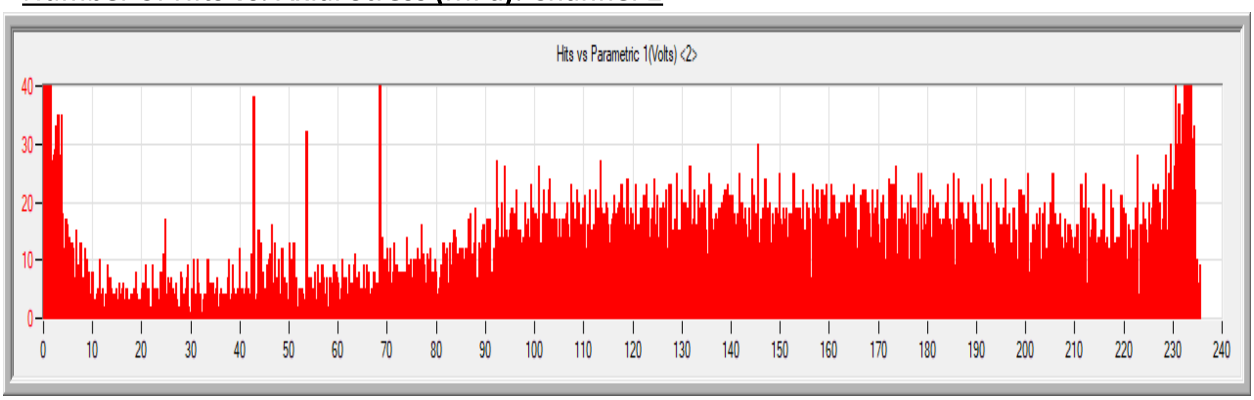

Number of Hits vs. Axial Stress (MPa): Channels 1+2

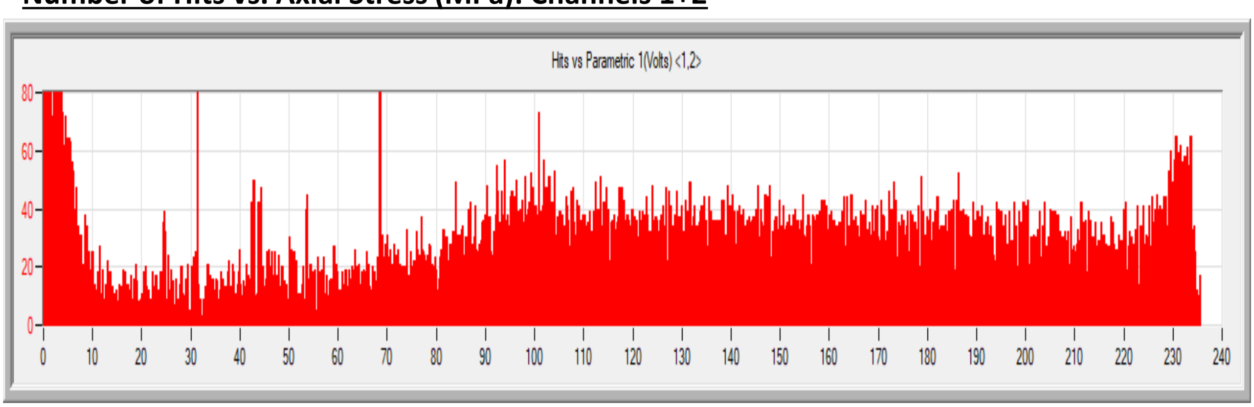

Cumulative Number of Hits vs. Axial Stress (MPa): Channel 1

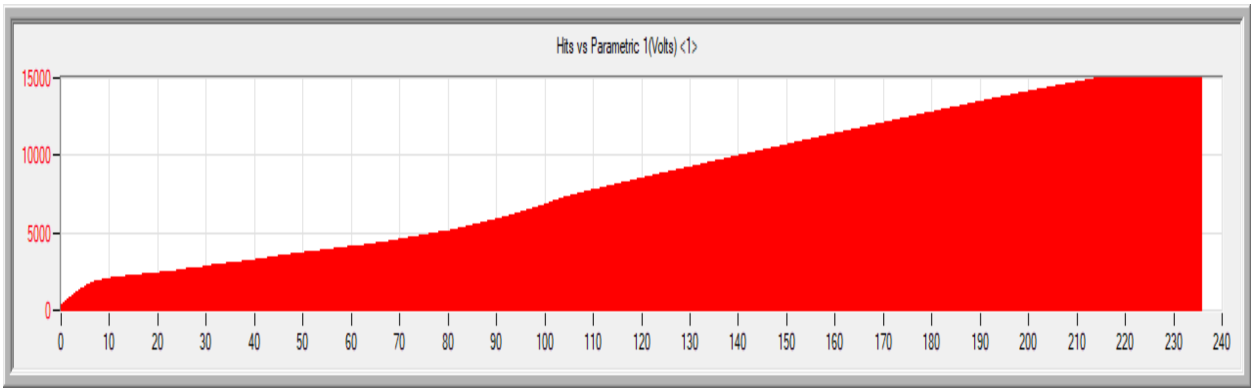

Cumulative Number of Hits vs. Axial Stress (MPa): Channel 2

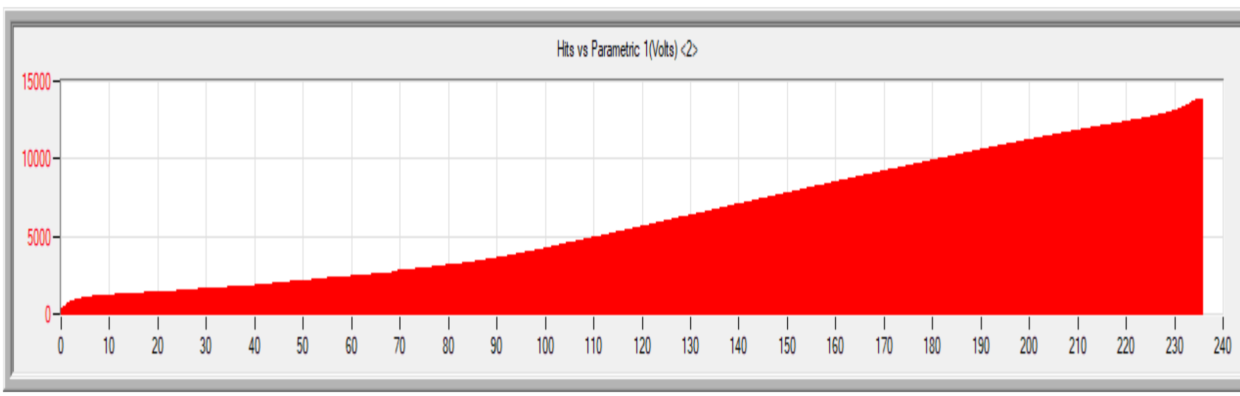

Cumulative Number of Hits vs. Axial Stress (MPa): Channels 1+2

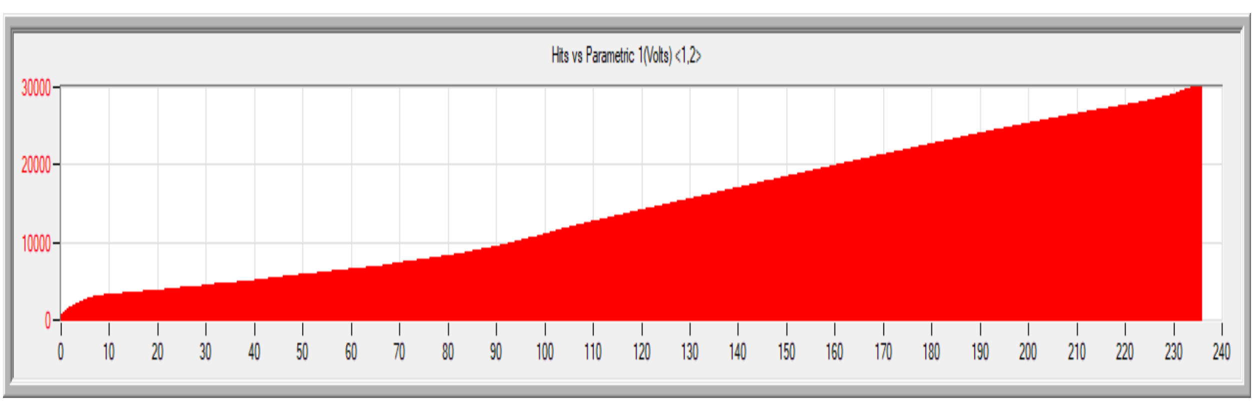

Test Summary

```
P:\lab data\S Gaines\P-002797.002_Golder_NWMO\Data\Batch 2 (Fall 2019)\AE\IG-UC002\IG-UC002.dta

Total AEHits   :       32656
Total TDDs     :          57
Total Waveforms:       32656
Total Resumes  :           1
Total Pauses   :           1
Total TimeMarks:           0

Channel         AEHits
      1          16050
      2          16606

HIT DRIVEN DATA:
         Feature Chan         Minimum         Maximum         Average         Std Dev
        Risetime    1          0.0000      13029.0000        120.0930        750.4650
          Counts    1          1.0000      29802.0000         63.5426        797.4984
          Energy    1          0.0000      65535.0000         70.4505       1750.2006
        Duration    1          0.0000    1000000.0000       1994.0675      37463.1778
       Amplitude    1         40.0000        100.0000         47.1238          7.5169
       Threshold    1         40.0000         40.0000         40.0000          0.0030
     SigStrength    1          0.0000 3001287168.0000     751249.3125   29479932.6739
       AbsEnergy    1          0.0000 5500637696.0000     679461.6875   46591227.7641
     Parametric1    1         -0.1138        234.8844        112.9279         72.2859
        Risetime    2          0.0000      13098.0000        114.4949        748.8632
          Counts    2          1.0000      32503.0000         64.0333        898.1848
          Energy    2          0.0000      65535.0000         63.7944       1664.5519
        Duration    2          0.0000    1000000.0000       1776.2404      34393.3204
       Amplitude    2         40.0000        100.0000         46.4751          7.4112
       Threshold    2         40.0000         40.0000         40.0000          0.0073
     SigStrength    2          0.0000 6785755648.0000     994579.9375   58096745.9619
       AbsEnergy    2          0.0000 27421265920.0000   2162575.5000  215828792.4912
     Parametric1    2         -0.1422        234.9413        111.3472         73.3799

TIME DRIVEN DATA:
         Feature Chan         Minimum         Maximum         Average         Std Dev
             asl    1         23.0000         66.0000         33.1053          9.2636
             asl    2         28.0000         63.0000         34.2807          7.5644
             asl   96          0.0000          0.0000          0.0000          0.0000
             asl  104          0.0000          0.0000          0.0000          0.0000
     Parametric1               0.5689        234.5146        119.5809         76.5524
```

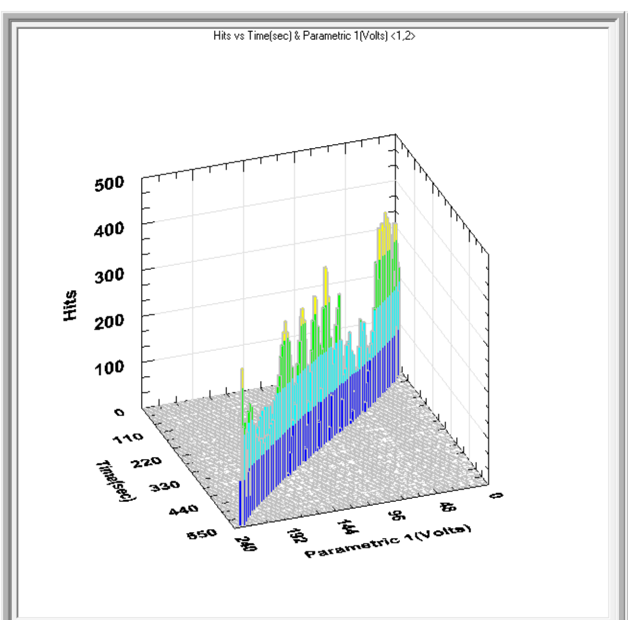

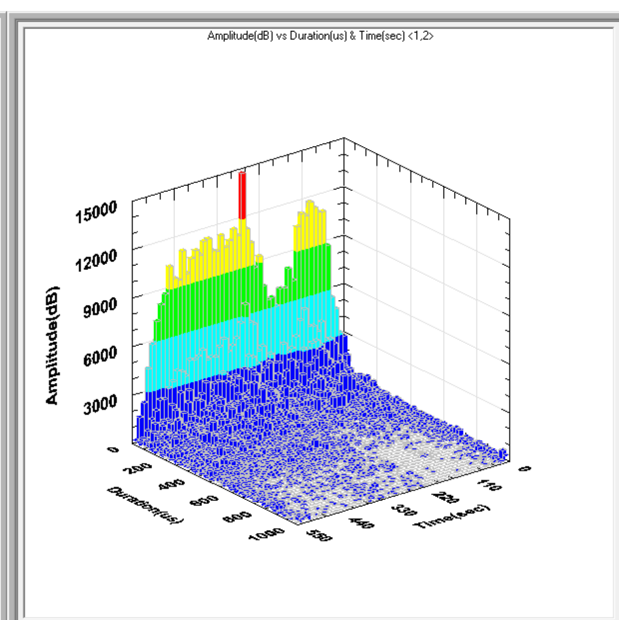

Number of Hits vs. Axial Stress (MPa): Channel 1

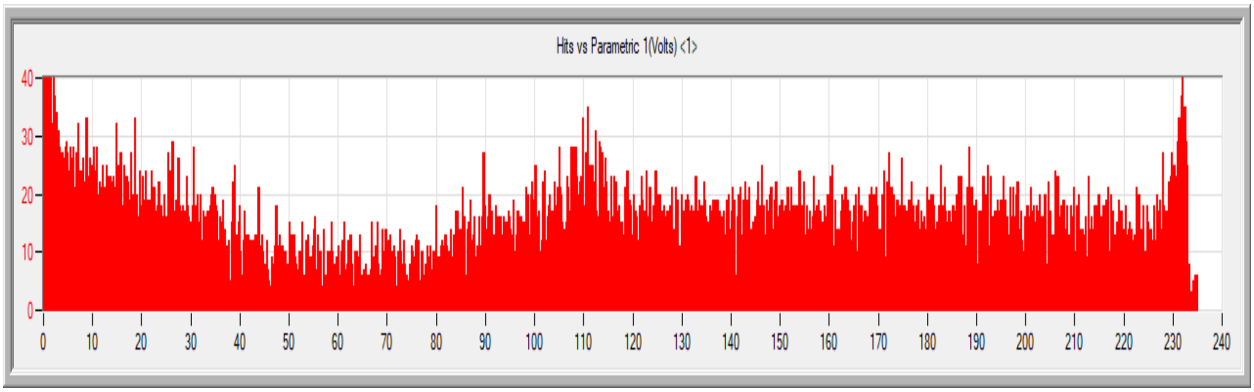

Number of Hits vs. Axial Stress (MPa): Channel 2

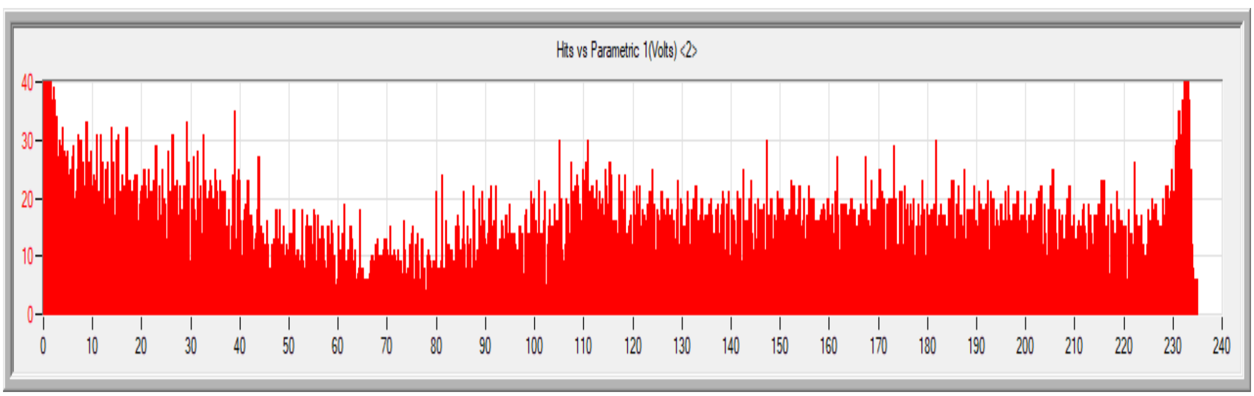

Number of Hits vs. Axial Stress (MPa): Channels 1+2

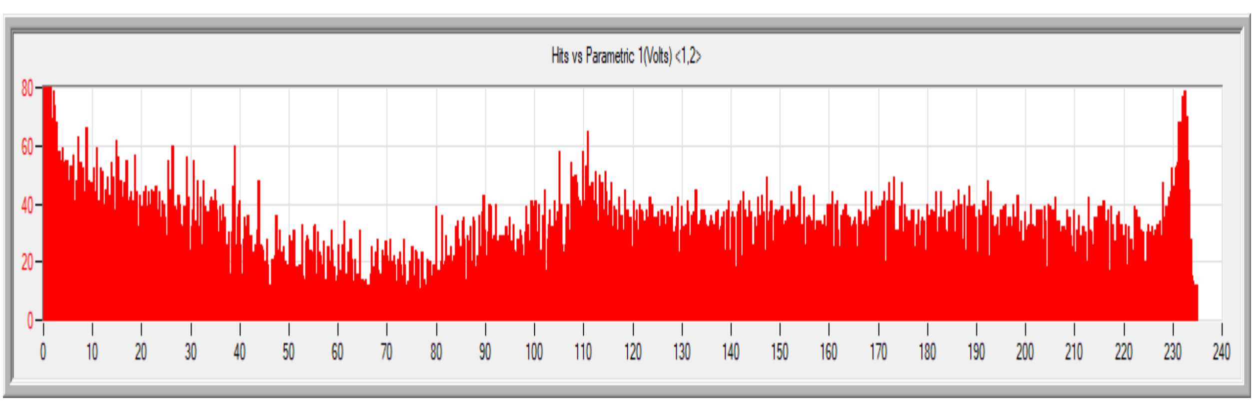

Cumulative Number of Hits vs. Axial Stress (MPa): Channel 1

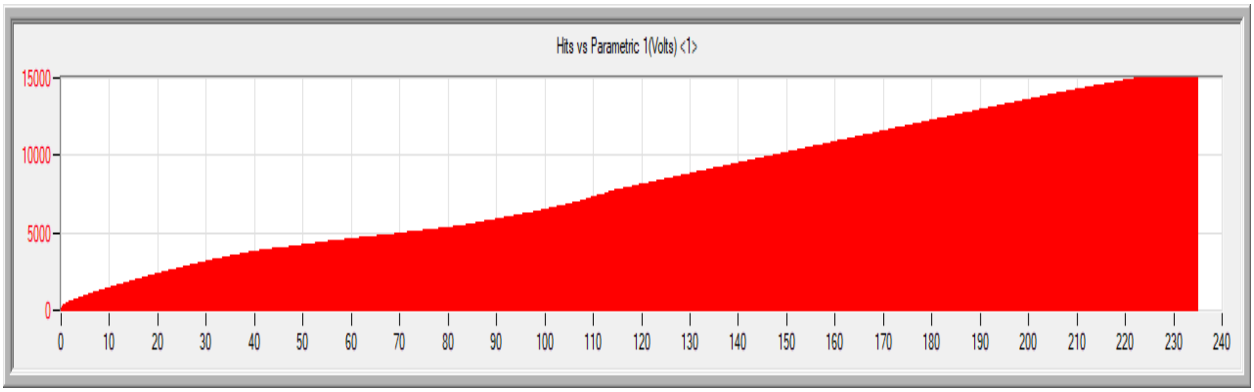

Cumulative Number of Hits vs. Axial Stress (MPa): Channel 2

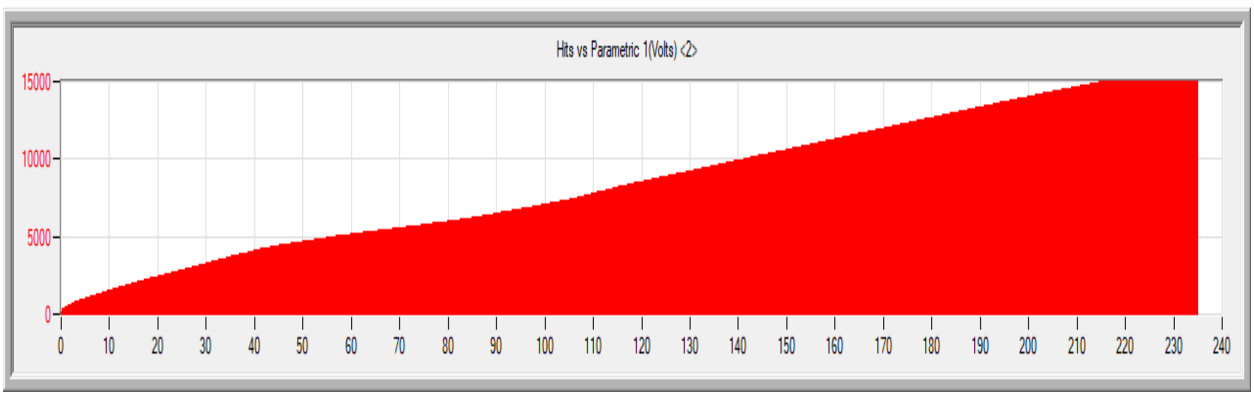

Cumulative Number of Hits vs. Axial Stress (MPa): Channels 1+2

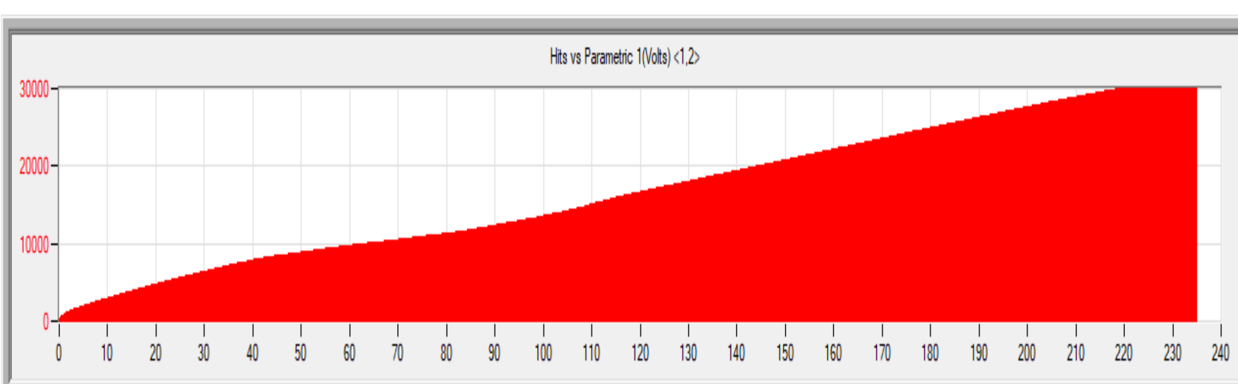

Test Summary

```
P:\lab data\S Gaines\P-002797.002_Golder_NWMO\Data\Batch 2 (Fall 2019)\AE\IG-UC003\IG-UC003.dta

Total AEHits    :        33773
Total TDDs      :           73
Total Waveforms:         33773
Total Resumes   :            1
Total Pauses    :            1
Total TimeMarks:             0

Channel          AEHits
      1           16635
      2           17138

HIT DRIVEN DATA:
         Feature Chan         Minimum          Maximum          Average          Std Dev
        Risetime    1          0.0000       12992.0000         160.5532         921.0056
          Counts    1          1.0000       31534.0000          93.3573         990.5601
          Energy    1          0.0000       65535.0000          80.6647        1810.0582
        Duration    1          0.0000     1000000.0000        2296.4880       37456.0890
       Amplitude    1         40.0000         100.0000          46.1859           7.8911
       Threshold    1         40.0000          40.0000          40.0000           0.0051
     SigStrength    1          0.0000  7710394880.0000     1153325.0000   64019992.7189
       AbsEnergy    1          0.0000 77017169920.0000     6400752.5000  626720785.2405
     Parametric1    1         -0.0853         246.6030         115.6407          76.5958
        Risetime    2          0.0000       12746.0000         145.2387         887.4167
          Counts    2          1.0000       32720.0000          91.8078        1089.4911
          Energy    2          0.0000       65535.0000          99.3144        2088.6320
        Duration    2          0.0000     1000000.0000        2535.4592       42232.8476
       Amplitude    2         40.0000         100.0000          47.0881           8.1000
       Threshold    2         40.0000          40.0000          40.0000          -1.#IND
     SigStrength    2          0.0000  7028843008.0000     1296524.0000   59319419.9529
       AbsEnergy    2          0.0000 57755860992.0000     5525467.5000  474163894.9677
     Parametric1    2         -0.1138         246.6030         110.5952          74.5849

TIME DRIVEN DATA:
         Feature Chan         Minimum          Maximum          Average          Std Dev
             asl    1         18.0000          61.0000          34.1781          10.0850
             asl    2         16.0000          69.0000          33.5479          11.8980
             asl   96          0.0000           0.0000           0.0000           0.0000
             asl  104          0.0000           0.0000           0.0000           0.0000
     Parametric1              0.1422         246.5461         104.1463          86.3767
```

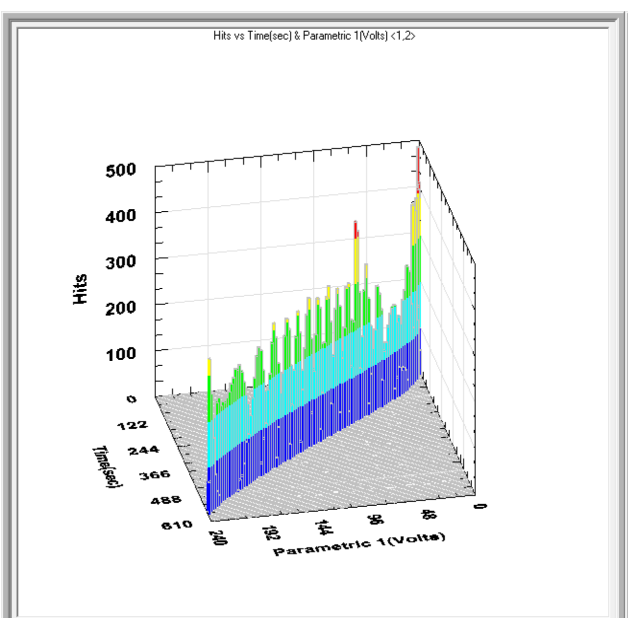

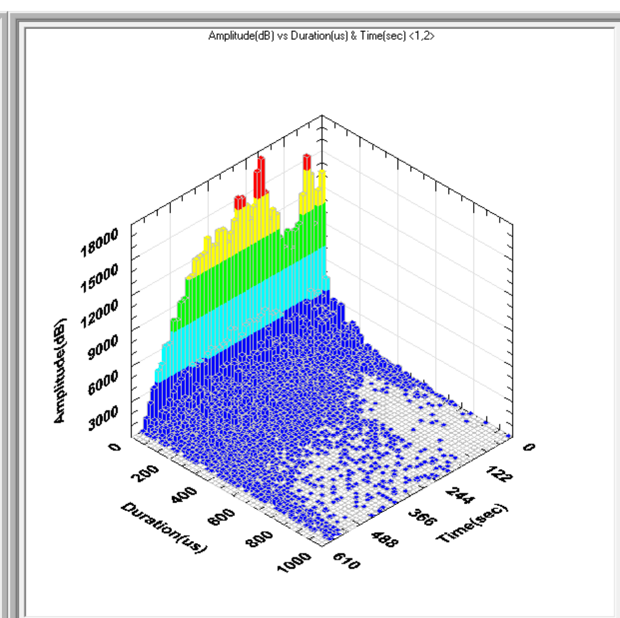

Number of Hits vs. Axial Stress (MPa): Channel 1

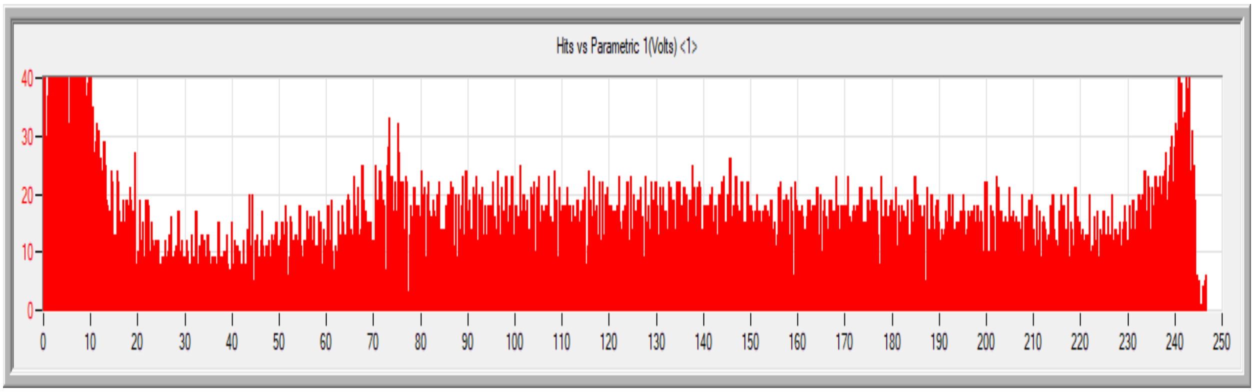

Number of Hits vs. Axial Stress (MPa): Channel 2

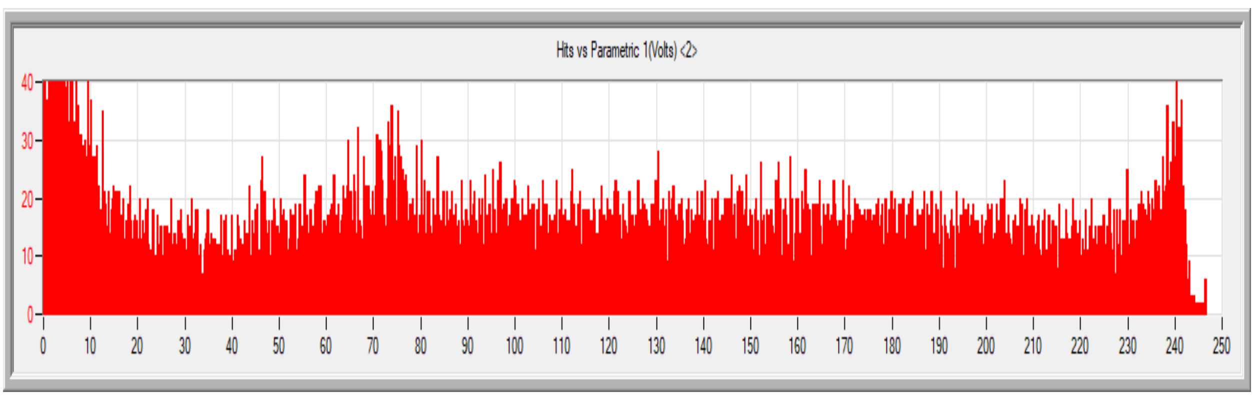

Number of Hits vs. Axial Stress (MPa): Channels 1+2

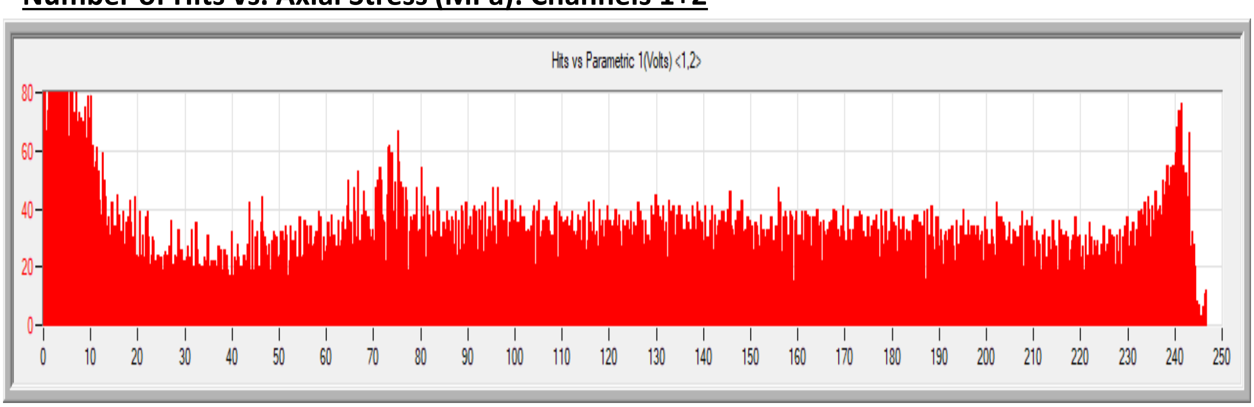

Cumulative Number of Hits vs. Axial Stress (MPa): Channel 1

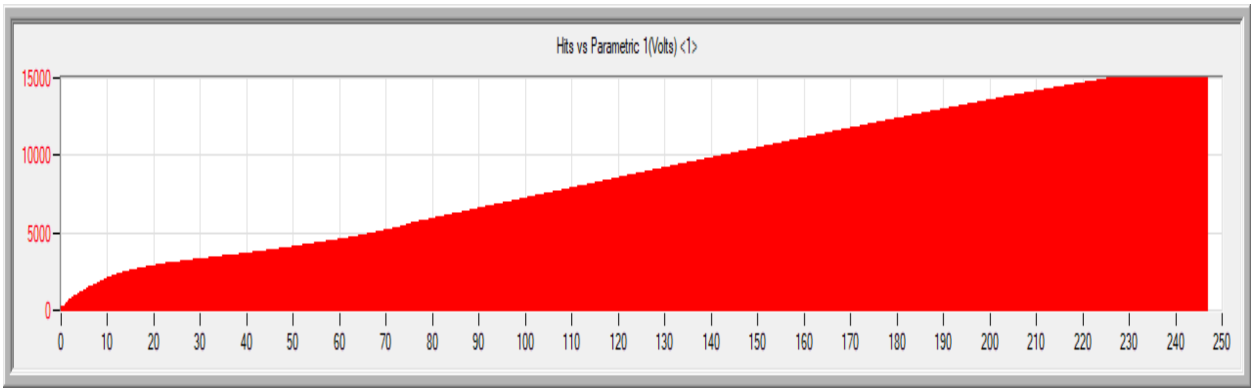

Cumulative Number of Hits vs. Axial Stress (MPa): Channel 2

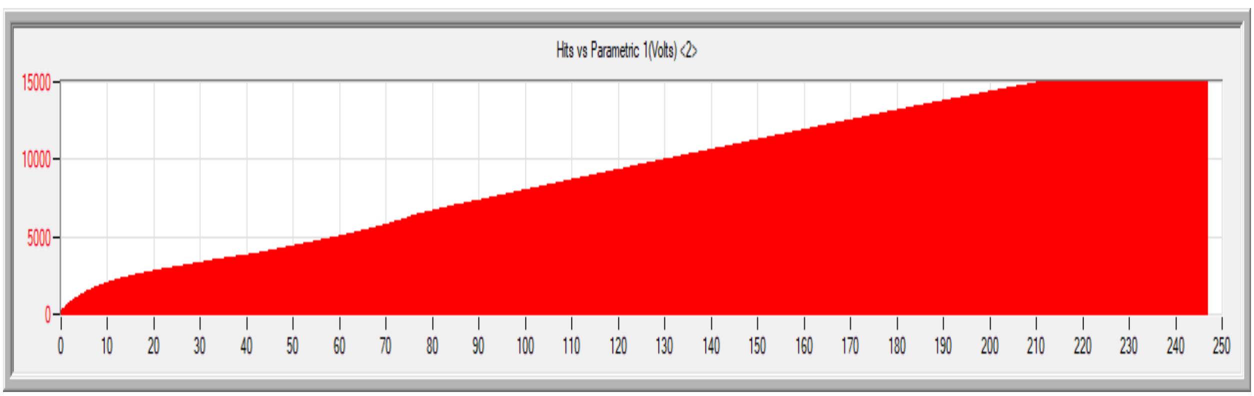

Cumulative Number of Hits vs. Axial Stress (MPa): Channels 1+2

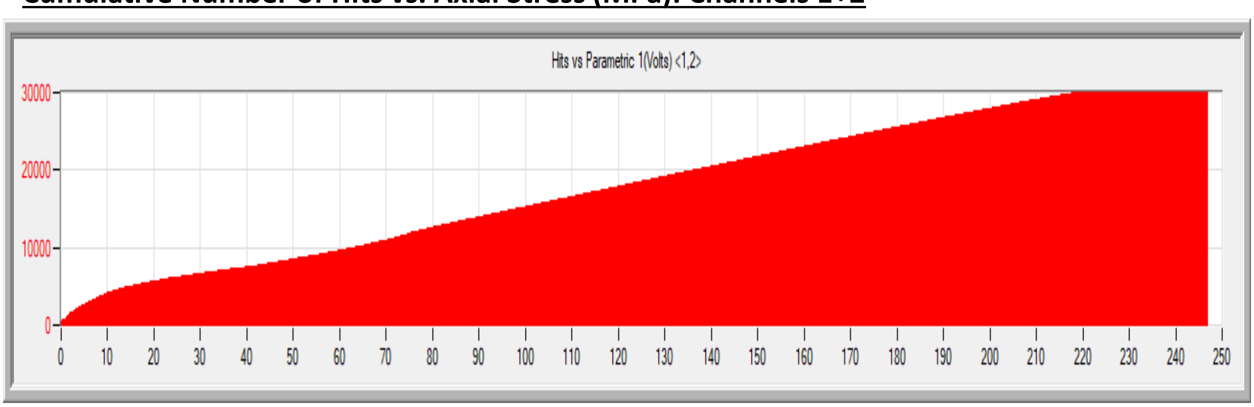

Test Summary

```
P:\lab data\S Gaines\P-002797.002_Golder_NWMO\Data\Batch 2 (Fall 2019)\AE\IG-UC004\IG-UC004.dta

Total AEHits    :        32268
Total TDDs      :           61
Total Waveforms:         32268
Total Resumes   :            1
Total Pauses    :            1
Total TimeMarks:             0

Channel          AEHits
      1           17068
      2           15200

HIT DRIVEN DATA:
         Feature Chan        Minimum        Maximum          Average          Std Dev
        Risetime    1         0.0000     13083.0000         113.4566         733.8923
          Counts    1         1.0000     31844.0000          49.2785         614.4119
          Energy    1         0.0000     65535.0000          66.2042        1905.3538
        Duration    1         0.0000   1000000.0000        1419.9692       30921.2946
       Amplitude    1        40.0000       100.0000          46.4777           7.3409
       Threshold    1        40.0000        40.0000          40.0000          -1.#IND
     SigStrength    1         0.0000 13022457856.0000   4247126.0000 188576566.1535
       AbsEnergy    1         0.0000 50635251712.0000  12551435.0000 635224292.0417
     Parametric1    1        -0.1138       238.8380         110.3038          71.8274
        Risetime    2         0.0000     12652.0000         110.8351         698.9798
          Counts    2         1.0000     28610.0000          42.5715         579.5028
          Energy    2         0.0000     65535.0000          69.1818        1954.7939
        Duration    2         0.0000   1000000.0000        1461.4098       32533.8338
       Amplitude    2        40.0000       100.0000          46.1692           7.3452
       Threshold    2        40.0000        40.0000          40.0000           0.0000
     SigStrength    2         0.0000 4338727936.0000    1601564.0000  63906570.5071
       AbsEnergy    2         0.0000 9154466816.0000    2266245.7500 113077505.3863
     Parametric1    2        -0.0853       238.8380         117.6574          72.7744

TIME DRIVEN DATA:
         Feature Chan        Minimum        Maximum          Average          Std Dev
             asl    1        28.0000        87.0000          36.6557          10.0554
             asl    2        28.0000        75.0000          35.1639           8.5836
             asl   96         0.0000         0.0000           0.0000           0.0000
             asl  104         0.0000         0.0000           0.0000           0.0000
     Parametric1              0.7395       238.4398         117.0314          76.7490
```

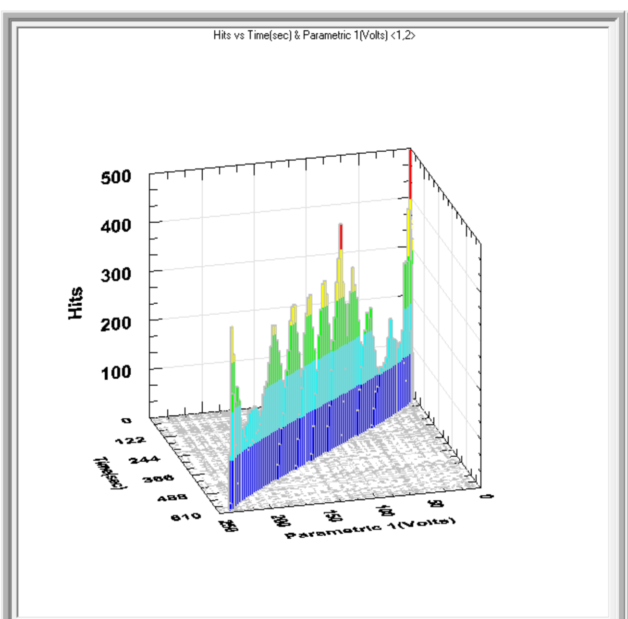

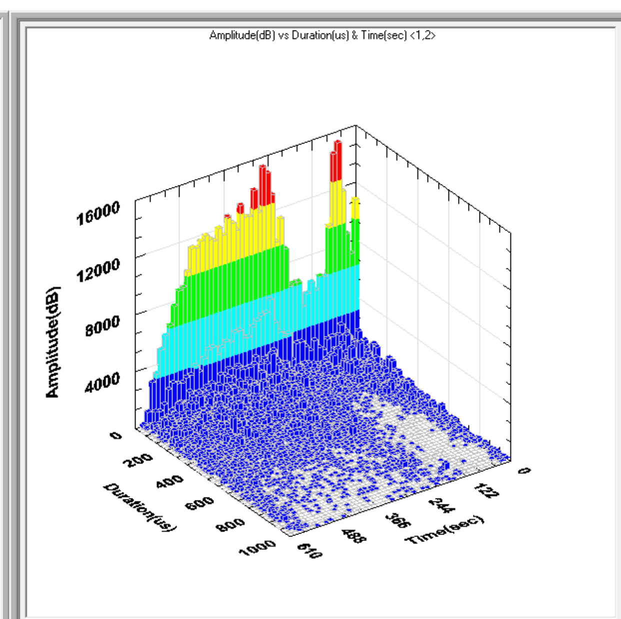

<u>Number of Hits vs. Axial Stress (MPa): Channel 1</u>

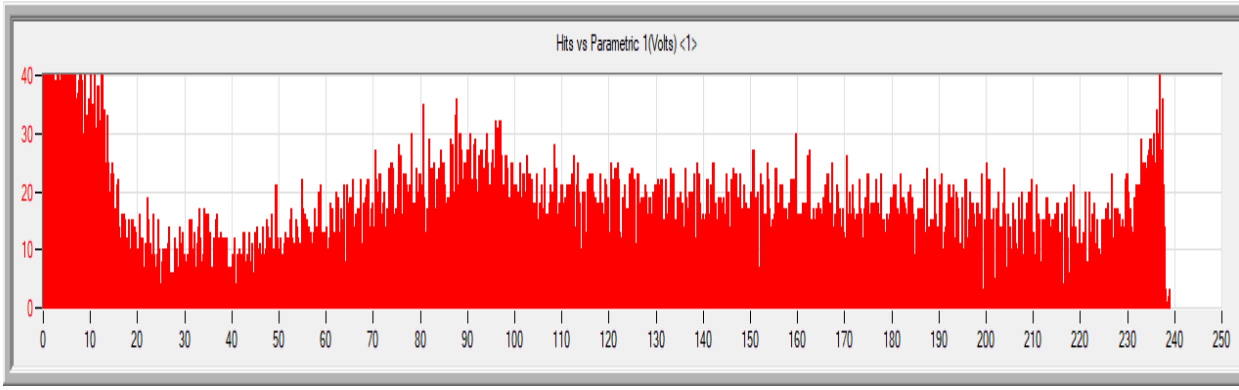

<u>Number of Hits vs. Axial Stress (MPa): Channel 2</u>

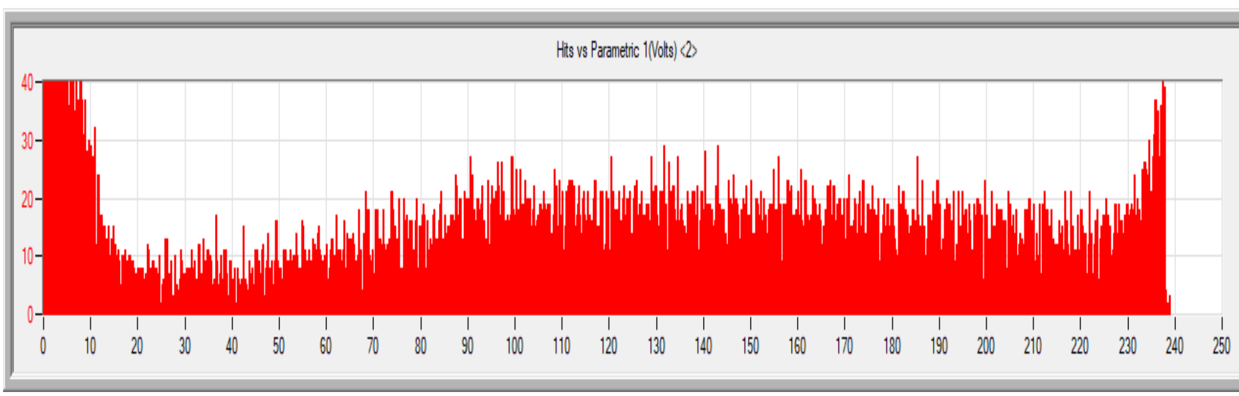

<u>Number of Hits vs. Axial Stress (MPa): Channels 1+2</u>

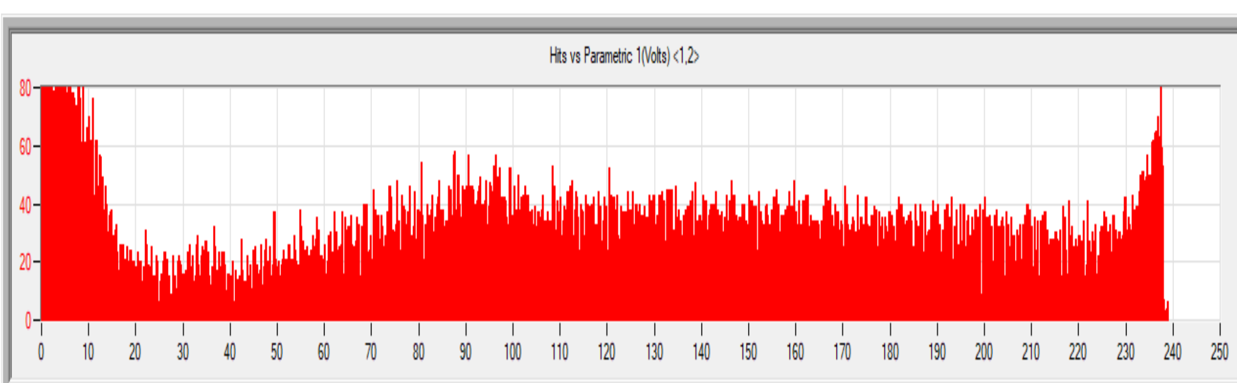

May 21, 2021

Cumulative Number of Hits vs. Axial Stress (MPa): Channel 1

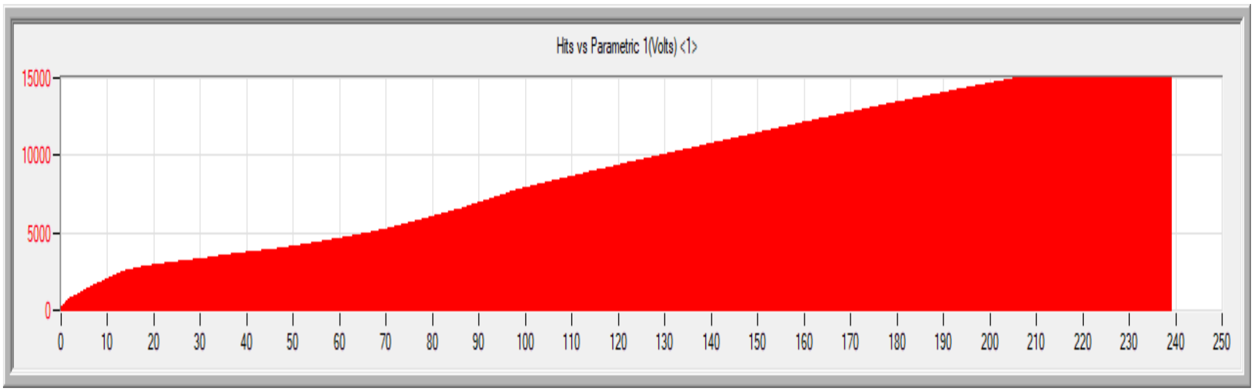

May 21, 2021

Cumulative Number of Hits vs. Axial Stress (MPa): Channel 2

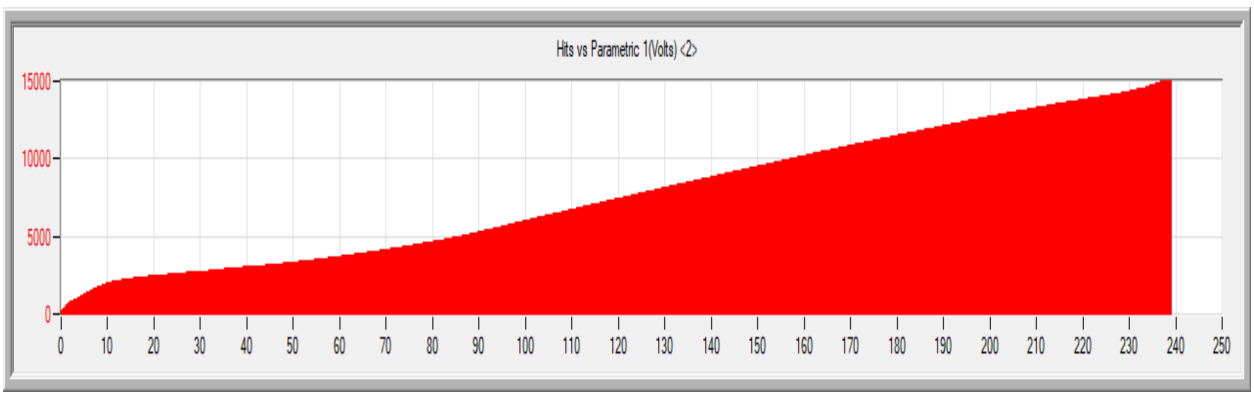

May 21, 2021

Cumulative Number of Hits vs. Axial Stress (MPa): Channels 1+2

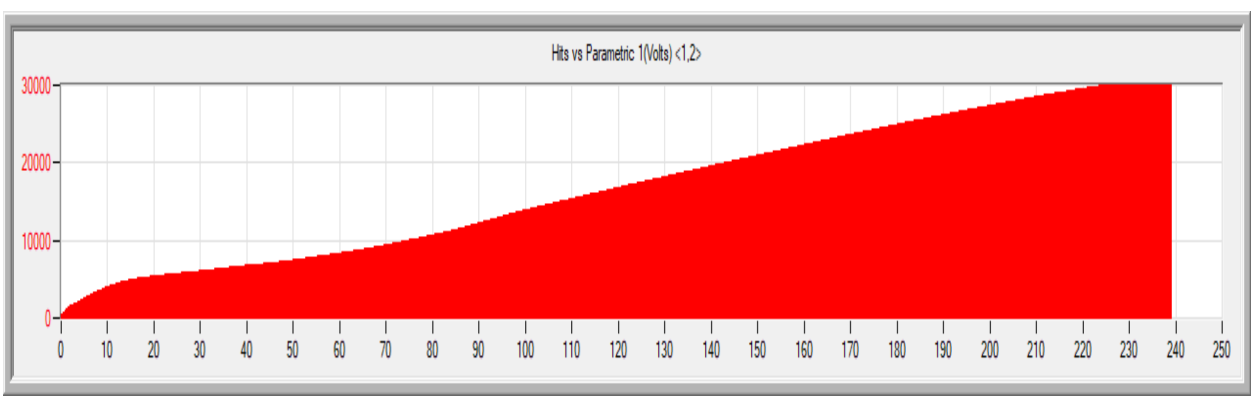

Test Summary

```
P:\lab data\S Gaines\P-002797.002_Golder_NWMO\Data\Batch 2 (Fall 2019)\AE\IG-UC005\IG-UC005.dta

Total AEHits   :      18918
Total TDDs     :         51
Total Waveforms:      18918
Total Resumes  :          1
Total Pauses   :          1
Total TimeMarks:          0

Channel         AEHits
      1          10137
      2           8781

HIT DRIVEN DATA:
         Feature Chan         Minimum         Maximum         Average         Std Dev
        Risetime    1          0.0000      12675.0000         96.0565        607.3259
          Counts    1          1.0000      21793.0000         33.2688        454.5408
          Energy    1          0.0000      65535.0000         23.1108        958.7919
        Duration    1          0.0000    1000000.0000        681.4039      15203.5086
       Amplitude    1         40.0000        100.0000         45.0755          5.9078
       Threshold    1         40.0000         40.0000         40.0000          0.0024
     SigStrength    1          0.0000 1741107200.0000     377257.9688   22366134.8135
       AbsEnergy    1          0.0000 7138859008.0000    1214785.5000   83239528.3689
     Parametric1    1          0.0000        223.5071        142.4773         80.8508
        Risetime    2          0.0000      11088.0000         48.3939        341.6838
          Counts    2          1.0000      22306.0000         20.6750        415.3261
          Energy    2          0.0000      65535.0000         26.7898       1220.3285
        Duration    2          0.0000     773138.0000        464.7469      13410.4724
       Amplitude    2         40.0000        100.0000         45.0771          5.4825
       Threshold    2         40.0000         40.0000         40.0000          0.0009
     SigStrength    2          0.0000  817433088.0000     246497.0625   12014555.5591
       AbsEnergy    2          0.0000 3495696896.0000     809330.9375   44671743.0565
     Parametric1    2          0.0284        223.4786        145.0988         80.1971

TIME DRIVEN DATA:
         Feature Chan         Minimum         Maximum         Average         Std Dev
             asl    1         26.0000         56.0000         30.6078          5.4596
             asl    2         25.0000         51.0000         27.9216          4.6478
             asl   96          0.0000          0.0000          0.0000          0.0000
             asl  104          0.0000          0.0000          0.0000          0.0000
     Parametric1              1.3368        223.2795        128.4860         70.3651
```

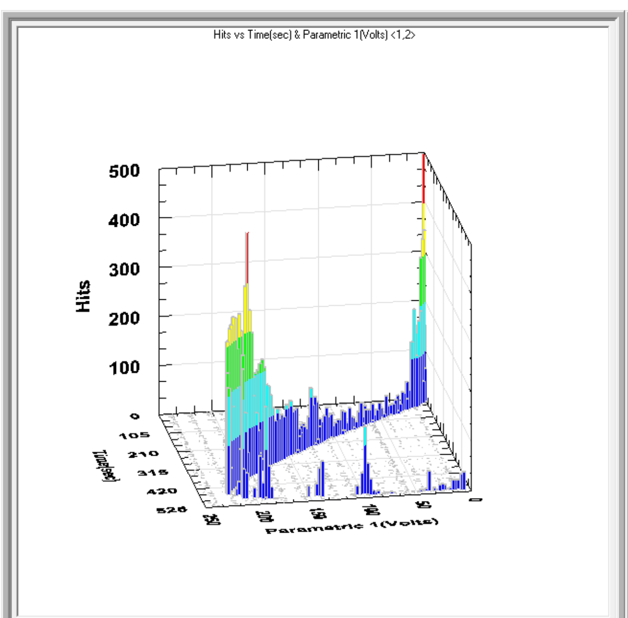

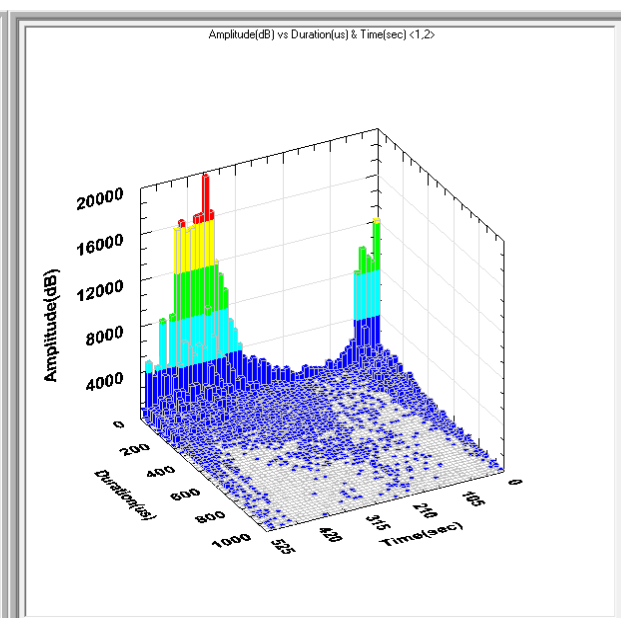

Number of Hits vs. Axial Stress (MPa): Channel 1

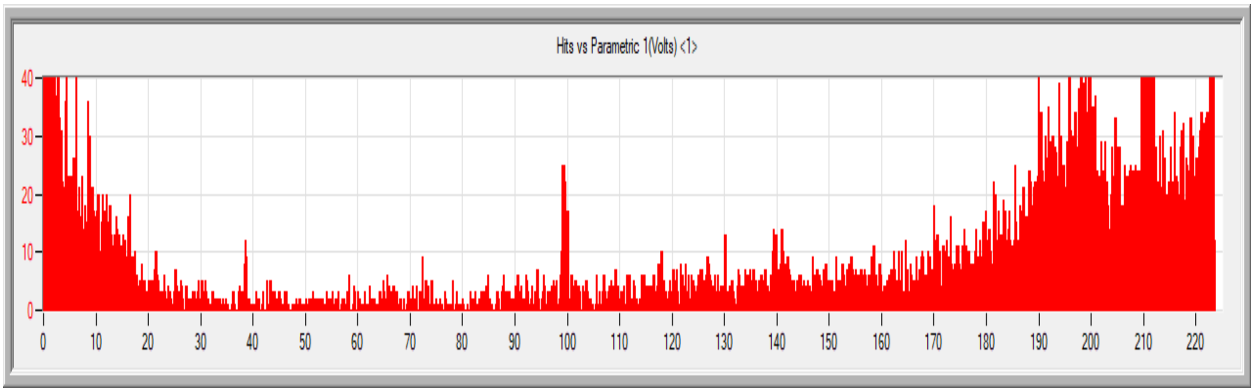

Number of Hits vs. Axial Stress (MPa): Channel 2

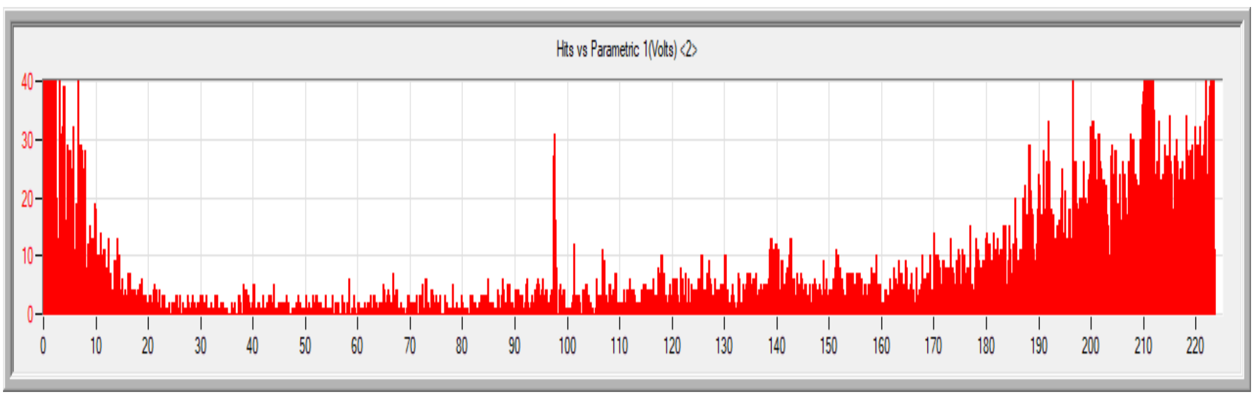

Number of Hits vs. Axial Stress (MPa): Channels 1+2

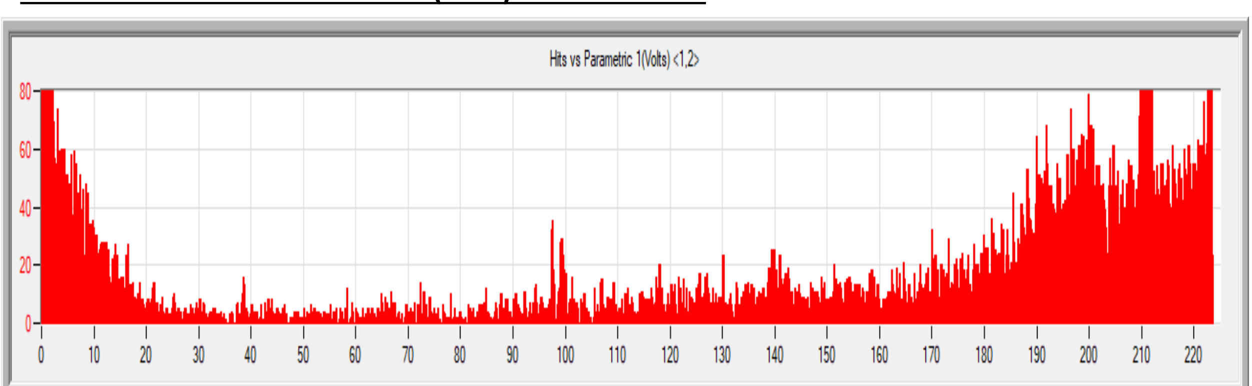

Cumulative Number of Hits vs. Axial Stress (MPa): Channel 1

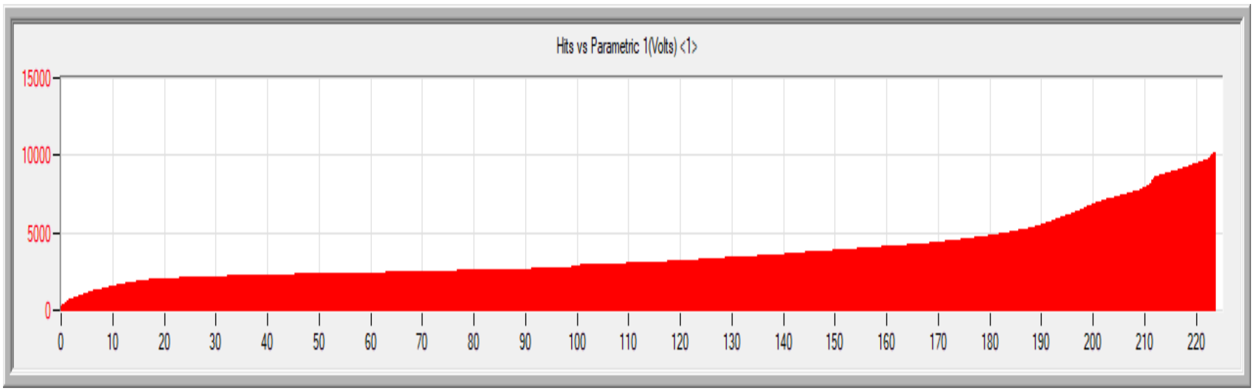

Cumulative Number of Hits vs. Axial Stress (MPa): Channel 2

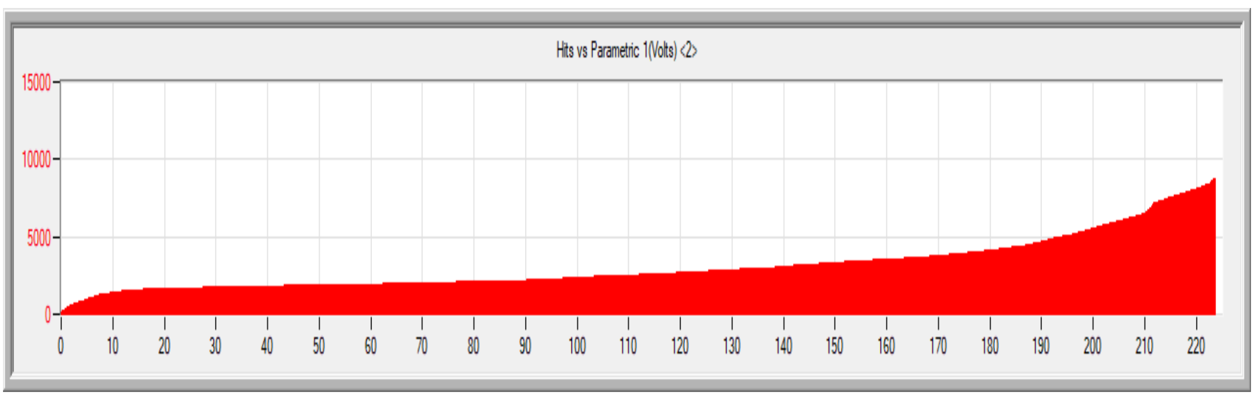

Cumulative Number of Hits vs. Axial Stress (MPa): Channels 1+2

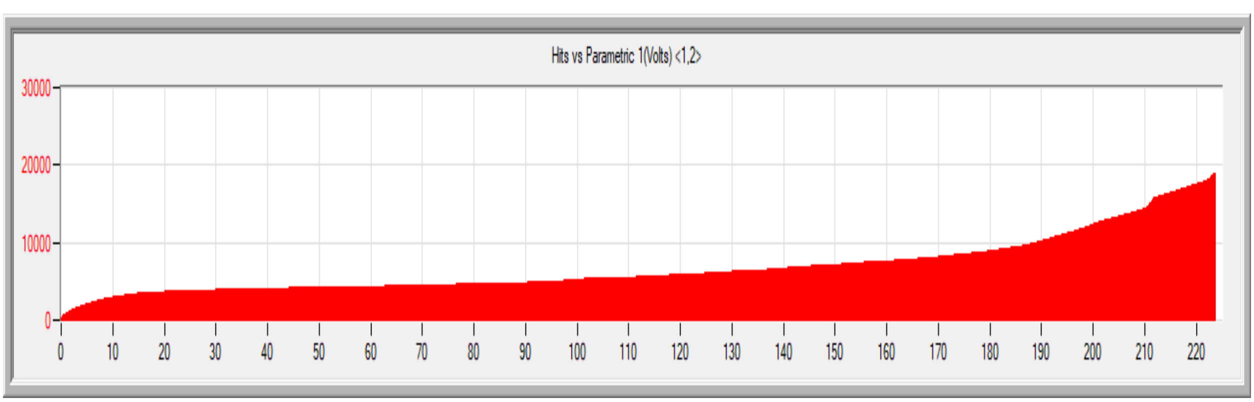

Test Summary

P:\lab data\S Gaines\P-002797.002_Golder_NWMO\Data\Batch 2 (Fall 2019)\AE\IG-UC006\IG-UC006.dta

Total AEHits	:	30175
Total TDDs	:	62
Total Waveforms	:	30175
Total Resumes	:	1
Total Pauses	:	1
Total TimeMarks	:	0

Channel	AEHits
1	13986
2	16189

HIT DRIVEN DATA:

Feature	Chan	Minimum	Maximum	Average	Std Dev
Risetime	1	0.0000	12940.0000	128.9941	833.3984
Counts	1	1.0000	31495.0000	80.5087	928.5723
Energy	1	0.0000	65535.0000	76.2403	1818.0314
Duration	1	0.0000	1000000.0000	1937.4819	34335.0956
Amplitude	1	40.0000	100.0000	47.2694	8.0305
Threshold	1	40.0000	40.0000	40.0000	0.0086
SigStrength	1	0.0000	11418544128.0000	2161105.2500	119511909.8579
AbsEnergy	1	0.0000	77157580800.0000	8176354.0000	682005591.6796
Parametric1	1	-0.0284	242.6778	129.9952	75.2469
Risetime	2	0.0000	13069.0000	140.1355	840.1137
Counts	2	1.0000	31355.0000	93.7932	1053.3918
Energy	2	0.0000	65535.0000	68.0190	1647.1239
Duration	2	0.0000	1000000.0000	1779.7452	29872.2294
Amplitude	2	40.0000	100.0000	46.7718	8.0090
Threshold	2	40.0000	40.0000	40.0000	-1.#IND
SigStrength	2	0.0000	3875485952.0000	1125785.1250	50186418.5728
AbsEnergy	2	0.0000	12835443712.0000	1917595.0000	123497599.8143
Parametric1	2	-0.0284	242.6209	120.9073	74.3009

TIME DRIVEN DATA:

Feature	Chan	Minimum	Maximum	Average	Std Dev
asl	1	23.0000	72.0000	33.4516	9.2748
asl	2	25.0000	69.0000	36.2419	8.0175
asl	96	0.0000	0.0000	0.0000	0.0000
asl	104	0.0000	0.0000	0.0000	0.0000
Parametric1		0.8533	242.3934	121.6316	79.0901

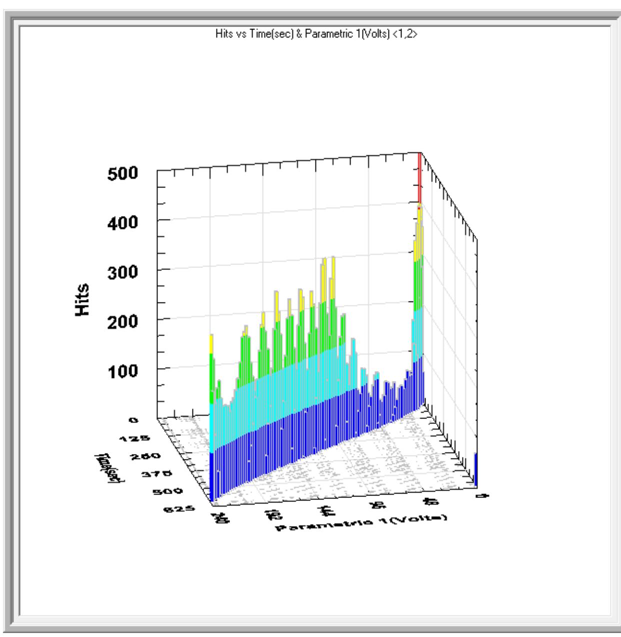

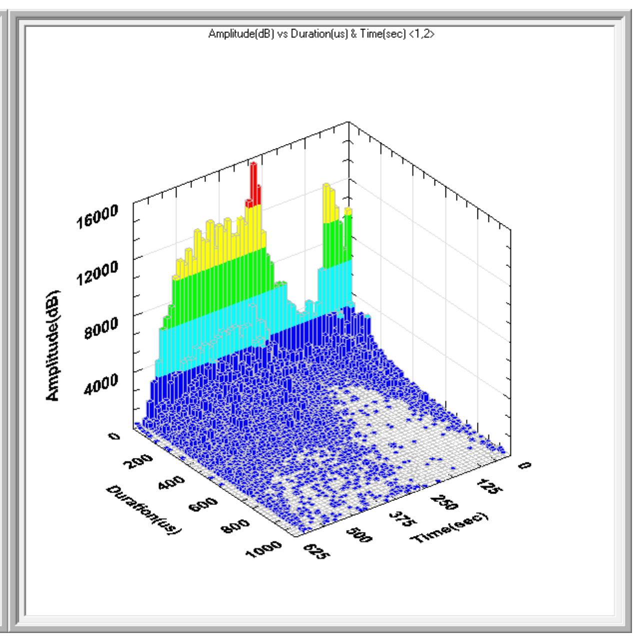

Number of Hits vs. Axial Stress (MPa): Channel 1

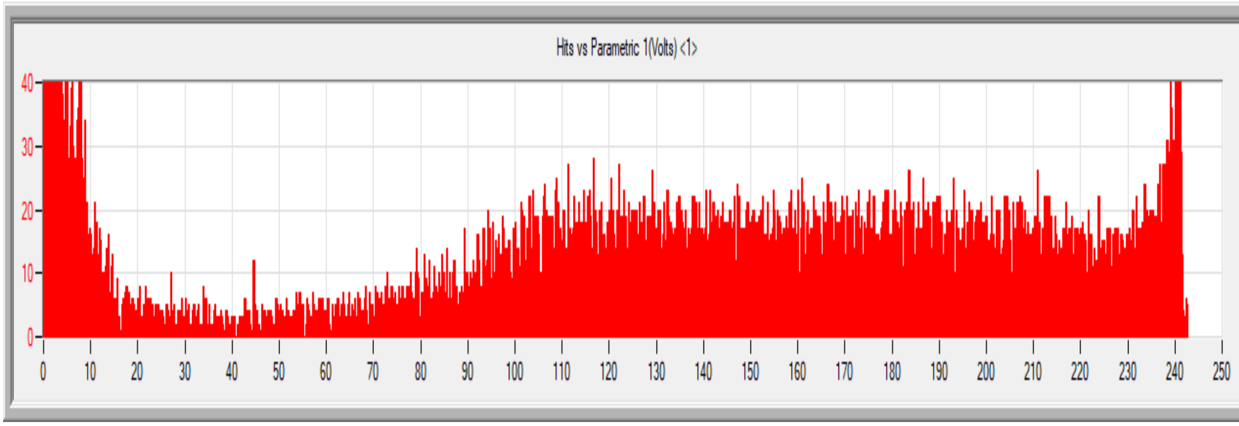

Number of Hits vs. Axial Stress (MPa): Channel 2

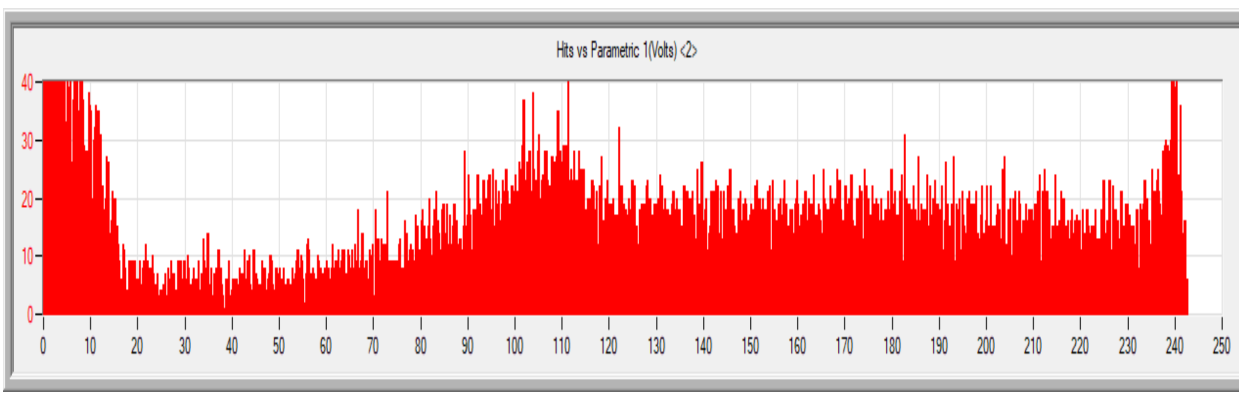

Number of Hits vs. Axial Stress (MPa): Channels 1+2

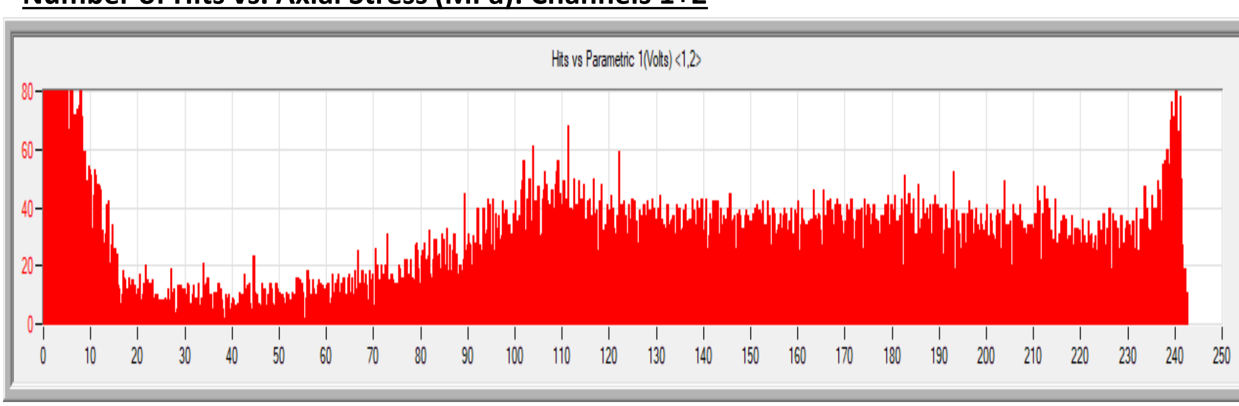

Cumulative Number of Hits vs. Axial Stress (MPa): Channel 1

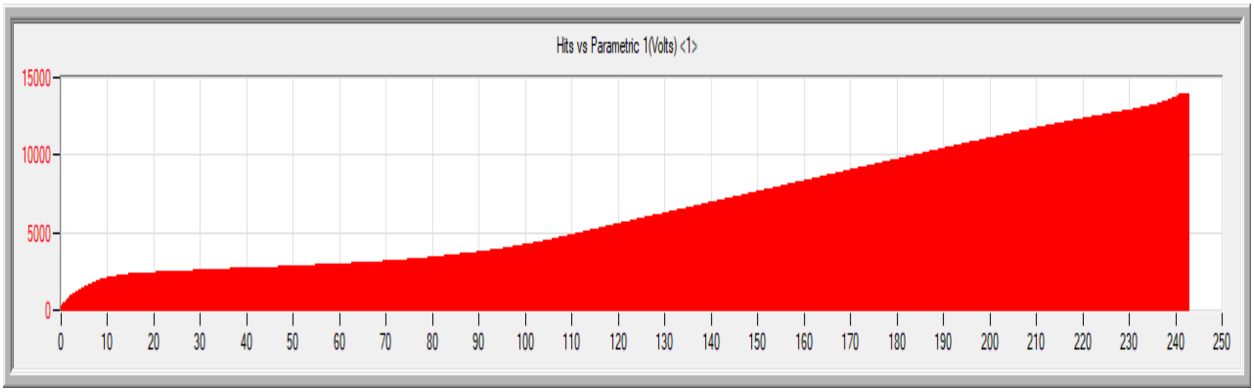

Cumulative Number of Hits vs. Axial Stress (MPa): Channel 2

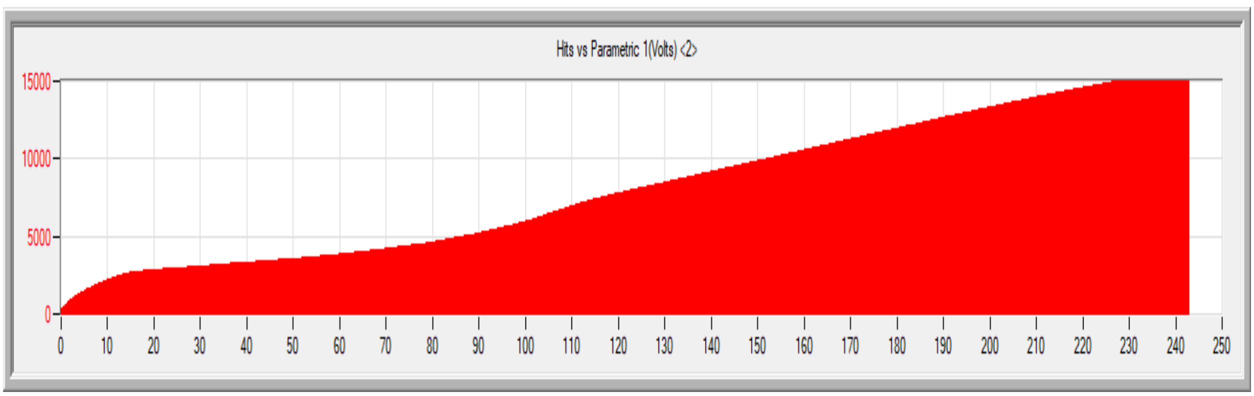

Cumulative Number of Hits vs. Axial Stress (MPa): Channels 1+2

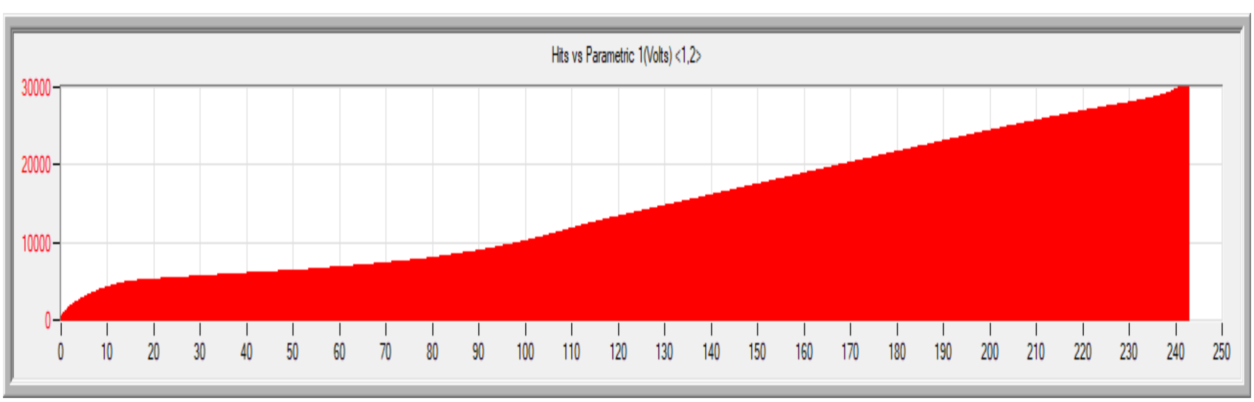

Test Summary

```
P:\lab data\S Gaines\P-002797.002_Golder_NWMO\Data\Batch 2 (Fall 2019)\AE\IG-UC-007\IG-UC007.dta

Total AEHits    :       27888
Total TDDs      :          62
Total Waveforms:        27888
Total Resumes   :           1
Total Pauses    :           1
Total TimeMarks:            0

Channel          AEHits
      1           14049
      2           13839


HIT DRIVEN DATA:
         Feature Chan         Minimum         Maximum         Average         Std Dev
        Risetime    1          0.0000      12914.0000        186.9875       1031.4310
          Counts    1          1.0000      30307.0000         93.0036       1003.5180
          Energy    1          0.0000      65535.0000         77.0878       1726.5174
        Duration    1          0.0000    1000000.0000       2424.3792      38117.8210
       Amplitude    1         40.0000        100.0000         46.8176          7.9593
       Threshold    1         40.0000         40.0000         40.0000         -1.#IND
     SigStrength    1          0.0000 8182845440.0000    1605621.2500    96121639.9561
       AbsEnergy    1          0.0000 53978836992.0000    6073285.0000 514765749.4770
     Parametric1    1          0.1707        243.7018        136.8745         59.1041
        Risetime    2          0.0000      12934.0000        159.2175        904.9362
          Counts    2          1.0000      31200.0000         90.3247        955.7763
          Energy    2          0.0000      65535.0000         60.8283       1460.7807
        Duration    2          0.0000    1000000.0000       1958.5786      32942.6472
       Amplitude    2         40.0000        100.0000         47.3184          8.1077
       Threshold    2         40.0000         40.0000         40.0000         -1.#IND
     SigStrength    2          0.0000 8807975936.0000    1305196.2500    85078795.0756
       AbsEnergy    2          0.0000 50371629056.0000    4581258.0000 439441347.0048
     Parametric1    2          0.2275        243.7587        142.3481         59.4034

TIME DRIVEN DATA:
         Feature Chan         Minimum         Maximum         Average         Std Dev
             asl    1         25.0000         59.0000         33.9355          7.7623
             asl    2         20.0000         57.0000         32.2581          8.0160
             asl   96          0.0000          0.0000          0.0000          0.0000
             asl  104          0.0000          0.0000          0.0000          0.0000
             asl  105          0.0000          0.0000          0.0000          0.0000
             asl  108         71.9924         71.9924         49.9302         33.1899
     Parametric1               1.0808        243.3889        120.9691         78.0923
```

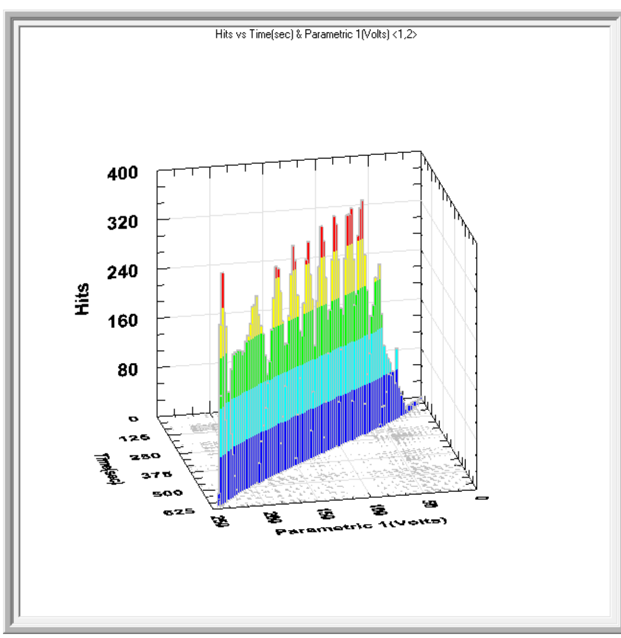

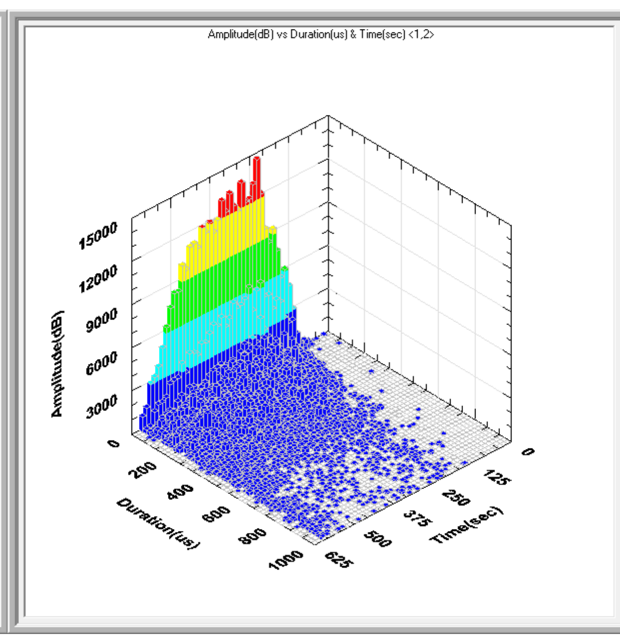

Number of Hits vs. Axial Stress (MPa): Channel 1

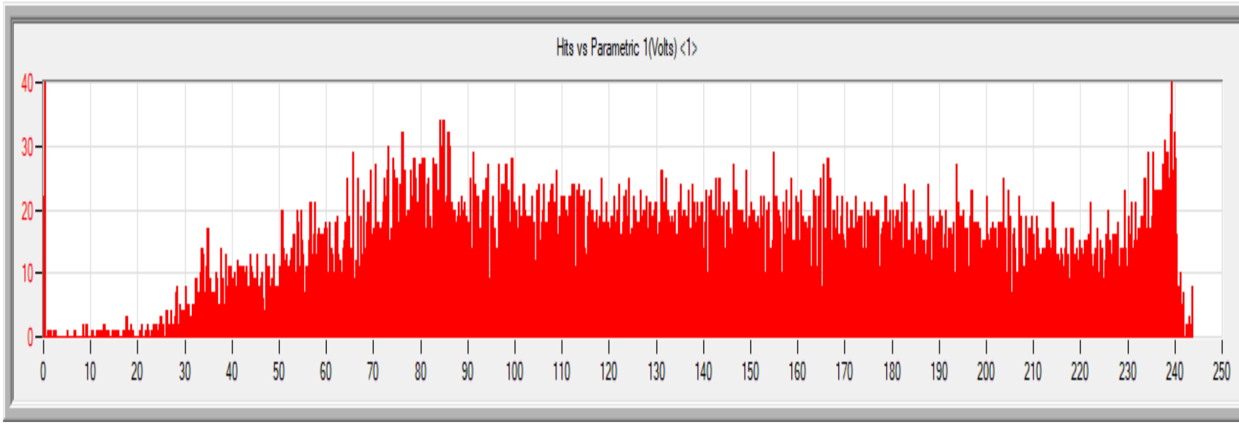

Number of Hits vs. Axial Stress (MPa): Channel 2

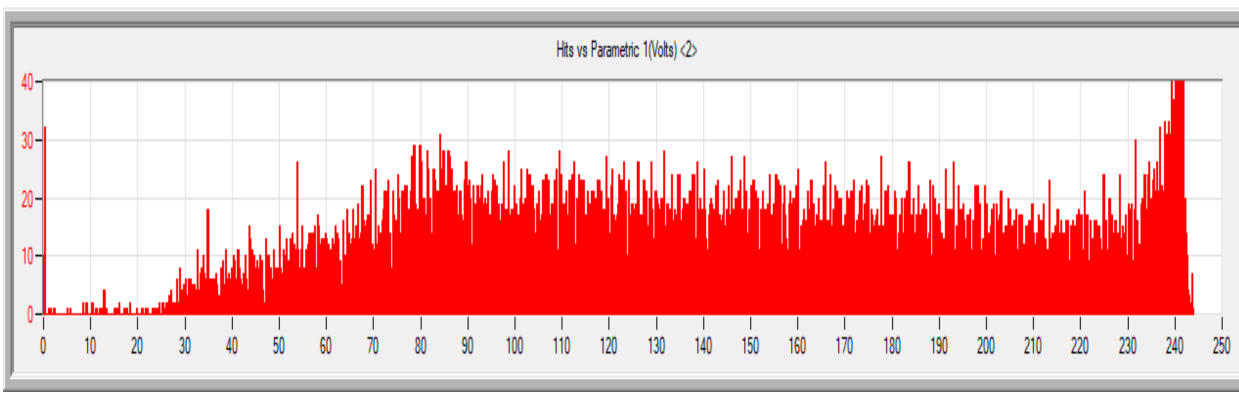

Number of Hits vs. Axial Stress (MPa): Channels 1+2

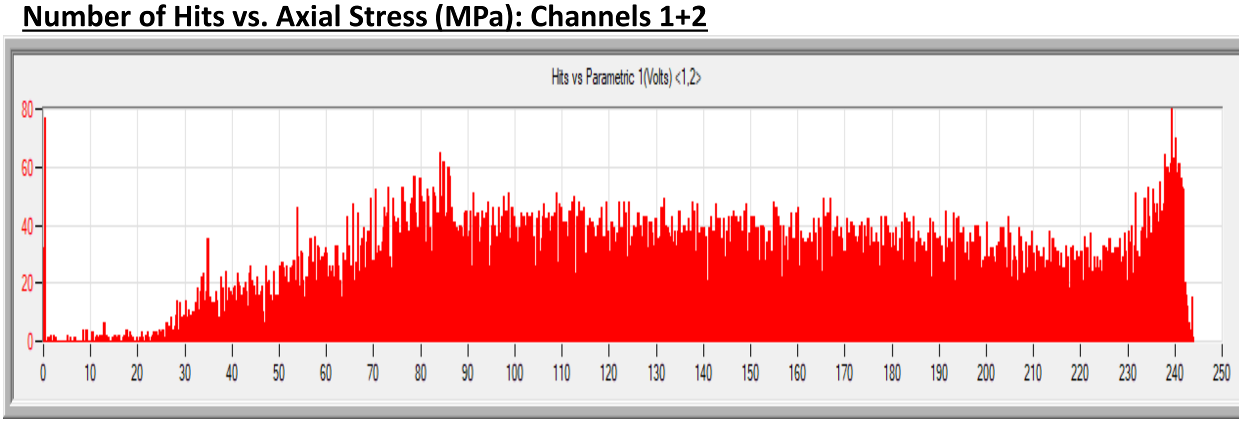

<u>Cumulative Number of Hits vs. Axial Stress (MPa): Channel 1</u>

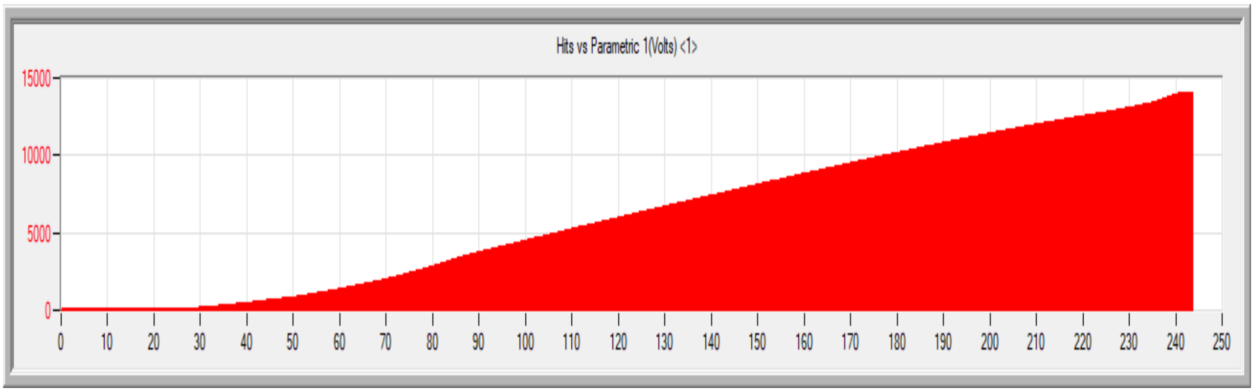

<u>Cumulative Number of Hits vs. Axial Stress (MPa): Channel 2</u>

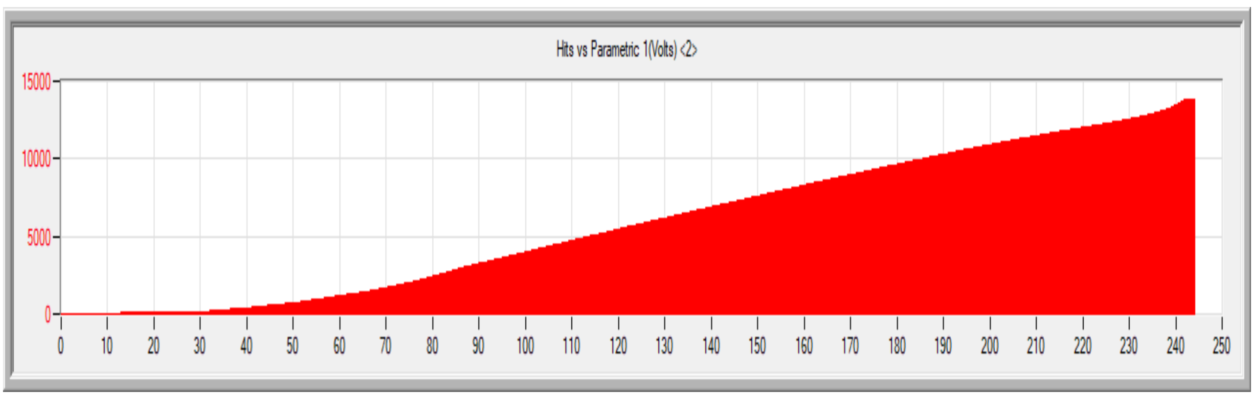

<u>Cumulative Number of Hits vs. Axial Stress (MPa): Channels 1+2</u>

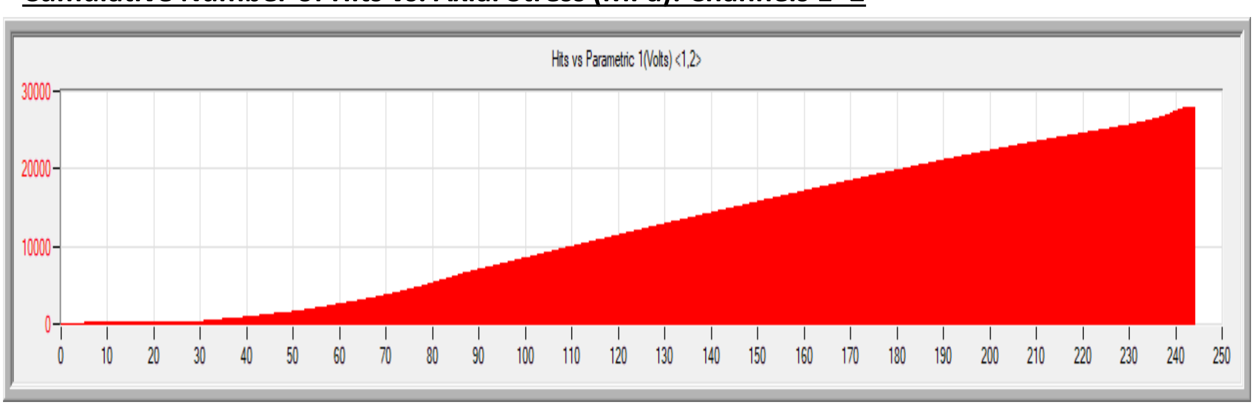

APPENDIX C

Indirect Tensile (Brazilian) Strength Tests: Load-Time and Stress-Displacement Graphs and Photographs of Intact and Broken Test Specimens

Table C-1: List of indirect tensile (Brazilian) test specimens

Specimen No.	**Depth (m)[1]**	**Rock Type**	**Page**
IG_BH01_BR001	416.20	Biotite Granodiorite-Tonalite	C-2
IG_BH01_BR002	455.42	Biotite Granodiorite-Tonalite	C-3
IG_BH01_BR003	494.73	Biotite Granodiorite-Tonalite	C-4
IG_BH01_BR004	540.42	Biotite Granodiorite-Tonalite	C-5
IG_BH01_BR005	551.80	Amphibolite	C-6
IG_BH01_BR006	582.82	Biotite Granodiorite-Tonalite	C-7
IG_BH01_BR007	662.81	Biotite Granodiorite-Tonalite	C-8

[1]Top depth of prepared sub-sample (depth along borehole)

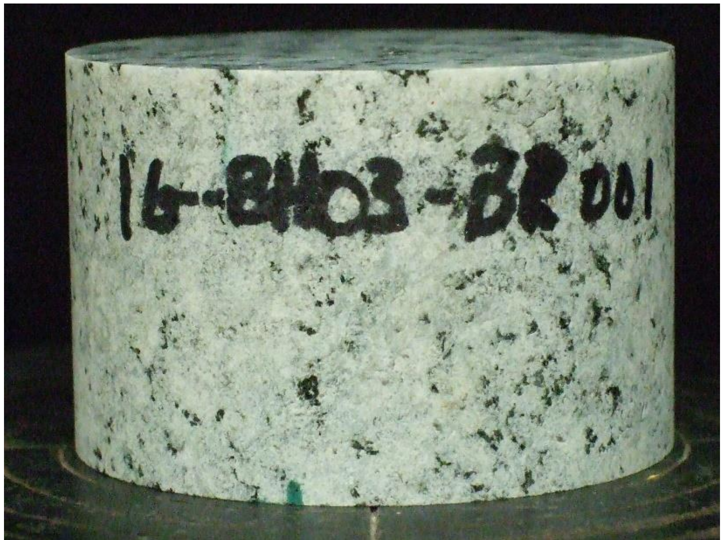

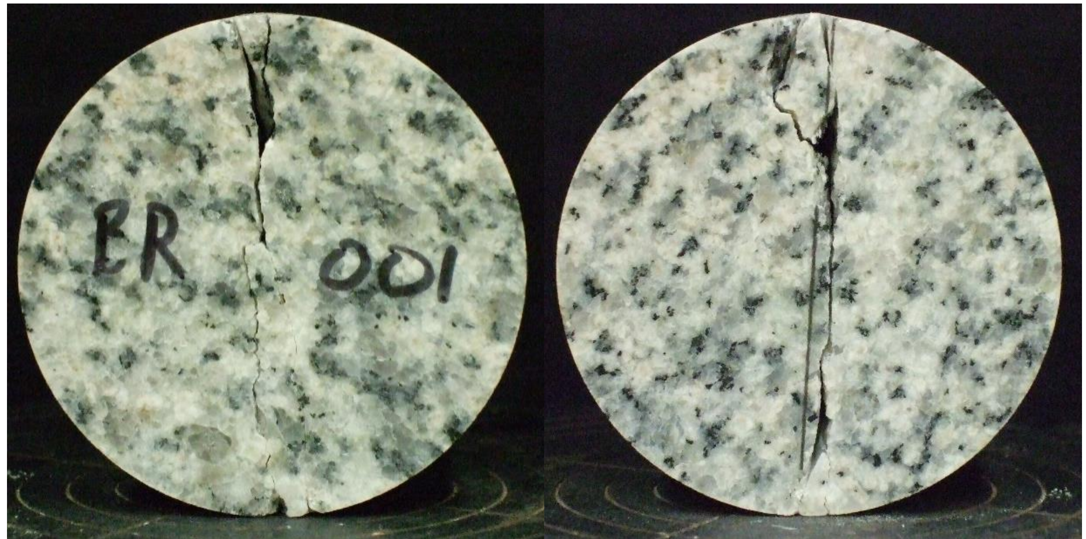

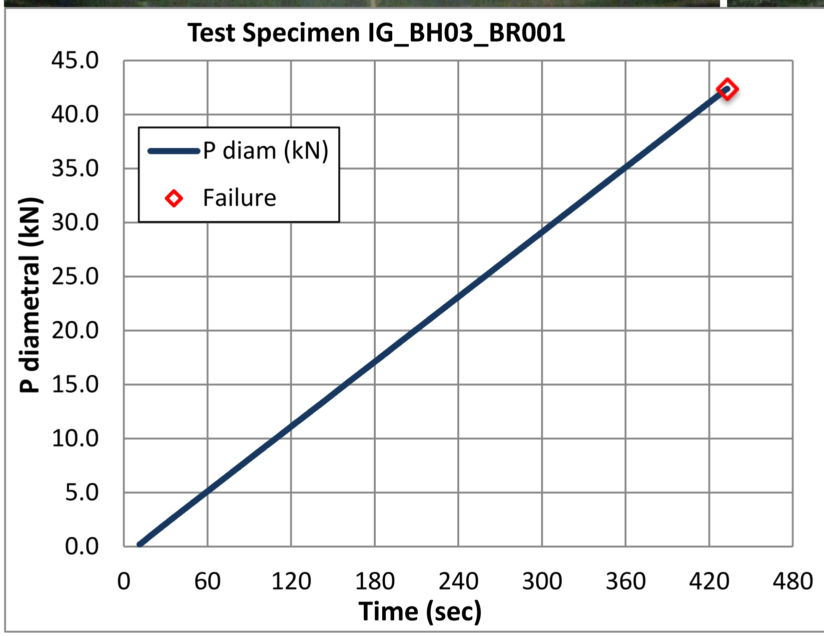

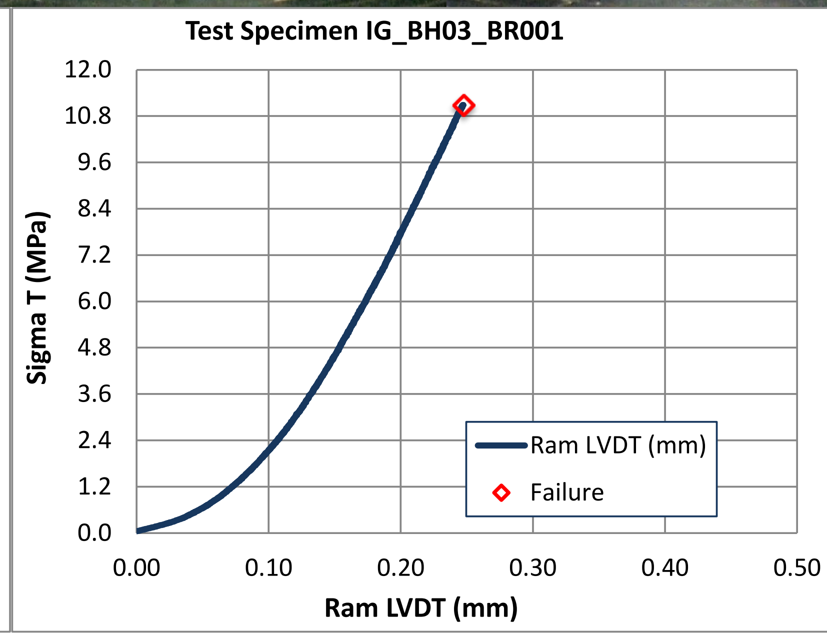

Test Specimen IG_BH03_BR001 – Depth = 416.20 m: Intact and broken specimen photographs; load-time and stress-displacement curves

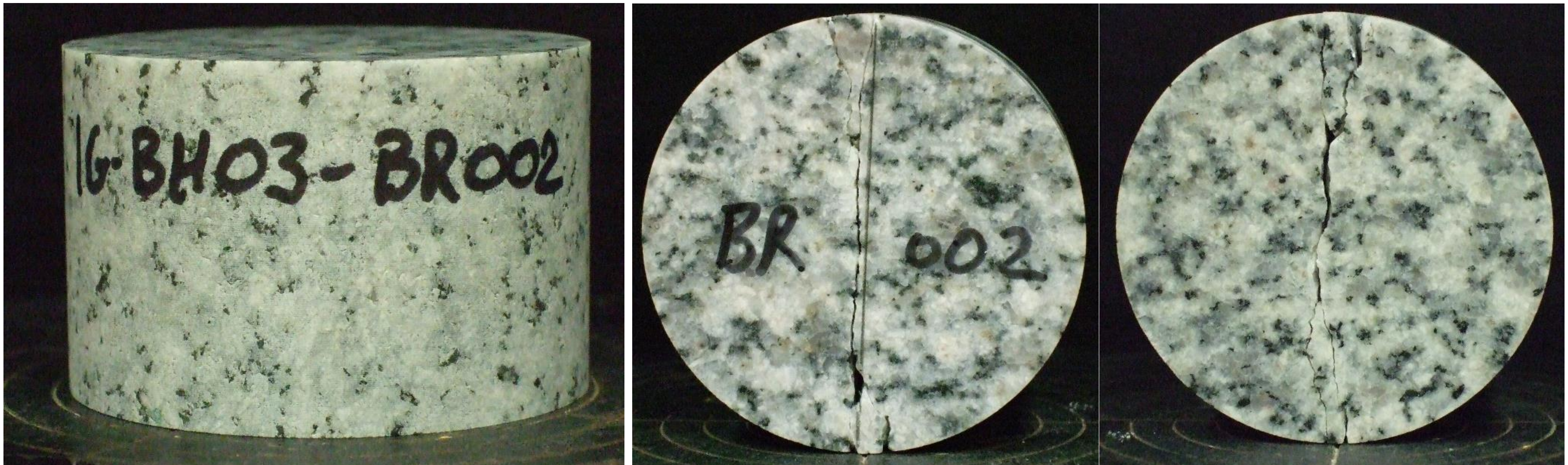

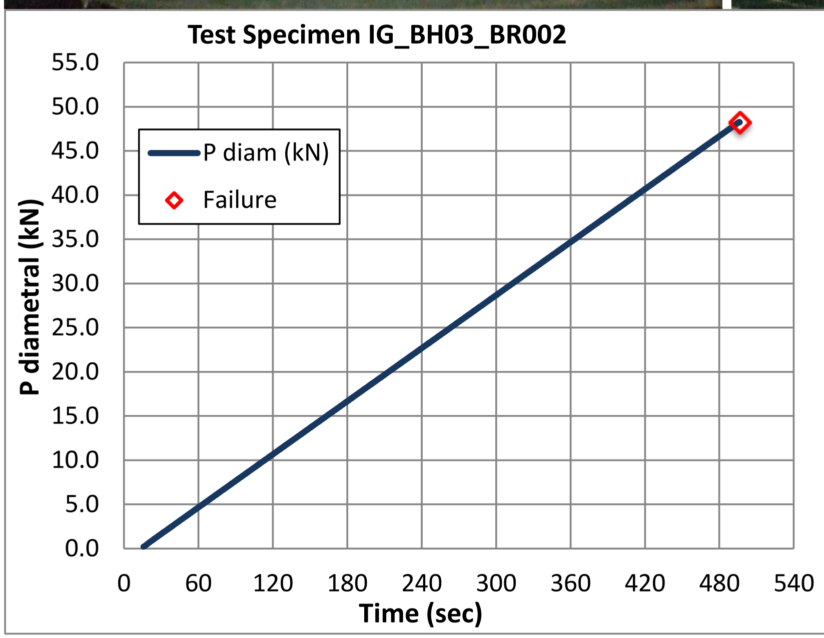

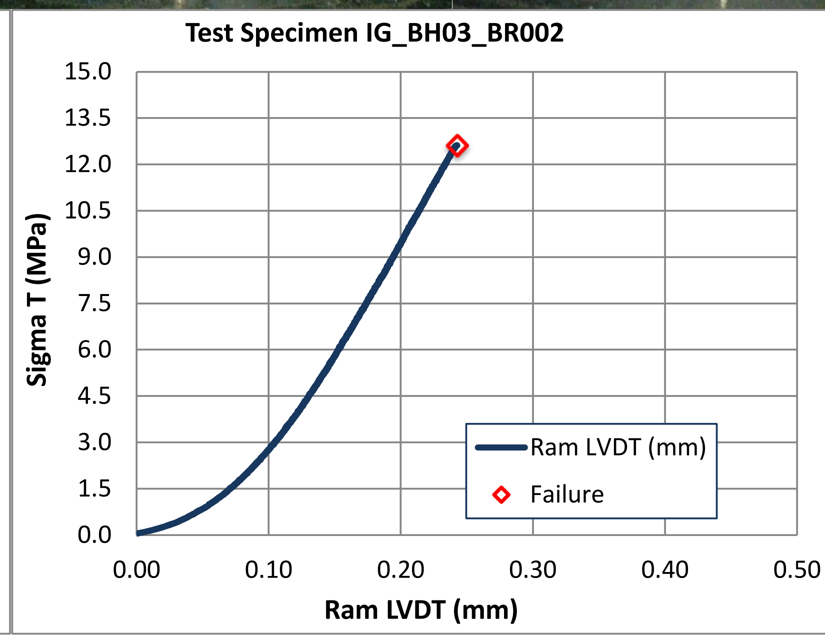

Test Specimen IG_BH03_BR002 – Depth = 455.42 m: Intact and broken specimen photographs; load-time and stress-displacement curves

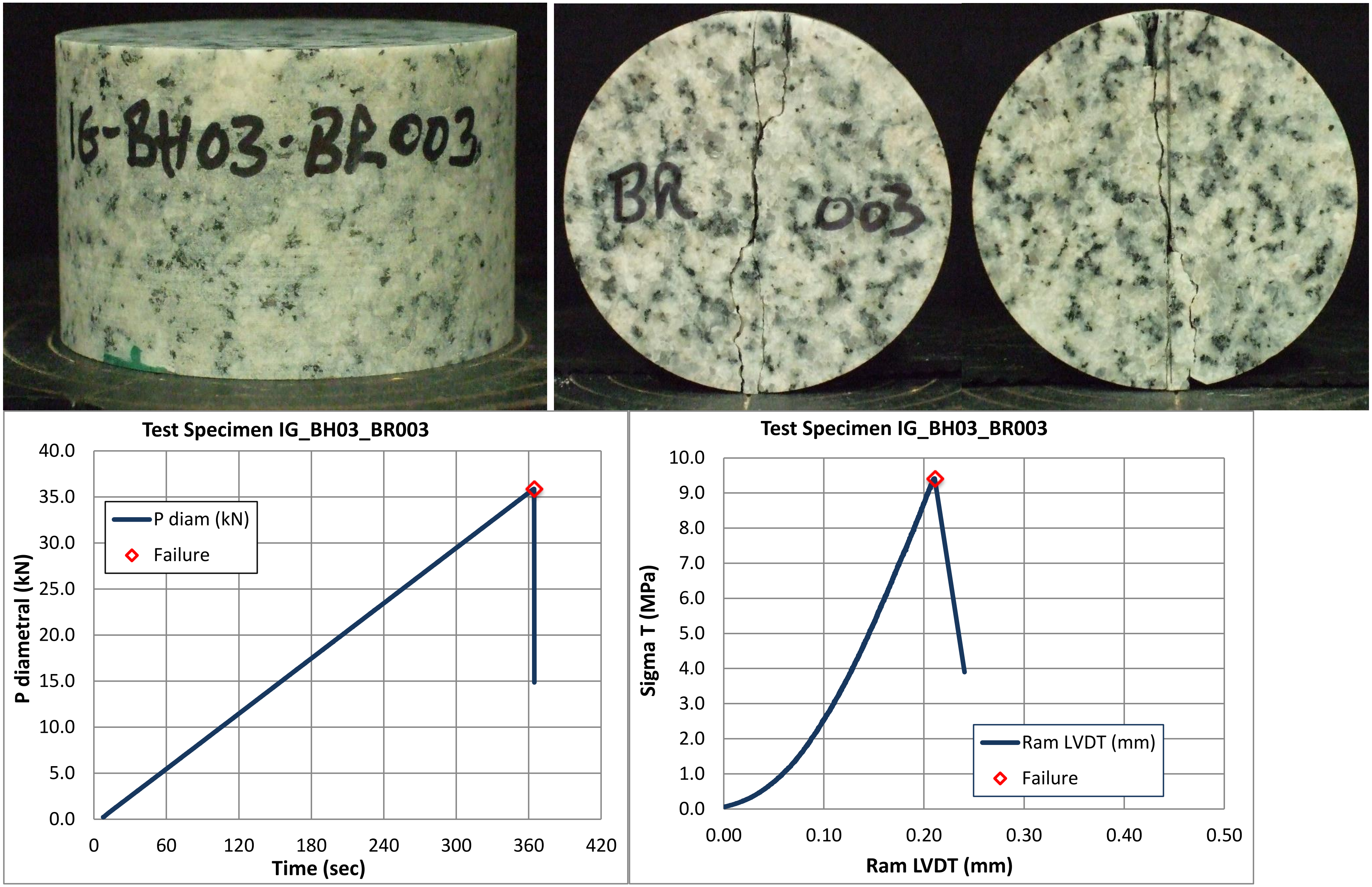

Test Specimen IG_BH03_BR003 – Depth = 494.73 m: Intact and broken specimen photographs; load-time and stress-displacement curves

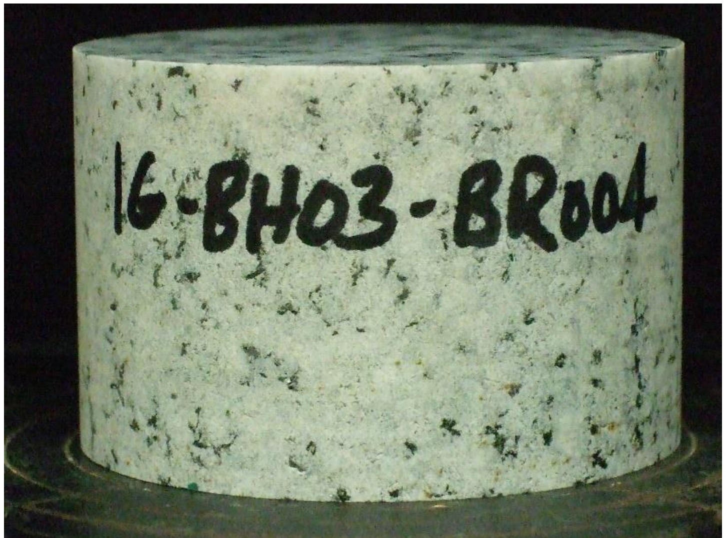

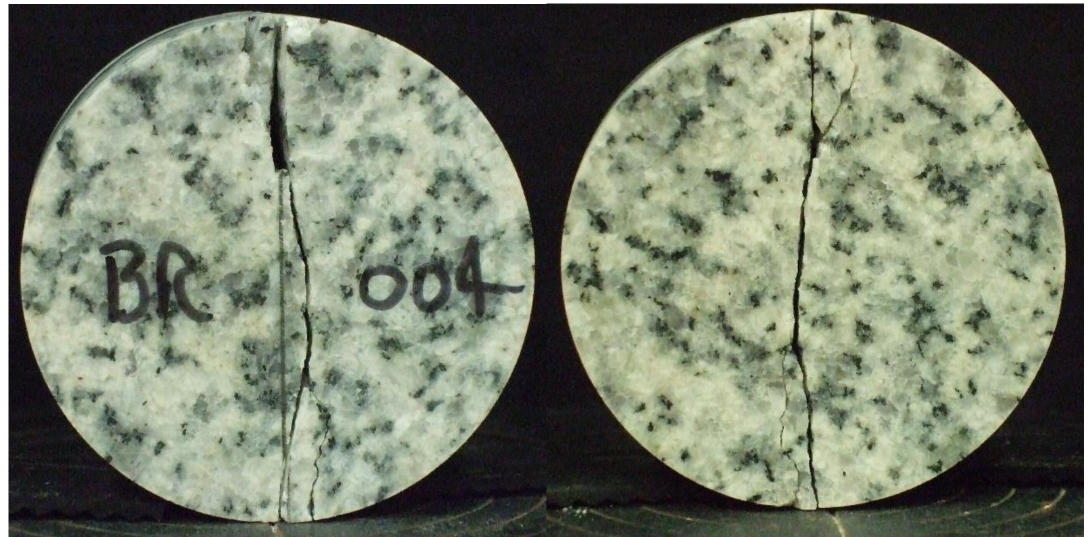

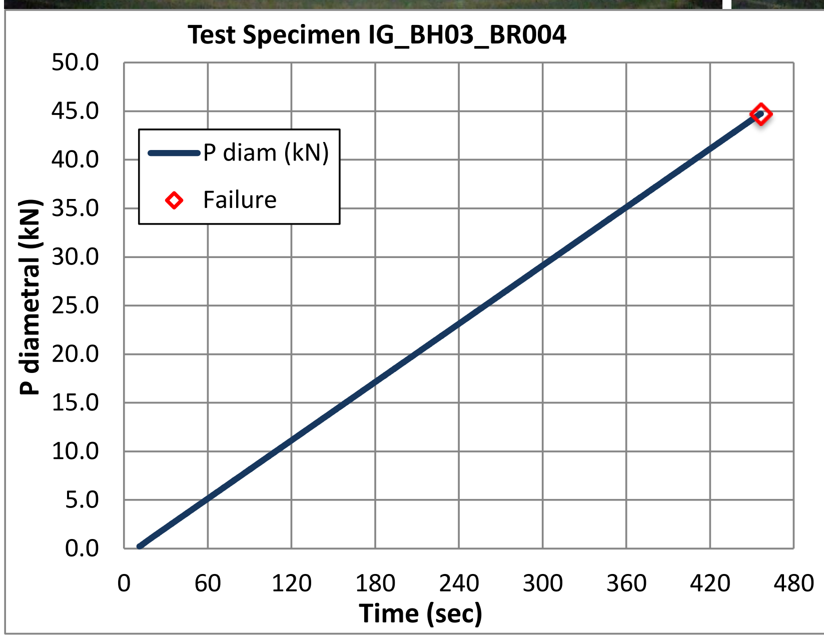

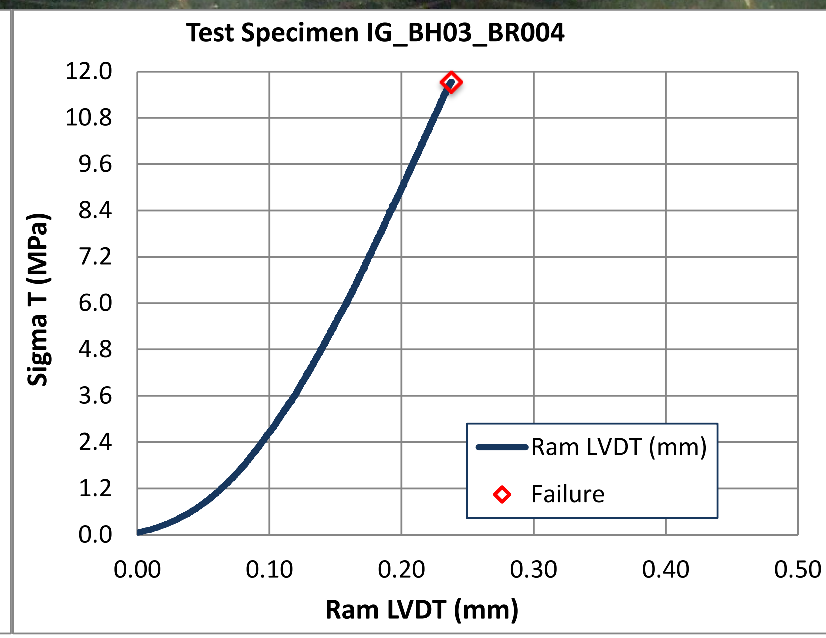

Test Specimen IG_BH03_BR004 – Depth = 540.42 m: Intact and broken specimen photographs; load-time and stress-displacement curves

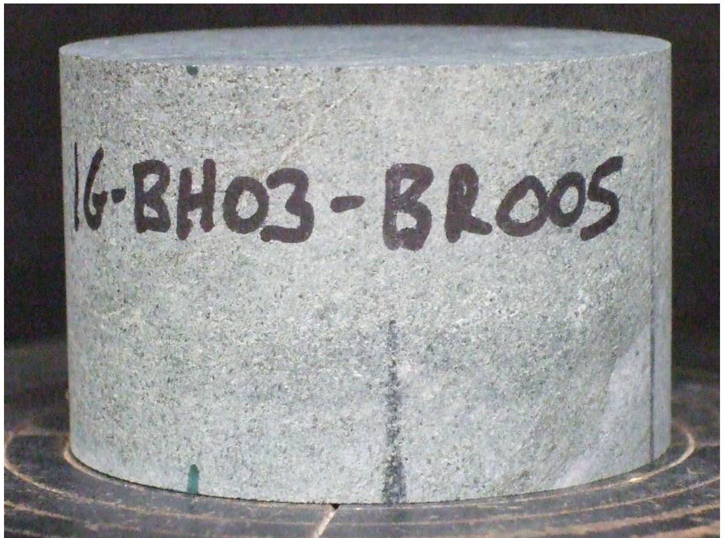

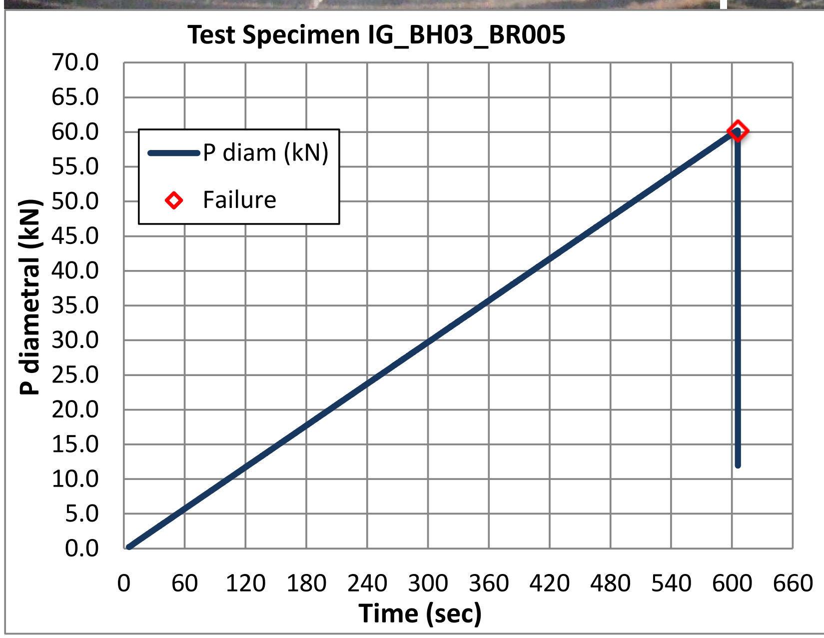

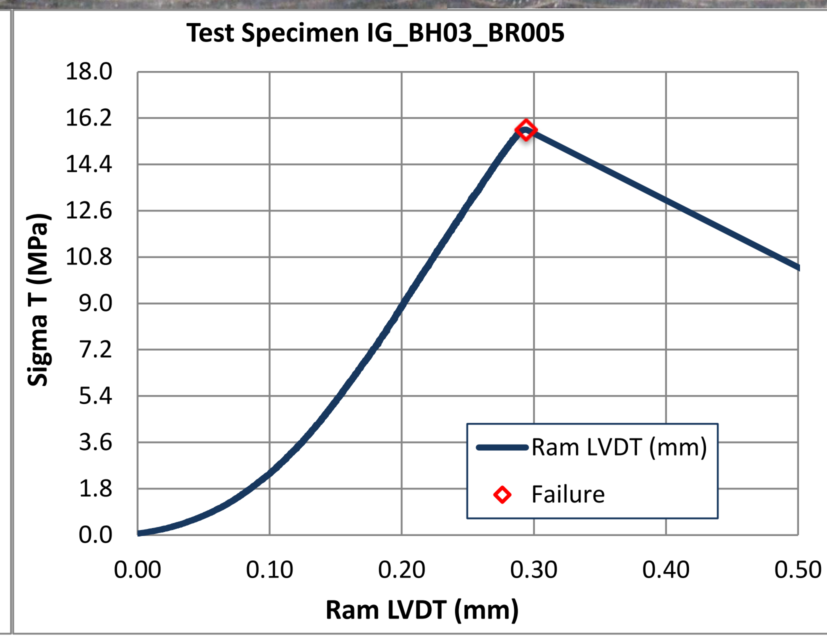

Test Specimen IG_BH03_BR005 – Depth = 551.80 m: Intact and broken specimen photographs; load-time and stress-displacement curves

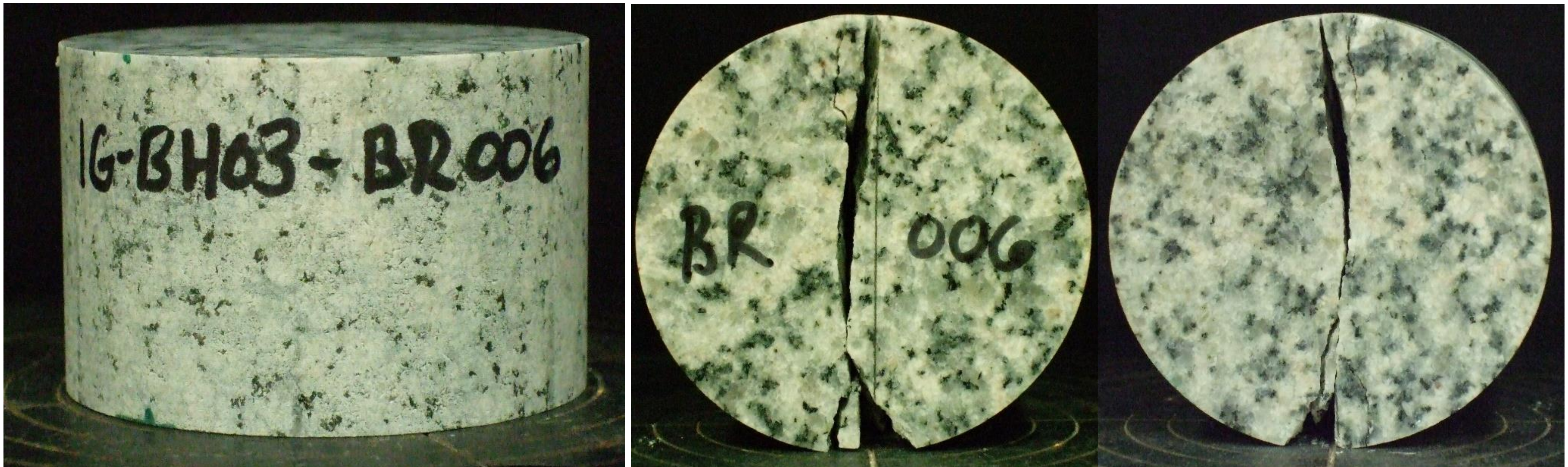

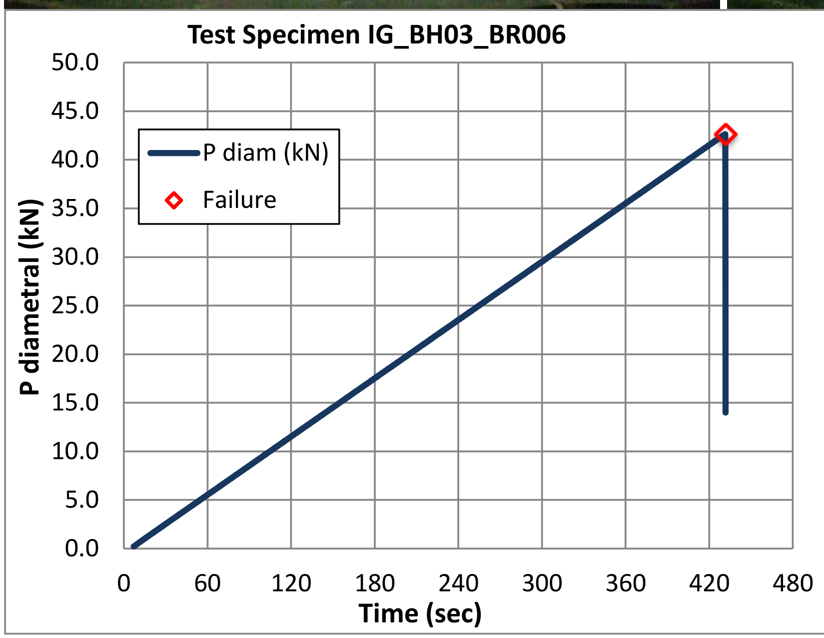

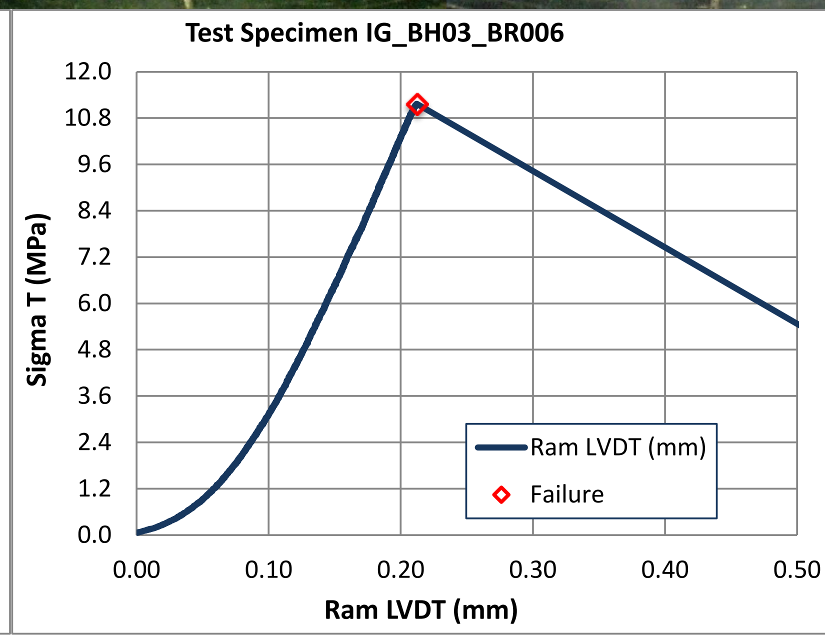

Test Specimen IG_BH03_BR006 – Depth = 582.82 m: Intact and broken specimen photographs; load-time and stress-displacement curves

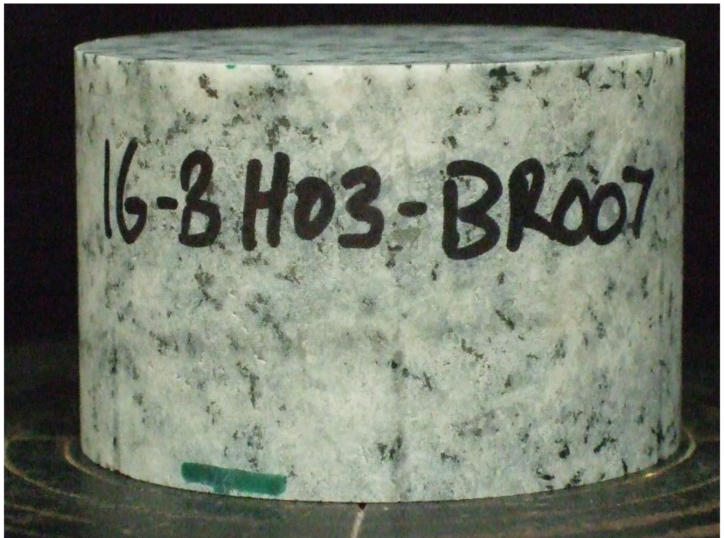

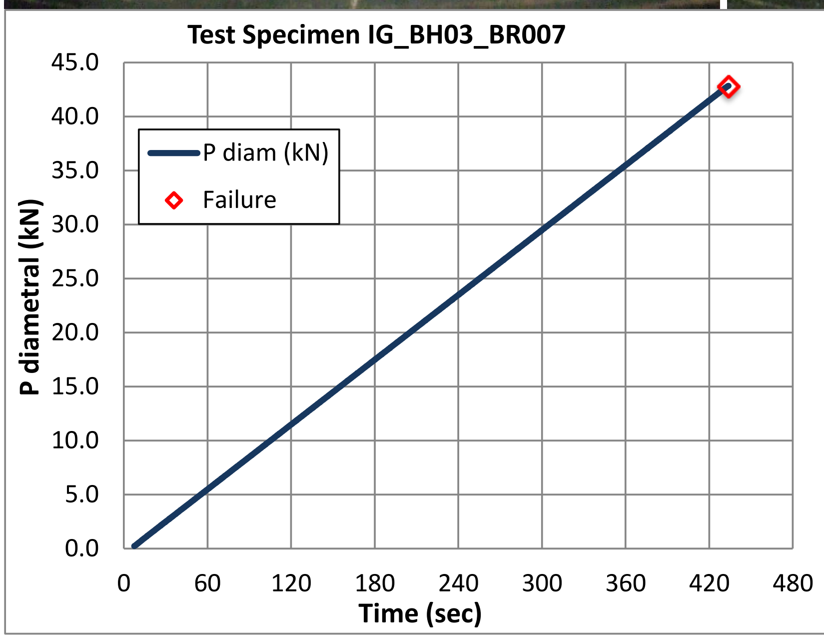

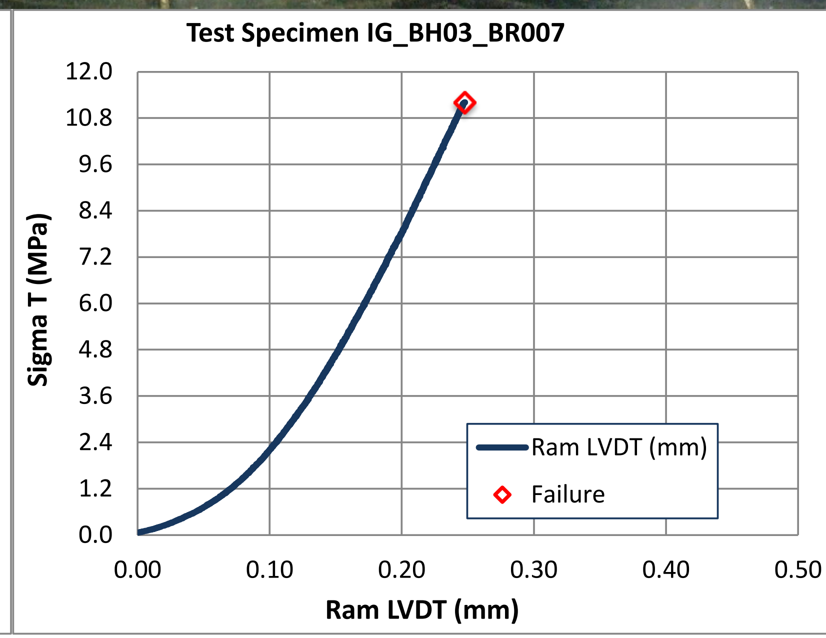

Test Specimen IG_BH03_BR007 – Depth = 662.81 m: Intact and broken specimen photographs; load-time and stress-displacement curves

APPENDIX D

Thermal Conductivity, Volumetric Heat Capacity and Thermal Diffusion Tests: Test Data and Graphs

Table D-1: List of thermal test specimens

Specimen No.	Depth (m)[1]	Rock Type	Page
IG_BH03_TH001[2]	304.71	Biotite Granodiorite-Tonalite	D-2
IG_BH03_TH002[2]	358.94	Biotite Granodiorite-Tonalite	D-4
IG_BH03_TH003[2]	416.43	Biotite Granodiorite-Tonalite	D-6
IG_BH03_TH004[2]	454.06	Biotite Granodiorite-Tonalite	D-8
IG_BH03_TH005[2]	495.01	Biotite Granodiorite-Tonalite	D-10
IG_BH03_TH006[2]	539.12	Biotite Granodiorite-Tonalite	D-12
IG_BH03_TH007[2]	548.19	Amphibolite	D-14
IG_BH03_TH008[2]	581.86	Biotite Granodiorite-Tonalite	D-16
IG_BH03_TH009[2]	800.64	Biotite Granodiorite-Tonalite	D-18
IG_BH03_TH011[3]	359.31	Biotite Granodiorite-Tonalite	D-20
IG_BH03_TH014[3]	495.54	Biotite Granodiorite-Tonalite	D-23
IG_BH03_TH016[3]	548.79	Amphibolite	D-26
IG_BH03_TH017[3]	582.25	Biotite Granodiorite-Tonalite	D-29
IG_BH03_TH018[3]	801.04	Biotite Granodiorite-Tonalite	D-32

[1] Top depth of prepared top sub-sample (depth along borehole).

[2] Preserved sample tested under as-received water content conditions. Sample was tested to temperatures beyond those specified in the Test Plan.

[3] Unpreserved samples. Sample was dried at 80°C before testing and at 110°C after testing.

GOLDER/NWMO/BH03TH001/304.71
IG_BH03_TH001

GOLDER/NWMO/BH03TH001/304.75
IG_BH03_TH001

Pretest Top Sample | **Posttest Top Sample** | **Pretest Bottom Sample** | **Posttest Bottom Sample**

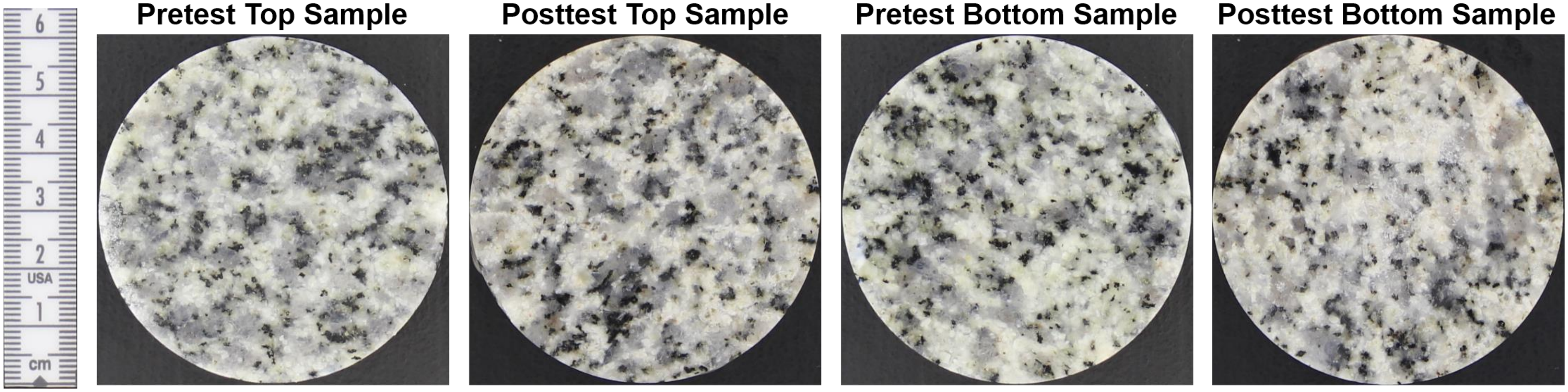

Test Specimen IG_BH03_TH001 – Depth = 304.71 m: specimen photographs

Table D-2: Hot Disk Results – Test Specimen IG_BH03_TH001 – Depth = 304.71 m

Average Temperature (°C)	Average Volumetric Specific Heat (MJ/m^3°K)	Average Thermal Conductivity (W/m°K)	Average Thermal Diffusivity (mm^2/s)
26.70	2.13	3.49	1.64
40.17	2.29	3.45	1.51
69.78	2.68	3.31	1.24
99.37	2.68	3.18	1.18
128.95	2.73	3.06	1.12
158.57	2.83	2.91	1.03
188.16	2.90	2.75	0.95
217.80	2.93	2.66	0.91
247.39	2.97	2.52	0.85
276.75	3.06	2.40	0.78
294.67	2.95	2.31	0.79

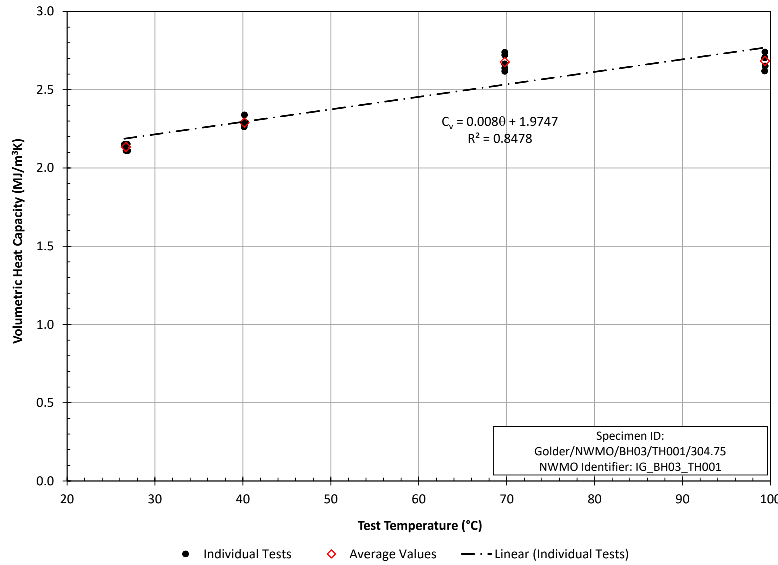

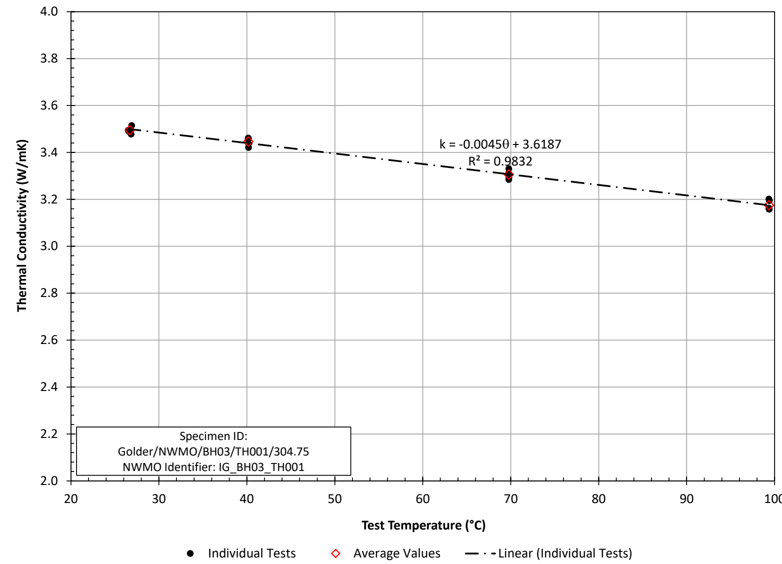

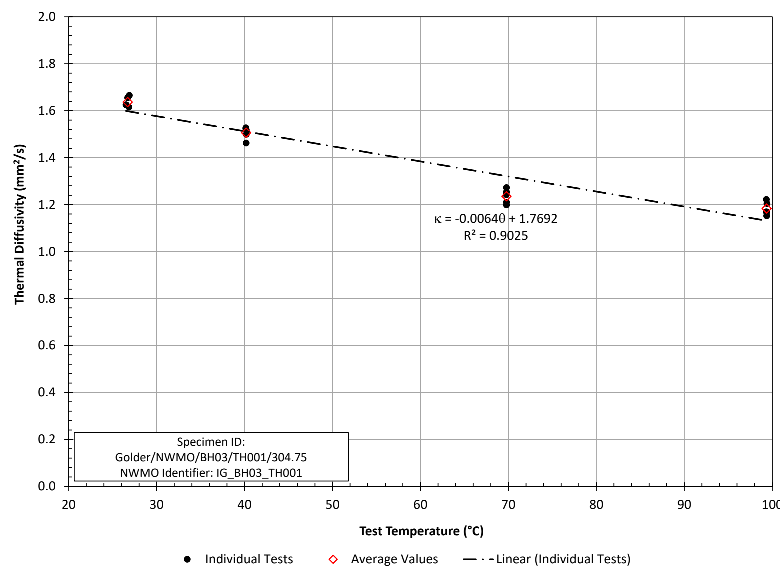

NOTE: Sample depths in the graph legends refer to the depth of the original sample as collected (part of the id), not the depth of the sub-samples

Test Specimen IG_BH03_TH001 – Depth = 304.71 m: Volumetric Heat Capacity, Thermal Conductivity and Thermal Diffusivity

GOLDER/NWMO/BH03TH002/358.94
IG_BH03_TH002

GOLDER/NWMO/BH03TH002/358.98
IG_BH03_TH002

Pretest Top Sample | **Posttest Top Sample** | **Pretest Bottom Sample** | **Posttest Bottom Sample**

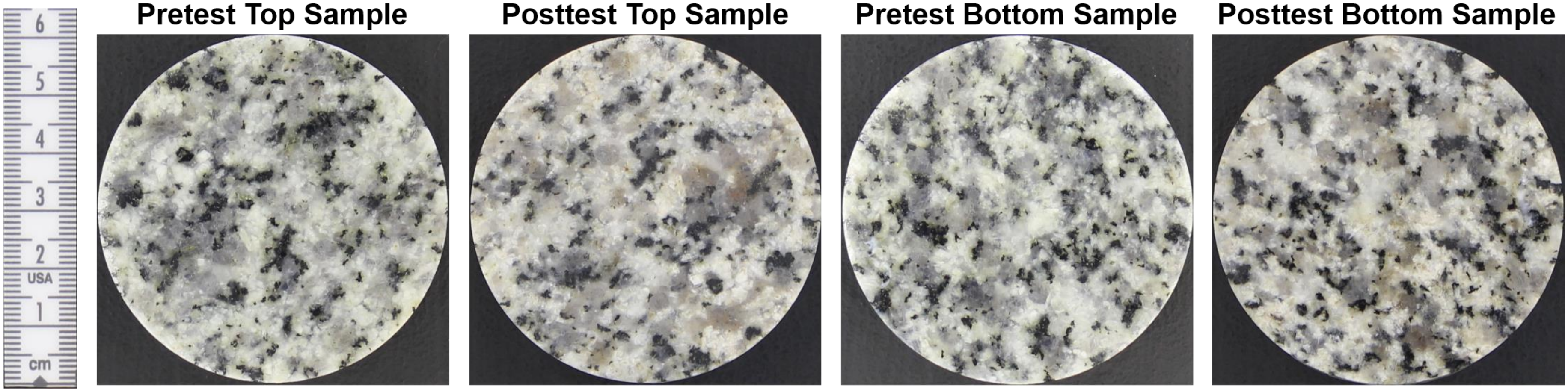

Test Specimen IG_BH03_TH002 – Depth = 358.94 m: specimen photographs

Table D-3: Hot Disk Results – Test Specimen IG_BH03_TH002 – Depth = 358.94 m

Average Temperature (°C)	Average Volumetric Specific Heat (MJ/m^3°K)	Average Thermal Conductivity (W/m°K)	Average Thermal Diffusivity (mm^2/s)
26.37	1.91	3.02	1.58
40.17	1.98	3.00	1.52
69.76	2.17	3.01	1.39
99.37	2.27	2.96	1.30
128.98	2.44	2.87	1.18
158.54	2.50	2.75	1.10
188.16	2.59	2.62	1.01
217.75	2.68	2.52	0.94
247.37	2.77	2.42	0.88
277.00	2.80	2.31	0.83
294.69	2.73	2.25	0.83

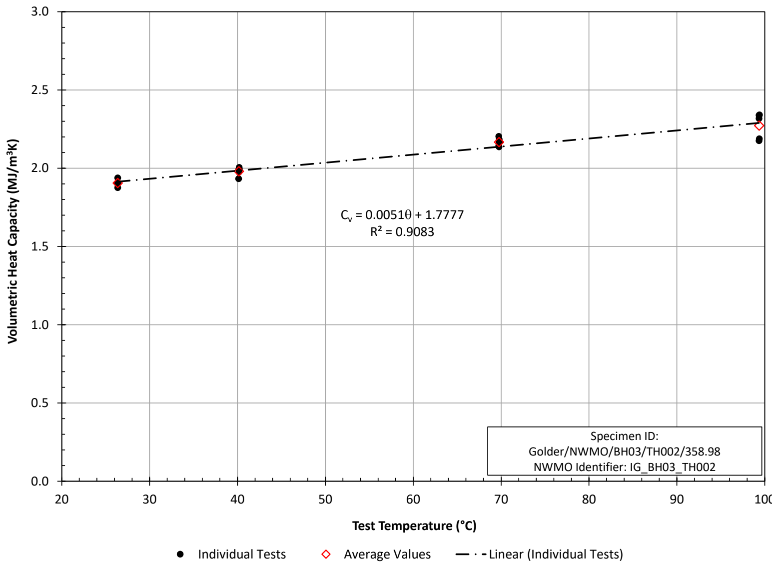

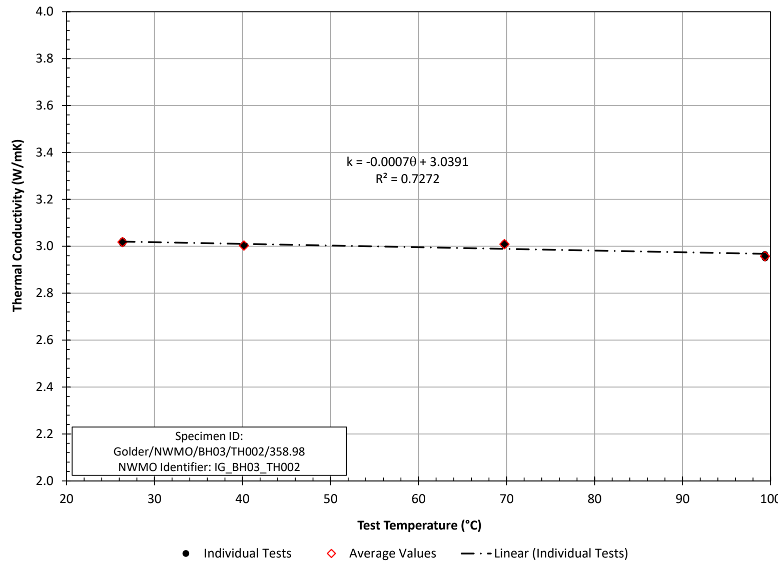

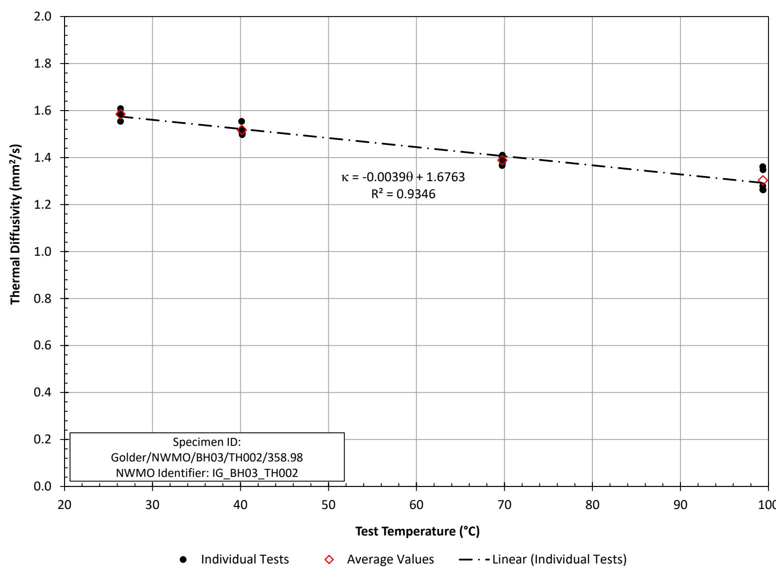

NOTE: Sample depths in the graph legends refer to the depth of the original sample as collected (part of the id), not the depth of the sub-samples

Test Specimen IG_BH03_TH002 – Depth = 358.94 m: Volumetric Heat Capacity, Thermal Conductivity and Thermal Diffusivity

GOLDER/NWMO/BH03TH003/416.43
IG_BH03_TH003

GOLDER/NWMO/BH03TH003/416.47
IG_BH03_TH003

Pretest Top Sample **Posttest Top Sample** **Pretest Bottom Sample** **Posttest Bottom Sample**

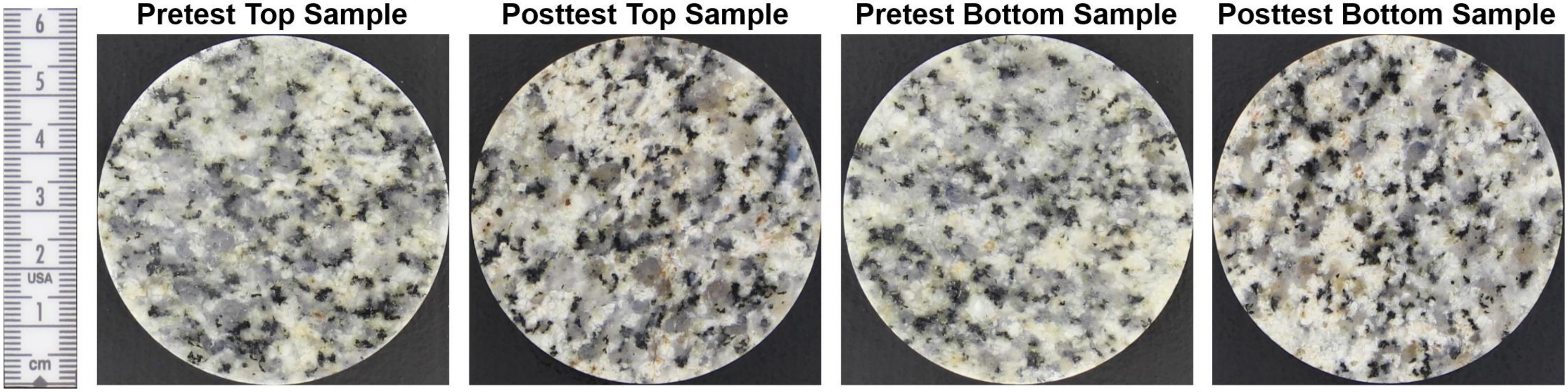

Test Specimen IG_BH03_TH003 – Depth = 416.43 m: specimen photographs

Table D-4: Hot Disk Results – Test Specimen IG_BH03_TH003 – Depth = 416.43 m

Average Temperature (°C)	Average Volumetric Specific Heat (MJ/m^3°K)	Average Thermal Conductivity (W/m°K)	Average Thermal Diffusivity (mm^2/s)
26.37	1.77	2.83	1.60
40.15	1.86	2.82	1.52
69.75	2.02	2.82	1.39
99.35	2.16	2.79	1.29
128.96	2.29	2.71	1.18
158.57	2.42	2.59	1.07
188.17	2.49	2.48	1.00
217.77	2.60	2.40	0.92
247.35	2.65	2.33	0.88
276.97	2.76	2.22	0.80
294.74	2.73	2.16	0.79

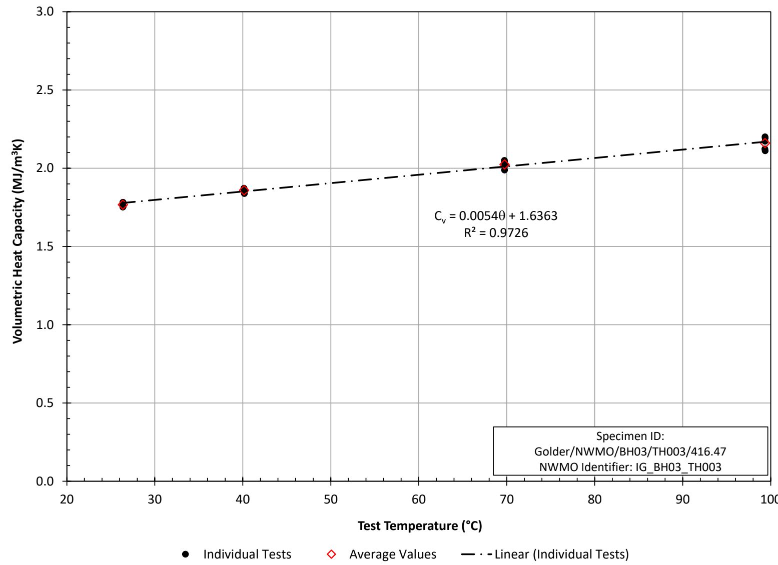

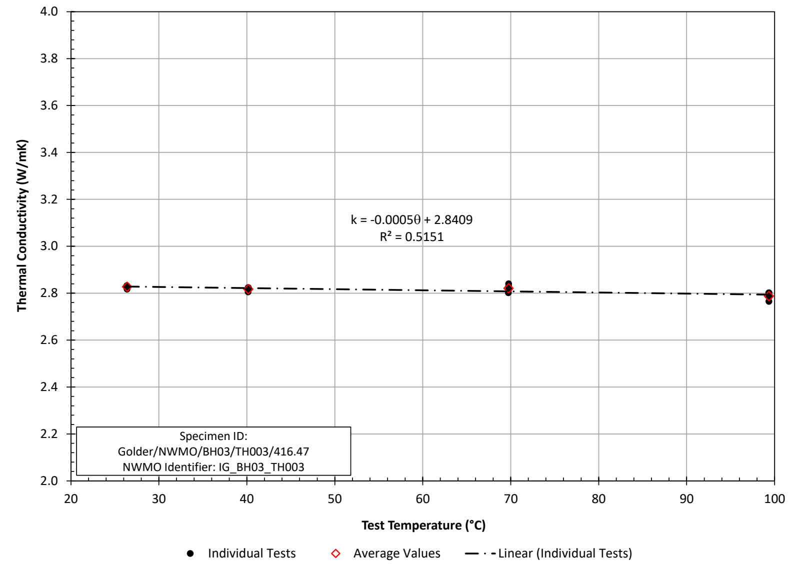

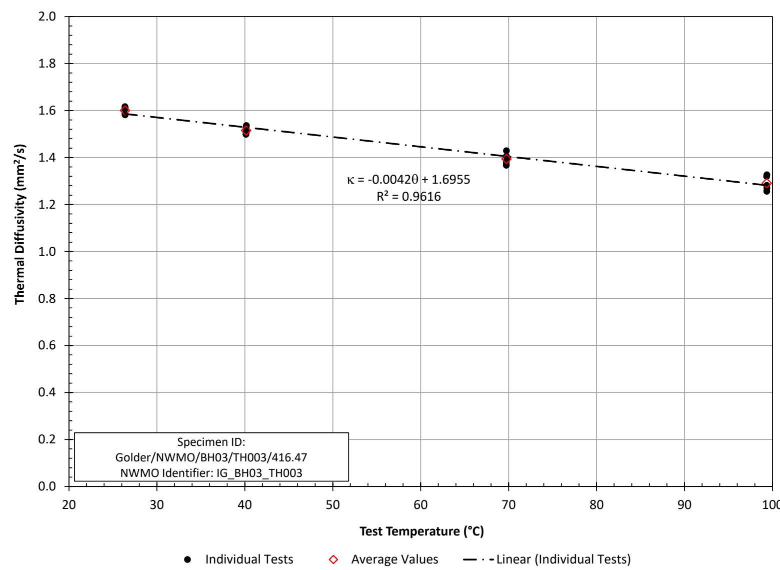

NOTE: Sample depths in the graph legends refer to the depth of the original sample as collected (part of the id), not the depth of the sub-samples

Test Specimen IG_BH03_TH003 – Depth = 416.43 m: Volumetric Heat Capacity, Thermal Conductivity and Thermal Diffusivity

GOLDER/NWMO/BH03TH004/454.06
IG_BH03_TH004

GOLDER/NWMO/BH03TH004/454.10
IG_BH03_TH004

Pretest Top Sample | **Posttest Top Sample** | **Pretest Bottom Sample** | **Posttest Bottom Sample**

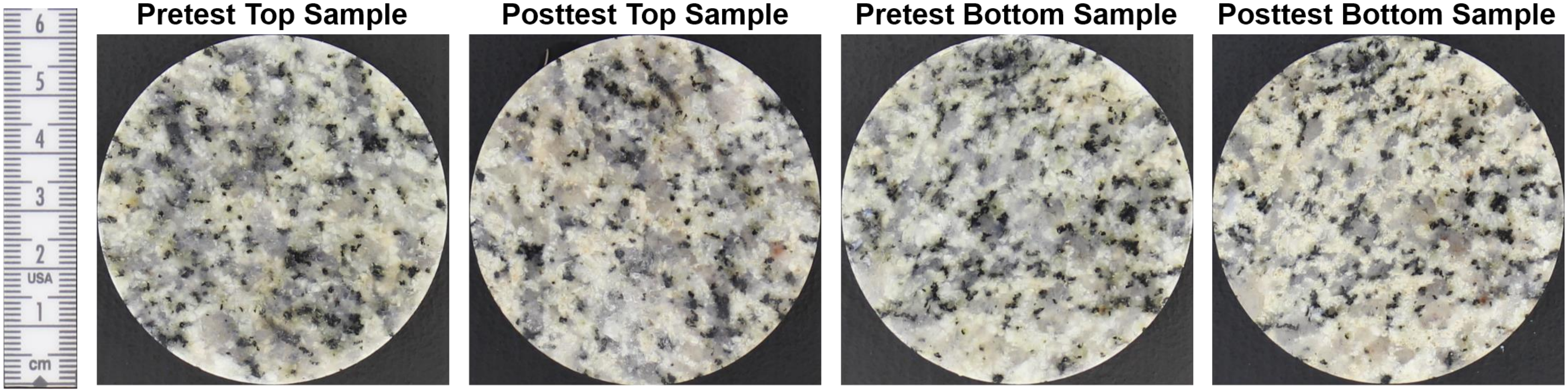

Test Specimen IG_BH03_TH004 – Depth = 454.06 m: specimen photographs

Table D-5: Hot Disk Results – Test Specimen IG_BH03_TH004 – Depth = 454.06 m

Average Temperature (°C)	Average Volumetric Specific Heat (MJ/m^3°K)	Average Thermal Conductivity (W/m°K)	Average Thermal Diffusivity (mm^2/s)
26.36	2.13	3.25	1.52
40.16	2.22	3.23	1.46
69.77	2.34	3.17	1.35
99.38	2.49	3.08	1.24
128.96	2.60	2.95	1.14
158.55	2.67	2.84	1.07
188.16	2.75	2.68	0.98
217.74	2.89	2.56	0.89
247.37	2.96	2.44	0.82
276.99	3.01	2.33	0.77
294.73	3.02	2.25	0.75

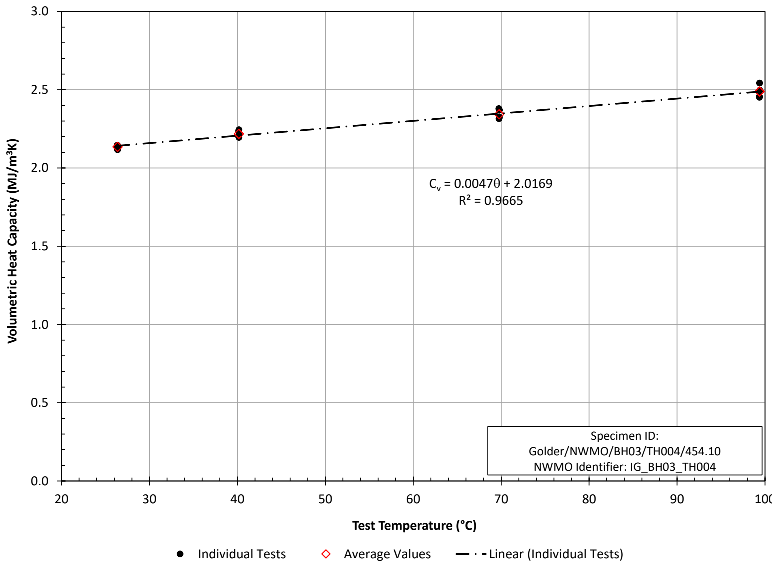

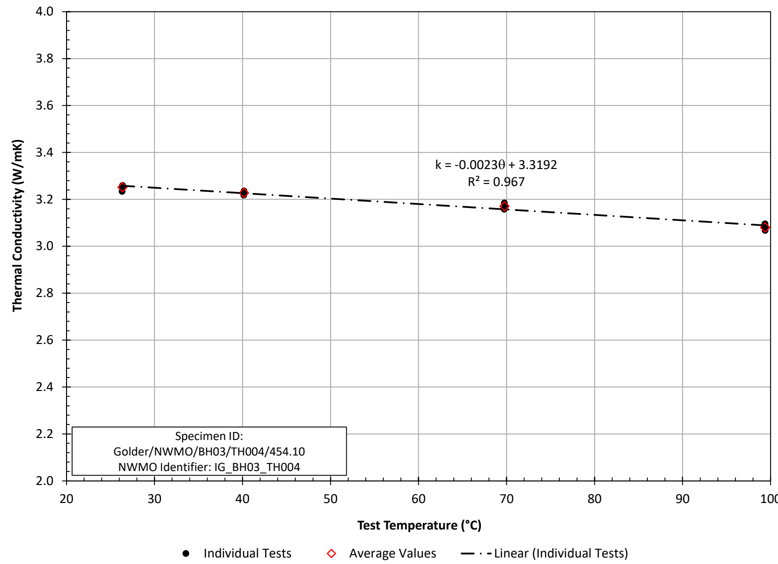

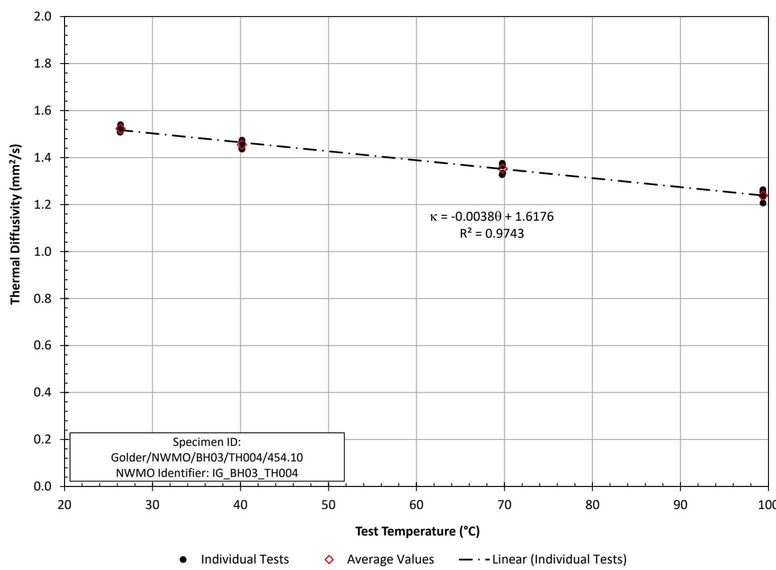

NOTE: Sample depths in the graph legends refer to the depth of the original sample as collected (part of the id), not the depth of the sub-samples

Test Specimen IG_BH03_TH004 – Depth = 454.06 m: Volumetric Heat Capacity, Thermal Conductivity and Thermal Diffusivity

GOLDER/NWMO/BH03TH005/495.01
IG_BH03_TH005

GOLDER/NWMO/BH03TH005/495.05
IG_BH03_TH005

Pretest Top Sample

Posttest Top Sample

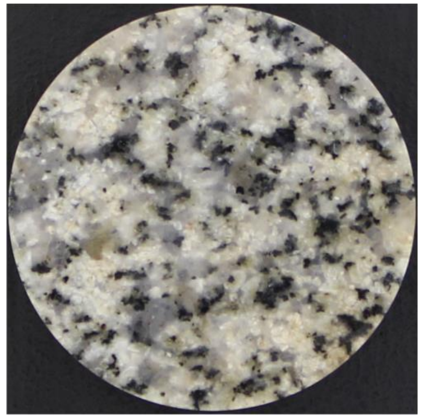

Pretest Bottom Sample

Posttest Bottom Sample

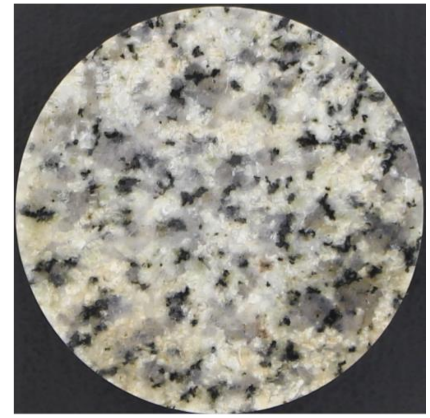

Test Specimen IG_BH03_TH005 – Depth = 495.01 m: specimen photographs

Table D-6: Hot Disk Results – Test Specimen IG_BH03_TH005 – Depth = 495.01 m

Average Temperature (°C)	Average Volumetric Specific Heat (MJ/m^3°K)	Average Thermal Conductivity (W/m°K)	Average Thermal Diffusivity (mm^2/s)
26.36	2.27	3.39	1.50
40.17	2.29	3.28	1.43
69.77	2.60	3.13	1.21
99.36	2.57	3.04	1.18
128.97	2.66	2.94	1.11
158.56	2.71	2.82	1.04
188.18	2.81	2.67	0.95
217.78	2.87	2.57	0.90
247.35	2.99	2.45	0.82
276.93	2.95	2.36	0.80
294.71	2.92	2.27	0.78

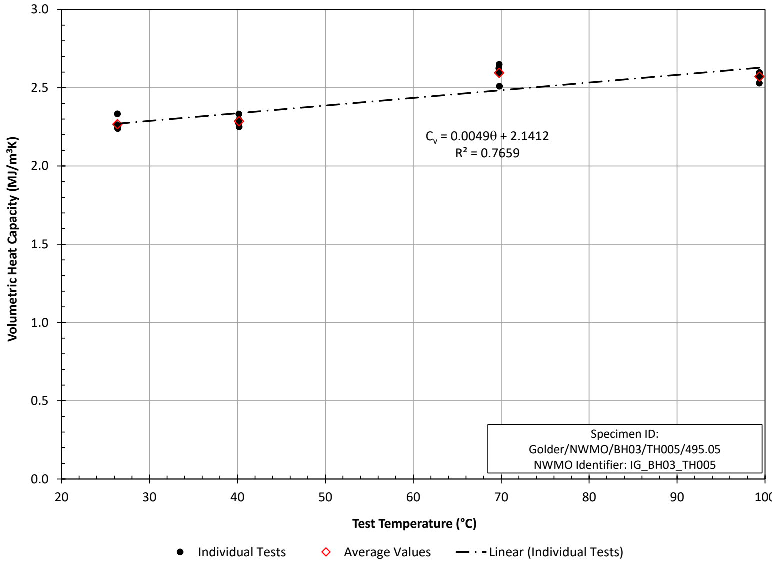

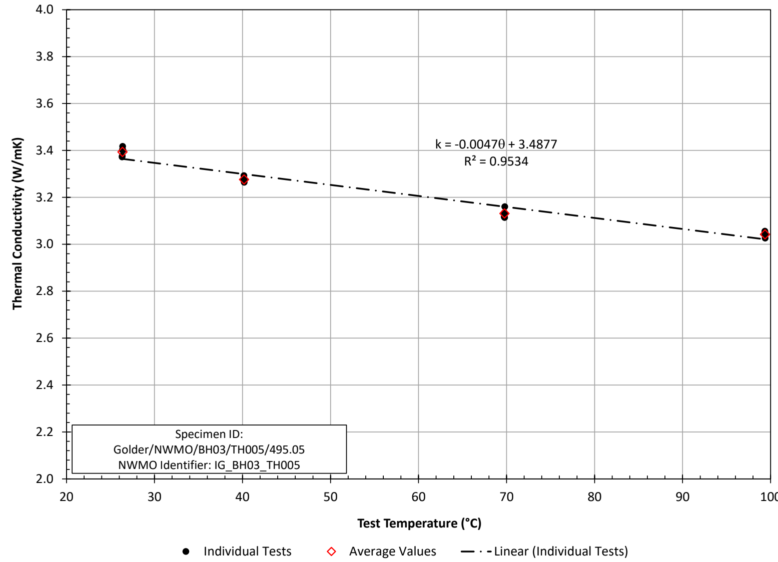

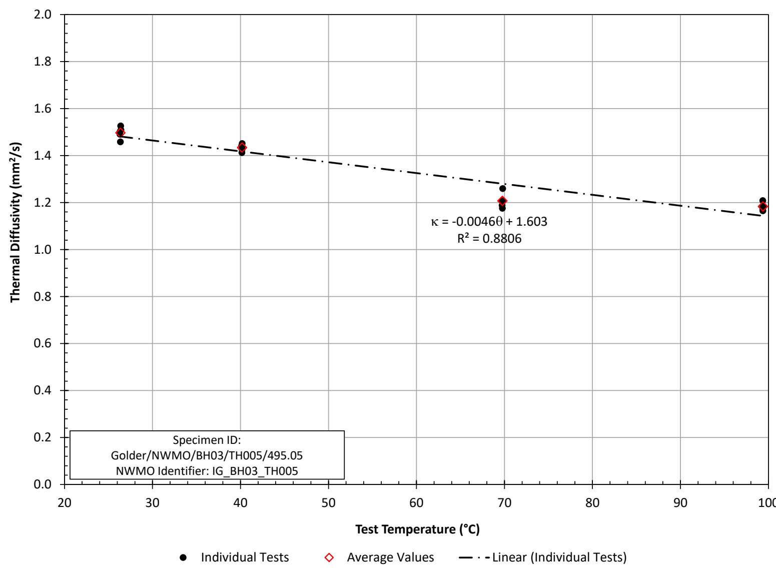

NOTE: Sample depths in the graph legends refer to the depth of the original sample as collected (part of the id), not the depth of the sub-samples

Test Specimen IG_BH03_TH005 – Depth = 495.01 m: Volumetric Heat Capacity, Thermal Conductivity and Thermal Diffusivity

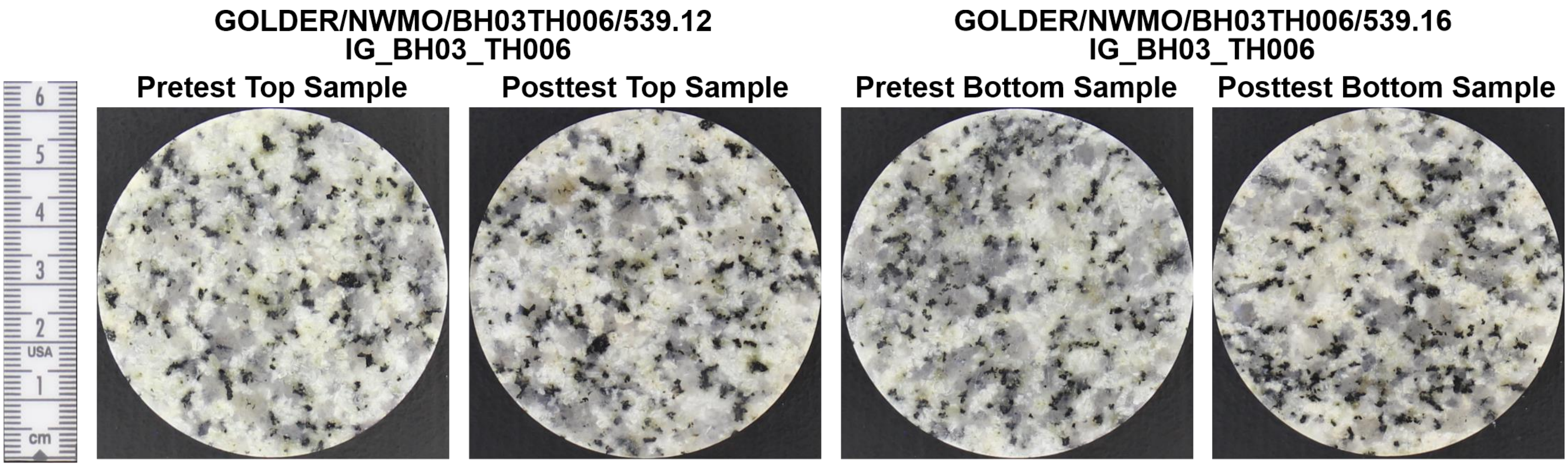

Test Specimen IG_BH03_TH006 – Depth = 539.12 m: specimen photographs

Table D-7: Hot Disk Results – Test Specimen IG_BH03_TH006 – Depth = 539.12 m

Average Temperature (°C)	Average Volumetric Specific Heat (MJ/m^3°K)	Average Thermal Conductivity (W/m°K)	Average Thermal Diffusivity (mm^2/s)
26.44	2.49	3.70	1.48
40.17	2.55	3.59	1.41
69.77	2.78	3.45	1.24
99.36	2.77	3.30	1.19
128.96	2.89	3.15	1.09
158.57	3.01	2.99	0.99
188.15	3.09	2.82	0.91
217.75	3.11	2.72	0.87
247.35	3.23	2.57	0.80
276.97	3.21	2.46	0.77
294.75	3.15	2.38	0.76

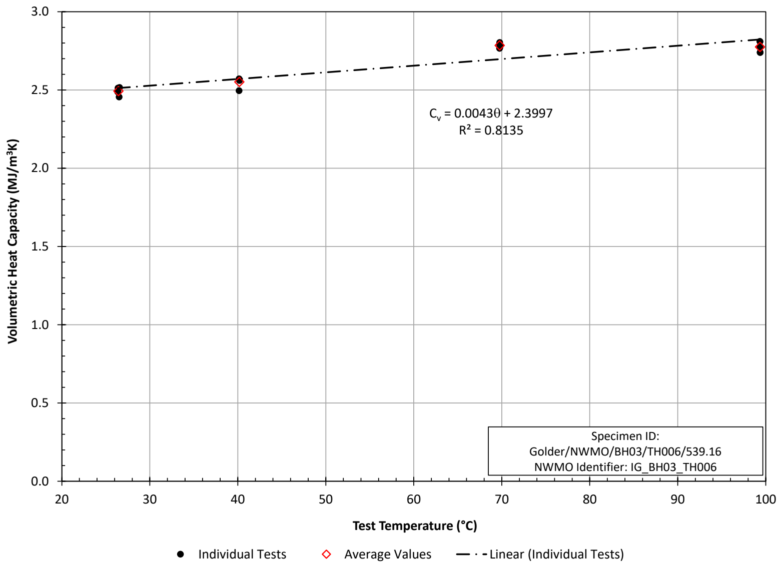

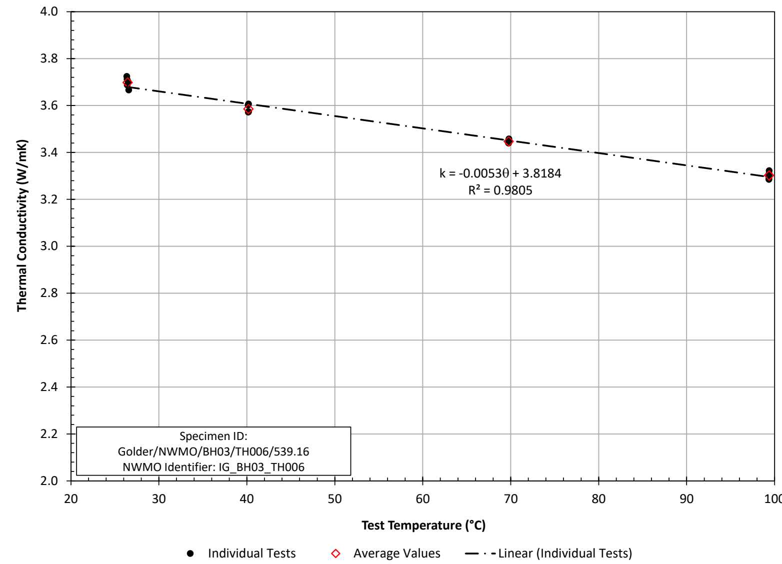

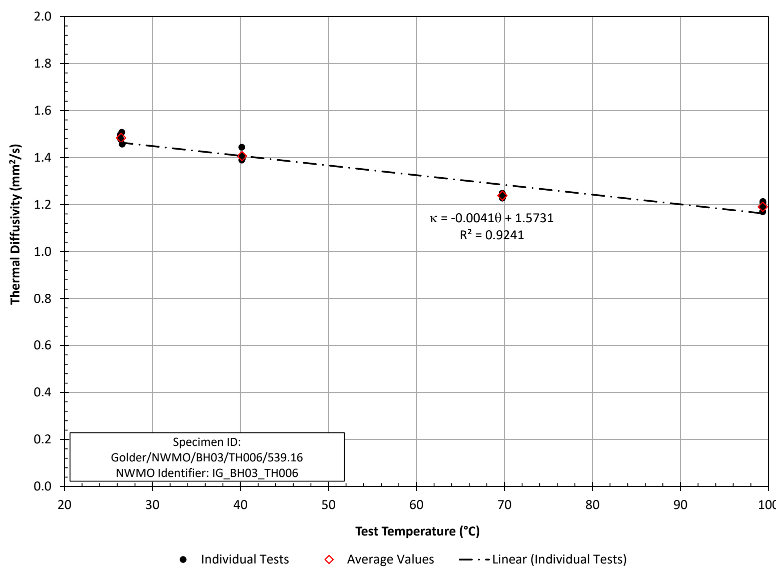

NOTE: Sample depths in the graph legends refer to the depth of the original sample as collected (part of the id), not the depth of the sub-samples

Test Specimen IG_BH03_TH006 – Depth = 539.12 m: Volumetric Heat Capacity, Thermal Conductivity and Thermal Diffusivity

GOLDER/NWMO/BH03TH007/548.19
IG_BH03_TH007

GOLDER/NWMO/BH03TH007/548.23
IG_BH03_TH007

Pretest Top Sample | **Posttest Top Sample** | **Pretest Bottom Sample** | **Posttest Bottom Sample**

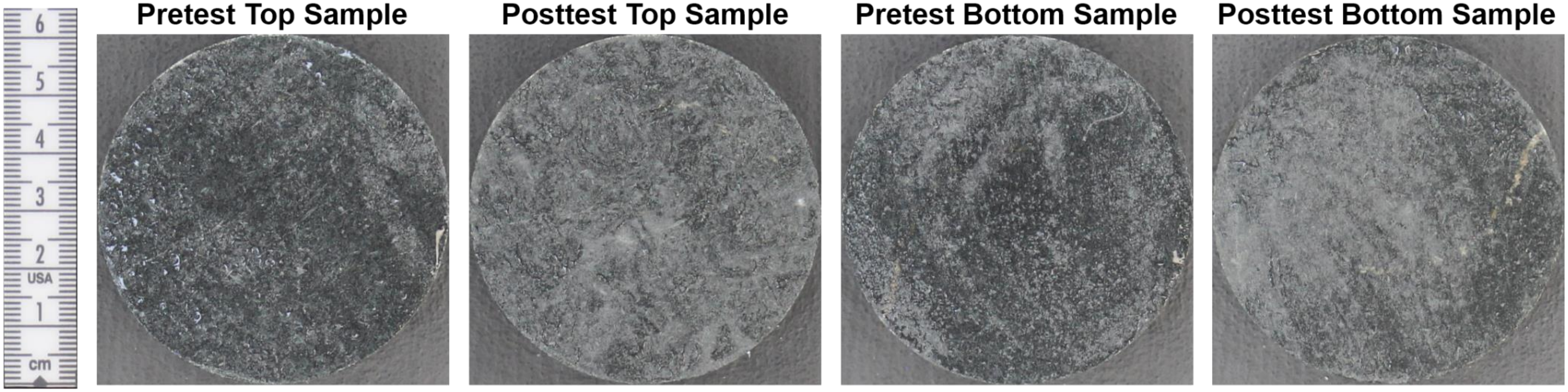

Test Specimen IG_BH03_TH007 – Depth = 548.19 m: specimen photographs

Table D-8: Hot Disk Results – Test Specimen IG_BH03_TH007 – Depth = 548.19 m

Average Temperature (°C)	Average Volumetric Specific Heat (MJ/m^3°K)	Average Thermal Conductivity (W/m°K)	Average Thermal Diffusivity (mm^2/s)
26.20	2.43	2.78	1.14
40.19	2.50	2.77	1.11
69.78	2.73	2.78	1.02
99.37	2.90	2.76	0.95
128.98	3.00	2.71	0.90
158.56	3.07	2.68	0.87
188.15	3.12	2.63	0.84
217.76	3.28	2.60	0.79
247.40	3.29	2.56	0.78
276.96	3.34	2.50	0.75
294.69	3.33	2.45	0.74

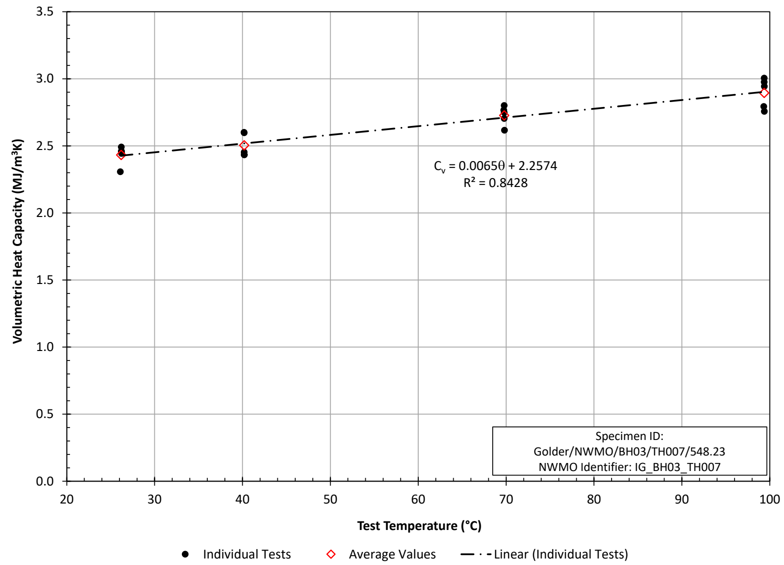

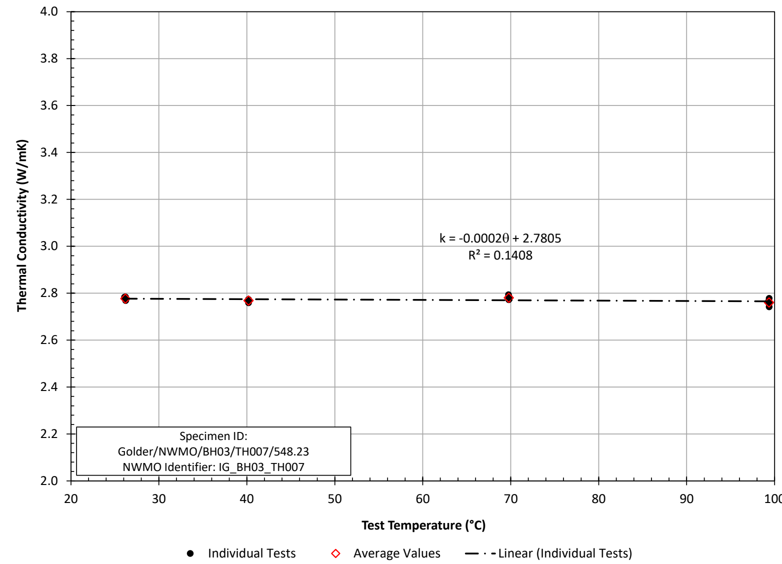

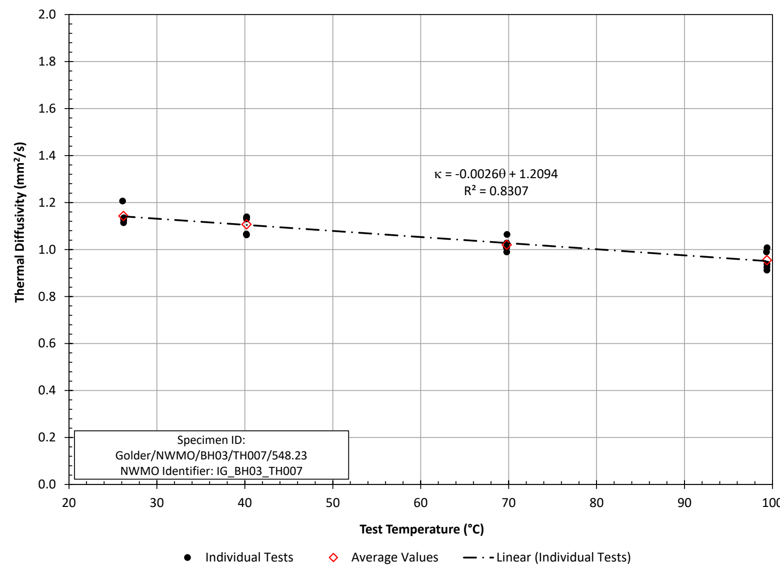

NOTE: Sample depths in the graph legends refer to the depth of the original sample as collected (part of the id), not the depth of the sub-samples

Test Specimen IG_BH03_TH007 – Depth = 548.19 m: Volumetric Heat Capacity, Thermal Conductivity and Thermal Diffusivity

GOLDER/NWMO/BH03TH008/581.86
IG_BH03_TH008

GOLDER/NWMO/BH03TH008/581.90
IG_BH03_TH008

Pretest Top Sample | **Posttest Top Sample** | **Pretest Bottom Sample** | **Posttest Bottom Sample**

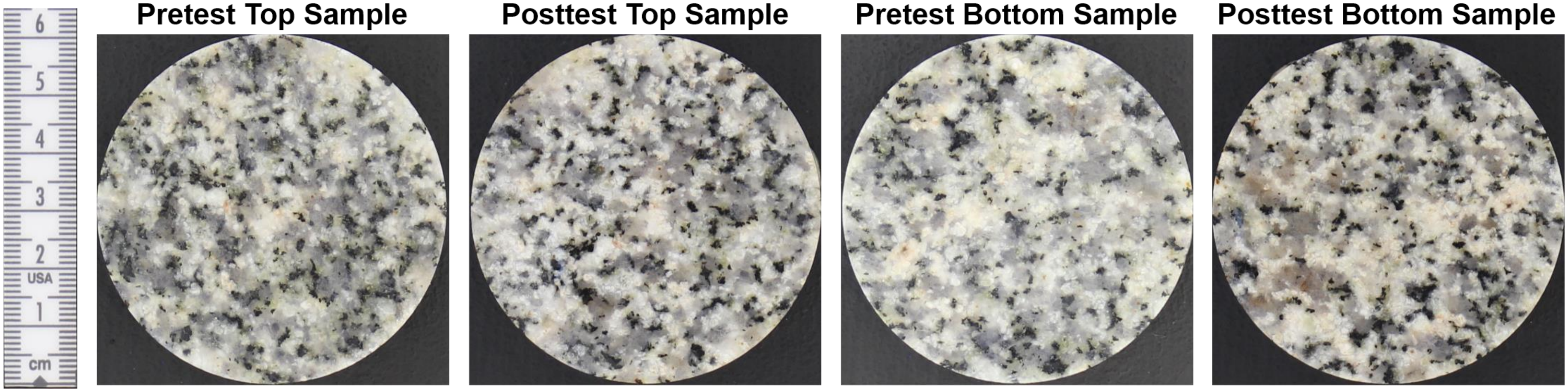

Test Specimen IG_BH03_TH008 – Depth = 581.86 m: specimen photographs

Table D-9: Hot Disk Results – Test Specimen IG_BH03_TH008 – Depth = 581.86 m

Average Temperature (°C)	Average Volumetric Specific Heat (MJ/m^3°K)	Average Thermal Conductivity (W/m°K)	Average Thermal Diffusivity (mm^2/s)
26.39	1.70	2.95	1.73
40.17	1.78	2.93	1.65
69.76	1.96	2.92	1.49
99.38	2.04	2.89	1.41
128.97	2.19	2.79	1.27
158.57	2.28	2.69	1.18
188.17	2.33	2.57	1.10
217.76	2.51	2.45	0.98
247.36	2.54	2.36	0.93
276.97	2.58	2.28	0.88
294.72	2.58	2.20	0.85

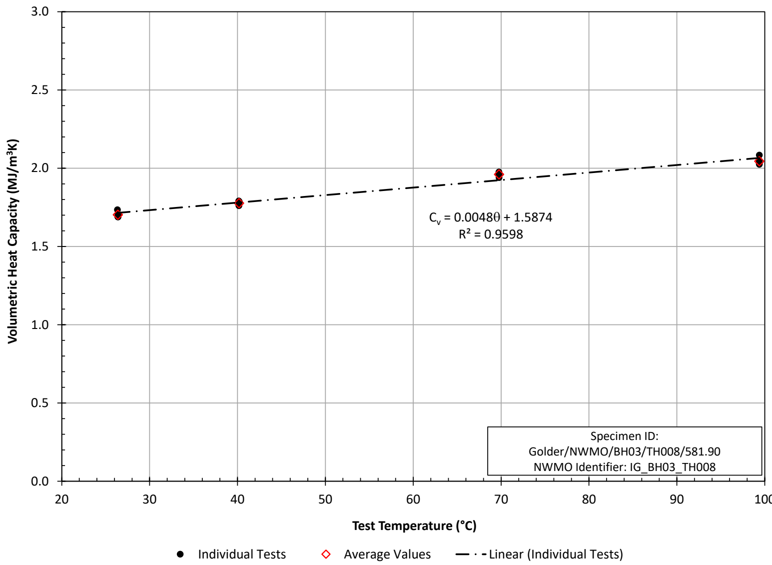

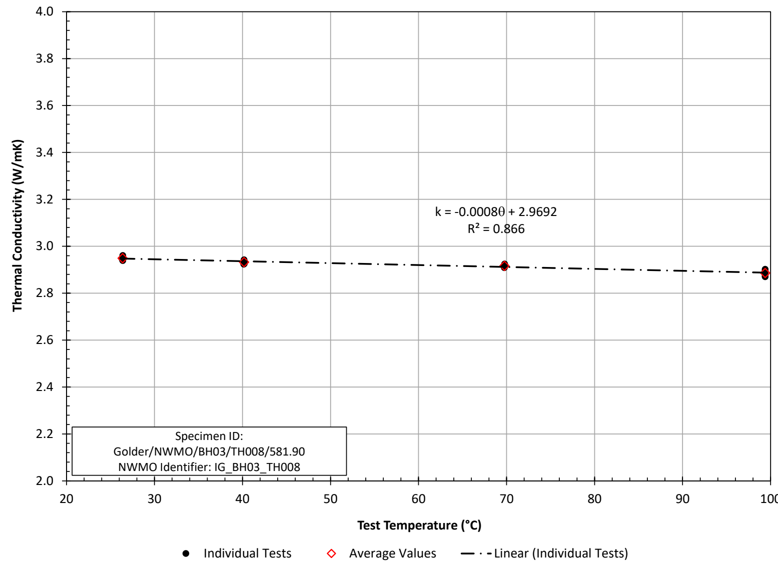

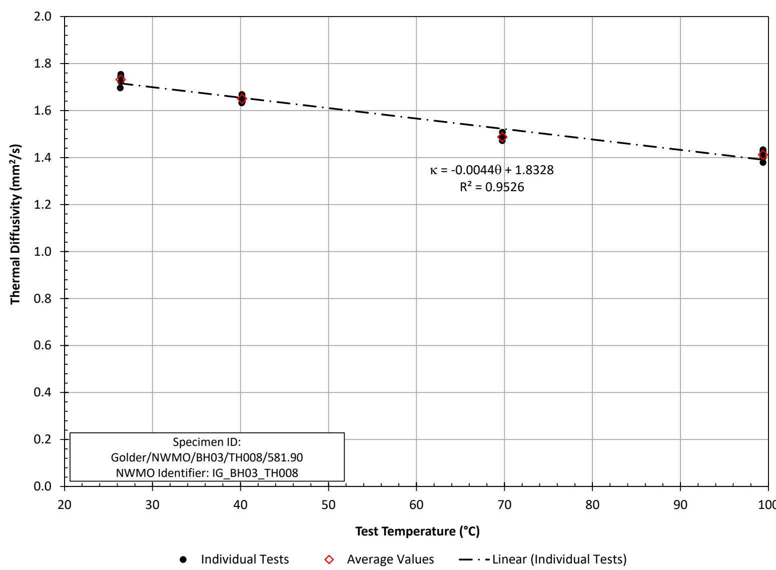

NOTE: Sample depths in the graph legends refer to the depth of the original sample as collected (part of the id), not the depth of the sub-samples

Test Specimen IG_BH03_TH008 – Depth = 581.86 m: Volumetric Heat Capacity, Thermal Conductivity and Thermal Diffusivity

GOLDER/NWMO/BH03TH009/800.64
IG_BH03_TH009

GOLDER/NWMO/BH03TH009/800.68
IG_BH03_TH009

Pretest Top Sample | **Posttest Top Sample** | **Pretest Bottom Sample** | **Posttest Bottom Sample**

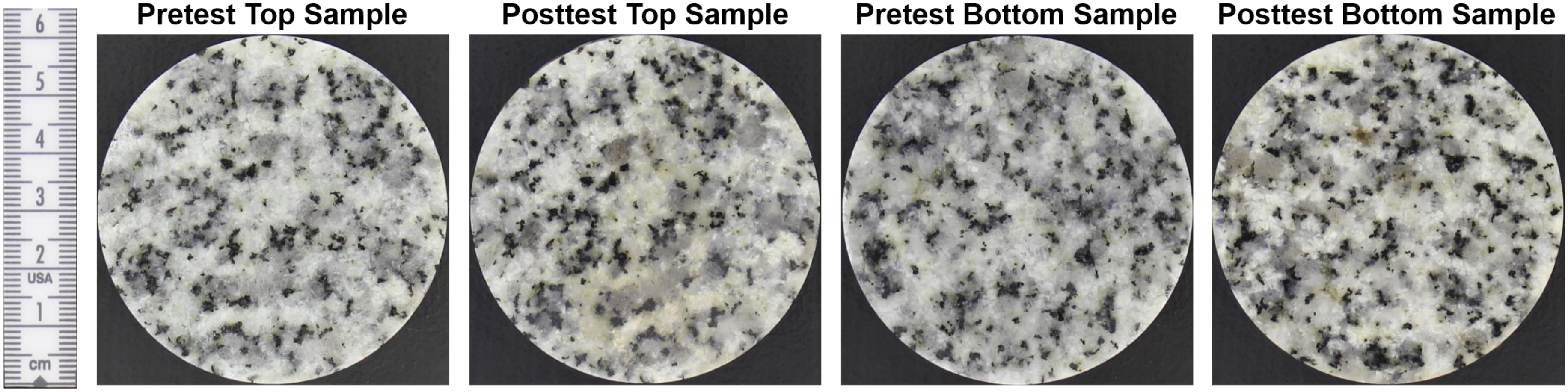

Test Specimen IG_BH03_TH009 – Depth = 800.64 m: specimen photographs

Table D-10: Hot Disk Results – Test Specimen IG_BH03_TH009 – Depth = 800.64 m

Average Temperature (°C)	Average Volumetric Specific Heat (MJ/m³°K)	Average Thermal Conductivity (W/m°K)	Average Thermal Diffusivity (mm²/s)
26.38	1.92	3.04	1.59
40.16	1.98	2.95	1.49
69.76	2.16	2.85	1.32
99.36	2.26	2.71	1.20
128.97	2.36	2.64	1.12
158.58	2.35	2.62	1.12
188.16	2.48	2.46	0.99
217.77	2.63	2.38	0.91
247.36	2.60	2.31	0.89
276.92	2.68	2.21	0.83
294.69	2.65	2.14	0.81

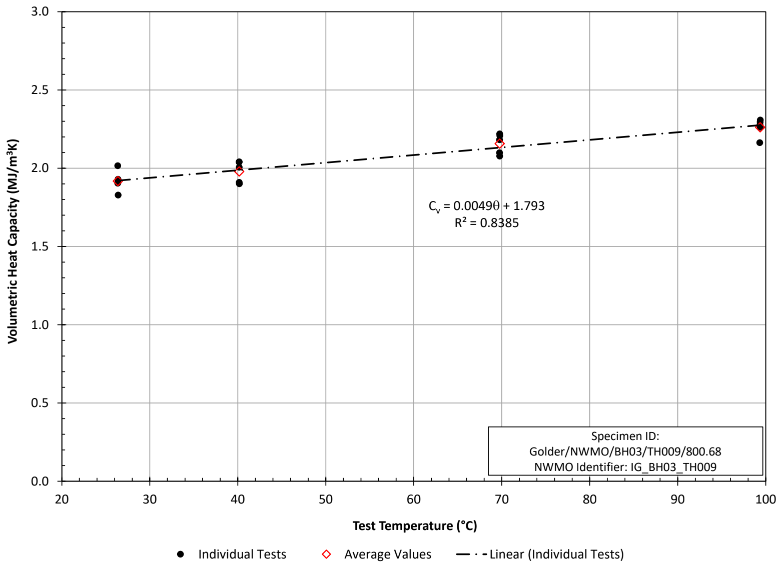

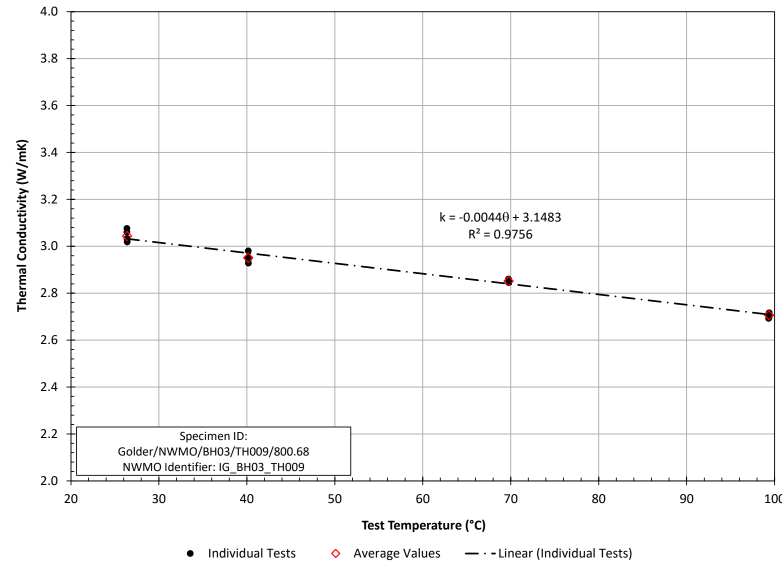

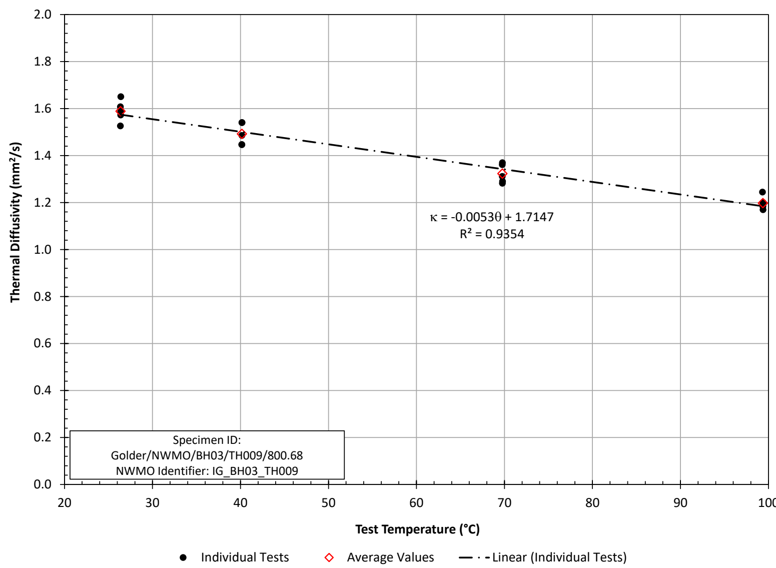

NOTE: Sample depths in the graph legends refer to the depth of the original sample as collected (part of the id), not the depth of the sub-samples

Test Specimen IG_BH03_TH009 – Depth = 800.64 m: Volumetric Heat Capacity, Thermal Conductivity and Thermal Diffusivity

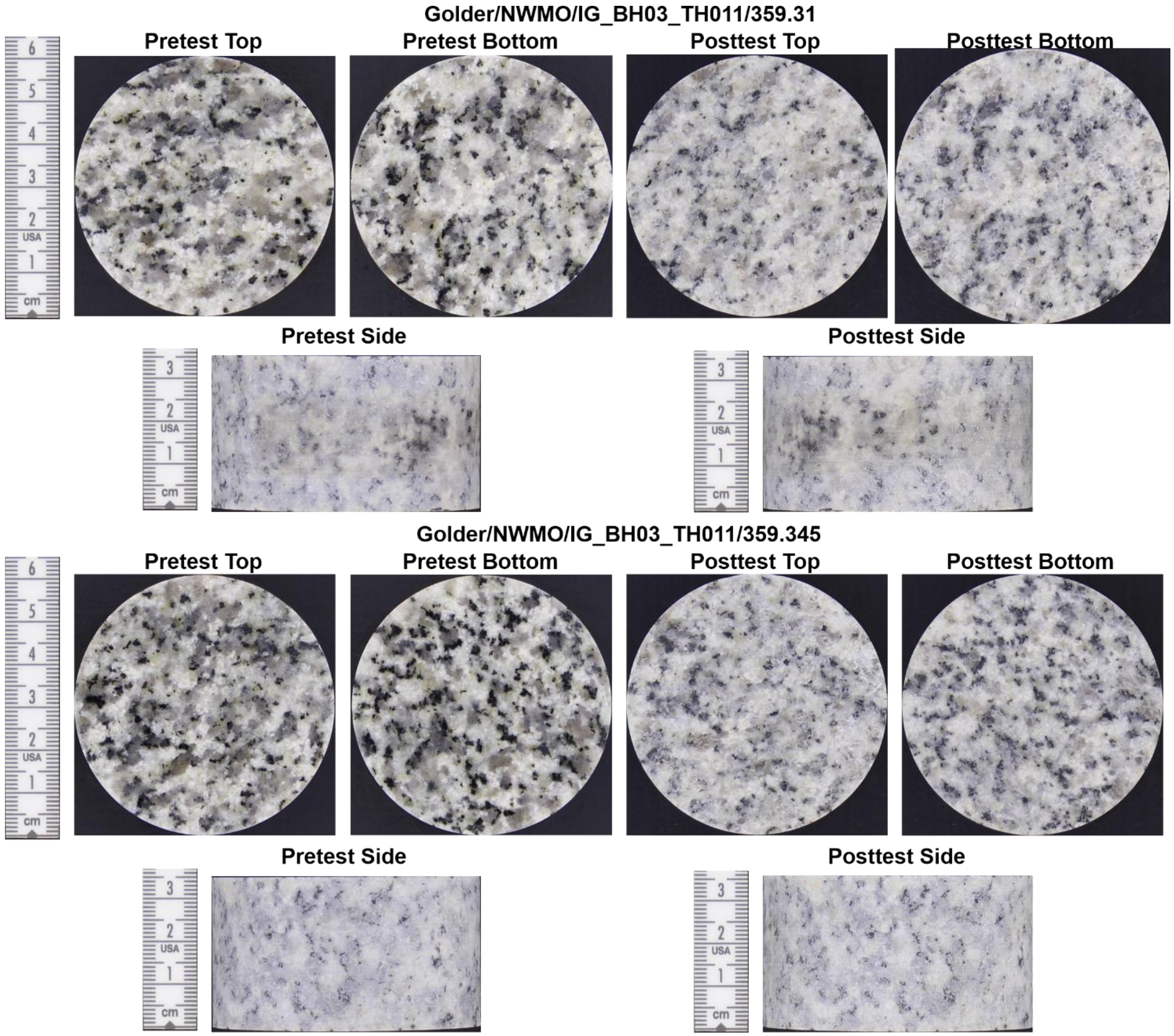

Test Specimen IG_BH03_TH011 – Depth = 359.31 m: specimen photographs

Table D-11: Hot Disk Results – Test Specimen IG_BH03_TH011 – Depth = 359.31 m

Average Temperature (°C)	Average Volumetric Specific Heat ($MJ/m^3°K$)	Average Thermal Conductivity (W/m°K)	Average Thermal Diffusivity (mm^2/s)
20.01	2.05	3.38	1.65
40.00	2.13	3.31	1.56
60.06	2.26	3.29	1.46
79.94	2.33	3.24	1.39
90.04	2.36	3.21	1.36
60.05	2.21	3.28	1.49

NOTE: Sample depths in the graph legends refer to the depth of the original sample as collected (part of the id), not the depth of the sub-samples

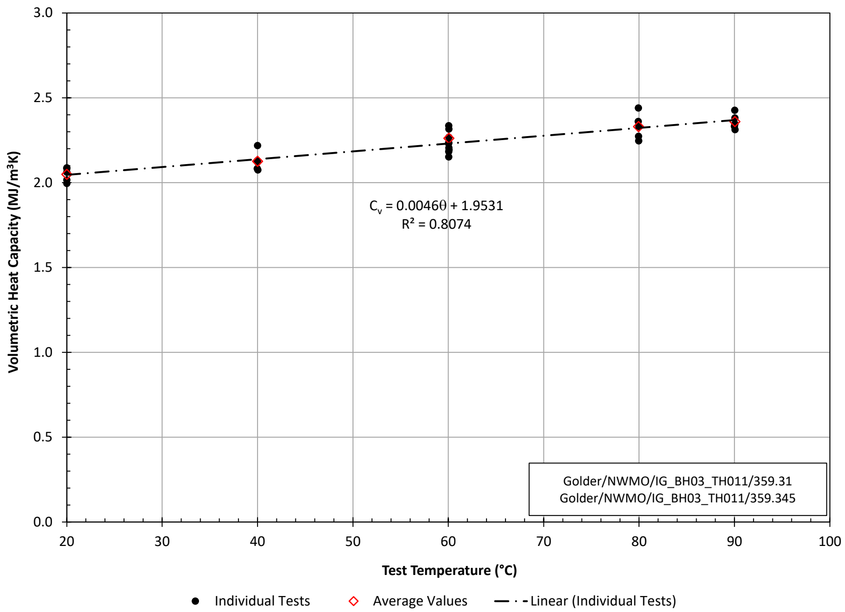

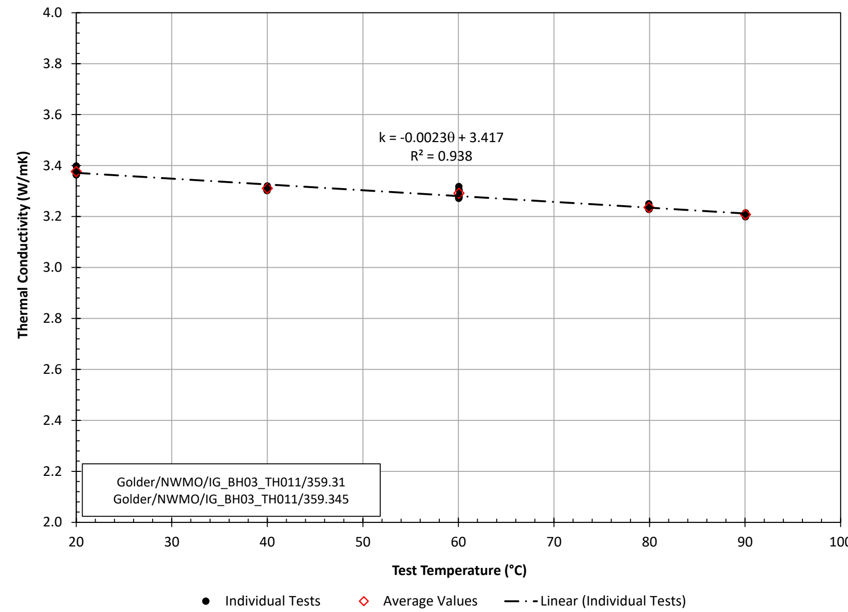

Test Specimen IG_BH03_TH011 – Depth = 359.31 m: Volumetric Heat Capacity and Thermal Conductivity

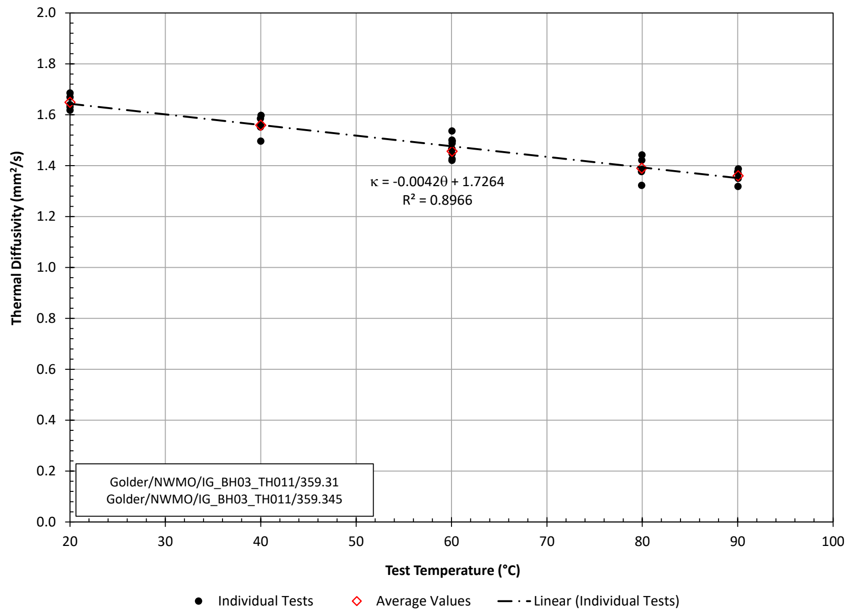

Test Specimen IG_BH03_TH011 – Depth = 359.31 m: Thermal Diffusivity

Golder/NWMO/IG_BH03_TH014/495.54

Pretest Top **Pretest Bottom** **Posttest Top** **Posttest Bottom**

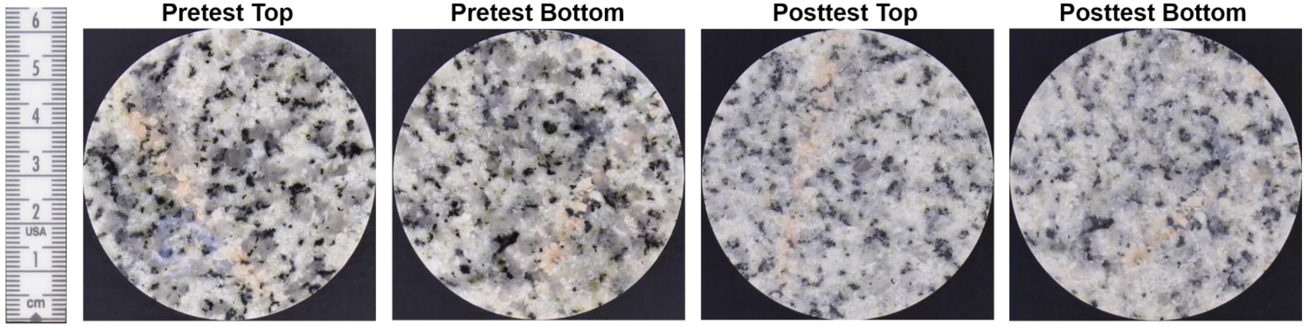

Pretest Side **Posttest Side**

Golder/NWMO/IG_BH03_TH014/495.575

Pretest Top **Pretest Bottom** **Posttest Top** **Posttest Bottom**

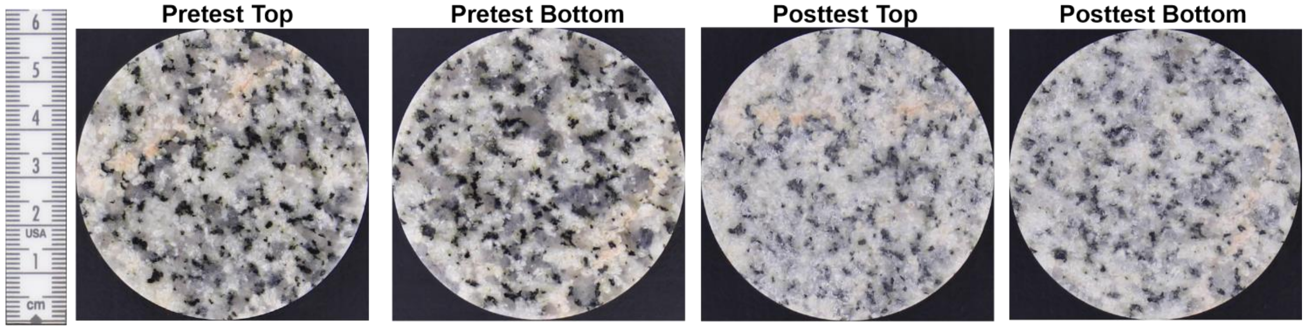

Pretest Side **Posttest Side**

Test Specimen IG_BH03_TH014 – Depth = 495.54 m: specimen photographs

Table D-12: Hot Disk Results – Test Specimen IG_BH03_TH014 – Depth = 495.54 m

Average Temperature (°C)	Average Volumetric Specific Heat (MJ/m³°K)	Average Thermal Conductivity (W/m°K)	Average Thermal Diffusivity (mm²/s)
20.01	2.10	3.16	1.50
40.01	2.14	3.11	1.45
60.05	2.26	3.10	1.37
79.96	2.34	3.06	1.31
90.05	2.40	3.04	1.27
60.03	2.27	3.08	1.36

NOTE: Sample depths in the graph legends refer to the depth of the original sample as collected (part of the id), not the depth of the sub-samples

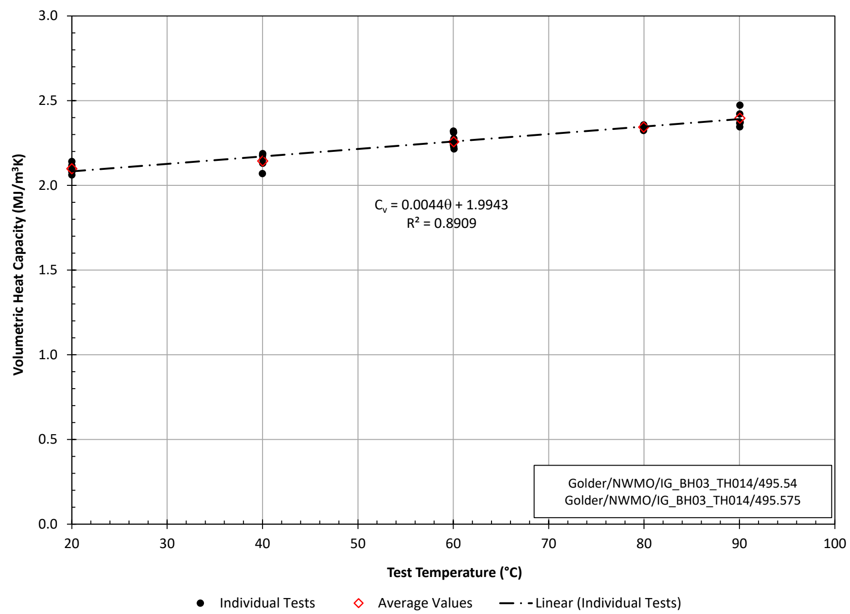

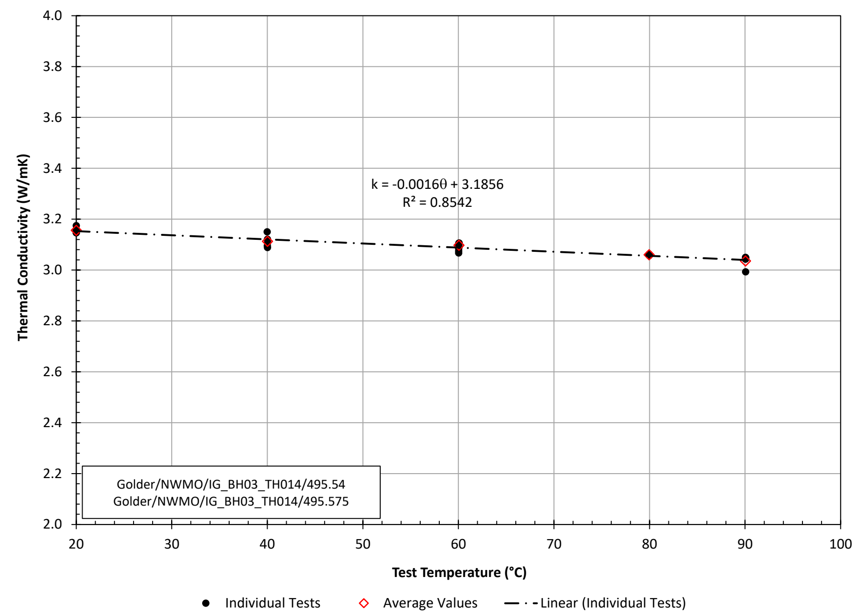

Test Specimen IG_BH03_TH014 – Depth = 495.54 m: Volumetric Heat Capacity and Thermal Conductivity

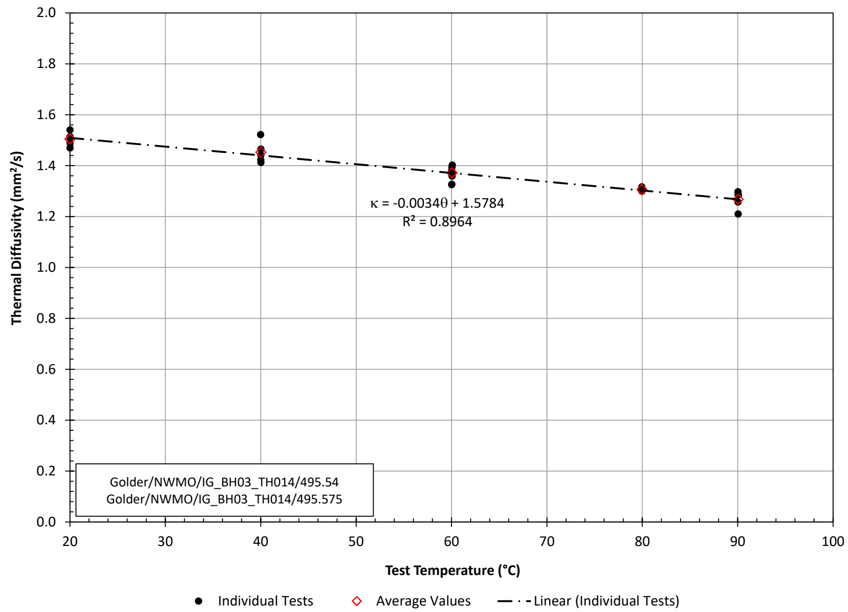

Test Specimen IG_BH03_TH014 – Depth = 495.54 m: Thermal Diffusivity

Golder/NWMO/IG_BH03_TH016/548.79

Pretest Top | **Pretest Bottom** | **Posttest Top** | **Posttest Bottom**

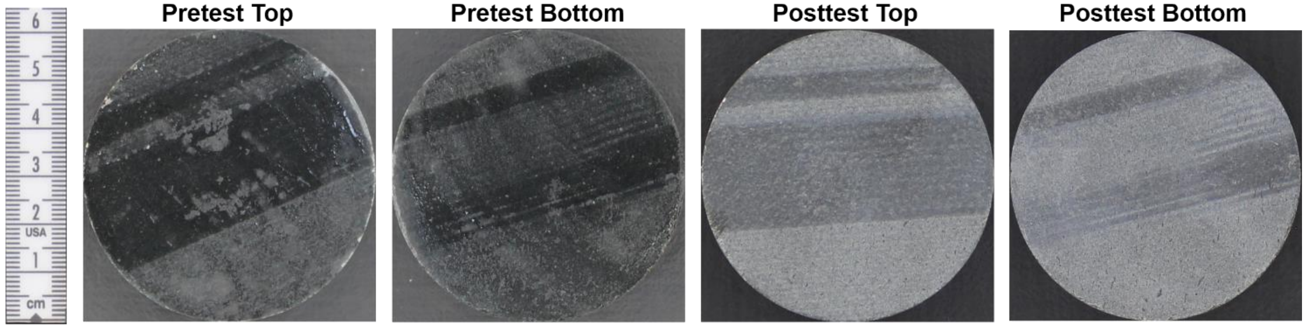

Pretest Side | **Posttest Side**

Golder/NWMO/IG_BH03_TH016/548.825

Pretest Top | **Pretest Bottom** | **Posttest Top** | **Posttest Bottom**

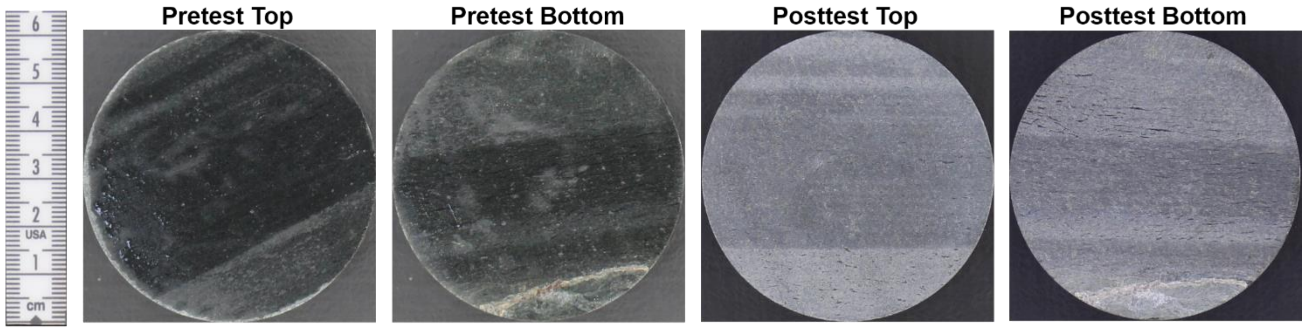

Pretest Side | **Posttest Side**

Test Specimen IG_BH03_TH016 – Depth = 548.79 m: specimen photographs

Table D-13: Hot Disk Results – Test Specimen IG_BH03_TH016 – Depth = 548.79 m

Average Temperature (°C)	Average Volumetric Specific Heat ($MJ/m^3°K$)	Average Thermal Conductivity (W/m°K)	Average Thermal Diffusivity (mm^2/s)
20.01	2.49	2.76	1.11
40.00	2.62	2.75	1.05
60.04	2.81	2.74	0.98
79.94	2.82	2.73	0.97
90.04	2.99	2.71	0.91
60.04	2.76	2.75	1.00

NOTE: Sample depths in the graph legends refer to the depth of the original sample as collected (part of the id), not the depth of the sub-samples

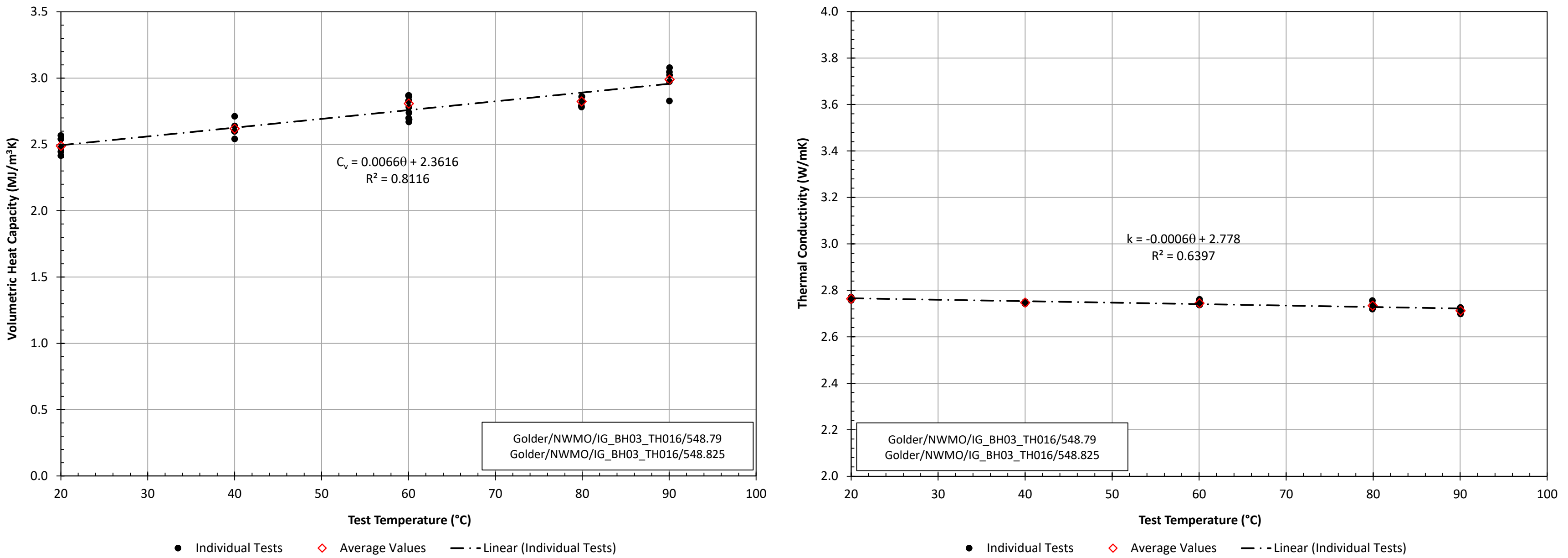

Test Specimen IG_BH03_TH016 – Depth = 548.79 m: Volumetric Heat Capacity and Thermal Conductivity

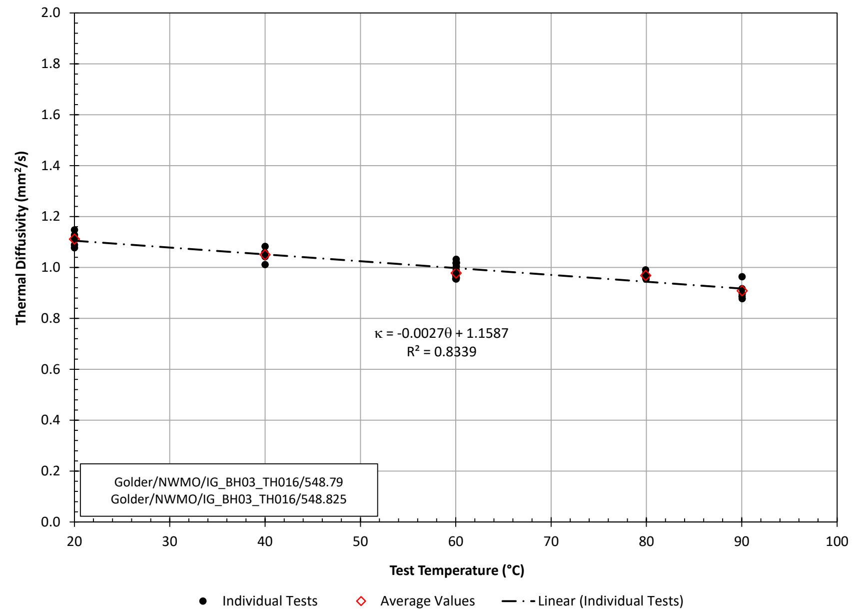

Test Specimen IG_BH03_TH016 – Depth = 548.79 m: Thermal Diffusivity

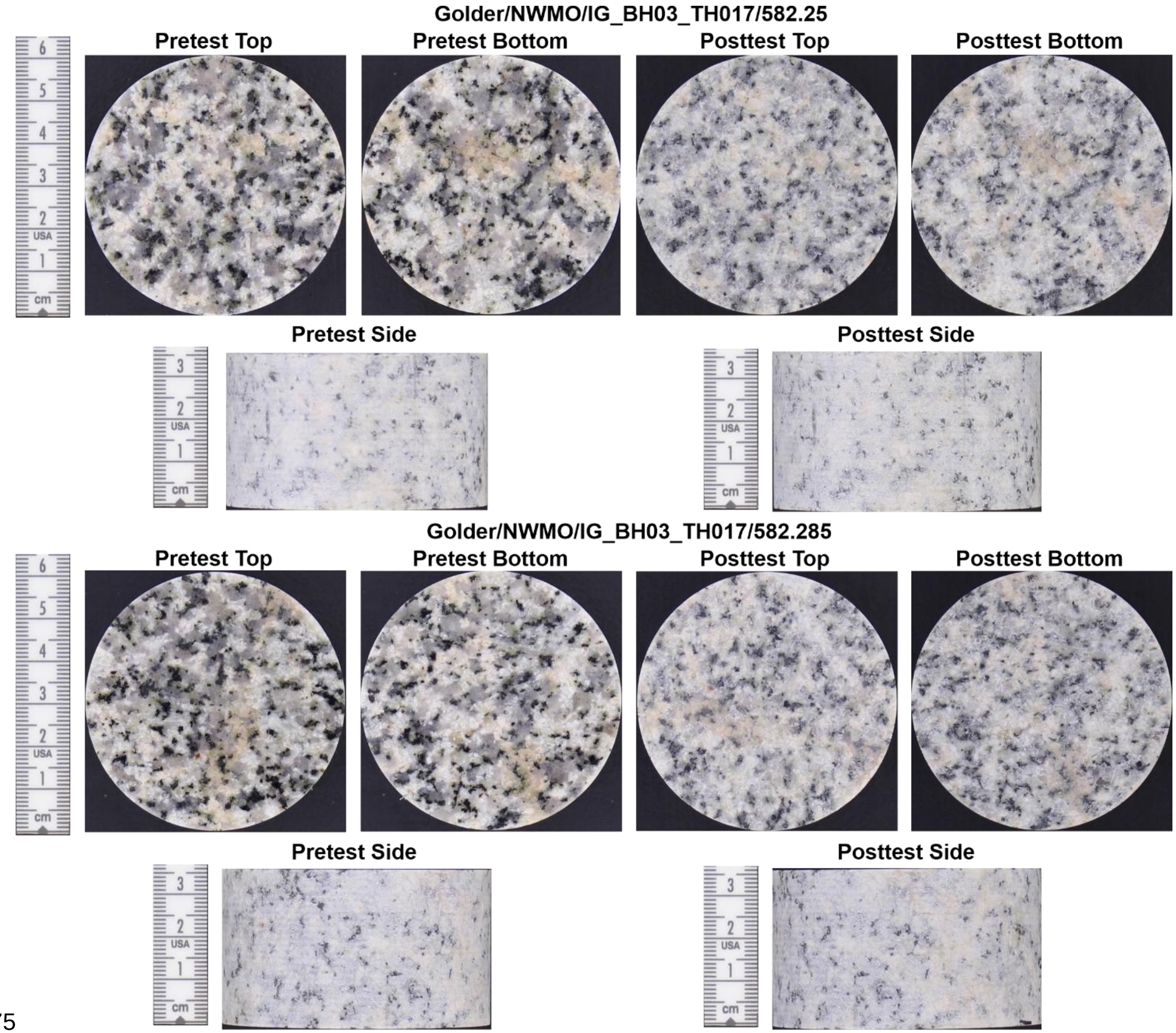

75

Test Specimen IG_BH03_TH017 – Depth = 582.25 m: specimen photographs

Table D-14: Hot Disk Results – Test Specimen IG_BH03_TH017 – Depth = 582.25 m

Average Temperature (°C)	Average Volumetric Specific Heat (MJ/m^3°K)	Average Thermal Conductivity (W/m°K)	Average Thermal Diffusivity (mm^2/s)
20.01	2.31	3.56	1.54
39.99	2.39	3.50	1.47
60.04	2.53	3.45	1.37
79.93	2.59	3.40	1.31
90.03	2.59	3.36	1.30
60.03	2.47	3.46	1.40

NOTE: Sample depths in the graph legends refer to the depth of the original sample as collected (part of the id), not the depth of the sub-samples

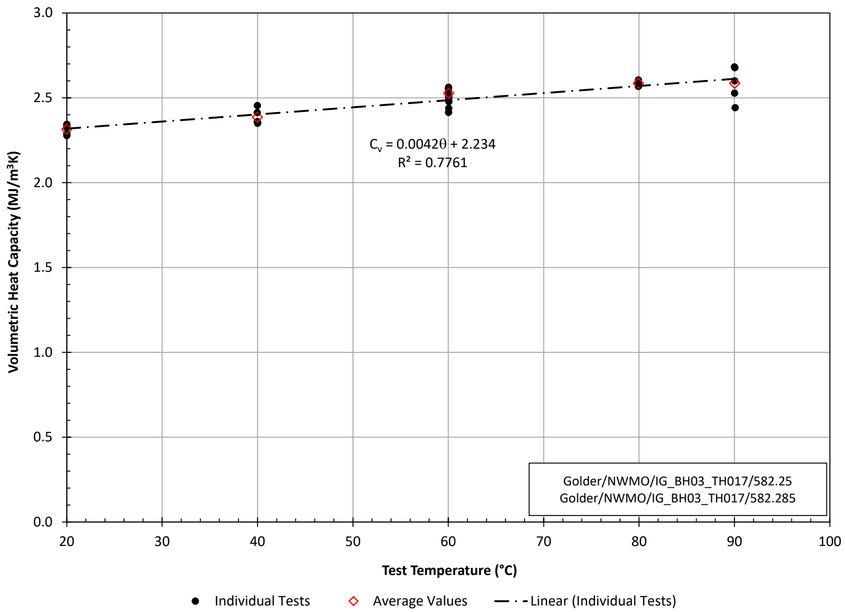

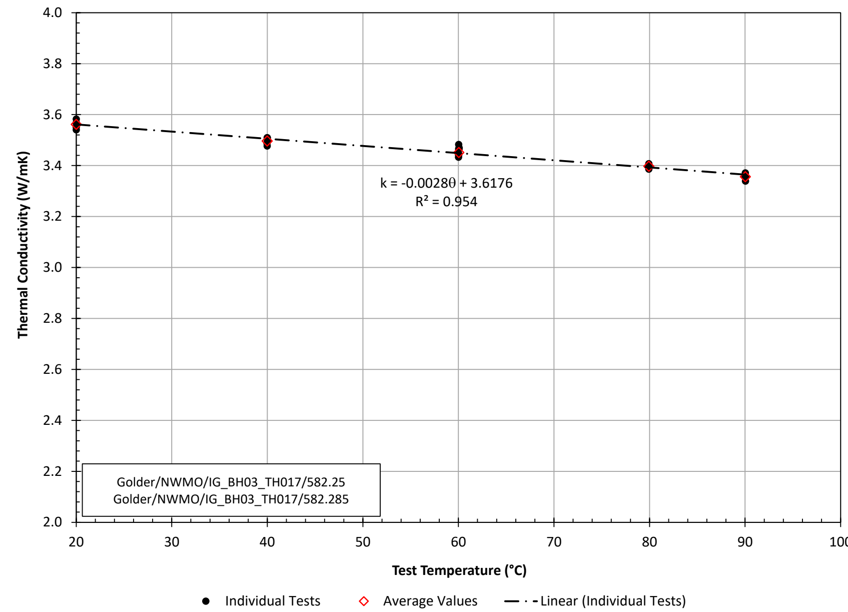

Test Specimen IG_BH03_TH017 – Depth = 582.25 m: Volumetric Heat Capacity and Thermal Conductivity

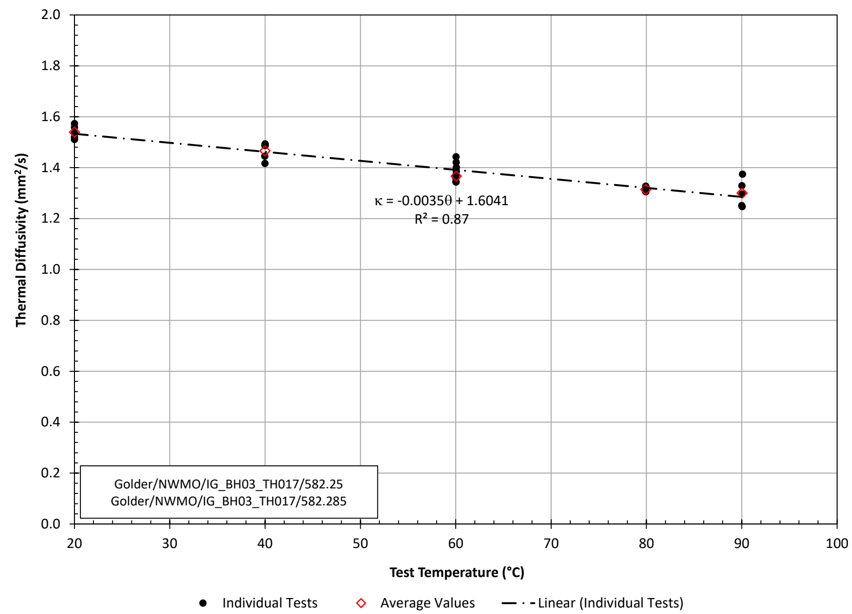

Test Specimen IG_BH03_TH017 – Depth = 582.25 m: Thermal Diffusivity

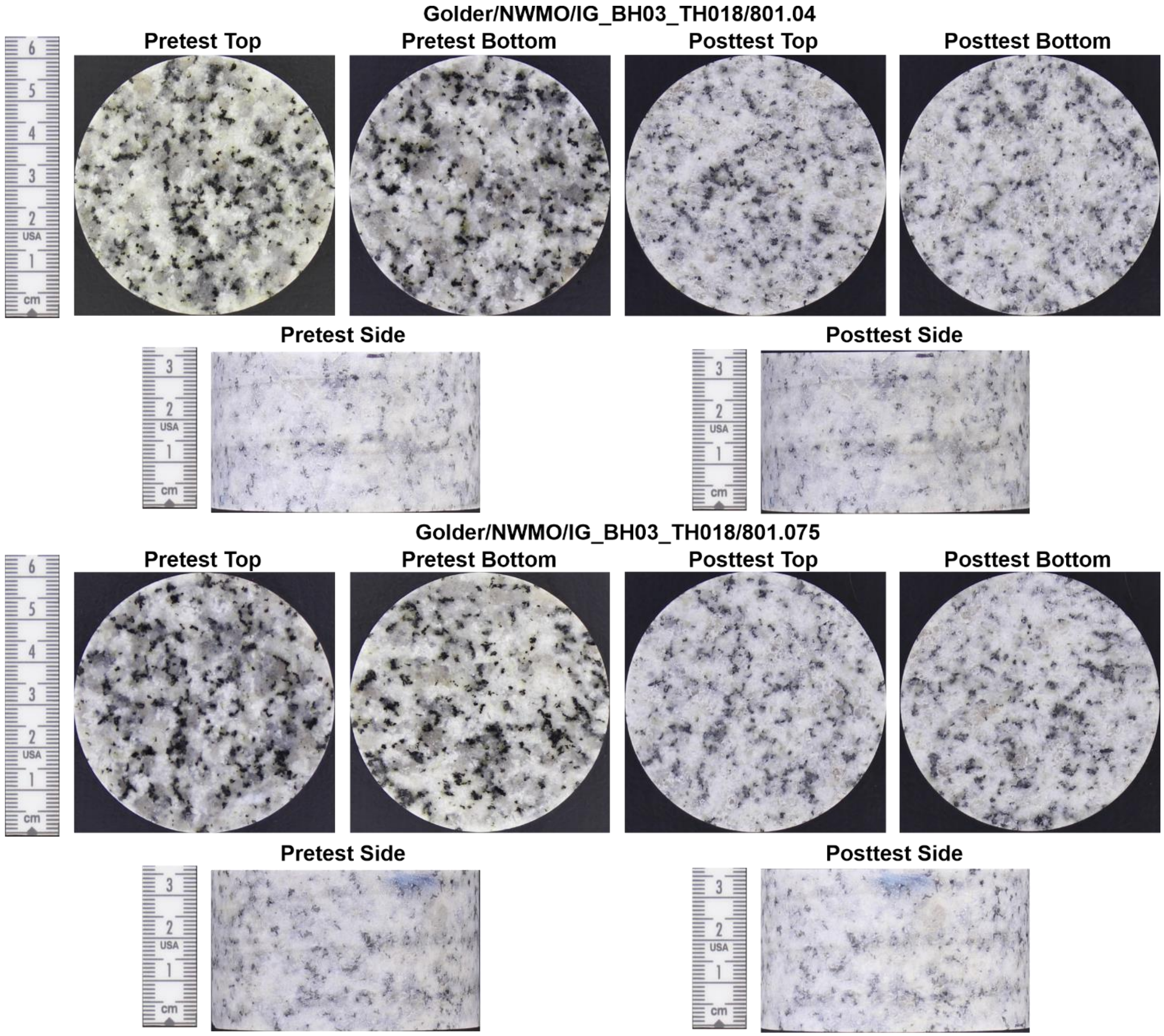

Test Specimen IG_BH03_TH018 – Depth = 801.04 m: specimen photographs

Table D-15: Hot Disk Results – Test Specimen IG_BH03_TH018 – Depth = 801.04 m

Average Temperature (°C)	Average Volumetric Specific Heat (MJ/m³°K)	Average Thermal Conductivity (W/m°K)	Average Thermal Diffusivity (mm²/s)
20.01	2.15	3.11	1.45
40.00	2.27	3.06	1.35
60.05	2.32	3.05	1.32
79.92	2.43	3.01	1.24
90.03	2.46	2.99	1.22
60.05	2.34	3.05	1.31

NOTE: Sample depths in the graph legends refer to the depth of the original sample as collected (part of the id), not the depth of the sub-samples

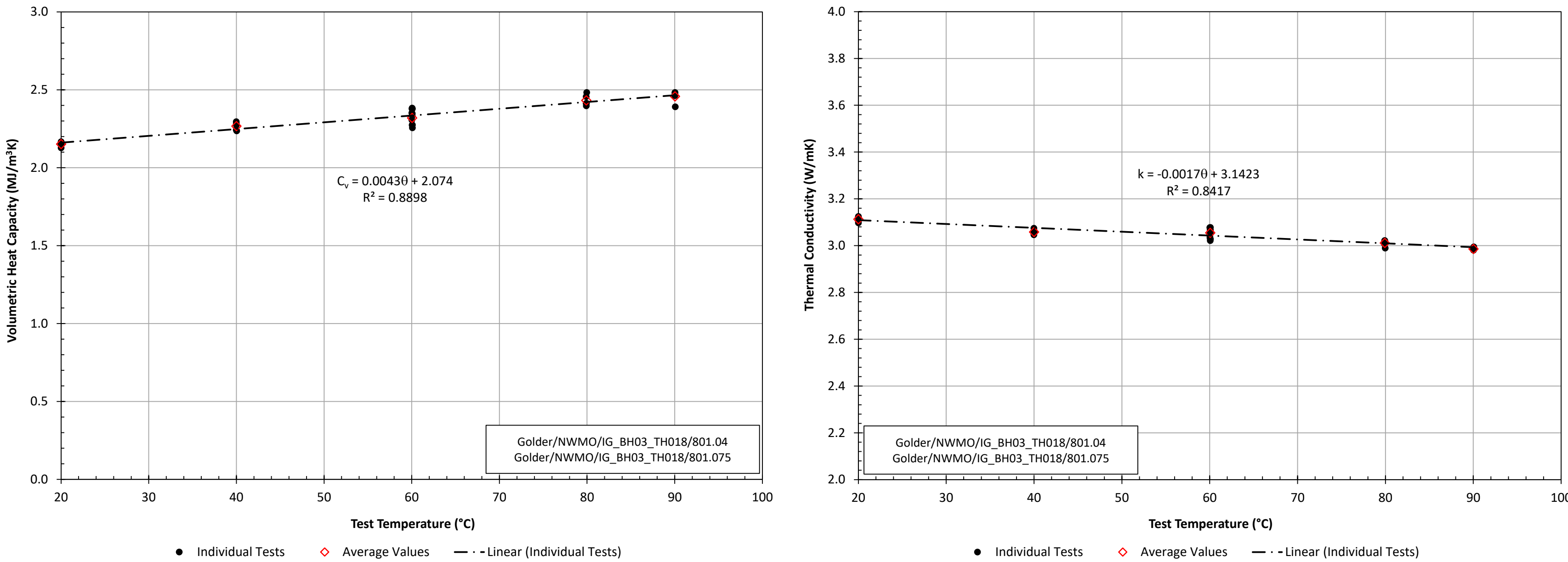

Test Specimen IG_BH03_TH018 – Depth = 801.04 m: Volumetric Heat Capacity and Thermal Conductivity

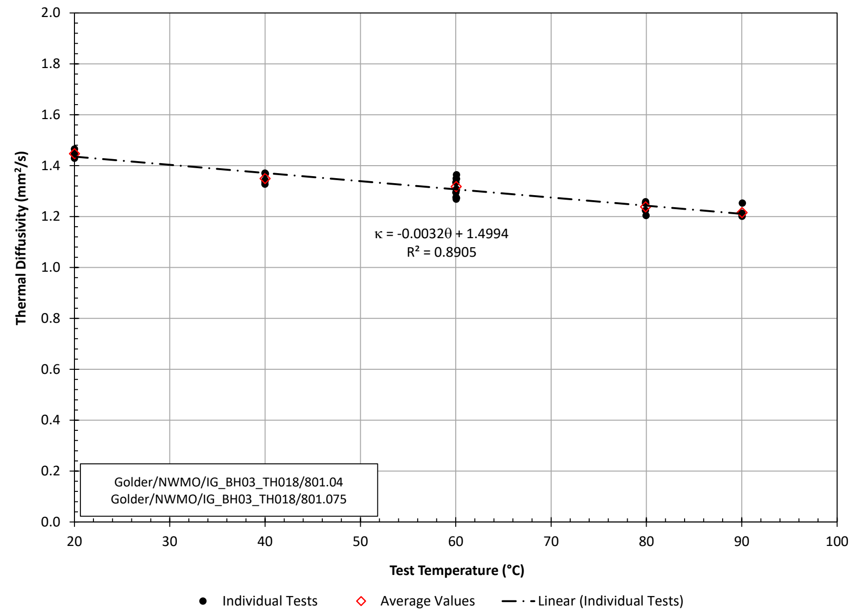

Test Specimen IG_BH03_TH018 – Depth = 801.04 m: Thermal Diffusivity

APPENDIX E

Thermal Expansion Tests: Test Data and Graphs

Table E-1: List of thermal test specimens

Specimen No.	Depth (m)[1]	Rock Type	Page
IG_BH03_TH010[2]	304.96	Biotite Granodiorite-Tonalite	E-2
IG_BH03_TH011[2]	359.20	Biotite Granodiorite-Tonalite	E-4
IG_BH03_TH012[2]	416.93	Biotite Granodiorite-Tonalite	E-6
IG_BH03_TH013[2]	454.64	Biotite Granodiorite-Tonalite	E-8
IG_BH03_TH014[2]	495.43	Biotite Granodiorite-Tonalite	E-10
IG_BH03_TH015[2]	538.74	Biotite Granodiorite-Tonalite	E-12
IG_BH03_TH016[2]	548.68	Amphibolite	E-14
IG_BH03_TH017[2]	582.14	Biotite Granodiorite-Tonalite	E-16
IG_BH03_TH018[2]	800.93	Biotite Granodiorite-Tonalite	E-18

[1] Top depth of prepared sub-sample (depth along borehole).

[2] Sample was saturated before testing.

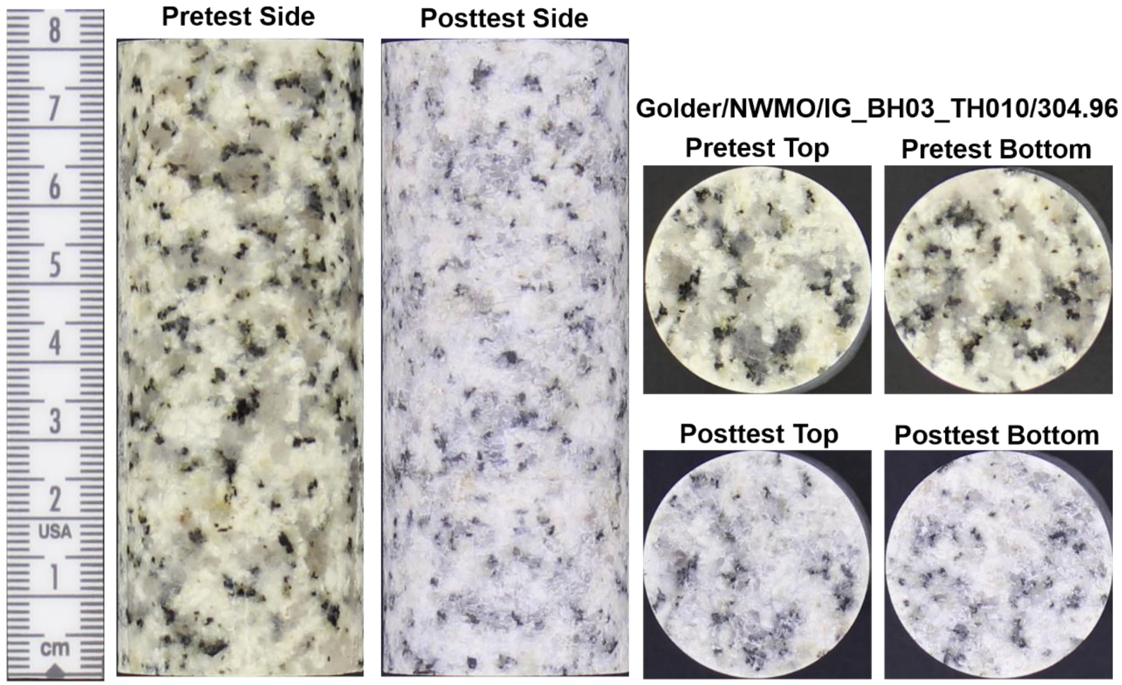

Test Specimen IG_BH03_TH010 – Depth = 304.96 m: specimen photographs

Table E-2: Thermal Expansion Results – Test Specimen IG_BH03_TH010 – Depth = 304.96 m

Average Temperature (°C)	Average Coeff. Linear Thermal Expansion – Linear (1/°K)	Coeff. Linear Thermal Expansion – Quadratic (1/°K)	Average Coeff. Linear Thermal Expansion – Linear (1/°K)	Coeff. Linear Thermal Expansion – Quadratic (1/°K)
	1st Temperature Cycle		2nd Temperature Cycle	
20	7.96E-06	5.92E-06	7.63E-06	6.47E-06
40		7.05E-06		7.11E-06
60		8.18E-06		7.75E-06
80		9.31E-06		8.38E-06
90		9.87E-06		8.70E-06

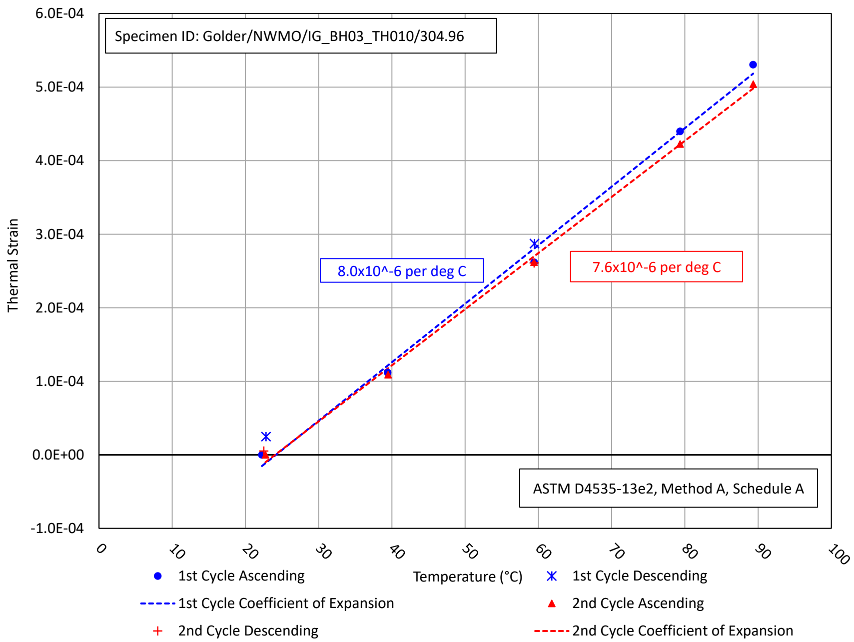

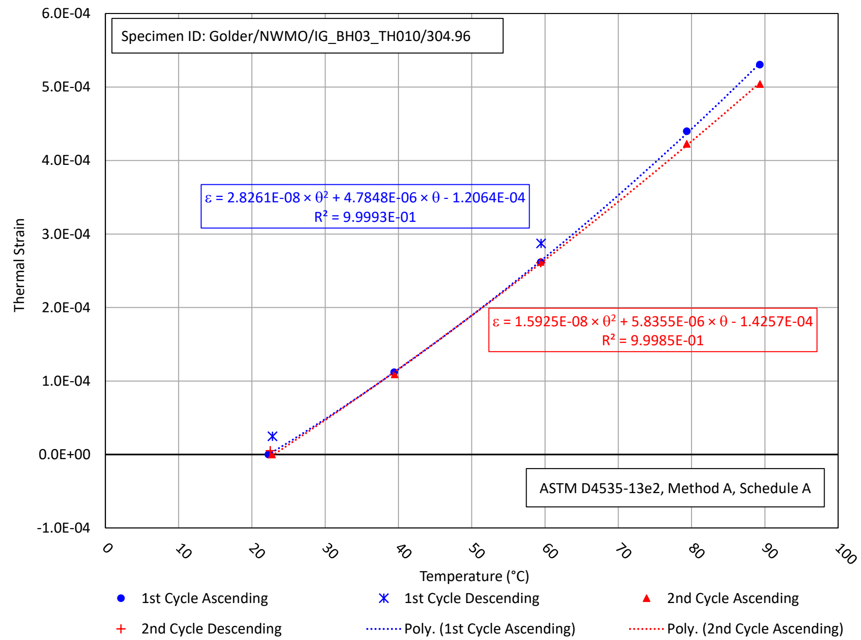

Test Specimen IG_BH03_TH010 – Depth = 304.96 m: Linear fit and quadratic fit for the thermal expansion data

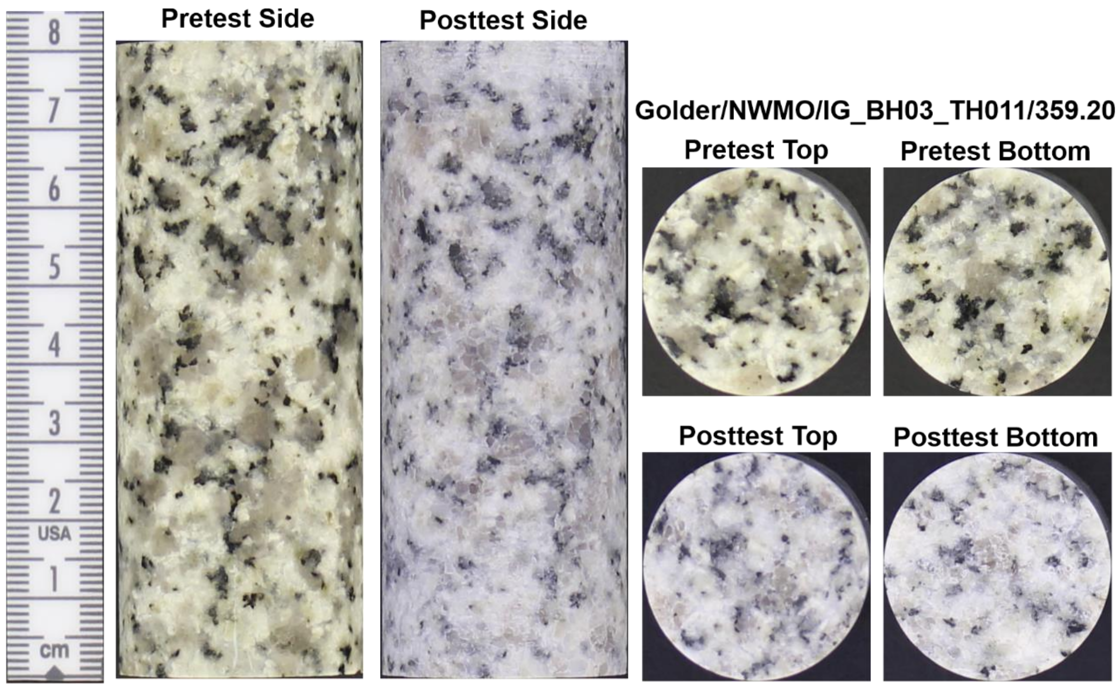

Test Specimen IG_BH03_TH011 – Depth = 359.20 m: specimen photographs

Table E-3: Thermal Expansion Results – Test Specimen IG_BH03_TH011 – Depth = 359.20 m

Average Temperature (°C)	Average Coeff. Linear Thermal Expansion – Linear (1/°K)	Coeff. Linear Thermal Expansion – Quadratic (1/°K)	Average Coeff. Linear Thermal Expansion – Linear (1/°K)	Coeff. Linear Thermal Expansion – Quadratic (1/°K)
	1st Temperature Cycle		2nd Temperature Cycle	
20	7.10E-06	5.37E-06	7.00E-06	5.92E-06
40		6.33E-06		6.52E-06
60		7.28E-06		7.11E-06
80		8.24E-06		7.70E-06
90		8.72E-06		8.00E-06

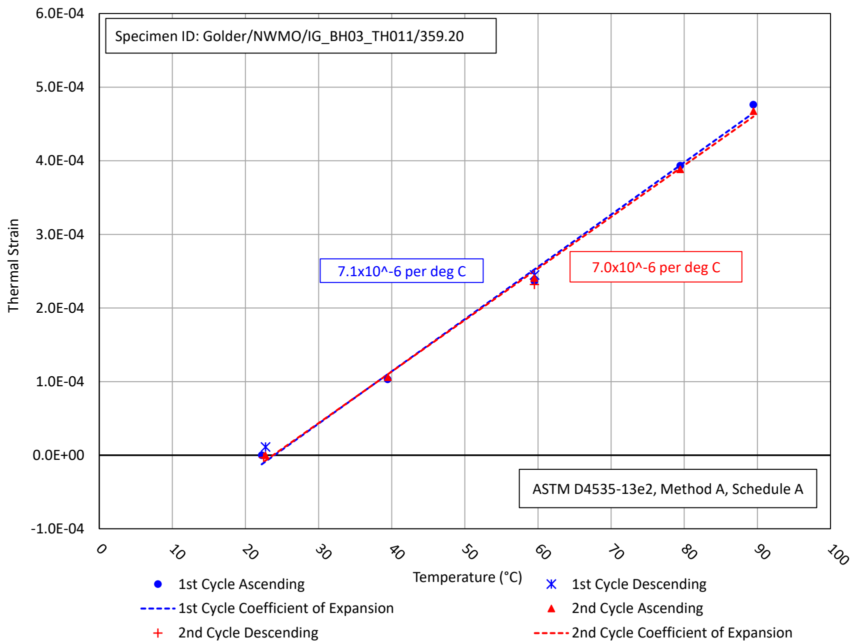

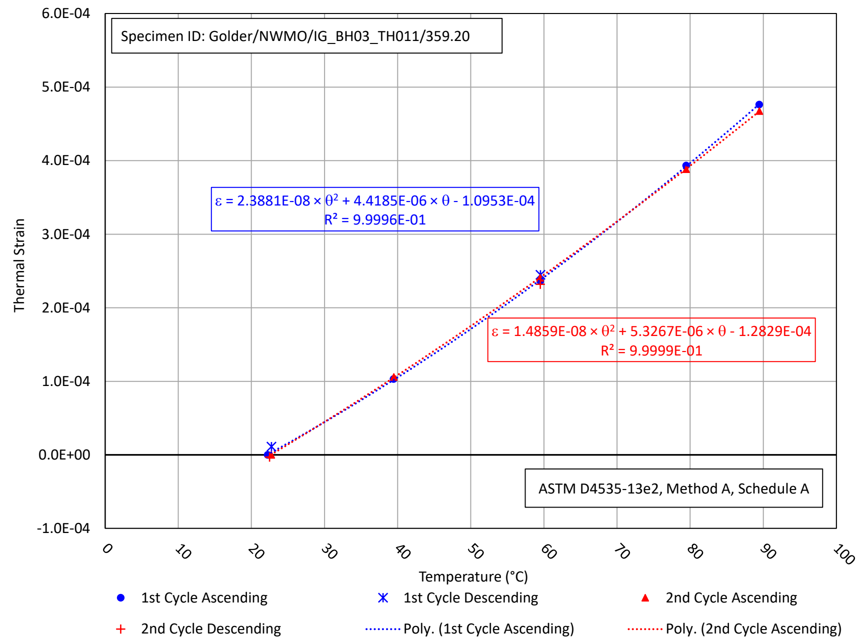

Test Specimen IG_BH03_TH011 – Depth = 359.20 m: Linear fit and quadratic fit for the thermal expansion data

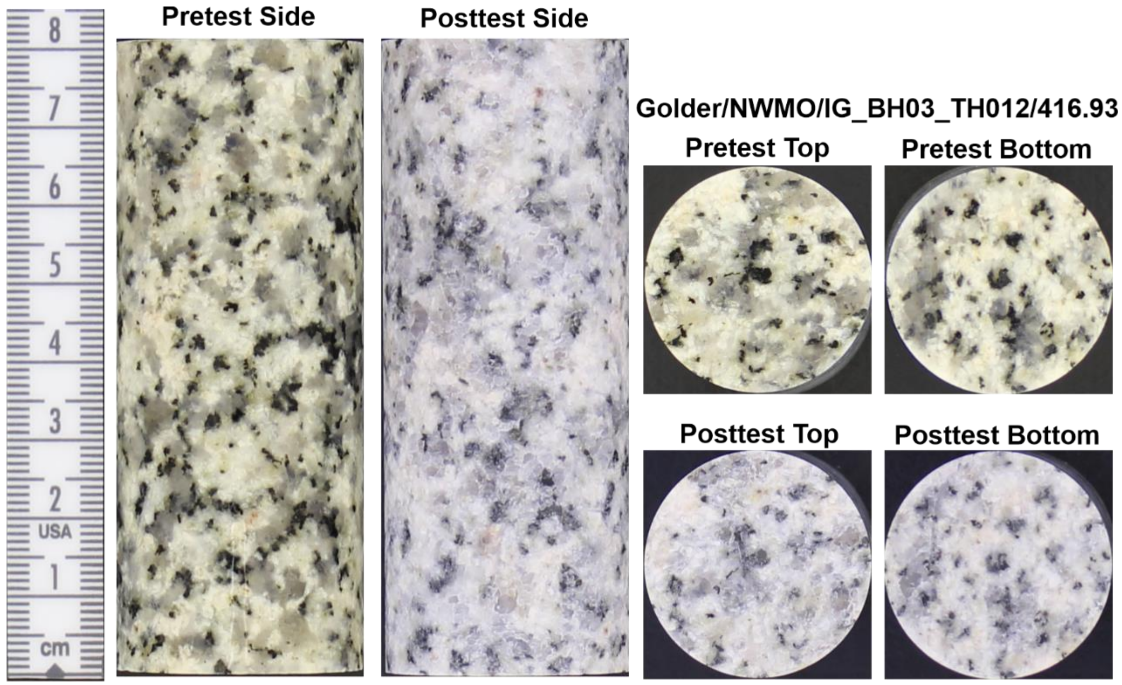

Test Specimen IG_BH03_TH012 – Depth = 416.93 m: specimen photographs

Table E-4: Thermal Expansion Results – Test Specimen IG_BH03_TH012 – Depth = 416.93 m

Average Temperature (°C)	Average Coeff. Linear Thermal Expansion – Linear (1/°K)	Coeff. Linear Thermal Expansion – Quadratic (1/°K)	Average Coeff. Linear Thermal Expansion – Linear (1/°K)	Coeff. Linear Thermal Expansion – Quadratic (1/°K)
	1st Temperature Cycle		2nd Temperature Cycle	
20	7.81E-06	5.80E-06	7.64E-06	6.60E-06
40		6.92E-06		7.18E-06
60		8.04E-06		7.75E-06
80		9.16E-06		8.32E-06
90		9.72E-06		8.61E-06

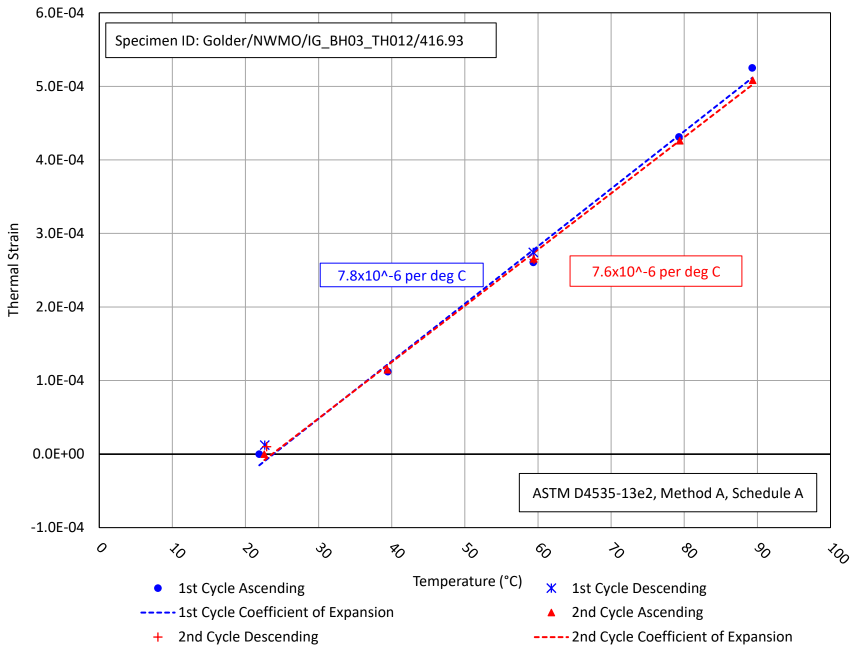

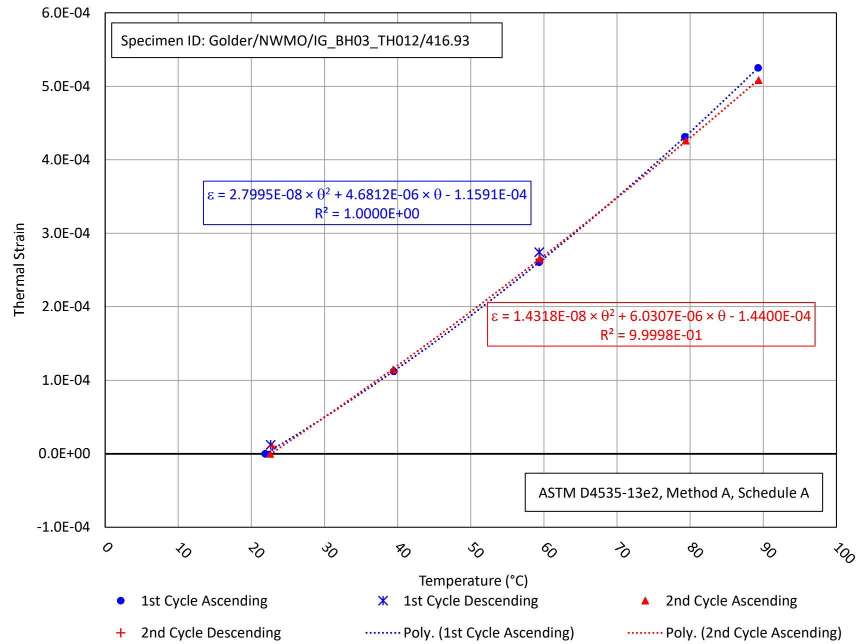

Test Specimen IG_BH03_TH012 – Depth = 416.93 m: Linear fit and quadratic fit for the thermal expansion data

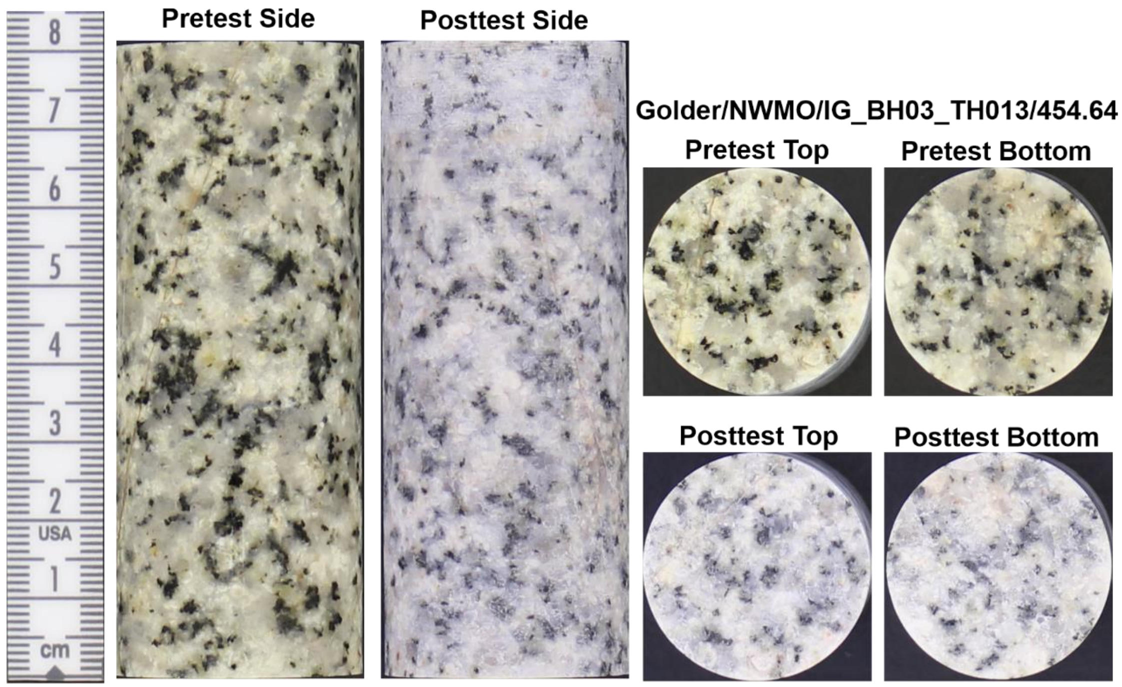

Test Specimen IG_BH03_TH013 – Depth = 454.64 m: specimen photographs

Table E-5: Thermal Expansion Results – Test Specimen IG_BH03_TH013 – Depth = 454.64 m

Average Temperature (°C)	Average Coeff. Linear Thermal Expansion – Linear (1/°K)	Coeff. Linear Thermal Expansion – Quadratic (1/°K)	Average Coeff. Linear Thermal Expansion – Linear (1/°K)	Coeff. Linear Thermal Expansion – Quadratic (1/°K)
	1st Temperature Cycle		2nd Temperature Cycle	
20	7.54E-06	5.80E-06	7.62E-06	6.79E-06
40		6.77E-06		7.25E-06
60		7.74E-06		7.70E-06
80		8.70E-06		8.16E-06
90		9.18E-06		8.39E-06

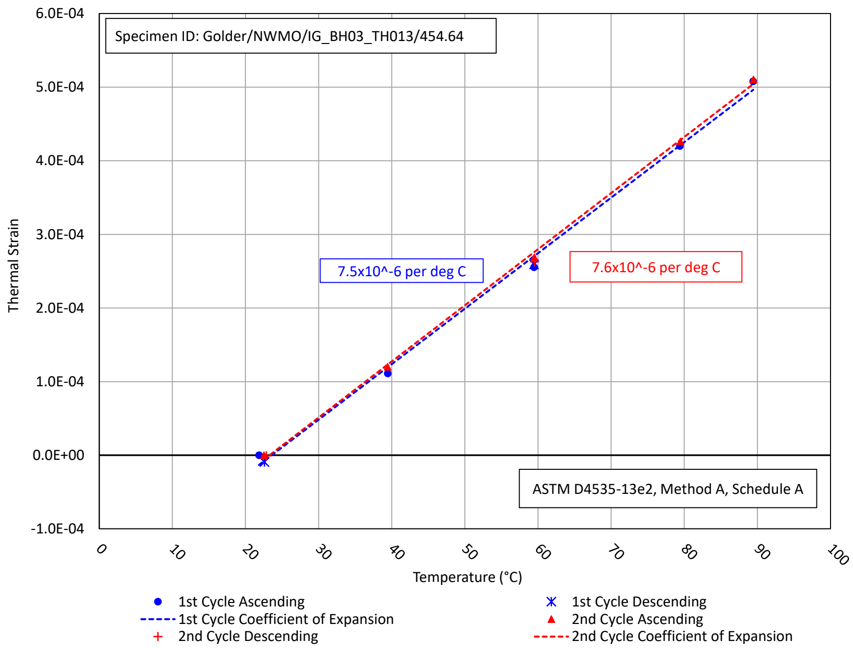

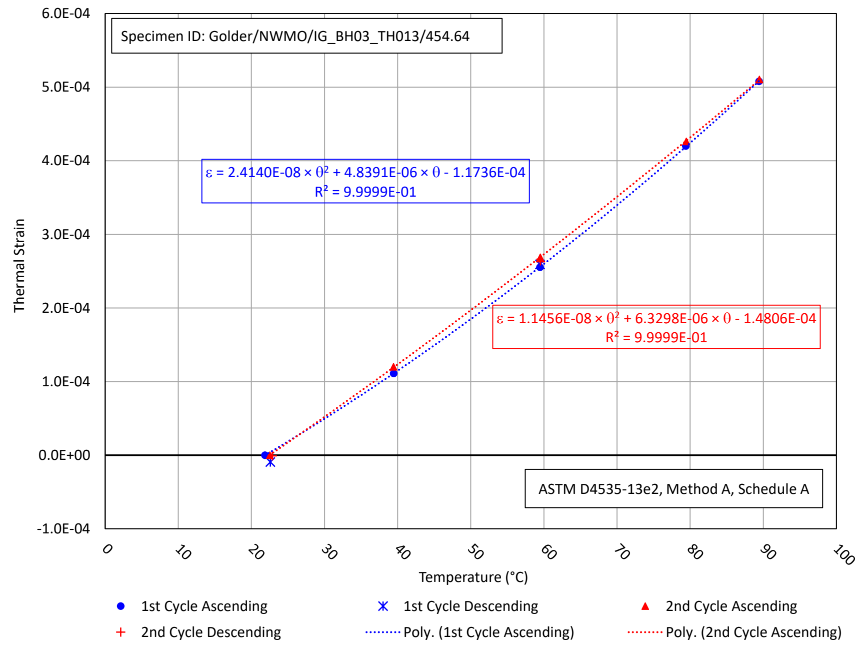

Test Specimen IG_BH03_TH013 – Depth = 454.64 m: Linear fit and quadratic fit for the thermal expansion data

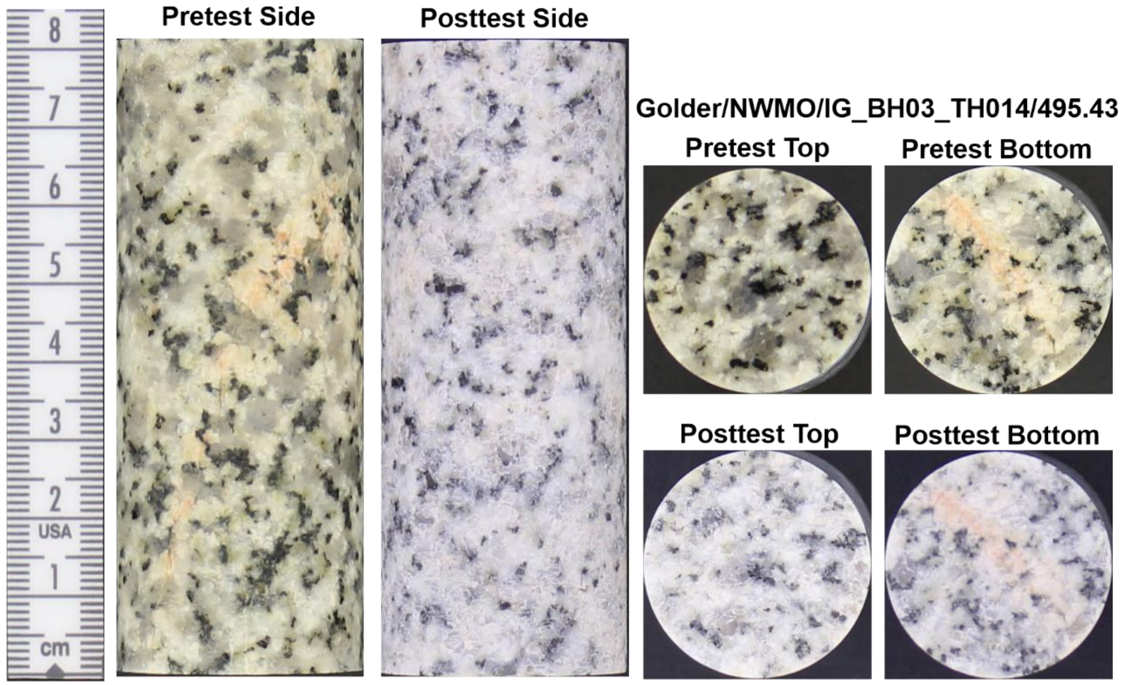

Test Specimen IG_BH03_TH014 – Depth = 495.43 m: specimen photographs

Table E-6: Thermal Expansion Results – Test Specimen IG_BH03_TH014 – Depth = 495.43 m

Average Temperature (°C)	Average Coeff. Linear Thermal Expansion – Linear (1/°K)	Coeff. Linear Thermal Expansion – Quadratic (1/°K)	Average Coeff. Linear Thermal Expansion – Linear (1/°K)	Coeff. Linear Thermal Expansion – Quadratic (1/°K)
	1st Temperature Cycle		2nd Temperature Cycle	
20	6.13E-06	4.21E-06	5.99E-06	4.26E-06
40		5.27E-06		5.21E-06
60		6.33E-06		6.16E-06
80		7.39E-06		7.11E-06
90		7.92E-06		7.59E-06

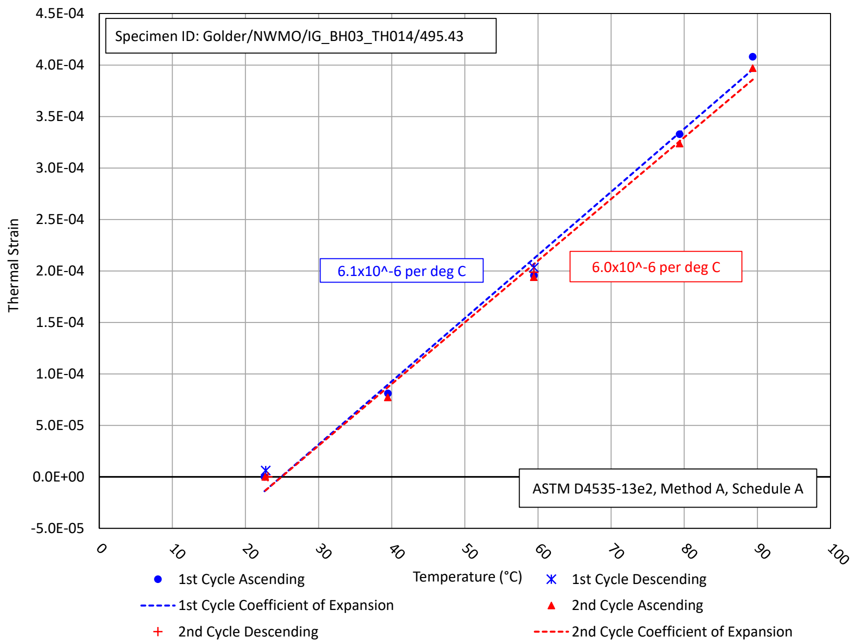

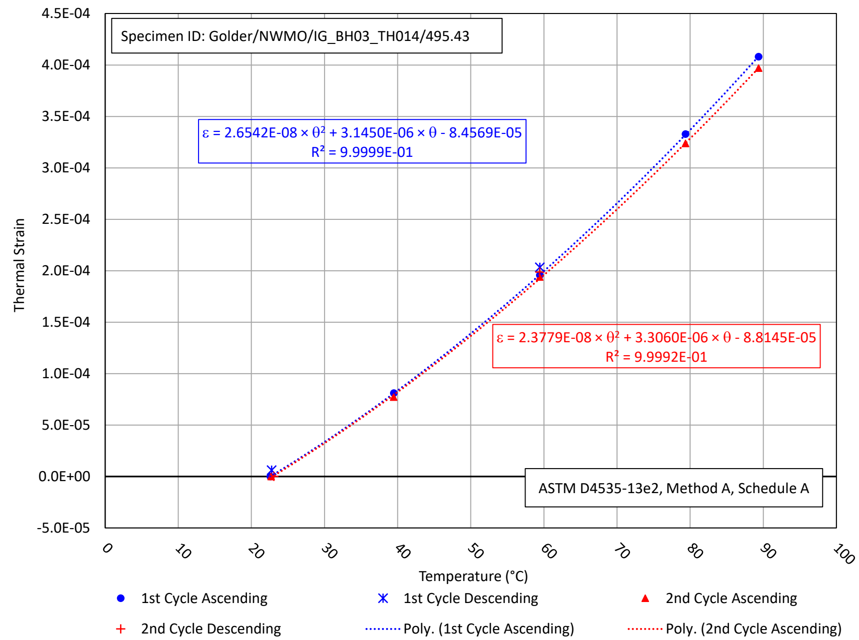

Test Specimen IG_BH03_TH014 – Depth = 495.43 m: Linear fit and quadratic fit for the thermal expansion data

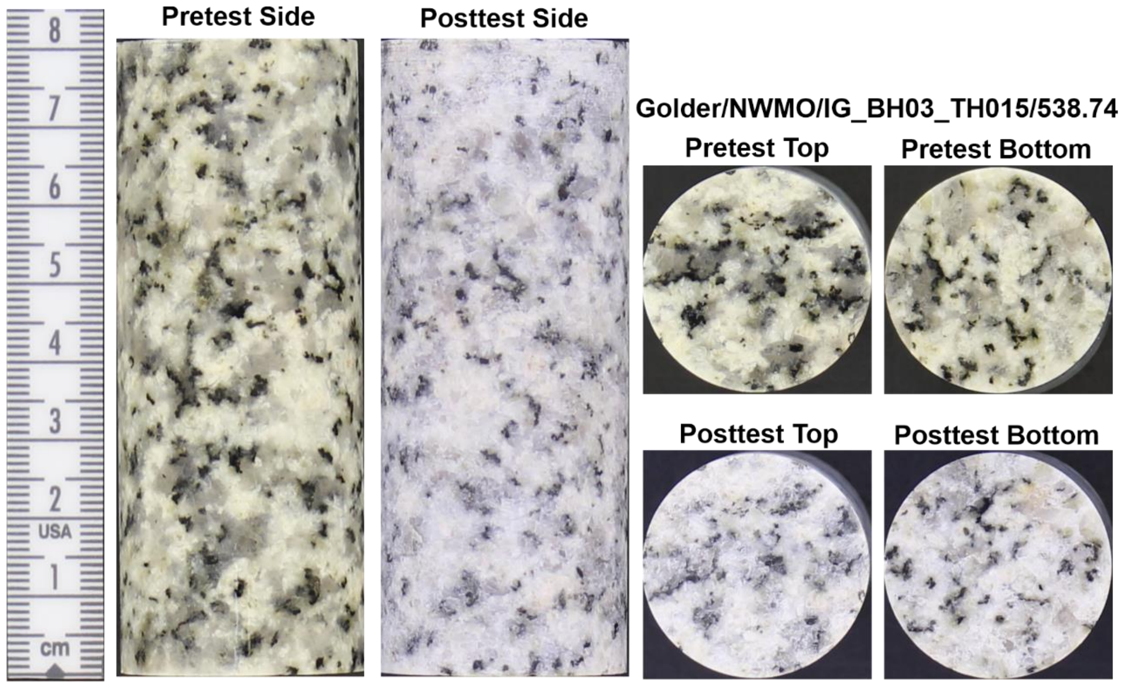

Test Specimen IG_BH03_TH015 – Depth = 538.74 m: specimen photographs

Table E-7: Thermal Expansion Results – Test Specimen IG_BH03_TH015 – Depth = 538.74 m

Average Temperature (°C)	Average Coeff. Linear Thermal Expansion – Linear (1/°K)	Coeff. Linear Thermal Expansion – Quadratic (1/°K)	Average Coeff. Linear Thermal Expansion – Linear (1/°K)	Coeff. Linear Thermal Expansion – Quadratic (1/°K)
	1st Temperature Cycle		2nd Temperature Cycle	
20	7.31E-06	5.32E-06	7.31E-06	6.14E-06
40		6.42E-06		6.78E-06
60		7.52E-06		7.42E-06
80		8.61E-06		8.07E-06
90		9.16E-06		8.39E-06

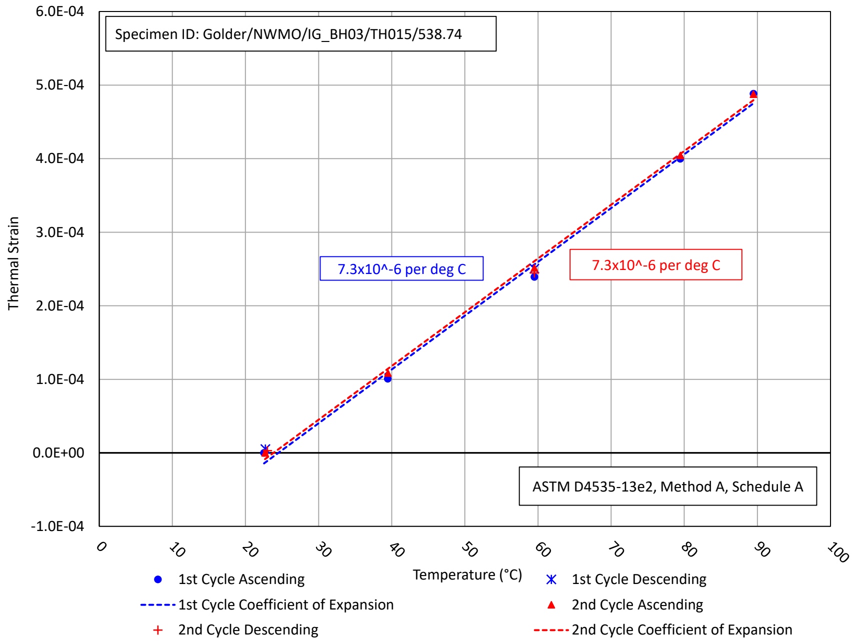

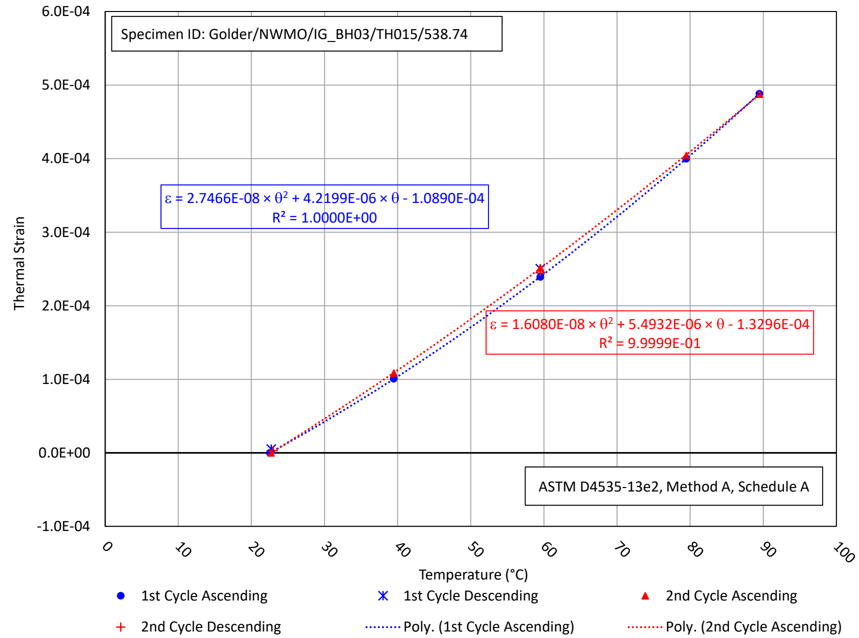

Test Specimen IG_BH03_TH015 – Depth = 538.74 m: Linear fit and quadratic fit for the thermal expansion data

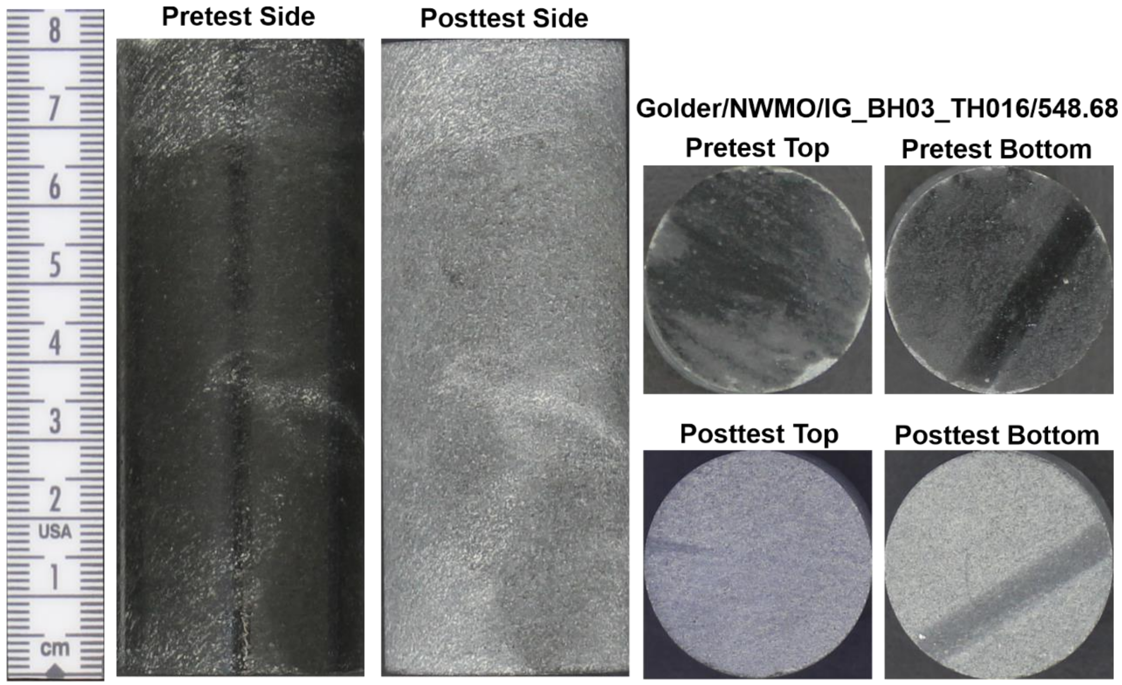

Test Specimen IG_BH03_TH016 – Depth = 548.68 m: specimen photographs

Table E-8: Thermal Expansion Results – Test Specimen IG_BH03_TH016 – Depth = 548.68 m

Average Temperature (°C)	Average Coeff. Linear Thermal Expansion – Linear (1/°K)	Coeff. Linear Thermal Expansion – Quadratic (1/°K)	Average Coeff. Linear Thermal Expansion – Linear (1/°K)	Coeff. Linear Thermal Expansion – Quadratic (1/°K)
	1st Temperature Cycle		2nd Temperature Cycle	
20	7.40E-06	6.51E-06	8.17E-06	7.83E-06
40		7.00E-06		8.02E-06
60		7.48E-06		8.21E-06
80		7.97E-06		8.40E-06
90		8.21E-06		8.49E-06

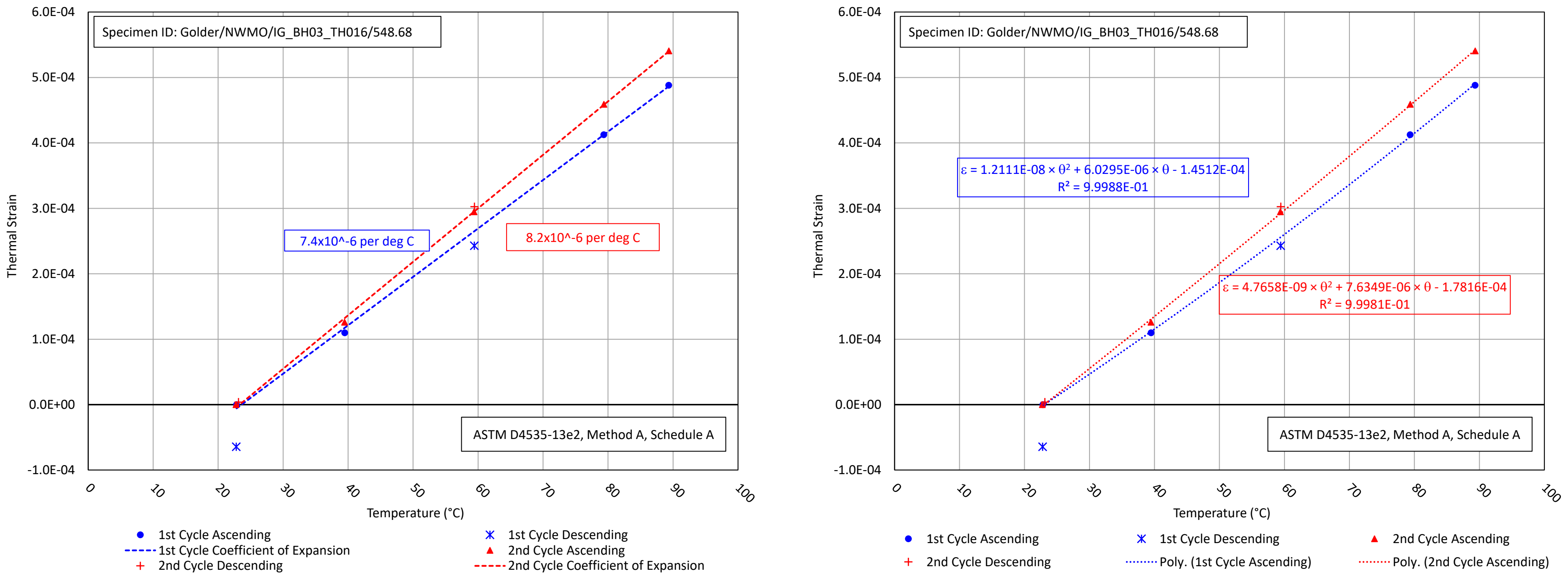

Test Specimen IG_BH03_TH016 – Depth = 548.68 m: Linear fit and quadratic fit for the thermal expansion data

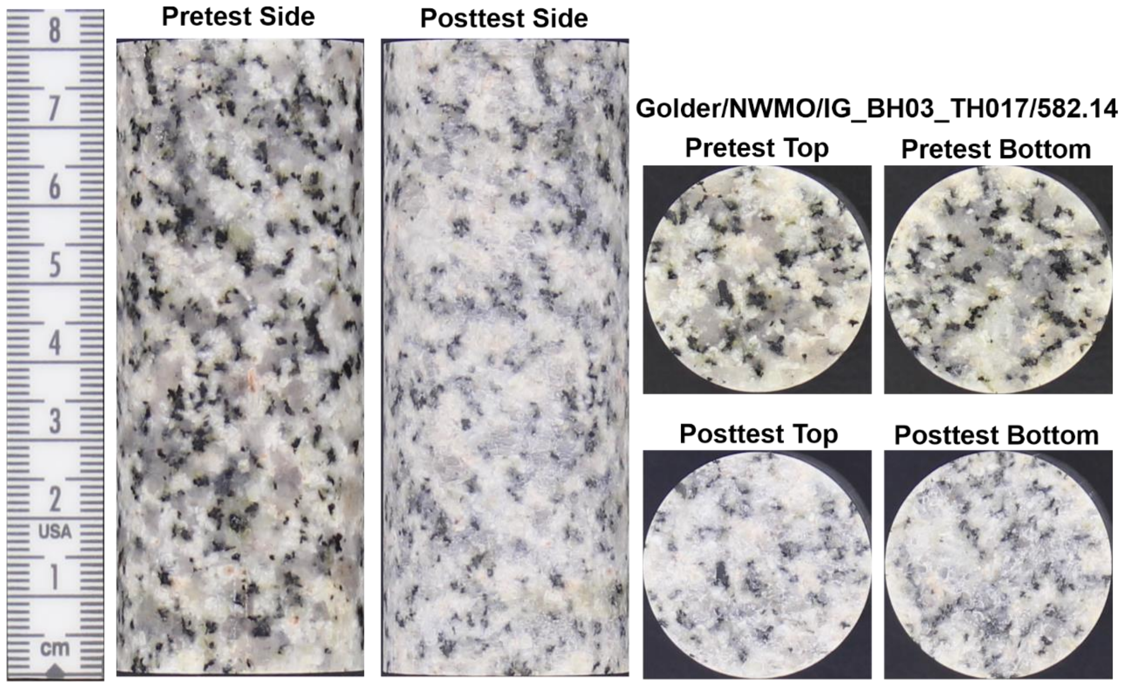

Test Specimen IG_BH03_TH017 – Depth = 582.14 m: specimen photographs

Table E-9: Thermal Expansion Results – Test Specimen IG_BH03_TH017 – Depth = 582.14 m

Average Temperature (°C)	Average Coeff. Linear Thermal Expansion – Linear (1/°K)	Coeff. Linear Thermal Expansion – Quadratic (1/°K)	Average Coeff. Linear Thermal Expansion – Linear (1/°K)	Coeff. Linear Thermal Expansion – Quadratic (1/°K)
	1st Temperature Cycle		2nd Temperature Cycle	
20	8.04E-06	6.35E-06	7.95E-06	7.08E-06
40		7.27E-06		7.56E-06
60		8.20E-06		8.03E-06
80		9.12E-06		8.50E-06
90		9.59E-06		8.74E-06

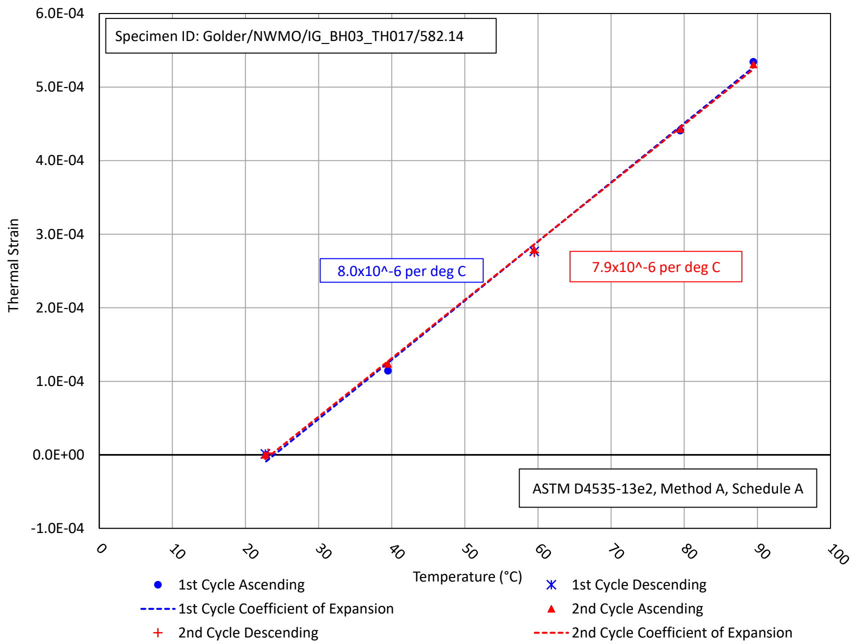

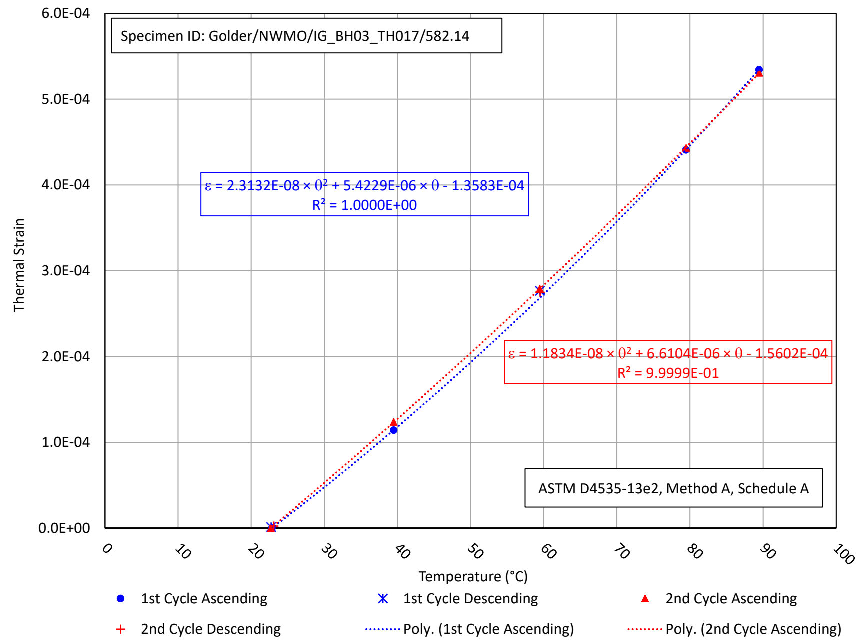

Test Specimen IG_BH03_TH017 – Depth = 582.14 m: Linear fit and quadratic fit for the thermal expansion data

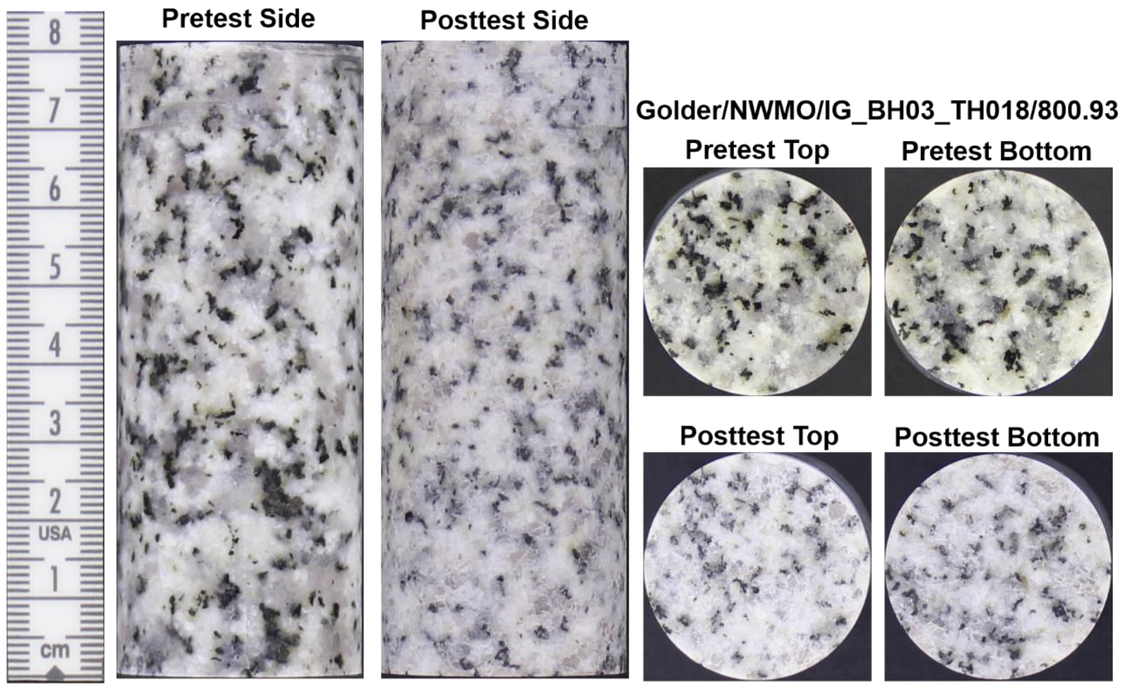

Test Specimen IG_BH03_TH018 – Depth = 800.93 m: specimen photographs

Table E-10: Thermal Expansion Results – Test Specimen IG_BH03_TH018 – Depth = 800.93 m

Average Temperature (°C)	Average Coeff. Linear Thermal Expansion – Linear (1/°K)	Coeff. Linear Thermal Expansion – Quadratic (1/°K)	Average Coeff. Linear Thermal Expansion – Linear (1/°K)	Coeff. Linear Thermal Expansion – Quadratic (1/°K)
	1st Temperature Cycle		2nd Temperature Cycle	
20	6.47E-06	5.59E-06	6.50E-06	5.76E-06
40		6.07E-06		6.16E-06
60		6.55E-06		6.57E-06
80		7.03E-06		6.97E-06
90		7.27E-06		7.18E-06

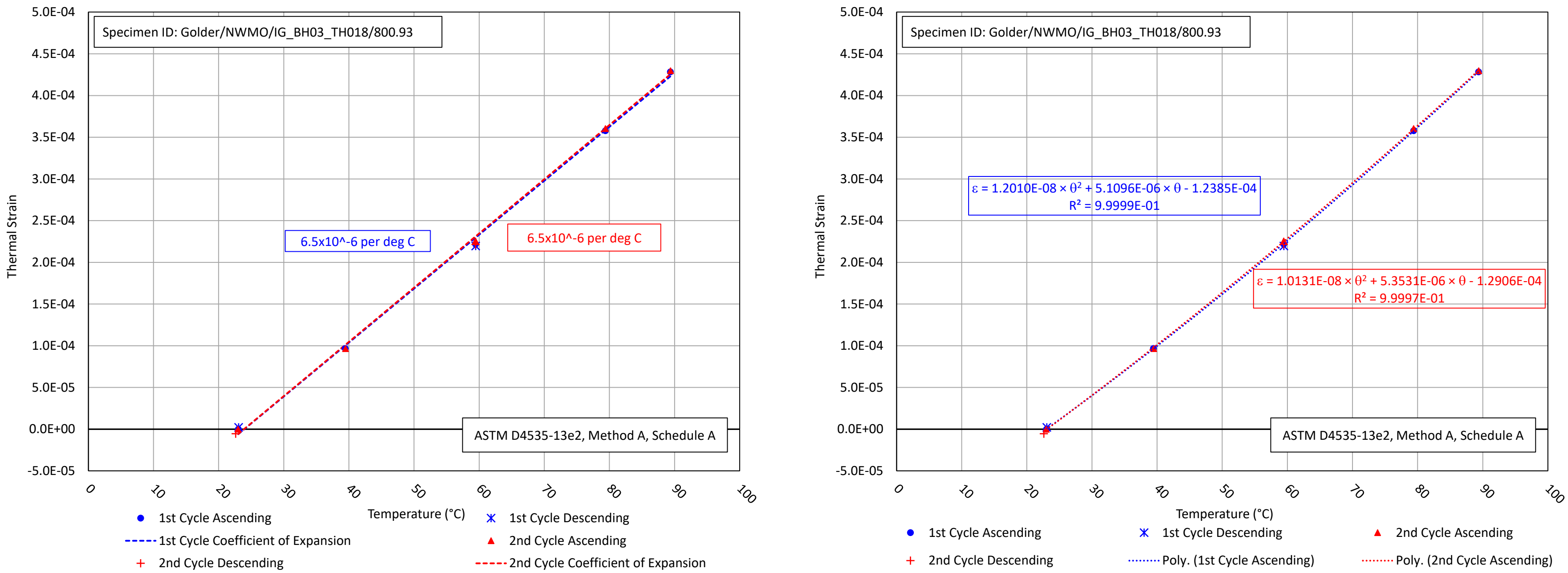

Test Specimen IG_BH03_TH018 – Depth = 800.93 m: Linear fit and quadratic fit for the thermal expansion data

GOLDER
MEMBER OF WSP

golder.com